UNIVERSITY OF OKLAHOMA

GRADUATE COLLEGE

FLEXIBLE AND OPTIMAL CARBON DIOXIDE CAPTURE SYSTEM DESIGN FOR FOSSIL-FUELED POWER PLANTS

A DISSERTATION

SUBMITTED TO THE GRADUATE FACULTY

in partial fulfillment of the requirements for the

Degree of

DOCTOR OF PHILOSOPHY

By

Javad Asadi

Norman, Oklahoma

2023

FLEXIBLE AND OPTIMAL CARBON DIOXIDE CAPTURE SYSTEM DESIGN FOR FOSSIL-FUELED POWER PLANTS

A DISSERTATION APPROVED FOR THE
SCHOOL OF AEROSPACE AND MECHANICAL ENGINEERING

BY THE COMMITTEE CONSISTING OF

Dr. Pejman Kazempoor, Chair

Dr. Farrokh Mistree

Dr. Zahed Siddique

Dr. Wilson Merchan Merchan

Dr. Hamidreza Shabgard

Dr. Paul Moses

Acknowledgments

During my time as a graduate student, I have been fortunate to have encountered remarkable individuals who have consistently provided me with unwavering support and encouragement when I needed it most. Their unwavering positivity and strength have played a pivotal role in shaping my scientific experience, as well as fostering my personal growth and eventual accomplishments.

First and foremost, I extend my heartfelt appreciation to my advisor, Dr. Pejman Kazempoor. His dedication, mentorship, and profound investment in my academic growth have been instrumental in shaping the trajectory of my research. Dr. Kazempoor's unwavering support, insightful feedback, and encouragement have continuously motivated me to strive for excellence in my work. The time and effort that Dr. Kazempoor dedicated to nurturing my scientific curiosity have been pivotal in enabling me to successfully complete this task. I am sincerely grateful for his mentorship and belief in my abilities.

I would like to express my gratitude to my esteemed committee members, Dr. Farrokh Mistree, Dr. Zahed Siddique, Dr. Wilson Merchan Merchan, Dr. Hamidreza Shabgard, and Dr. Paul Moses. Their valuable insights, expertise, and constructive feedback have significantly enhanced the quality and rigor of this dissertation. Their collective wisdom and guidance have broadened my perspective and enriched the overall contributions of this research.

I want to express my deepest gratitude to my mother, Zivar, my father, Mohammad, my sisters, Sahar and Zahra, and my niece and nephew, Benita and Barsam, whose love, encouragement, and guidance kept me motivated in pursuing my dreams. Above all, I am extremely grateful for the continuous support, encouragement, and love that my wife, Dorna, has provided me throughout the entire process of completing my Ph.D. Her presence by my side has been an extraordinary source of love, strength, and motivation, elevating this journey to new heights of meaning and fulfillment.

To my Mom and Dad, for sacrificing their lives to support and nurture my dreams. This achievement is as much yours as it is mine.

Table of Contents

List of Figures

List of Tables

Abstract

Fossil fuel consumption remains a significant contributor to global greenhouse gas emissions, accounting for approximately 90% of the overall emissions, with fossil fuel power generation systems identified as a major source of CO_2 emissions. Given the ongoing industrial activities and increasing energy demand, completely discontinuing the use of nonrenewable resources for power production is not feasible in the near future. CO_2 capture and storage (CCS) technologies offer a promising option for continuing to utilize fossil fuels in a cleaner and more sustainable manner. The wide deployment of carbon capture technologies alone has the potential to decrease power plant emissions by as much as 90%. However, the current CCS technologies face several challenges for broad implementation, specifically significant energy requirements, high capital cost, and flexible operation. The current CCS technologies lead to a decrease in the net power output of the plant by approximately 25-40% and result in a substantial increase in power generation costs, potentially up to 70%. Another challenge is the requirement for flexible operation of CCS, as with the increasing penetration of renewable energy sources in the power grid, fossil fuel-fired power plants need to operate in a load-following manner to ease the integration of intermittent renewable sources. Consequently, significant fluctuations in the power plant flue gas necessitate flexible operation of the downstream carbon capture system to adapt to these changes.

The above challenges necessitate implementing innovative solutions in the operation and design of carbon capture systems to reduce the energy penalty and cost of CO_2 capturing and improve the flexible operation of CCS to accommodate both base-load and load-following operating of the power plants. Membrane systems offer promising advantages for separating CO_2 from other components of power plant flue gas, although the process encounters several technical and economic challenges. These challenges must be addressed to optimize their design and integration with fossil-fueled power plants and enhance the feasibility of this environmentally-friendly technology for extensive adoption.

This dissertation is focused on the development of flexible and efficient membrane-based carbon capture technologies for large-scale implementation and integration with both base-load and load-following fossil-fueled power plants under high renewable energy integration. This dissertation aims to address and provide insights into the current challenges by employing

advanced modeling, simulation, and optimization techniques. An efficient and flexible multi-stage membrane-based CCS process is developed and optimized to address the challenge of energy requirements and cost penalties of the system. In this context, a comprehensive techno-economic model for the possible designs and operating strategies of the membrane separation process is developed in order to investigate the potential and viability of the membrane-based CCS system. Furthermore, the optimal process design and the possible trade-offs between performance indicators of the membrane-based CCS are presented with the aim of reducing energy and cost penalties. Finally, the transient behavior of the membrane-based process is further investigated at different disturbances and variations in the power plant operation imposed by the plant load-following behavior to address the required flexibility of the carbon capture system. The results substantiate that the proposed system could be an optimal and flexible option for the decarbonization of power plants operating in a load-following manner. The best possible trade-offs between objective functions show that the CO_2 capture cost and energy penalty of the process could be as low as 13.1 \$/tCO_2 and 10% at optimal design and operating conditions. Also, the results show that the response of the membrane module to step-change in feed flowrate conditions is much faster than the conventional CO_2 capture process, making this technology promising for flexible integration. This study provides valuable insight into membrane separation and can be used by decision-makers for the sustainable development of fossil-fueled power plants.

Moreover, to address CCS integration challenges for the power plant operating at base-load mode, a hybrid solar-assisted membrane-amine CCS equipped with thermal energy storage is developed in order to improve the power plant operation and reduce the low-carbon electricity cost and the energy penalty associated with the CO_2 capturing. In this regard, the conventional amine-based CCS is hybridized with a multi-stage membrane process for selective CO_2 recirculation to improve the separation driving force and decrease both CCS equipment size and energy penalty. Furthermore, the solar energy field with 4-hour thermal energy storage is integrated with the developed CCS to provide the required thermal energy and flexibility for capturing 90% of released CO_2. The results proved that the specific reboiler duty and total packing volume in the case of the proposed design could be significantly reduced by 4.3-6.9% and 39-44%, respectively, compared to the baseline case. Also, due to the change in the inlet air properties and integration of the solar field to the CO_2 capture plant, the output power of the system in the proposed designs can be increased by 13.8-19.4% in comparison to the conventional case. Moreover, the results

revealed that the developed design represents the lowest levelized cost of electricity and CO_2 avoided cost, 81.43 $/MWh and 101.66 $/tonne$CO_2$, among the other CCS-equipped power plant.

The proposed designs and system investigation conducted in this dissertation and for addressing the technology challenges of the CO_2 capture process hold considerable promise in facilitating the ideal reduction of carbon emissions from fossil-fueled power plants and promoting sustainability within the power sector. These advancements and developments, along with appropriate governmental policies and incentive programs, can potentially enhance the economic viability and desirability of CO_2 capture systems, making them increasingly favorable for widespread implementation.

Chapter 1. Introduction and Research Objectives

1.1 Climate change mitigation and carbon capture and storage

Carbon dioxide, a significant gas present in the atmosphere, plays a crucial role in sustaining life on Earth. This molecule is essential for the process of photosynthesis, which provides energy to plants, the primary resource of food as well as a source of oxygen which is vital for human life [1]. However, recent evidence suggests that human activities associated with energy production are causing an excessive buildup of carbon dioxide (CO_2) in the atmosphere [2]. A significant increase in atmospheric CO_2 concentration has been reported, surpassing 415 parts per million (ppm) in 2019 from the pre-industrial revolution level of 280 ppm, as energy demands have increased globally [3]. This accumulation of CO_2 has surpassed the capacity of Earth's natural cycles to balance it, and CO_2 has become the most abundant greenhouse gas (GHG) generated by human activities, and it is expected to lead to severe environmental issues in the future through climate change [4]. As presented in Fig. 1-1, CO_2 has been responsible for the major GHG emission and associated negative impacts since 1990 in the United States [5]. These potential environmental impacts include the melting polar ice caps, rising sea levels, drastic changes in

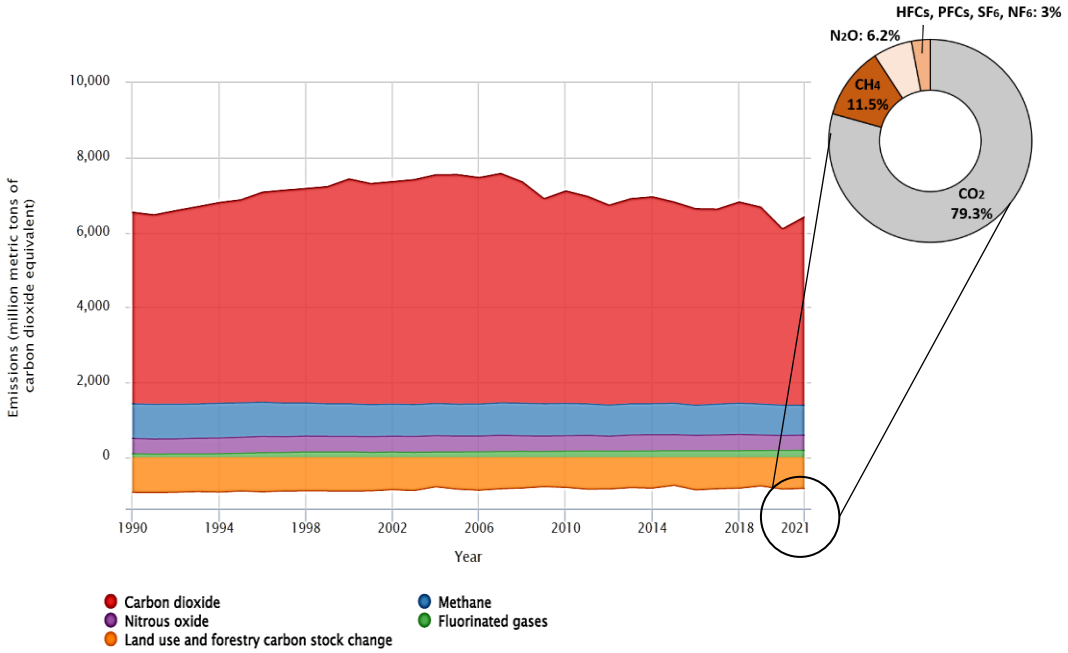

Fig. 1-1. The contribution of different GHG components in the U.S. emissions since 1990 [5]

weather patterns, warming and acidification of the oceans, depletion of the ozone layer, and poor air quality, which subsequently endanger human, plant, and animal life [6].

Since the start of the industrial revolution, carbon dioxide emissions have dramatically risen primarily due to the combustion of fossil fuels for power generation. This anthropogenic activity, which currently accounts for 80% of the world's energy supply, has steadily increased atmospheric CO_2 levels [7]. Specifically, global CO_2 emissions from energy combustion and industrial processes in 2022 reached 36.6 gigatons (Gt) of CO_2, marking the highest amount ever recorded [8]. As depicted in Fig. 1-2, the United States emitted around 5.6 $GtCO_2$ in 2021 through energy production and industrial activity, which is about 15.3% of global annual CO_2 emissions [5]. Although a decrease in recent decades has been reported in GHG emissions, mainly due to switching coal to natural gas power plants, there still are large GHG emissions from the energy sectors that need to be addressed to prevent climate change issues.

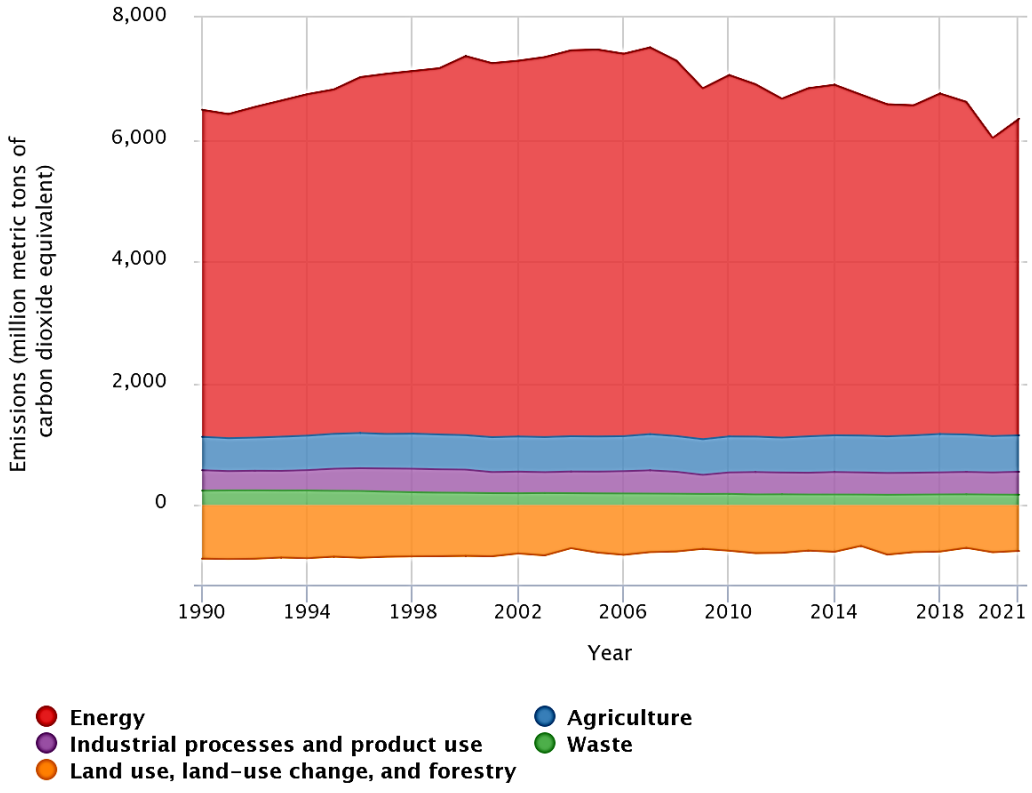

Fig. 1-2. U.S. GHG emission by inventory sector from 1990 to 2021 [5]

Simultaneously, we are witnessing a significant surge in the global population and a remarkable expansion in energy usage, fueled by the increasing number of countries adopting industrialization. It is expected that energy consumption will continue to escalate in the 21st century as The International Energy Agency (IEA) projected a 50% surge in energy demand by 2050 [9]. Accordingly, decarbonizing fossil fuel power plants is of paramount importance to align with the environmental goal of achieving zero emissions by 2050 outlined by the Intergovernmental Panel on Climate Change (IPCC) [10].

Various options exist for decreasing CO_2 emissions from conventional power plants, including enhancing fuel conversion efficiency through advanced technologies like integrated gasification combined cycle (IGCC) [11], supercritical and ultra-supercritical pulverized coal power plants [12], and natural gas combined cycle (NGCC) [13]. Another approach is fuel switching involves transitioning from carbon-intensive fuels (such as coal) to less carbon-intensive alternatives like natural gas [14]. Additionally, the most emerging technology is carbon capture and storage (CCS), which could be integrated with fossil fuel combustion plants to capture the emitted CO_2. CCUS, which stands for Carbon Capture, Utilization, and Storage, plays a crucial role in facilitating the shift toward achieving net zero emissions through various means. It addresses emissions stemming from current energy infrastructures, offers solutions in sectors where emission reduction is particularly challenging, such as cement production, aids in the significant expansion of low-emission hydrogen generation, and allows for extracting certain amounts of CO_2 from the atmosphere [15].

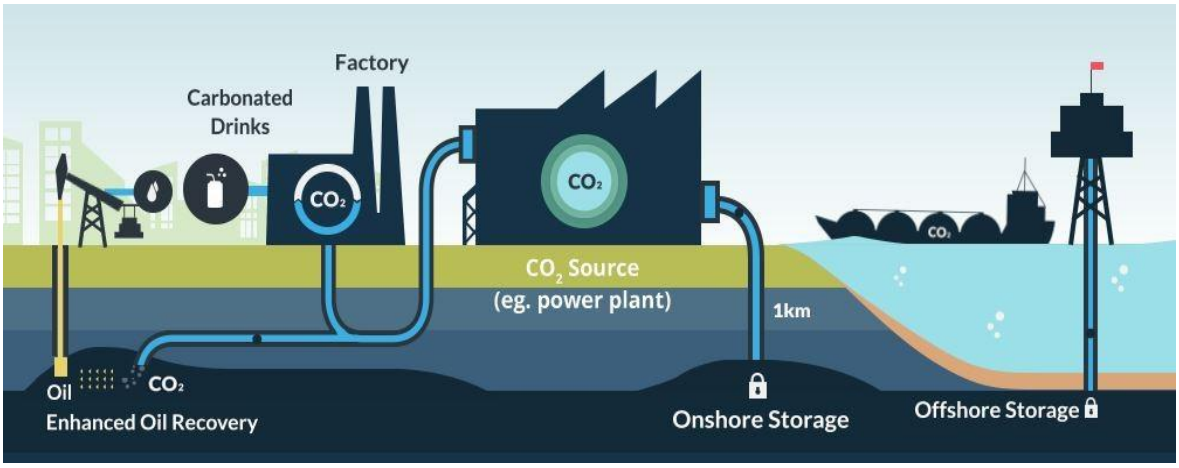

Fig. 1-3. Schematic of carbon capture and storage technologies [16]

CCS technology involves the process of capturing CO_2 emissions from sources, such as power plants or industrial facilities, and transporting them to a storage site where it is deposited in sinks like geological reservoirs or aquifers or directed to CO_2 utilization plants for being converted to valuable products. The schematic of the CCS chain is depicted in Fig. 1-3 [16]. There are two major approaches for capturing CO_2, including point source CO_2 capturing and direct air CO_2 capturing. Point-source capture refers to the process of capturing and redirecting CO_2 emissions from significant sources such as power plants and industrial facilities. This technology enables the capture of CO_2, preventing it from being released into the atmosphere. Additionally, there are methods available to address historical CO_2 emissions that are already present in the atmosphere. These methods include direct air capture and storage (DAC), which involves capturing CO_2 directly from the air, and bioenergy with capture and storage (BECCS), which combines bioenergy production with CO_2 capture and storage [17]. These approaches offer potential solutions for mitigating and reducing CO_2 levels in the atmosphere. Given that power production is a major contributor to CO_2 emissions, capturing CO_2 from electricity plants presents an attractive solution for reducing the CO_2 output associated with fossil fuel combustion. To achieve the net-zero emissions target, CO_2 capture technologies enable fossil-fueled power plants to continue operating while reducing their environmental impact, providing a bridge toward a cleaner and sustainable energy future [18].

Due to the potential and importance of CCS technologies in climate change and net zero emission scenarios, there has been a notable surge in the CCS facilities, which now encompasses

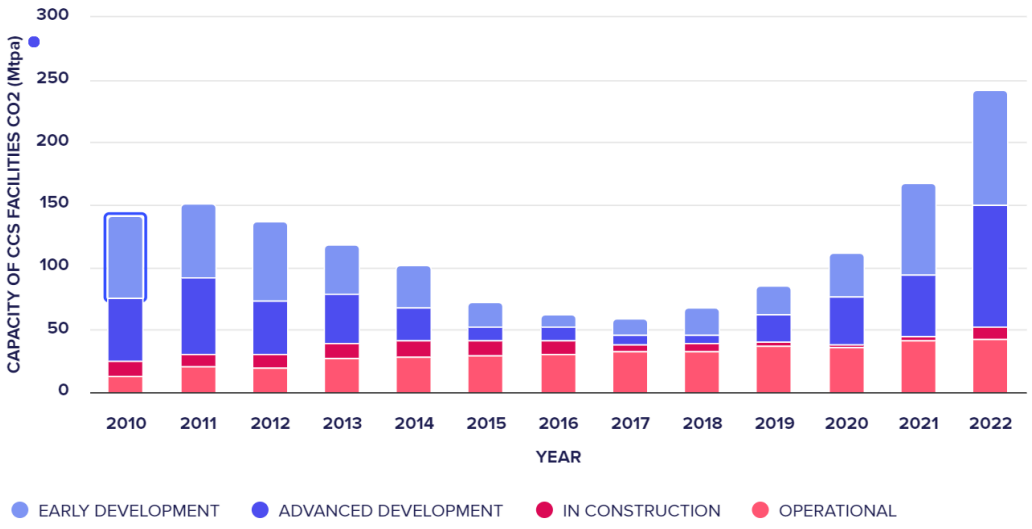

Fig. 1-4. Capacity of CCS facilities in the world at different stages from 2010 to 2022 [19]

a total of 196 projects worldwide. The trend of CCS facilities capacity in the world is presented in Fig. 1-4, which emphasizes the remarkable progress and momentum in recent years. However, there are only 30 operational commercial-scale CCS facilities in the world, with a total capture capacity of 42 million tonnes of CO_2 per year [19].

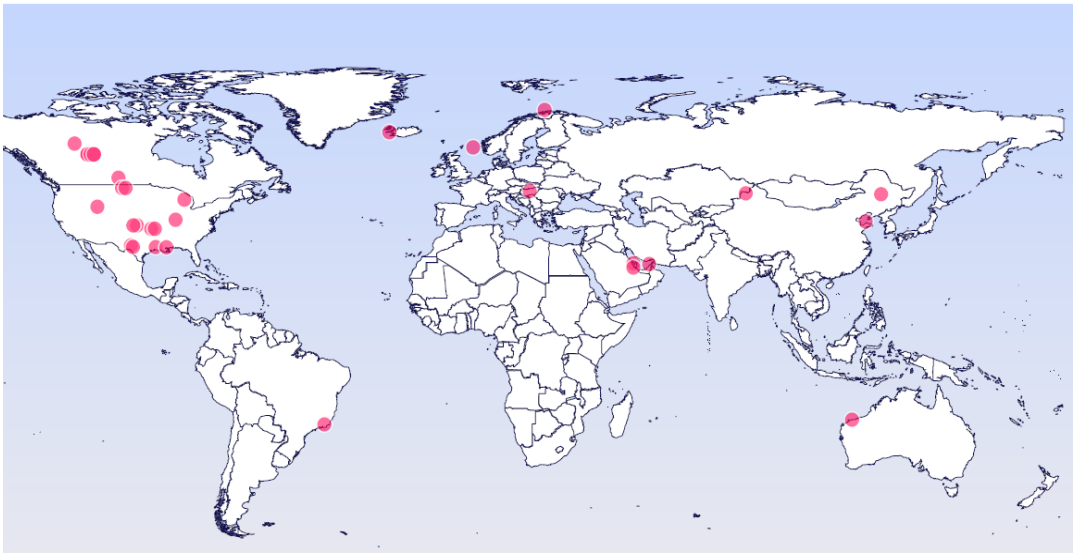

Fig. 1-5. World map indicting operational commercial CCS facilities [19]

Fig. 1-5 presents the distribution of these facilities worldwide, indicating that the U.S. is the leading country with 15 operation CCS facilities. The number of these facilities is expected to increase significantly in the near future due to potential advancement in the process and design as well as government investment and incentive programs [20].

In the context of achieving Net Zero Emissions (NZE) by 2050, it is estimated that the amount of CO_2 captured by CCS technology significantly increases from the current annual amount of 42 million tonnes to 7600 million tonnes by 2050, representing a remarkable increase of at least a hundred times the current levels [9]. As illustrated in Fig. 1-6, this amount is divided among different sources, with fossil fuel combustion contributing around 50% of the captured CO_2, industrial processes accounting for 20%, and the combination of bioenergy utilization with CO_2 capture and Direct Air Capture (DAC) methods making up approximately 30% [9].

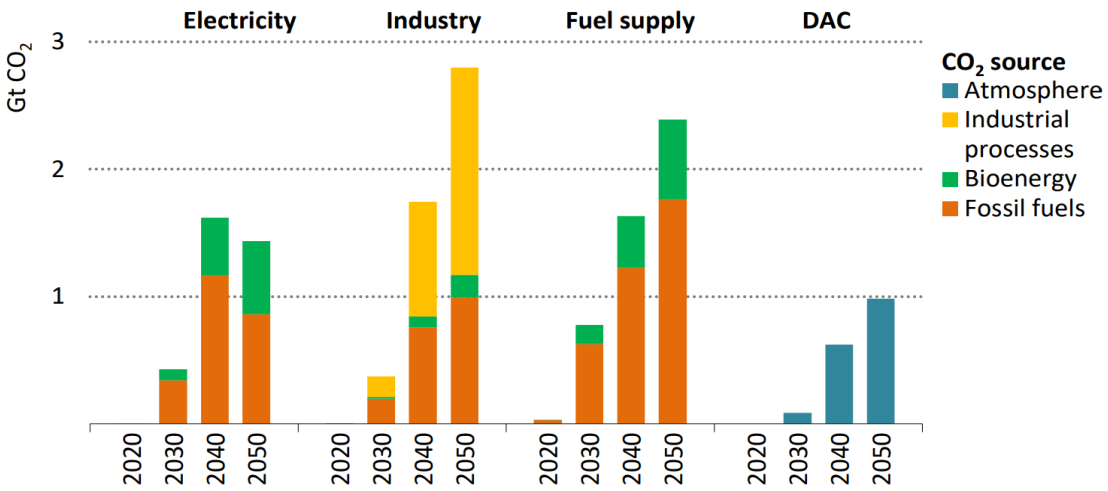

Fig. 1-6. CCS by sector and emissions source in the Net Zero Emission scenario outlined by IEA [9]

It is worth noting that the utilization of CCS with fossil fuels is expected to drive nearly 70% of the overall growth in CCS until 2030 within the NZE framework. However, various factors, including economic, political, and technical challenges, contribute to the uncertainty surrounding the future growth of CCS, which creates obstacles that hinder the widespread adoption and scaling up of CCS technologies.

To effectively combat climate change, it is crucial to transition towards cleaner energy sources and technologies such as renewable energy resources. Anticipated advancements in the global energy mix include a gradual transition towards renewable energy resources like solar and wind power. As of 2021, the share of renewables in global electricity generation has already reached 28.7%. [15,21]. However, despite the increasing installed capacity of renewables, the intermittency and non-dispatchability of these sources impose a significant obstacle in achieving a smooth integration with electricity grids [22]. Fossil fuel plants offer several advantages over emerging renewable sources, such as their ability to respond swiftly to short-term changes in peak power demand, provide backup during electricity production using sources like wind or solar, generate larger quantities of energy at a lower cost, and adapt to short and long-term shifts in energy requirements [23,24]. By considering the increasing demand for electricity, the continued presence of fossil-fueled power plants equipped with CCS, along with a high share of renewable energy in the electricity mix, is expected in the foreseeable future [25–27]. This approach ensures a reliable and stable electricity supply by leveraging the strengths of each energy source. While

intermittent renewables contribute to reducing carbon emissions, conventional thermal power plants provide a reliable baseload capacity that can be flexibly adjusted to meet fluctuating demand.

1.2 Motivations and challenges

Although CCS is widely acknowledged as a crucial technology for mitigating CO_2 emissions in the fossil-fueled power sector, the substantial costs involved and the significant energy requirements associated with its implementation are the primary obstacles to its widespread deployment [28,29]. One notable challenge is the increased energy requirements associated with CO_2 separation technologies, leading to reduced overall efficiency of the power plant and economic viability of the power plant. Additionally, the costs of implementing capture systems contribute to both the initial capital investment and the ongoing operating costs of power plants. The current CCS technologies can lead to a decrease in the net power output of the plant by approximately 25-40% and result in a substantial increase in power generation costs, potentially up to 70% [30–32]. Accordingly, balancing the potential environmental benefits with the associated energy and costs penalties is crucial in determining the practicality and viability of the wide implementation of carbon capture technologies into power plants.

Another challenge that limits the widespread deployment of CCS is the requirement for flexible design and operation of CCS integrated with fossil-fueled power plants. As the penetration of intermittent renewable energy sources continues to increase in the electric grid, conventional thermal power plants are faced with the challenge of frequently cycling their load and operating under low-load conditions [33]. The fluctuating output from renewable sources can lead to sudden surges or drops in power production, requiring thermal power plants to quickly adjust their operations to maintain grid stability [34]. This often involves ramping up or down the output of conventional power plants to compensate for the intermittent nature of renewable energy. Consequently, the downstream carbon capture plant, which is integrated with the power plant, needs to be responsive to these rapid changes imposed by the shifting load demands. To respond to the changing load demands, the carbon capture plant must have the flexibility and adaptability to adjust its capture and storage processes accordingly. It should be capable of handling varying flow rates and concentrations of carbon dioxide to ensure efficient carbon capture throughout different operating conditions. Additionally, due to the increasing share of renewable energy and

the potential integration of energy storage facilities, the thermal power plant may need to operate at a reduced load. Thus, the capability of carbon capture system for operating efficiently and flexibly during partial load conditions has become a challenge that need to be addressed.

1.3 Problem statement and research objectives

Among the available technologies for point source CO_2 capturing, the conventional and widely-implemented process is the absorption of CO_2 into amine solvents, such as monoethanolamine (MEA), which has proved to have notable advantages. Although extensive research studies have been undertaken to showcase the viability and potential of this technology, significant challenges are still remained for large-scale commercial implementation [35–41]. These challenges include the high thermal energy requirement to regenerate solvent along with high capital and operating cost, resulting in a substantial reduction in energy efficiency and an escalation in the cost of electricity. On the other hand, membrane technology is considered to be one of the promising and fast-developing alternatives for CO_2 capture purposes [42]. Membrane processes offer advantages such as selective separation, scalability, and flexibility, while conventional absorption processes are known for their high capture efficiency. Despite the fact the current membrane technologies face the same challenge of costs and energy requirements, the continuous advancements in membrane materials and innovative process designs hold the potential for membrane technology to become a key player in the development of sustainable power generation systems [43]. There are significant gaps in the field of CO_2 capture technologies to make them technically and commercially viable and appropriate for the large-scale decarbonization of fossil-fueled power plants. Accordingly, considering the research gaps in the field that have been discussed in the next chapter, seven research questions (RQ) have been proposed that addressing them makes significant contributions and generates new knowledge.

- **RQ1:** What are the current status, challenges, and progress of CO_2 capture technologies for integrating with fossil-fueled power plants?
- **RQ2:** How can the technical performance of membrane-based carbon capture technologies be improved to enhance their efficiency and effectiveness in capturing and storing carbon dioxide?

- **RQ3:** What are the key factors influencing the economic and energy performance of membrane-based carbon capture systems, and how can they be optimized to reduce costs and increase energy effectiveness?
- **RQ4:** How is the dynamic performance of membrane-based integrated with load-following power plants, and how can the flexibility of membrane-based carbon capture systems be enhanced to accommodate different industrial processes and varying carbon capture requirements?
- **RQ5:** What novel process design and integration can be developed to overcome the limitations of the current carbon capture systems? How can the integration of power plants with renewable energy sources and membrane-based CCS be optimized to create a hybrid system that combines efficient carbon capture with sustainable power generation?
- **RQ6:** What are the impacts of commercial-scale deployment of the proposed hybrid design on the capital cost, operational costs, equipment size, capture cost, and electricity cost of the system?
- **RQ7:** How is the performance of the proposed novel hybrid system in the case of off-design and partial load performance?

Overall, given the global importance of implementing CCS technology and its significant potential in reducing CO_2 emissions from fossil fuel power plants, this dissertation addresses key challenges mentioned in the research questions. Accordingly, the primary goal is to develop an innovative and practical solution for the optimal design, operation, and flexible integration of CCS with fossil-fueled power plants. To accomplish this objective, it is crucial to employ advanced approaches in the development and enhancement of carbon capture systems. These methods should focus on reducing the energy and cost implications of CO_2 capture, as well as improving the flexibility of CCS systems to accommodate both base-load and load-following operations of power plants. By implementing these measures, the efficiency and effectiveness of CCS technologies can be optimized, making them more economically viable and adaptable to different operational requirements of power plants. To achieve the main goal of this dissertation, five research objectives with their corresponding research questions and tasks have been proposed as follows:

- ***Objective 1:*** *Literature review in the CCS field* ***(RQ1)***

Approach: A comprehensive literature review is conducted to give insight into the progress and developments in CO_2 capture technologies as well as associated challenges and potential opportunities for flexible carbon capture technologies.

New knowledge: Overview of recent progress, developments, and challenges in CO_2 capture technologies design and integration.

- ***Objective 2:*** *Component and system-level simulations and techno-economic investigation of the membrane-based CCS* ***(RQ2)***

Approach: Despite the membrane-based CCS potentials for CO_2 capturing purposes, the process encounters several techno-economic challenges that need to be addressed to enhance the feasibility of this environmentally-friendly technology for extensive adoption. Accordingly, this dissertation addresses and provides insights into this objective by employing advanced technical models involving lumped parameter models for the balance of plants and a mechanistic membrane model. Furthermore, an economic model comprising different cost factors for the capital cost and operational cost of the system components is developed to investigate techno-economic performance and sensitivity analysis of several designs and operating parameters of the system.

New Knowledge: Understanding the technical performance and cost of membrane technologies in various designs and operations imposed by upstream power plants

- ***Objective 3:*** *Development of an economically viable design of multi-stage membrane-based CCS with a flexible operation for integration with power plant under load following operation* ***(RQ3 and RQ4)***

Approach: An efficient and flexible multi-stage membrane-based CCS process must be developed using a rigorous process optimization approach to address the challenge of the system. The optimal process design of membrane-based CCS is proposed, and the possible trade-offs between performance indicators of the membrane-based CCS are presented with the aim of reducing energy and cost penalties. Moreover, the transient behavior of the membrane-based process is further investigated at different disturbances and variations in the power plant operation imposed by the plant load-following behavior to address the required flexibility of the carbon capture system.

New knowledge: Optimal multi-stage membrane-based CCS process and possible trade-offs for energy and cost penalty - Flexible operation and transient behavior of membrane process for integration with power plant under load following operation.

- ***Objective 4.*** *Development of a novel solar-assisted hybrid membrane-amine carbon capture system for flexible and sustainable decarbonization of natural gas-fired combined cycle power plant* ***(RQ5)***

Approach: To address the technical and economic challenges associated with the conventional amine-based CCS process and its integration with the base-load power plant, a new hybrid CO_2 capture process is developed and investigated. The aim of this hybrid design is to improve the power plant operation and reduce the low-carbon electricity cost and the energy penalty associated with CO_2 capture. In this regard, the conventional amine-based CCS is hybridized with a multi-stage membrane process for selective CO_2 recirculation to improve the separation driving force and decrease both CCS equipment size and energy penalty. Furthermore, the solar energy heating system with thermal energy storage is integrated with the developed CCS to provide the required thermal energy and flexibility for the integrated system.

New knowledge: An Efficient and robust design of a CCS process by hybridization of membrane-amine process and solar heating field for flexible and sustainable decarbonization of natural gas-fired combined cycle (NGCC) power plant.

- **Objective 5.** *Investigation of part load performance and economic viability of the natural gas combined cycle power plant integrated with solar-assisted hybrid carbon capture system* ***(RQ6 and RQ7)***

Approach: The part load operation and economic analysis of the developed solar-assisted hybrid membrane-amine CCS for flexible and sustainable decarbonization of the NGCC power plant are investigated in detail. An advanced process modeling and simulation is performed by utilizing several software and custom models in off-design conditions, where the power plant turbine load decreases from 100% to 50%. Furthermore, an accurate economic model based on a well-known methodology is developed to calculate the levelized cost of electricity and CO_2 avoided cost. The economic performance of the system is evaluated, and a detailed comparison with other cases, as well as sensitivity analysis of parameters on the economic indicators, are provided.

New Knowledge: Insight into part load performance and economic viability of the natural gas combined cycle power plant integrated with the proposed design.

1.4 Dissertation structure

The current Ph.D. dissertation consists of an additional five chapters that correspond to the five research objectives mentioned earlier. Additionally, it includes a compilation of five journal papers that are associated with the conducted tasks in the dissertation to address research objectives two to five.

Chapter two, corresponding to the approach of the first objective, serves as the technical background on the CO_2 capture process, emphasizing the current development and progress in the field with a specific focus on its application in the power sector. It discusses the challenges associated with balancing power generation and the need for flexible CO_2 capture plants. Furthermore, it explores various aspects of integrating natural gas combined cycle power plants with the CO_2 capture process.

Chapters three to six of the dissertation align directly with approaches performed in the second to fifth research objectives. The analysis and results of these chapters have been published or submitted to prestigious peer-reviewed journals. The specific mapping of the chapters to the respective publications is as follows:

- **Chapter 3: Multi-stage Membrane-based Process for Power Plant Decarbonization**

Published paper: *Asadi, J., & Kazempoor, P. (2021). Techno-economic analysis of membrane-based processes for flexible CO_2 capturing from power plants. Energy Conversion and Management, 246, 114633*

- **Chapter 4: Optimal Design and Dynamic Behavior of Membrane-based CCS**

Published paper: *Asadi, J., & Kazempoor, P. (2022). Sustainability Enhancement of Fossil-Fueled Power Plants by Optimal Design and Operation of Membrane-Based CO_2 Capture Process. Atmosphere, 13(10), 1620.*

Published paper: *Asadi, J., & Kazempoor, P. (2022). Dynamic response and flexibility analyses of a membrane-based CO_2 separation module. International Journal of Greenhouse Gas Control, 116, 103634.*

- **Chapter 5: A Novel Solar-assisted Hybrid Design of CCS Process for Flexible Integration**

Under review paper: *Asadi, J., & Kazempoor, P. (2023). Advancing Power Plant Decarbonization with a Flexible Hybrid Carbon Capture System, Energy Conversion and Management*

- **Chapter 6: Off-design Operation and Economic Viability of the Integrated System**

Under review paper: *Asadi, J., & Kazempoor, P. (2023). Dynamic Performance and Economics of Solar-Assisted Hybrid Carbon Capture for Natural Gas Combined Cycle Power Plant, Applied Energy*

Fig. 1-7 presents the summary of the dissertation structure and the connection between research questions and new knowledge in each chapter. Each of these chapters concludes with a summary section that highlights the significant points and insights derived from the obtained results. Finally, in Chapter seven, all the pertinent findings are consolidated, and the main conclusions of the work and the direction of future research in the field are presented.

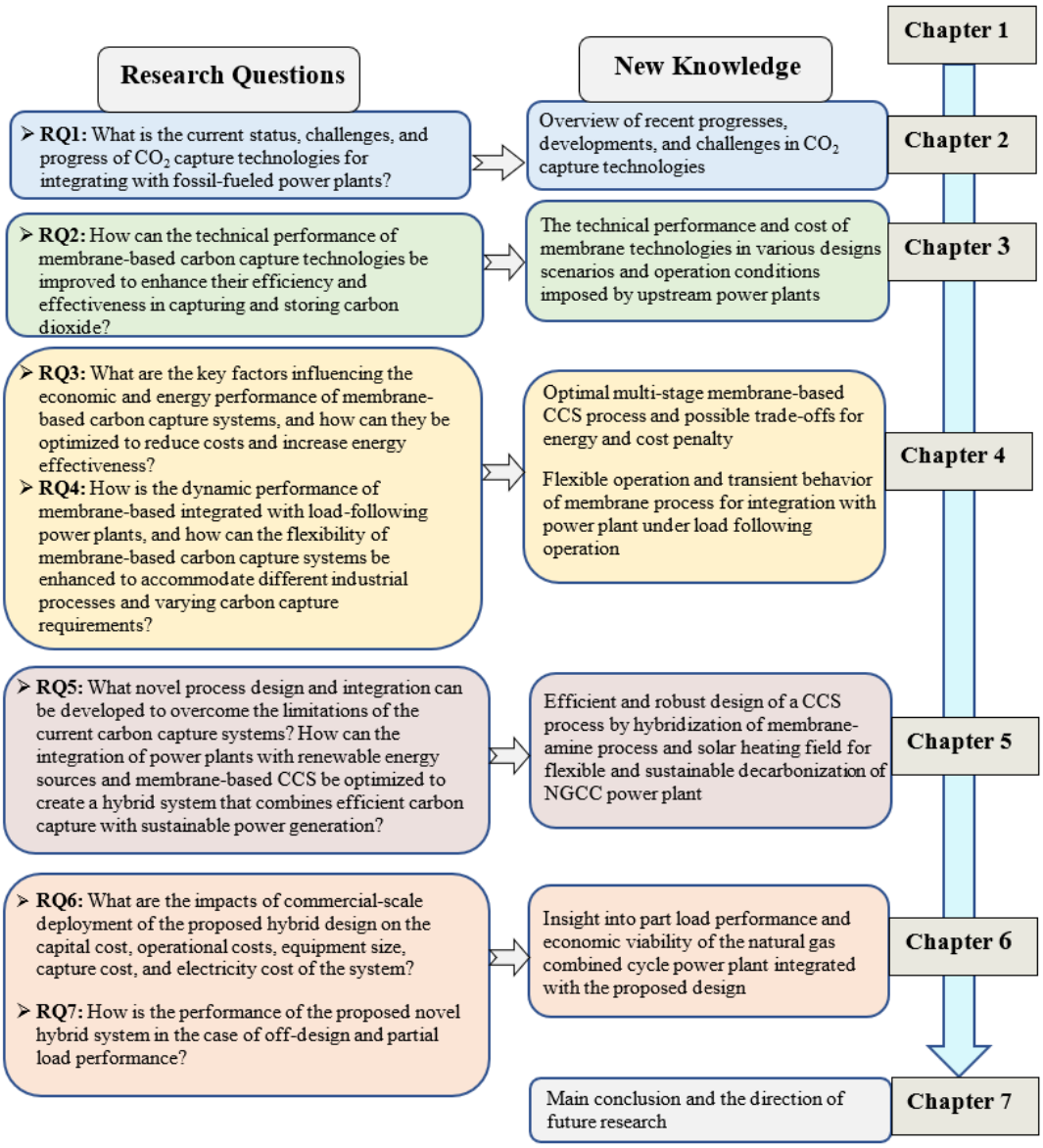

Fig. 1-7. Dissertation structure and chapters connections with research questions and new knowledge

Chapter 2. Background and Literature Review

- ? **Research Question: RQ1**-What is the current status, challenges, and progress of CO_2 capture technologies for integrating with fossil-fueled power plants?
- ➢ **Objective:** Performing literature review in the CCS field
- ✓ **New Knowledge:** Overview of recent progress, developments, and challenges in CO_2 capture technologies

The current chapter is organized as follows to provide a background and a detailed literature review regarding the primary goal and research objectives of this dissertation: In Section 2.1, common types of power plants that could be integrated with the CO_2 capture process are introduced and discussed. Section 2.2 is devoted to an overview of CO_2 capture and storage methods for point source capturing, including post-combustion, pre-combustion, and oxy-fuel combustion, is provided along with a discussion about the pros and cons of each method. Section 2.3 comprises the potential gas separation technologies for CO_2 capture systems that can effectively separate CO_2 from other gas components, with a specific focus on absorption and membrane CO_2 separation technologies. Section 2.4 includes a comprehensive review of various studies centered around the modeling, simulation, and optimization of the membrane and absorption processes. Furthermore, Section 2.5 delves into the flexible operation and design of CCS technologies. Moreover, Section 2.6 reviews various strategies for the hybridization of CO_2 separation methods and integration of CCS with renewable resources and natural gas combined cycle power plants. Lastly, Section 2.7 provide conclusions and remarks on this chapter.

2.1 Fossil-fueled power plants

Fossil-fueled power plants are electricity-generating facilities that rely on the combustion of fossil fuels, such as coal, oil, and natural gas, to produce energy. Most thermal power stations worldwide use fossil fuel, outnumbering nuclear, geothermal, biomass, or concentrated solar power plants, to meet the growing demand for electricity worldwide [44]. The most common fossil-fueled power plants include pulverized coal-fired power plants (PC), natural gas-fired combined cycles (NGCC), and integrated gasification combined cycles (IGCC).

Fig. 2-1 displays simple block diagrams illustrating the configuration of pulverized coal-fired power plants. Initially, coal and air are introduced into the boiler, where they undergo combustion to produce steam. This steam is then utilized to generate electricity. Subsequently, the flue gas generated in the boiler is directed towards a flue gas desulfurization (FGD) section, where the removal of sulfur compounds takes place [45]. The resultant flue gas, which is now clean and saturated, is released into the atmosphere. A typical 550 MWe pulverized supercritical coal-fired power plant has an efficiency of 39.3% and produces 821 kg/s flue gas with a CO_2 concentration of 13.5 mol.% [30]. The average CO_2 intensity of the coal power plant is the highest among other types of power plants, equal to 961 kgCO_2/MWh [46]. Currently, approximately 8,500 operational coal power plants spread across the globe possess a capacity exceeding 2,000 gigawatts, contributing to over one-third of the total global electricity generation [47]. Remarkably, coal power plants stand out as the largest individual source of greenhouse gas emissions worldwide, accounting for one-fifth of the global total. This highlights their significant role in the production of carbon dioxide and other greenhouse gases that contribute to climate change. Accordingly, the properties of flue gas from this type of power plant has been considered in this dissertation for integrating with carbon capture and storage process.

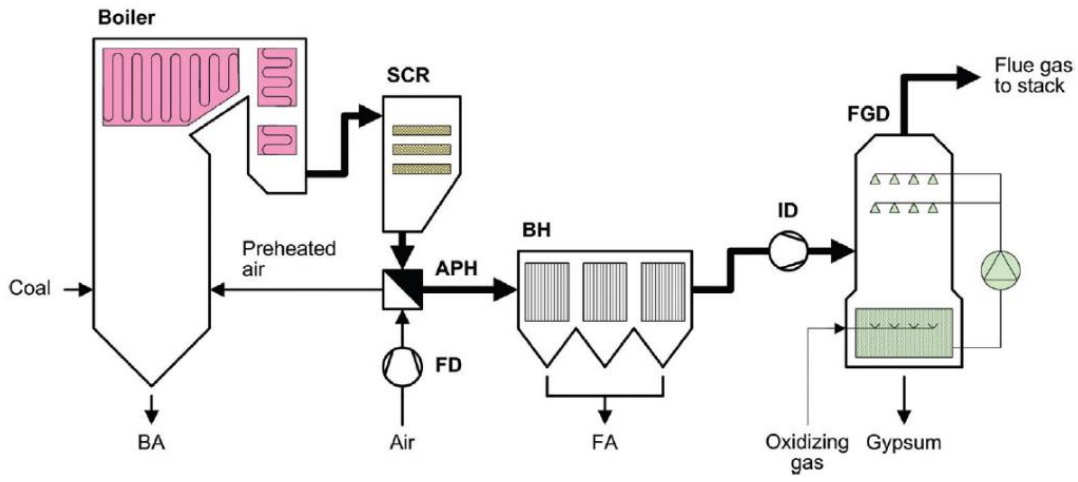

Fig. 2-1. Schematic of typical pulverized coal fired power plant [45]

The NGCC power plant mainly consists of three sub-processes, combined cycle gas turbine, heat recovery and steam generation (HRSG) system, and steam turbines, as presented in Fig. 2-2. The gas turbine compresses air, which is then heated through the combustion of injected fuel. The resulting energy is harnessed as the hot product gases expand through an expander, driving the rotor that directly powers both the compressor and the generator. The generated exhaust gases with temperatures ranging from 550 to 650°C are then used in a heat recovery system to produce steam at different pressures for expansion through a steam turbine to generate additional electricity [48]. NGCC power plants demonstrate a higher efficiency of 50%. A typical NGCC plant with a capacity of 555 MWe produces 897.4 kg/s flue gas with a CO_2 concentration of 4 mol.% [49]. Accordingly, the NGCC plants, compared with coal-fired power plants, are more efficient with lower CO_2 emissions (425 $kgCO_2$/MWh) [50]. In 2021, NGCC plants accounted for 32% of the total electricity generation in the U.S., while coal-fired power generation held the second position with a share of 22% [51]. In the present dissertation, the NGCC power plant, as one of the widely used sources of power, is considered for modification and integration with CCS.

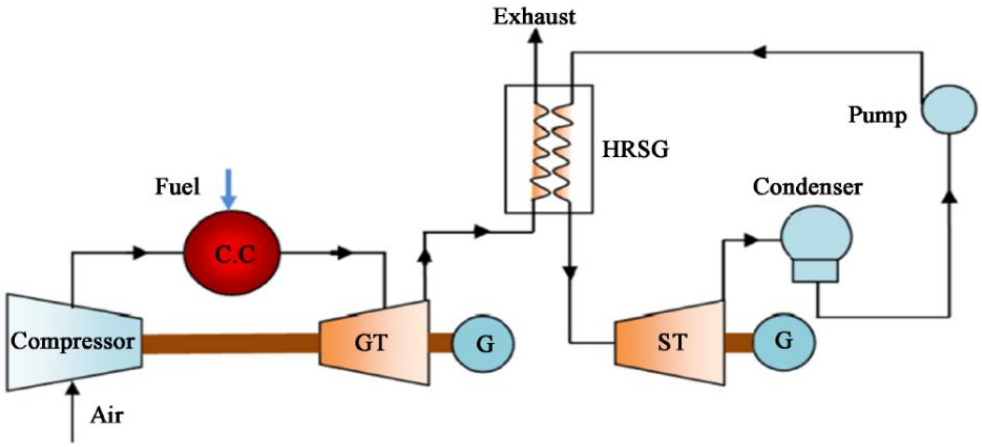

Fig. 2-2. Schematic of typical NGCC power plant [48]

Fig. 2-3 presents the schematic of an Integrated Gasification Combined Cycle (IGCC) power plant, which is a type of advanced power generation facility that converts coal or other solid fuels into synthesis gas (syngas) through a process called gasification [52]. The syngas is then used to generate electricity through a combined cycle system, similar to an NGCC plant. IGCC plants are designed to achieve higher efficiency and lower emissions than conventional coal-fired power plants by utilizing gasification technology and advanced pollution control systems. A typical IGCC

plant with 640 MWe capacity produces 1100 kg/s flue gas with a CO_2 concentration of 7-14 mole% [49]. This type of fossil-fueled power plant demonstrates a net plant efficiency of 43% with a CO_2 intensity of 602 kgCO_2/MW. Although the performance of IGCC plants in terms of both efficiency and emission has been improved compared to the traditional coal-fired power plants, 20-47% higher capital costs for IGCC plants, along with many technical challenges and operation complexity, are the main barrier to replacing the conventional coal power plants [53].

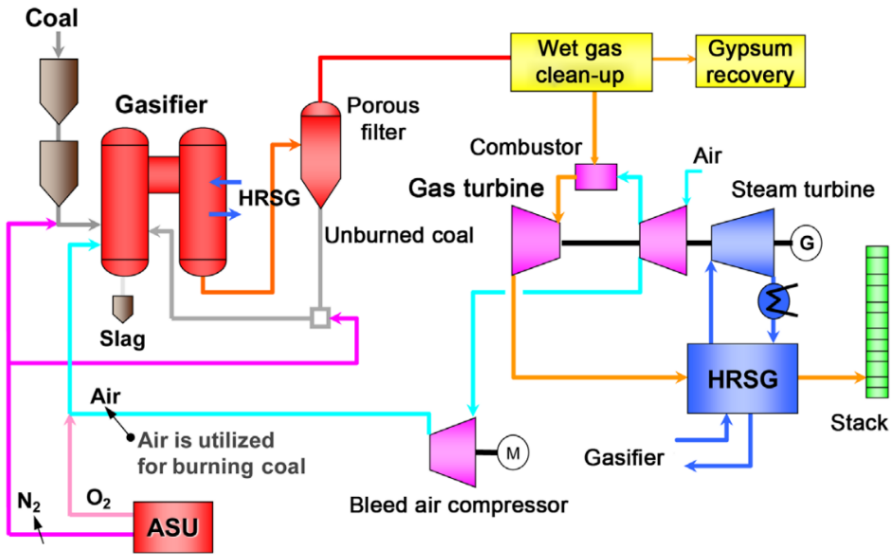

Fig. 2-3. Schematic of IGCC power plant [52]

2.2 CO_2 capture and storage methods for point source capturing

CCS technologies are comprised of three distinct components. The carbon capture process, constituting the first part, is the most expensive component, accounting for approximately 50% of the total costs [54]. When CO_2 compression is included, the costs can escalate and reach up to 90% of the total expenses [49]. The second part of CCS technologies involves the transportation of CO_2, acting as a crucial link between the capture stage and the third part, which focuses on storage. While the transportation and storage aspects may not be as cost-intensive as carbon capture, they present significant challenges in terms of planning and implementation [55]. Carbon dioxide can be captured from different sources according to its partial pressure, operating conditions, and composition of the gas mixture. In thermal power generation, including fossil fuels, biomass, and

other waste-to-energy plants, the capturing approaches can be broadly categorized into three main processes: pre-combustion, oxy-fuel combustion, and post-combustion [56].

2.2.1 Pre-combustion CO_2 capturing

In the pre-combustion process, the fuel undergoes oxidation through a gasification process, and CO_2 is captured before the fuel is burned in a combustor. As presented in Fig. 2-4, this process involves reforming or converting the fossil fuel into syngas, which is a mixture containing hydrogen (H2), carbon dioxide, and carbon monoxide (CO) [57]. The CO in the syngas undergoes a shift reaction, where it reacts with steam to produce more hydrogen and carbon dioxide. The carbon dioxide is then separated from the gas mixture, typically through a physical or chemical absorption process [58]. As a result, a hydrogen-rich stream is obtained, which can be utilized in various applications such as boilers, furnaces, gas turbines, engines, and fuel cells [59]. The pre-combustion capture method benefits from higher concentrations and pressures of CO_2 compared to other capture processes, enabling low energy penalty due to CO_2 capturing [54]. However, this process has a complex operation since the capture plant is in the middle of design, and the power plant needs significant modification [60]. Also, this method is limited to the gasification-based power plant; integrated coal gasification combined cycle (IGCC) plant serves as an example of this technology [61]. It is important to note that the fuel conversion process in pre-combustion capture is costly and is typically more suitable for new plant projects [62].

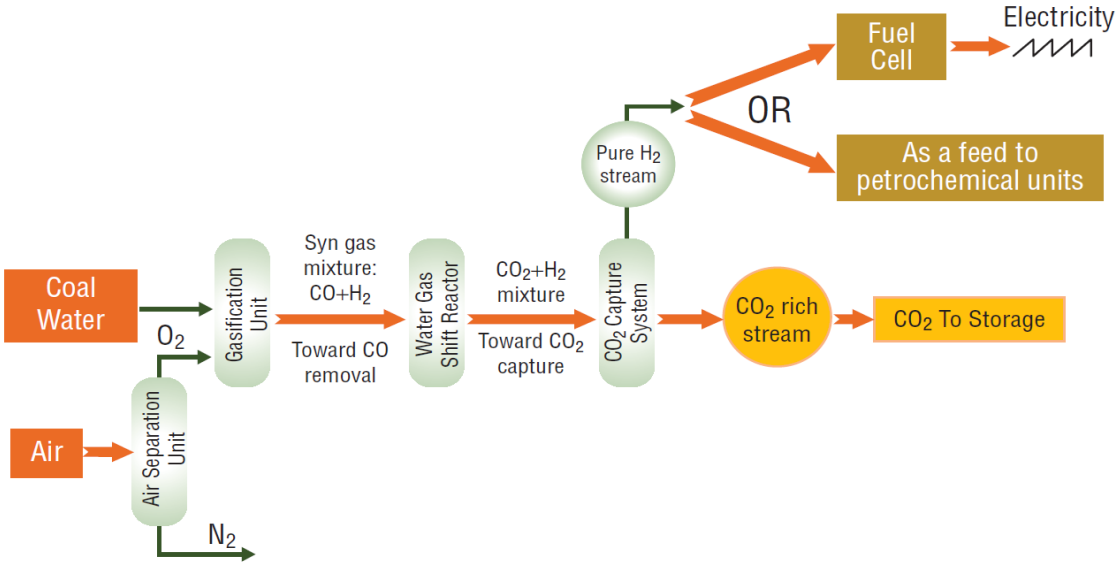

Fig. 2-4. Schematic of pre-combustion CCS [4]

2.2.2 Post-combustion CO_2 capturing

Post-combustion technology is presently the most common method for capturing CO_2. As depicted in Fig. 2-5, CO_2 is removed from the exhaust flue gases of power plants in the post-combustion process, which typically exits at atmospheric pressure. One of the primary advantages of post-combustion capture is its ease of integration with existing power plants [63]. However, a significant challenge in this process is that the concentration of CO_2 in these flue gases is generally very low (10-15% for coal-based power plants and 4 mole% for NGCC) [64]. Therefore, capturing CO_2 from post-combustion flue gases requires efficient separation technologies to handle low concentration levels and large flowrate [65]. Hence, identifying a cost-effective approach for capturing CO_2 from flue gas is crucial. Additionally, the presence of various contaminants such as SOx, NOx, and fly ash in the flue gas further increases the complexity and cost of the separation process using this technology [66]. Due to its simple integration with power plants, post-combustion capture technology requires a lower auxiliary system to ensure smooth operation compared to the pre-combustion method [67]. Consequently, the capital cost associated with implementing and maintaining this system tends to be lower than the pre-combustion capture systems. Also, previous studies showed that when utilizing natural gas as fuel, the pre-combustion carbon capture process results in a 14% decrease in efficiency compared to the reference power plant [68,69]. On the other hand, the post-combustion carbon capture process shows a relatively lower efficiency drop of 8% compared to the reference power plant when natural gas is used as fuel [69]. These efficiency drops reflect the energy requirements and process complexities

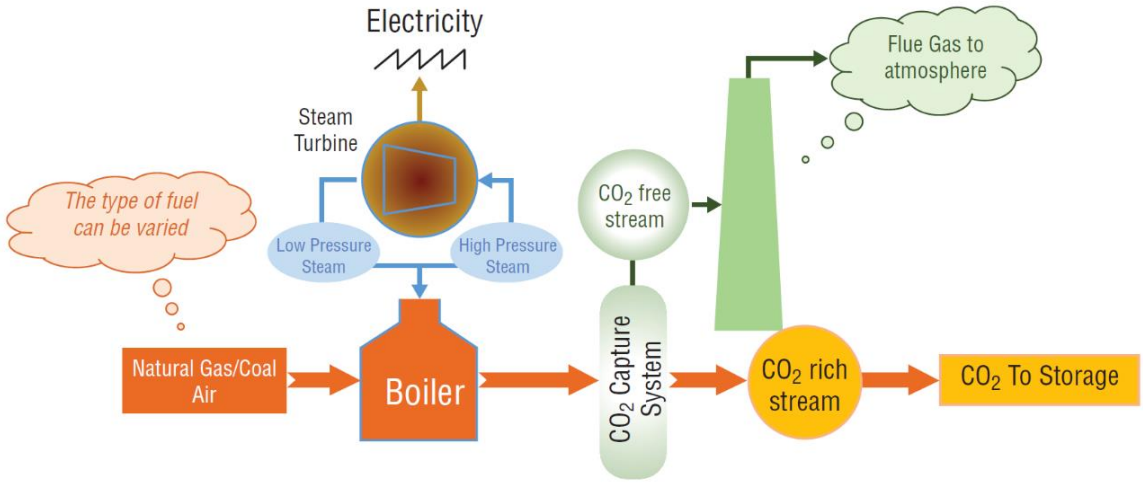

Fig. 2-5. Schematic of Post-combustion CCS [4]

associated with capturing and separating carbon dioxide from the flue gases generated during combustion. It is essential to consider these efficiency losses when evaluating the feasibility and cost-effectiveness of implementing carbon capture technologies in power plants [70].

2.2.3 Oxy-fuel combustion capture system

Oxy-combustion involves burning fuel in an oxygen-enriched environment, resulting in the primary emissions of carbon dioxide and water vapor while minimizing the presence of nitrogen [71]. The general scheme for the process using the oxy-combustion method is presented in Fig. 2-6. The use of pure oxygen in fuel combustion, instead of air, leads to the absence of nitrogen in the flue gas and an increased concentration of CO_2. Oxy-combustion technology is primarily applied to solid fuel-fired boilers, such as pulverized coal boilers and circulating fluidized bed boilers [72]. The advantages of oxy-combustion include reduced nitrogen oxide (NOx) emissions, smaller boiler dimensions, a simplified method for capturing CO_2 compared to other technologies, the possibility of retrofitting existing technologies, and a lower mass flow rate of exhaust gases (approximately 75% less compared to combustion in the air)[73]. However, oxy-combustion also has its drawbacks, such as the high energy requirement for the separation of oxygen from the air, which typically has a purity level of 95-99%, the need for high-temperature-resistant materials, and high initial capital costs [74].

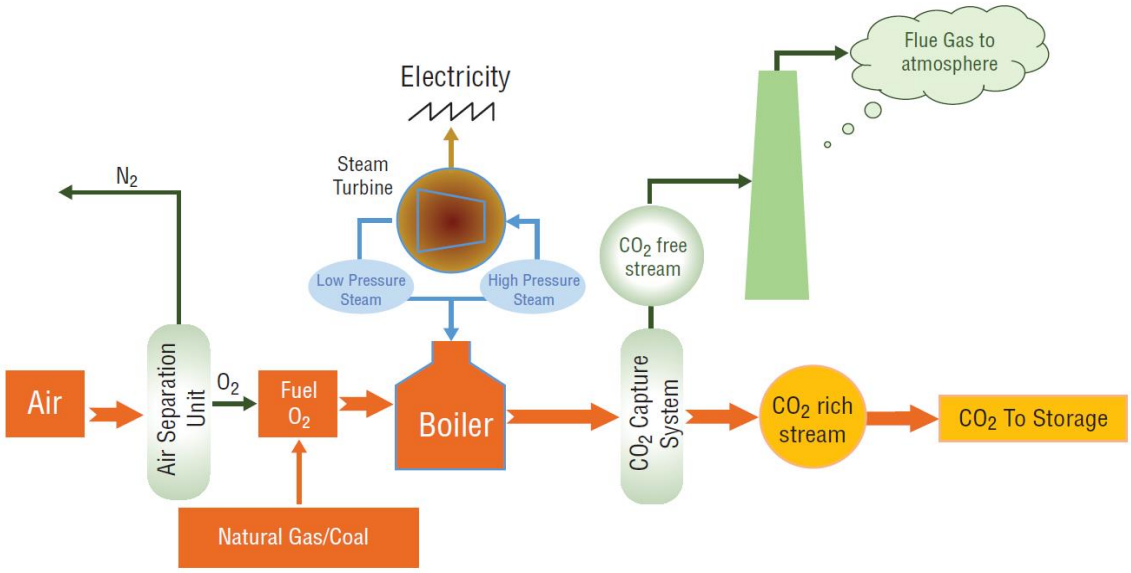

Fig. 2-6. Schematic of oxy-fuel combustion capture process [4]

2.2.4 Comparison of CO_2 capture technologies

Table 2-1 shows the limitations and advantages of each capturing method based on the available literature. It can be concluded that the post-combustion CCS has great potential to be integrated into both existing and new power plants, although there are some technical challenges that need to be addressed. Addressing these technical challenges to pave the way for the commercialization and large-scale application of post-combustion CO_2 capture technology is one of the aims of this Ph.D. dissertation.

Table 2-1. Advantages and limitations of CO_2 capturing methods

CO_2 Capture method	Advantages	Limitations and challenges	Related References
Pre-combustion	• Lower energy requirement for CO_2 separation and compression • The feed gas to the CCS unit has a high pressure, which improves the CCS performance • The presence of CO_2 at much higher concentrations in syngas makes CO_2 capture less expensive	• It can only be applied in gasification-based power plants like IGCC. • It cannot be retrofitted to the existing power plant as this method needs lots of change in the process. • It requires a complicated chemical plant in front of the turbine, which can cause extra shut-down of the plant.	[62], [57], [75], [59], [76], [58]
Oxy-combustion	• high concentration of CO_2 for easy separation • As a result of decreased flue gas volume, the cost of carbon capture in oxyfuel combustion is low. • Massive reduction in NOx emissions	• It cannot be retrofitted to the existing power plant as this method needs lots of change in the process. • High cost and energy requirement of air separation and flue gas recirculation • Material of construction to withstand high temperatures is needed.	[74], [77], [78], [79], [73]
Post-combustion	• It leads to a lower total electricity cost compared to others which makes this method favorable for power plants owner. • It can be easily retrofitted to both existing and new power plants • It can be used for different types of power plants, coal-fired, IGCC and NGCC • It will not affect the operation and reliability of the power plant since the CO_2 capturing is after the power supply	• There is a technical challenge due to the low thermodynamic driving force for CO_2 capture • A large amount of energy is required for CO_2 capturing and separation • The presence of impurities, such as SOx and NOx in the flue gas, needs to be separated before CCS	[64], [80], [81], [82], [83]

2.2.5 CO_2 transportation and storage

CO_2 transportation is the intermediary step in the CCS supply chain, connecting the capture site to the storage location. Various transportation methods can be utilized, including pipelines, rail, road tankers, and ships, depending on the specific CO_2 capture and storage scenarios [84].

Pipelines are well-suited for transporting CO_2 over long distances and at large scales, while road tankers are more appropriate for short distances and smaller capacities.

CO_2 storage is a crucial process that involves safely and securely storing the captured and transported CO_2 in different types of storage sites [56]. There are several potential options for CO_2 storage, including:

1. Geological storage [85]: This involves injecting CO_2 into deep geological formations, such as saline aquifers (porous rock formations filled with saline water) or depleted oil and gas reservoirs that are no longer productive. These formations act as natural traps, securely storing the CO_2 underground.
2. Enhanced Oil and Gas Recovery (EOR/EGR) [86]: In this method, CO_2 is injected into depleted oil and natural gas reservoirs to enhance the recovery of remaining resources. The injected CO_2 not only aids in the extraction process but also remains trapped within the reservoir, effectively storing the CO_2 underground.
3. Submarine sediment Layers [87]: Deep underwater, CO_2 can be injected into suitable sediment layers beneath the ocean floor, where it can be stored safely over long periods.

These various storage options offer different advantages and considerations, and the choice of storage site depends on factors such as geological characteristics, proximity to CO_2 sources, and local regulations [88]. Implementing a combination of these storage methods can contribute to effective CO_2 management to mitigate climate change.

After capturing and separating CO_2, compression will occur at different stages in the CCS process. It can occur after the initial capture process, preparing the CO_2 for transportation via pipelines, ships, or other means. Additionally, compression may be required before injecting the CO_2 into storage sites (100-150 bar), ensuring it reaches the appropriate pressure for long-term storage [89].

2.3 CO_2 separation technologies

Various gas separation technologies can be utilized for separating CO_2 from other components of flue gas in the post-combustion phase. The primary methods include physical and chemical absorption, absorption, cryogenic separation, and membrane processes. Fig. 2-7 provides

a schematic representation of the potential technologies and methods for CO_2 separation, which are under investigation in both academia and industry. Except for cryogenic separation, all other methods mentioned in the figure require material carriers. Also, selecting the appropriate technology for CO_2 capture depends on the specific characteristics of the flue gas stream, which are primarily influenced by the power plant technology used. Chemical absorption is the most implemented technology for CCS, while membrane technology is the most potential and promising one [90]. A brief description of these technologies with a specific focus on chemical absorption and membrane technologies is presented below.

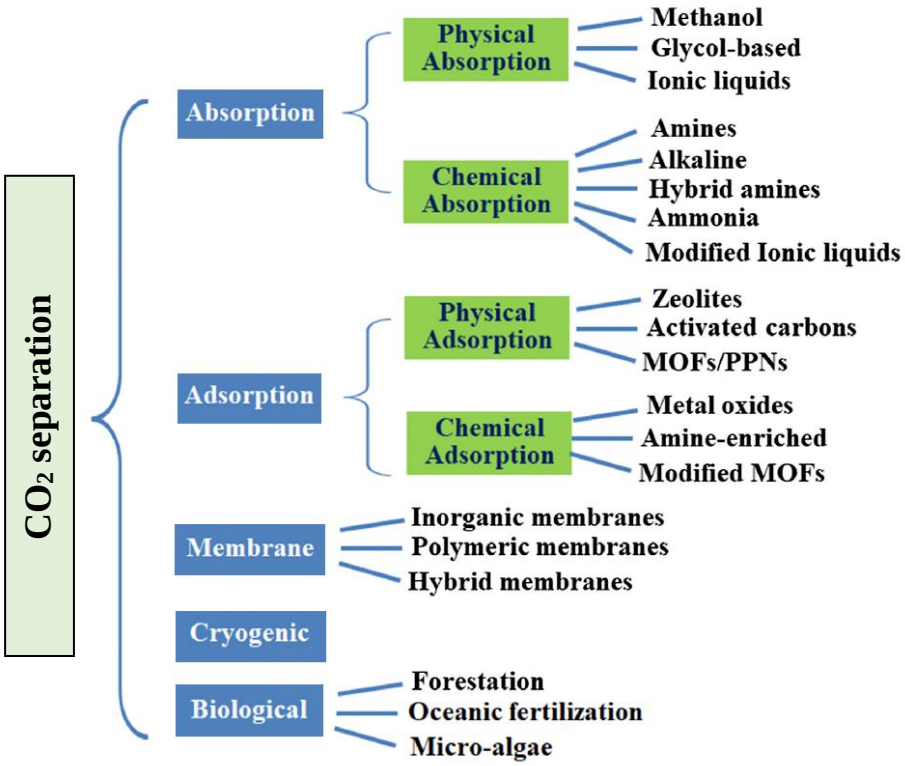

Fig. 2-7.Various CO_2 separation technologies for post-combustion CO_2 capturing

2.3.1 CO_2 absorption processes

Among the mentioned methods for capturing CO_2, the most well-established and commercially accessible technology is liquid absorption, particularly in the petroleum and chemical industries [75]. Absorption of CO_2 using the solvent occurs either with physical or chemical absorption. In this process, a gas stream reacts with a liquid to degrade components. If

remarkable chemical reactions are not implemented between liquid and gas, the interaction between absorbent and gas is generally defined as physical absorption. At the same time, if it takes place as reversible or irreversible, this interaction is described as chemical absorption [58].

- **Physical absorption**

Physical absorption involves utilizing organic or inorganic solvents to physically capture CO_2 without undergoing chemical reactions with the solvent. This method is primarily employed for gas streams containing concentrated CO_2 at high pressures. Commercially, it is utilized to eliminate acid gases, such as CO_2 and H2S, from natural gas, as well as to extract CO_2 from synthesis gas in ammonia, hydrogen, and methanol production processes [11]. Physical absorption occurs according to Henry's Law under operating conditions, where temperature and pressure affect efficient CO_2 removal [91]. In physical absorption, since the reaction of CO_2 and absorbent is low, the energy needed for regeneration is lower than the chemical absorption of CO_2. Physical solvents are also associated with certain drawbacks, including low CO_2-H2 selectivity, high solvent viscosity, limited thermal stability, flammability, corrosiveness, and toxicity [22]. Some of the commercial absorption processes of CO_2 physically can be listed as the Selexol process using dimethyl ether or propylene glycol as an absorbent, the Fluor process using propylene carbonate as an absorbent, the Rectisol process using methanol as an absorbent, and the Purisol process using N-methyl pyrrolidone as an absorbent [92].

- **Chemical absorption**

Chemical absorption processes are currently favored for post-combustion CO_2 capture due to the relatively low partial pressure of CO_2 in exhaust gases. This method is suitable for removing CO_2 present in low concentrations (low partial pressure). However, this technology faces challenges in power plant CO_2 capture, mainly related to the high energy requirements for solvent regeneration and degradation. Chemical solvents such as amine solutions, aqueous ammonia, and carbonates are utilized to remove CO_2 from the gas stream through chemical reactions that occur in the absorption column. An ideal chemical solvent for this purpose should possess the following characteristics:

- Minimized energy/cost requirements for regenerating the solvent.
- The enhanced absorption rate promotes the efficient capture of CO_2.

- Increased reactivity in capturing CO_2.
- Affordable solvent cost.
- Improved stability, with reduced degradation and lower corrosive properties.
- Reduced environmental impact.

Alkanolamines like Monoethanolamine (MEA) in aqueous solution is the commonly employed solvents and have become the standard amine for CO_2 capture in power plants due to their effective CO_2 transfer rates, relatively affordable cost, and biodegradability [93]. Fig. 2-8 illustrates a schematic diagram of the chemical absorption process, which occurs in two stages. In the first stage, the flue gas reacts with the solvent in the absorber to capture CO_2. Subsequently, the CO_2-rich solution is transported to the stripper, where CO_2 is regenerated at high temperatures. The solution without CO_2 (lean-loading solution) is then returned to the absorber column. The stripper produces a high-purity carbon dioxide stream, which can be compressed, stored, or utilized. The absorber and stripper model incorporates multiple equilibrium and kinetic reactions.

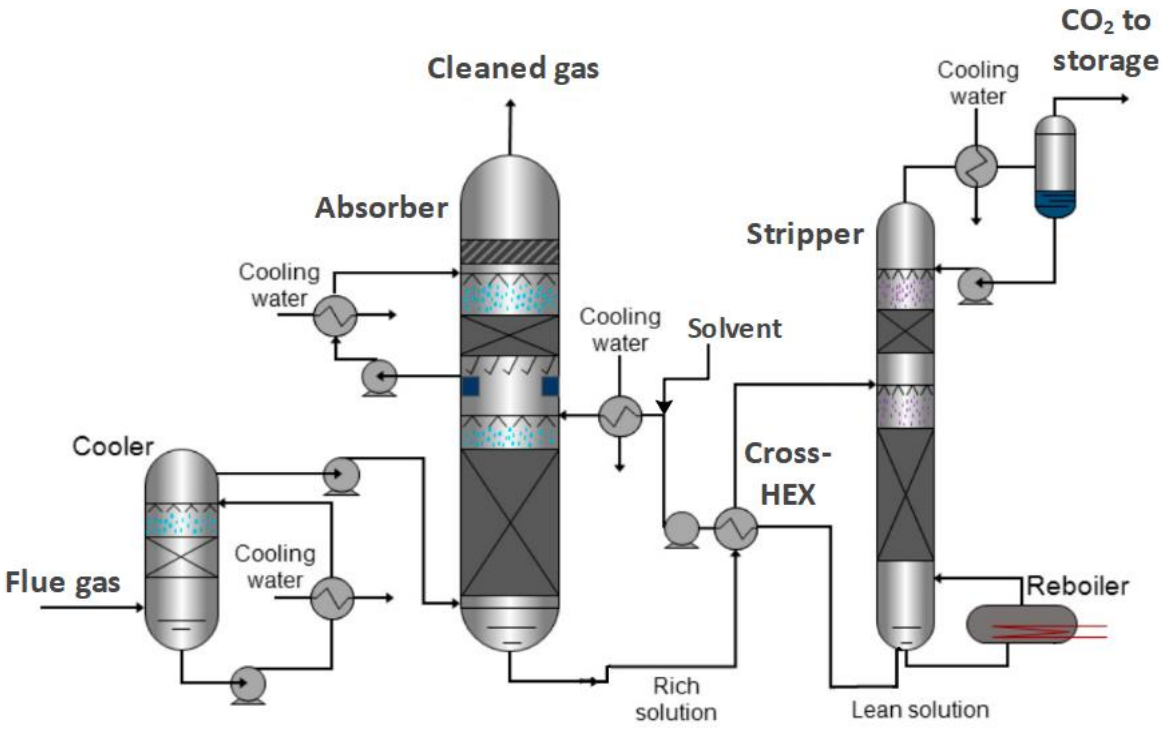

Fig. 2-8. Schematic of chemical absorption CO_2 separation method

Chemical absorption has long been utilized in the chemical industry, with 30% MEA and MDEA solutions being commonly used due to their high process efficiency and carbon dioxide purity [94].

However, the chemical absorption method is energy-intensive as it requires a significant amount of heat for the stripper. It is estimated that approximately 30-40% of the heat supplied to the steam in the boiler should be directed to the CCS installation, depending on the absorber used, in the case of a steam unit fired with hard coal [95]. In the process of CO_2 capture, besides MEA with the chemical formula $C_2H_7NO_2$, other primary amines such as diglycolamine (DGA) with the formula $C_4H_{11}NO_2$, secondary amines include 2,2'-iminodiethanol (DEA) with the formula $C_4H_{11}NO_2$, diisopropanolamine (DIPA) with the formula $C_6H_{15}NO_2$ have been utilized as the solvent [96]. Also, tertiary amines such as N-methyl-2,2-iminodiethanol (MDEA) with the formula $CH_3N(C_2H_4OH)_2$ are also utilized for removing sour gases such as H2S and CO_2 in gas treatment processes [97]. The reaction between CO_2 and amines is reversible, as the weak bond formed is easily broken when the liquid is heated. When CO_2 reacts with MEA, it forms a carbamate and bicarbonate solution while releasing 83.6 kJ/mol, as shown in equation (1) [98]. By heating the MEA solution, the MEA carbamate and bicarbonate decompose, regenerating the amine and releasing CO_2.

$$C_2H_4OHNH_2 + H_2O + CO_2 \leftrightarrow C_2H_2OHNH_3^+ + HCO_3^-$$

In addition to the conventional solvents, there have been developments in other solvents for CO_2 capture. Specifically, steric hindrance amines, such as 2-amino-2-methyl-1-propanol (AMP), and cyclic diamine, such as piperazine (PZ), have been commercially used for CO_2 capture [99]. AMP exhibits exceptional absorption and desorption characteristics, including lower energy consumption for desorption, higher degradation resistance, and a higher loading capacity of 1 mol CO_2/mol amine [100]. PZ is commonly used as an activator in other amine systems for CO_2 capture due to its rapid reaction rate with CO_2, which improves mass transfer rates and kinetics [101]. However, PZ's solubility in water is very low, requiring CO_2 capture with high PZ content solutions to be conducted at high temperatures [102]. Furthermore, Solvent blends have shown the potential to enhance absorption properties by combining different types of solvents since primary and secondary amines exhibit high absorption rates, while tertiary amines have a higher capacity. For example, blending MEA with a small amount of PZ can improve the absorption rate, as PZ is 50 times faster than MEA [99]. Another option is using a solution of AMP promoted with PZ,

which has been suggested as a good alternative to MEA [93]. Furthermore, ionic liquids have emerged as novel alternatives to amines. These low melting point salts consist of a large organic cation and an arbitrary anion, allowing for physical or chemical absorption of CO_2 depending on the pressure [103]. New-generation solvents have been proposed to reduce energy consumption, including water-free solvents and biphasic solvents. Since the presence of water in a solvent increases the energy demand for the regeneration process, novel water-free solvents such as non-aqueous organic amine blends (methanol, ethylene glycol), aminosilicones, or amines with a superbase have been under investigation [104]. Each of these solvents has some advantages and disadvantages for CO_2 separation application, as summarized in Table 2-2. Overall, fundamental research and pilot plant studies are necessary to understand further the behavior of new solvents for absorption technology to facilitate the application of post-combustion CO_2 capture.

Table 2-2. Pros and cons of various solvents for chemical absorption CO_2 capturing process [94,96,105,106]

Solvent type	Advantage	Disadvantage
MEA	• strong reactivity with CO_2 • Widely available and cost-effective • Rapid absorption rate	• Elevated vapor pressure • Strong corrosive properties • High energy requirement for regeneration
MDEA	• Minimal corrosive properties • Highly resistant to degradation • Selective to H2S absorption	• Slow reaction rate with CO_2
DEA	• Low corrosivity and minimal foaming • Reduced energy requirements	• Generation of corrosive acids • Incapable of handling low-pressure gases
DIPA	• Non-corrosive • Low vapor requirements for recovery	• Poor CO_2 absorption capability
PZ	• Demonstrates high absorption capacity, twice that of MEA • Formation of carbamate during CO_2 reaction	• Limited concentration
AMP	• Efficient absorption and high CO_2 loading • Lower corrosiveness compared to other solvents	• Inferior amine-CO_2 mass transfer compared to MEA
Ionic liquid	• Exhibits low vapor pressure • Eco-friendly solvent • Reduced energy demand for recovery	• Higher cost compared to amine solvents • Reduced CO_2 absorption capacity compared to MEA • Hindered mass transfer due to high viscosity

Moreover, Extensive research studies have been undertaken to showcase the viability and potential chemical absorption process for large-scale commercial implementation [35–41]. However, a significant challenge lies in the high thermal energy consumption in the stripper column to regenerate solvent, resulting in a substantial reduction in energy efficiency and a subsequent escalation in the cost of electricity. In response, extensive efforts have been dedicated

to developing more reliable and cost-effective designs for CO_2 separation from other flue gas components. Over the past decade, besides research on improving solvents properties and developing efficient solvents, further process improvement approaches such as thermal integration [107,108], novel and hybrid process design, and process optimization [95,109,110] are implemented to reduce costs and enhance the effectiveness of absorption-based CO_2 capture process. These studies are reviewed and discussed in the next sections.

2.3.2 Membrane-based CO_2 separation

- **History of membrane technology**

Over the past few decades, membrane-based gas separations have gained significant industrial adoption due to their various advantages, including reduced environmental impact and lower capital and operating costs compared to conventional separation processes [111]. The concept of membrane-based gas separation was initially proposed by Graham in 1866 [112]. The first commercialized membrane gas separation process was in 1979, which sparked further interest and led to the development of different gas separation processes that could compete with existing technologies [113]. Currently, membrane gas separation is widely used in industrial applications worldwide, including air separation (for nitrogen production and oxygen enrichment), hydrogen recovery from ammonia purge streams, separation of hydrocarbons and light gases, and CO_2 removal from natural gas [114].

- **Membrane materials**

Membrane materials used for CO_2 separation can be categorized into two main types: porous and non-porous membranes [115]. Non-porous membranes, also referred to as dense film membranes, are typically made of polymers that are above their glass transition temperature. In this state, the polymers exhibit a more liquid-like behavior [116]. Membrane permeability and selectivity are important parameters in the characterization and comparison of various membrane materials. They determine the ability of a membrane to selectively allow certain substances to pass through while restricting the passage of others. Membrane permeability refers to the rate at which a specific substance can permeate or pass through a membrane. It is a measure of the transport capability of the membrane for a particular component.

Two commonly used polymeric membranes for gas separations are glassy and rubbery membranes. Glassy membranes are rigid and have a glass-like nature. They operate below their glass transition temperatures. On the other hand, rubbery membranes are flexible and soft, and they operate above their glass transition temperatures. Rubbery polymers often have high permeability but low selectivity, whereas glassy polymers have low permeability but high selectivity [117]. Glassy polymeric membranes are predominantly used in industrial membrane separations due to their excellent gas selectivity and favorable mechanical properties. Commercial glassy polymeric membrane includes polysulfones, polyimides, polyaramides, and polycarbonates [42].

Inorganic membranes, including zeolite-based membranes such as DDR zeolite, SAPO-34 zeolite, and Zeolite-T, have been utilized for CO_2 separation under high temperature, pressure, and harsh conditions where organic membranes may not be suitable [118]. However, their applicability is limited due to several factors, including high cost, low processability, and membrane poisoning. Metal-organic frameworks (MOFs) are a promising class of hybrid materials that consist of metal ions as coordination centers covalently bonded with organic linkers. MOFs exhibit high porosity, large surface area, and high CO_2 uptake capacity, making them potential candidates for CO_2 separation [119]. Developing continuous MOF membranes poses several challenges due to their inherent characteristics. These challenges include poor intergrowth, low stability at high moisture content, low reproducibility, and limited molecular sieving by the organic linker [120]. Mixed matrix membranes (MMMs) combine inorganic materials, such as zeolite, alumina, silica nanoparticles, carbon nanotubes, graphene oxide, and zeolitic imidazolate frameworks (ZIFs), with a polymeric matrix [121]. Including these inorganic fillers provides molecular sieving properties, enhancing the separation performance of the membrane. MMMs can have an asymmetric structure with a thin skin layer supported by a porous sub-layer [122]. One significant disadvantage of MMMs is the inadequate ability to disperse inorganic particles evenly throughout the polymer matrix. Insufficient dispersion results in particle aggregation, which causes defects in the membrane structure. These defects have a negative impact on the overall performance of the MMM, leading to a decrease in its effectiveness [120]. Facilitated transport membranes (FTMs) offer an alternative approach to CO_2 separation, demonstrating the potential to achieve higher permeances and selectivities compared to conventional polymeric membranes [123]. In FTMs, CO_2 selectively permeates through the membrane via a reversible reaction with a complexing

agent-carrier incorporated in the membrane [124]. Non-reacting gases like H2, N2, and CH4 permeate exclusively through the solution-diffusion mechanism. Complex membrane fabrication, sensitivity to operating conditions, and limited stability are the main drawbacks of this membrane type [125].

As mentioned before, several kinds of membrane materials have been proposed for the CO_2 capture process, such as inorganic, organic-inorganic, and polymeric membranes, although most of them are not tested in pilot-scale CCSs. Among the proposed CO_2-selective polymeric membranes, Membrane Technology Research Inc. developed the Polaris membrane, which can provide remarkable permeance values of 1000–2000 GPU ((1 GPU = 10^{-6} cm^3 (STP)/(s cm^2 cmHg))) and moderate CO_2/N_2 selectivity of 50 and is applied into several pilot plants CCS [126,127]. On the other hand, higher CO_2/N_2 selectivity and CO_2 permeance can be reached by facilitated transport membranes such as polyvinylamine (PVAm)/piperazine glycinate (PG), presented the selectivity of more than 140 and the permeance of greater than 700 GPU at the normal flue gas conditions [128,129]. It is reported that CO_2/N_2 selectivity higher than 40 and CO_2 permeance higher than 500 GPU makes the membrane separation competitive to solvent-based absorption for CCS [90]. However, a more comprehensive understanding of membrane properties' effects on the system performance and economy is critically important to enhance the viability of membrane separation in a flexible CO_2 capture system.

- **Mechanism of gas transport in membrane**

In membrane gas separation, gas molecules are selectively separated from their mixture. Membrane contactors, however, promote the contact between two phases, i.e., liquid and gas phases [130]. Membranes form semi-permeable barriers to separate compounds through various mechanisms, including convective flow, Knudsen diffusion, molecular sieving, and solution diffusion [131]. Two widely recognized models are used to describe gas permeation in membranes: the pore flow model for porous membranes and the solution-diffusion model for dense (nonporous) membranes [132]. Fig. 2-9 provides an illustration of the gas permeation mechanisms in membranes. While both porous and dense membranes have the potential to be used for selective gas separation, it is worth noting that all commercially available gas separation membranes currently rely on dense polymer membranes.

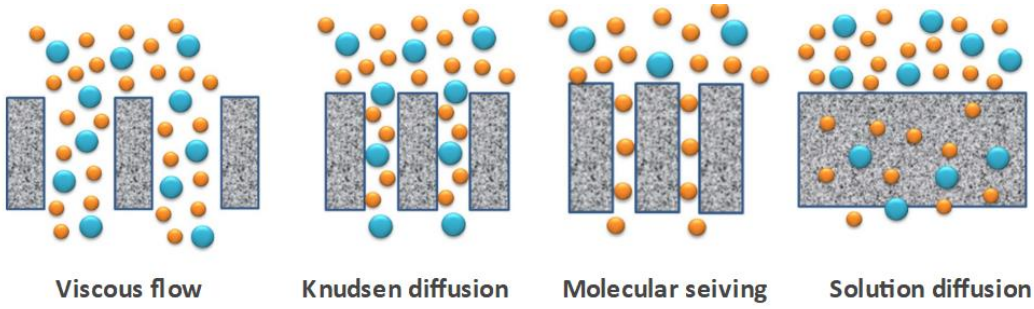

Fig. 2-9. Mechanisms of Gas permeation through the membrane

The mechanism of gas transport through membranes is influenced by several factors, including the physical and chemical structure of the membrane, the characteristics of the permeating gas species (such as size, shape, and polarity), and the interaction between the membrane and the gas [133]. The distinction between the solution-diffusion and pore flow mechanisms is based on the size and continuity of the pores within the membrane. In the solution-diffusion mechanism, the transport occurs through tiny spaces known as free-volume elements or pores. These pores are created by the thermal motion of the polymer molecules and are considered gaps between the polymer chains. The transport process in this mechanism is described by Fick's law and follows the principles of solution-diffusion [131]. In contrast, the pore flow mechanism, described by Darcy's law, involves relatively large and fixed pores within the membrane. These pores do not fluctuate in position or volume on the timescale of gas movement and are interconnected. In this mechanism, gas transport occurs through the continuous channels provided by these relatively large pores [134].

- **Membrane modules**

In industrial-scale separation processes, a significant amount of membrane material, ranging from hundreds to thousands of square feet, is required. Efficient packing of these membrane materials into modules is essential to ensure economic viability and practicality. While cost is an important factor in selecting membrane modules, issues like fouling and concentration polarization often take precedence. There are several types of membrane modules available, including plate-and-frame modules, tubular modules, spiral-wound modules, and hollow fiber modules. Among them, spiral-wound modules and hollow fiber modules are the most commonly

used in gas separation applications [135]. Fig. 2-10 presents the schematic of these membrane modules.

Spiral-wound modules are well-suited for gas separation applications involving high-flux feed gases with contamination and concentration polarization concerns. These modules consist of a flat sheet membrane material wound around a central permeate tube, creating a spiral structure. This design allows for a large membrane surface area within a compact module, facilitating efficient mass transfer [126]. On the other hand, hollow fiber modules are more suitable for high-volume applications that require low flux and low selectivity membranes. Hollow fiber modules consist of numerous small, hollow fiber membranes bundled together in a similar configuration to shell and tube heat exchangers [130]. Hollow fiber membranes are highly desirable in membrane processes due to their large membrane area per unit volume, ease of construction, and self-supporting structure. These characteristics contribute to the overall performance and economic feasibility of membrane processes. Currently, the majority of gas separation membranes are manufactured in the form of hollow fiber modules, with less than 20% being produced as spiral-wound modules [130]. This membrane module type has been considered for CO_2 capture application in this dissertation.

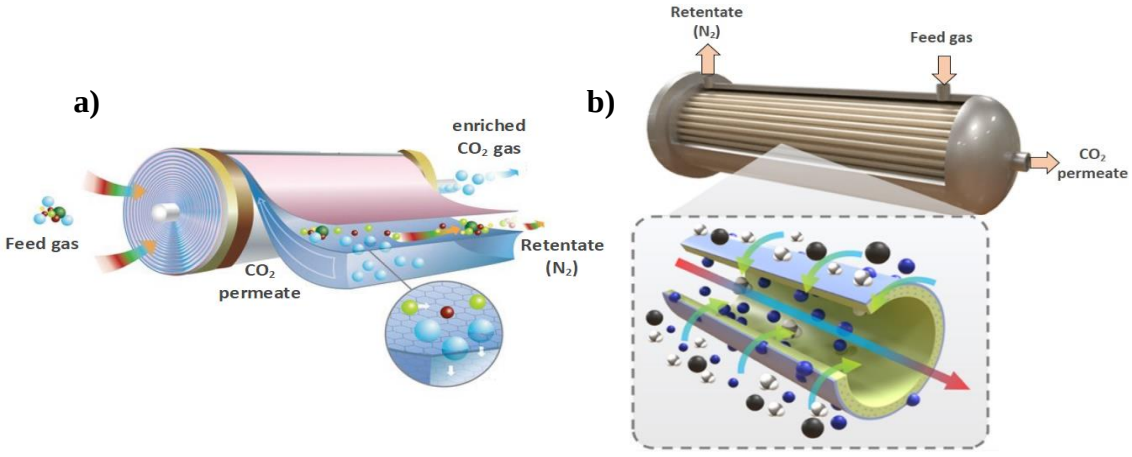

Fig. 2-10. Schematic of membrane modules, (a) spiral wound membrane contactor, (b) hollow fiber membrane contactor

Also, flow configuration in the membrane modules can be categorized into two types: parallel flow and cross-flow membrane module, as presented in Fig. 2-11. Cross-flow modules

mainly depend on the feed-to-permeate pressure ratio as a driving force. The parallel flow module is also categorized as co-current flow, counter-current flow, and counter-current flow with sweep gas [136]. Counter-current flow is widely recognized for enhancing mass transfer in the case of a limited pressure ratio [137]. Due to complexity and flow distribution, counter-flow modules are currently limited in their applications, mainly used for air dehydration and some nitrogen-from-air processes. Most membrane-based gas separations utilize cross-flow modules because of simple operation. Counter-flow modules are expected to be employed when it comes to separating CO_2 from flue gas in power plants. This is because counter-flow operation offers clear advantages: it increases the concentration of CO_2 in the permeate from 29% to 41%, reduces the required membrane area by 38%, and decreases power consumption by 18% [127]. In the sweep module, a small portion of the residue gas is introduced to the permeate side at the end of the module. This has a dramatic effect due to additional driving force; the membrane area needed for separation is significantly reduced by almost 40%.

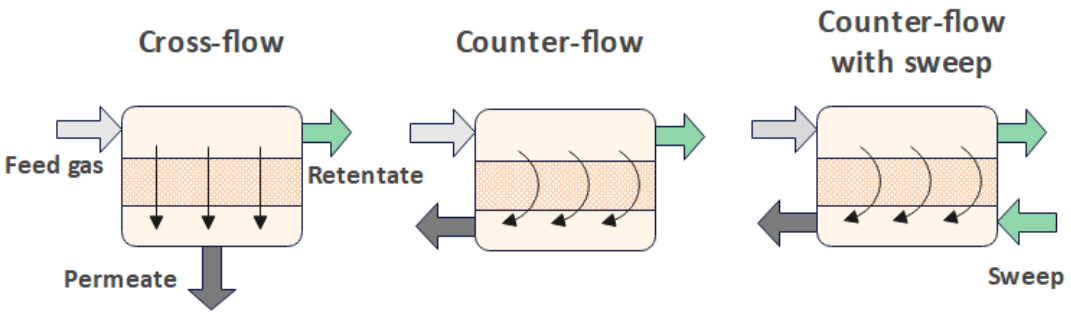

Fig. 2-11. Schematic cross-flow, counter-flow, and counter-flow with sweep module designs

- **Membrane-based process for CO_2 capturing**

The membrane gas separation is considered as a potential and cost-effective technology for flexible post-combustion CO_2 capturing due to several known benefits, such as low energy consumption [138]. Besides the post-combustion method, the membrane modules for CO_2 capturing can be used in the pre-combustion strategy, which involves CO_2 capturing before power generation via the combustion process [139]. Also, oxygen transport membranes have a wide application in the oxy-combustion CO_2 capturing method, which consists of a combustion process with oxygen instead of air [140,141]. However, A technical challenge for cost-efficient CO_2

capturing by the membrane process is the low CO_2 partial pressure (typically 0.15 atm.) in power plant flue gas, which implies a low thermodynamic driving force for the CO_2 separation. To reach the desired CO_2 capture rate and CO_2 purity, the permeability and selectivity of available membranes are not adequate for a single-stage membrane process [133]. To address this challenge, many research works are devoted to both the development of new membranes and the improvement of membrane process designs.

Fig. 2-12 shows a two-stage membrane process schematic for post-combustion CO_2 capturing. The flue gas must be compressed prior to being supplied to the membrane unit to provide the necessary driving force required for the gas separation. Membrane separation for CO_2 capture is simple and does not involve chemicals or regeneration. However, membrane CO_2 separation, based on the flue gas CO_2 partial pressure, needs a considerable inlet pressure to provide enough driving force for CO_2 separation and reduce the required membrane area [142]. Hence in the case of low partial CO_2 pressure in post- combustion flue gas, the main challenge is high compressor and membrane cost, where process design and optimization based on multistage membrane systems could offer a solution. A detailed review of the current design and potential improvements in the membrane-based CO_2 capture process is presented in the next section.

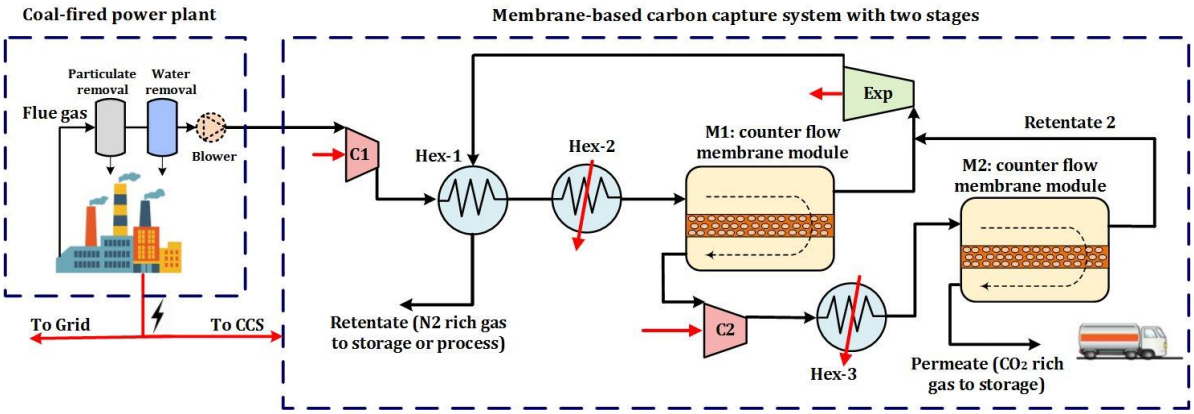

Fig. 2-12. Schematic of two stage membrane-based CCS process

2.3.3 Adsorption-based CO_2 separation

In adsorption processes, molecules adhere to the porous surface of a solid either by physical and/or chemical forces. The adsorption separation process typically consists of three steps: the

adsorption step, where a film of the adsorbate (CO_2) is formed on the surface of the adsorbent (molecular sieves or activated carbon); a purging step, where the other gases are purged from the vessel; and a desorption step, where the CO_2 is desorbed from the adsorbent. Fig. 2-13 indicates the simple CO_2 adsorption process, which consists of adsorption and desorption steps [143]. Typically, single bed CO_2 adsorption employs four distinct regeneration cycles, namely pressure swing adsorption (PSA), temperature swing adsorption (TSA), electrical swing adsorption (ESA), and vacuum swing adsorption (VSA) [144]. TSA heats the adsorbents for regeneration leading to a larger sorbent inventory as well as a high energy requirement. In the ESA, electricity is passed through the bed to heat up and regenerate the adsorbent. In pressure swing adsorption, the pressure of the adsorbent is reduced to achieve desorption of CO_2. Vacuum swing adsorption is a specialized form of pressure swing adsorption used when the feed gas pressure is close to the ambient pressure [145].

2.3.4 Cryogenic-based CO_2 separation

The cryogenic method of carbon capture technology utilizes liquefied natural gas (LNG) to generate the necessary cold energy for capturing CO_2. It is employed in both oxyfuel combustion and post-combustion carbon capture processes to separate CO_2 from flue gas. Cryogenic CO_2 capture enables the production of highly pure CO_2, reaching levels of up to 99%. This method involves several steps, including compression, expansion, separation, and cooling. However, the cryogenic process is considered less desirable than other technologies due to its high operational costs [146].

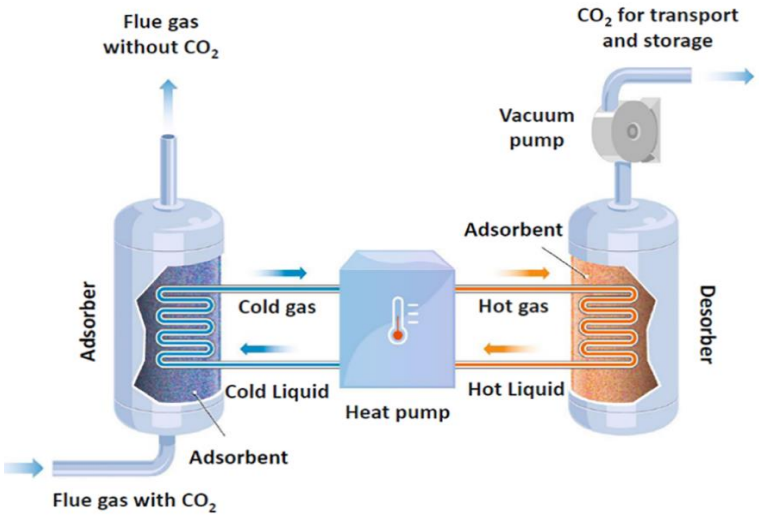

Fig. 2-13. CO_2 separation process using adsorption technology [143]

2.3.5 Comparison of CO_2 separation technologies

Table 2-3 summarizes the above-described CO_2 separation technologies along with their pros and cons. While absorption remains the most widely used method for carbon capture, membrane separation shows significant potential in the field as a less energy-intensive and cost-effective technique. Additionally, membrane systems are often compact, modular, and scalable, allowing for easier implementation and integration into existing processes. These factors contribute to the affordability and feasibility of membrane separation for carbon capture applications. While further research and development are needed to optimize membrane materials, enhance selectivity, and improve efficiency, membrane separation holds promise as a viable alternative to absorption methods in the field of carbon capture.

Table 2-3. Characteristics of different CO_2 separation technologies

Separation technology	Description	Main advantages	Main disadvantages
Chemical absorption [147]	Chemical absorption of carbon dioxide with a solvent such as MEA, piperazine, sodium hydroxide, or potassium hydroxide.	• High carbon dioxide absorption per unit of solvent • No methane losses • Strong selectivity • Simple operation	• High energy penalty in the regeneration • High capital and operating cost • Possibility of amine emissions
Membrane separation [127]	This technique is based on the different sizes of molecules. Carbon dioxide is permeated through a porous membrane while methane is retained over the membrane surface.	• Low costs • No need to use chemical agents or anti-fouling • No hazardous emissions • High recovery	• Need of a previous stage to remove minor contaminants
Adsorption [148]	Zeolite, molecular sieve, and other solid adsorbents are used to adsorb CO_2. By changing the temperature and pressure, CO_2 is released from adsorbents.	• Simple operation • Low energy consumption • Fast sorbent regeneration	• High gas losses in the desorption stage due to the pressure release • The adsorbent has limited capacity and low selectivity
Cryogenic [149]	CO_2 has different condensing temperatures; hence a gradual decrease of flue gas temperature is performed until pure gas flows are achieved.	• High CO_2 purity Simple and easy to use	• High costs and low recovery

Table 2-4 shows the status of post-combustion CO_2 capture development. Among various separation technologies, the absorption process has reached a relatively advanced stage of development. However, it still requires careful consideration of equipment corrosion and entails high costs for solvent regeneration. On the other hand, adsorption processes face limitations in

terms of low CO_2 adsorption capacity and susceptibility to the influence of other gases on adsorbents. Overcoming these barriers necessitates the development of new adsorbent materials. Membrane technology shows promise due to its energy efficiency, but research is required to optimize its performance at low CO_2 concentrations and high capacities. Continued exploration and development in these areas will contribute to advancing carbon capture and separation technologies.

Table 2-4. Status of post-combustion CO_2 capture development [81]

	Absorption	**Adsorption**	**Membrane**
Commercial usage in chemical process industries	High	Moderate	Low
Operational confidence	High	High but complex	moderate
The primary source of the energy penalty	Solvent regeneration	Solid sorbent regeneration	Compression
Regeneration energy (MJ/kgCO_2)	2.2–6	0.5–3.12	0.5–6
Efficiency penalty (%)	8.2–14	5.4–9.0	6.4–8.5
Development trends	New solvent, thermal integration	New sorbent, process configuration	New membrane, process configuration

2.4 Challenges and advances in the design and operation of CO_2 capture plants

In this section, a literature review is conducted on the current challenges in the design and operation of chemical absorption CO_2 capture plants, the conventional processes, as well as membrane-based CO_2 capture plants as the promising option for widespread implementation for decarbonizing power plants. Furthermore, recent literature about advances and progress in the field is critically reviewed.

2.4.1 Challenges and advances in Chemical absorption

Aqueous amine-based technology is a chemical absorption process recognized as the most mature for post-combustion capture (PCC) of CO_2. Aqueous MEA has been globally considered a fundamental solvent because of its high separation selectivity for CO_2 and its rapid rate of reaction [75]. Even though this technique is quite old and has been commercialized, the solvent-based PCC

process faces challenges due to the large flow rate and low CO_2 concentration in the flue gas, requiring significant heat for solvent regeneration. These challenges impose energy and cost penalties on the power plants, affecting the viability and feasibility of the process. The heat duty for regenerating the amine solvent comprises three main components: (i) the desorption energy needed to break the chemical bond between the solvent and carbon dioxide, (ii) the sensible heat required to raise the temperature of the aqueous amine solution, and (iii) the energy needed to vaporize water for CO_2 stripping. Generally, desorption heat accounts for half of the total energy requirement for regeneration. Typically, the required heat for a stripper is obtained from steam drawn-off from the medium/low-pressure turbine crossover in a power plant [150]. The thermal energy needed for solvent regeneration is a crucial performance indicator in absorption-based CO_2 capture processes commonly measured by the adsorbent regeneration energy required to capture 1 tonne of CO_2. Traditional solvents like MEA typically require around 3.5-4 GJ of regeneration energy per tonne of CO_2 [151]. However, advanced solvents such as Shell's CANSOLV® and Fluor's ECONAMINE FG PLUS™ have achieved lower regeneration energy consumption, ranging between 2.5 GJ/tCO_2 and 2.9 GJ/tCO_2 [49]. This reduction in regeneration energy indicates improved efficiency and cost-effectiveness of the CO_2 capture process using these advanced solvents.

To mitigate this energy efficiency penalty, extensive research has focused on four areas: (1) developing solvents with improved properties like high CO_2 absorption capacity and lower regeneration heat [102]; (2) modifying process configurations, such as intercooler, vapor recompression, and split-stream techniques [152]; (3) optimizing process parameters like absorber/stripper sizes, solvent flow rate, and re-boiler temperature/pressure [153]; and (4) effectively integrating the PCC plant with the power plant [154,155].

Abu-Zahra et al. [156] have identified key process parameters, such as CO_2 lean-loading, reboiler pressure, and MEA concentration, that directly impact the heat duty of the reboiler. Other factors, like solvent temperature and column height, play a less significant role in reboiler energy consumption. Abu-Zahra et al. have suggested that optimizing these parameters can lead to a 20% reduction in reboiler duty and a 23% reduction in regeneration energy when using 40 wt% MEA. Aboudheir et al. [157] conducted a study where they modified the solvent capacity and concentration to optimize reboiler duty and cost. Damartzis et al. proposed alternative flowsheet designs for MEA-based CO_2 capture systems and used techniques like orthogonal collocation on

finite elements to improve performance and reduce solvent flowrate [158]. Moullec et al. [159] explored various process modifications for MEA-based CCS categorized into heat integration, absorption enhancement, and heat pump to analyze their impact. Their study found that the reduction in regeneration energy range could be up to 45% depending on the complexity of the process modification. Julien et al. conducted two studies aimed at reducing reboiler energy consumption [15]. They explored new solvent technologies beyond MEA and investigated different process configurations, such as stripper split feed, lean vapor compressor, and combinations of the two, to optimize operational costs and processes. Also, Sultan et al. [160] assessed the advantages of three different modifications to the stripping process to reduce energy requirements and cost. These modifications are lean vapor compression, stripper overhead exchanger, and an advanced hybrid configuration combining both techniques. Gbadago et al. used CFD simulation to evaluate an MEA absorption process for CO_2 removal on an AMT-SP 350Y structured packing in an industrial-scale pilot plant [161]. They found that multi-packed bed columns with interbed liquid distributors are ideal for studying industrial-scale CO_2 absorbers. Also, regarding the ratio of CO_2 recovery in the MEA absorption process, it is generally recommended to set the optimal CO_2 capture degree (CO_2 amount in product stream/CO_2 amount in the flue gas) in the range of 80-90% for economic considerations, with a common value of 90% used in most designs [32,65].

The absorption process in CO_2 capture can be modeled using either a simple equilibrium stage model or a rigorous rate-based model. For a large-scale CO_2 capture process, the rate-based process modeling and simulation has been considered a vital approach for evaluating different configurations' performance and gaining better and more accurate insight into the process design and development [162]. The rate-based models, based on both two-film and eddy diffusion theories, have been shown to provide more reasonable predictions compared to the simple equilibrium stage models [163]. The CO_2 desorption models in amine-based processes are similar to the absorption section, including heat and mass transfer models and thermodynamic considerations. However, treating chemical reactions in the stripper column, which operates at a wider temperature range (e.g., 100-130 °C), requires careful consideration [164]. Kinetic data for reactions at this temperature range are often limited. Some models assume instantaneous chemical reactions dominated by chemical equilibrium in the liquid phase, while others use kinetic models [165]. Developing a model that incorporates available kinetic models and relevant process

parameters would improve the accuracy of describing the MEA-absorption process and provide a more comprehensive understanding of the process. Several process simulators have been used to ensure solution efficiency for this system, and they include Aspen Plus [166], HYSYS [167], ProMax [168], and UniSim [95]. These tools have been extensively used in multiple process modifications and for the identification of optimum operating conditions in comparison with the conventional configuration. In the work by Ahn et al. [95], they evaluated ten different designs of MEA technologies for a coal-fired boiler power plant using UniSim. They proposed that the use of multiple strategies can help in reducing energy consumption for integrated carbon capture and in the compression unit. They achieved a 0.9 % net increase in plant efficiency coupled with a 37% reduction in steam consumption. Likewise, Moullec and Kanniche [169] used Aspen Plus to assess and compare several flowsheet modifications found in literature through modeling.

The optimization of the CO_2 absorption operating parameters is crucial for cost reduction and energy penalty in large-scale testing. Many studies focus on simulation, mathematical modeling, and optimization of the integrated CO_2 capture process using common commercial software stated above. Various flowsheet configurations can be achieved by manipulating variables or adding additional process units. Several decision variables, including temperature, pressure, composition, gas, and solvent flow rates, CO_2 loadings, process unit sizes, heat loads, and CO_2 recovery level, are typically optimized [170]. Choi et al. [171] investigated superstructure-based optimization to identify optimal operating conditions and configurations with high energy savings in CO_2 capture. Yulia et al. [172] optimized a CO_2 absorption system by selecting exhaust gas temperature, MEA molar flow rate, and reboiler duty as decision variables. The goal was to maximize exergy and minimize exergoenvironmental impacts, improving system efficiency and reducing environmental consequences. The combination of process optimization and systematic optimization algorithms proves to be a practical approach to evaluating the CO_2 capture process.

When assessing capture technologies and proposing new designs, it is essential to consider various process characteristics and design implications as well as the economic evaluation of the process. These evaluations help assess the technical advantages and economic impacts of the capture technology in a fair and standardized manner, allowing for effective comparison and decision-making. In techno-economic assessments (TEAs) of capture technologies, the cost to capture or avoid one tonne of CO_2 is commonly used as a performance and economic indicator

[173]. This metric considers all cost elements associated with the technology, including equipment purchase, installation, labor, operating costs, and more [174]. Previous studies demonstrated considerable cost penalties associated with CO_2 capturing mainly due to high capital and operating cost. For instance, by integrating amine-based CCS with an NGCC plant, the power plant's net efficiency decreases by 7%, and the cost of electricity could increase from 57.1 to 84.3 $/MWh, resulting in a capture cost of 86.6 $/ton of CO_2 [13,49]. Li et al. [175] evaluated the technical and economic performance of an MEA-based post-combustion capture process integrated with a 650-MW coal-fired power station. The techno-economic model estimated a capital investment of US$1357/kW with a CO_2 avoided cost of US$75.1/tonne. Also, Yun et al. [65] conducted a techno-economic analysis (TEA) for a coal-fired power plant integrated with an MEA-based CO_2 capture process that requires 3.57 GJ of regeneration energy per tonne of CO_2. The TEA estimated the CO_2 capture cost as 62.8 $ per tonne of CO_2, while the avoidance cost was calculated to be 97.7 $ per tonne of CO_2.

A higher CO_2 concentration in the gas phase has several benefits in CO_2 capture processes. It can enhance the amount of CO_2 chemically or physically bound to solid materials or liquid solvents, as well as improve the permeation rates in membrane-based processes. This is particularly advantageous for coal-fired power plants (10-14 mole% CO_2) compared to the NGCC power plant (4 mole% CO_2), affecting the capturing cost and energy penalty. Accordingly, increasing the CO_2 concentration in the flue gas could be an effective method to reduce the energy penalty and equipment size of CO_2 capture processes and lead to improved capital cost (CAPEX), cost of electricity, and CO_2 avoidance cost [32,67]. This area of improvement in chemical absorption and its potential effect on the operation of the upstream power plants, capture cost, and cost of electricity has been comprehensively addressed in this dissertation.

Overall, the high cost and energy penalty associated with the MEA absorption process for CO_2 capture highlight the need for significant improvements in various areas of the process. To facilitate widespread implementation, it is crucial to focus on developing advanced CO_2 separation technologies. Additionally, optimal process design and integration strategies are vital in minimizing the thermal energy demand and overall capture cost in post-combustion carbon capture processes. Addressing these aspects makes it possible to enhance the efficiency and cost-effectiveness of CO_2 capture, making it more viable for large-scale deployment.

2.4.2 Challenges and advances in the membrane-based CO_2 capture process

Compared with the conventional MEA absorption method, membrane-based CO_2 separation is considered an attractive alternative for CO_2 capture, mainly because of its lower energy requirement and operation cost [176]. In spite of the fact that the membrane-based CO_2 separation method hasn't been used commercially for CO_2 capturing from power plants, recent developments in membrane materials plus easy scaling-up, high packing density, small footprint, and mobility make the membrane separation method a potential candidate for environmentally friendly and sustainable CO_2 capture [115]. Using membrane technology in coal and natural gas power plants presents the major challenge of low CO_2 concentration (4-15%), which requires the use of compressors on the feed side or vacuum pumps on the permeate side to enhance driving force across the membrane [177].

The selectivity and permeability of the membranes available on the market make a single-stage membrane process unsuitable for recovering CO_2 at more than 90% purity from diluted- CO_2 flue gases in fossil gas combustion [178]. There have been a number of membrane improvements proposed to overcome the challenge of CO_2 capturing from the power industry. Membrane materials with high selectivity and permeability, including polymeric, organic, and inorganic materials, have been the subject of much research in recent years. It has been demonstrated that Polaris membranes developed by Membrane Technology Research Inc. can provide significant CO_2 permeances of 1000–2000 while the CO_2 /N_2 selectivity is acceptable at 50 [126]. The use of facilitated transport membranes, such as Polyvinylamine/Pirazine Glycinate-based membranes, can also provide higher CO_2/N_2 selectivity (about 140) under normal flue gas conditions [128]. It has been shown that membranes with high CO_2 permeability reduce the area and cost of membranes. In contrast, membranes with high CO_2/N_2 selectivity reduce the energy consumption and cost of operation of the system. Accordingly, future developments in membrane materials require deep insight into how membrane properties affect the operation and economy of the carbon capture system. By considering the limited permeability and selectivity of commercially available membranes, the process design of gas membrane systems plays a crucial role in determining their economic viability. This involves determining the size and configuration of the membrane system to meet the project's scope and specifications. The design of membrane processes can vary significantly depending on the specific application and module configurations. Membrane module is the central component of any membrane process, and multiple modules are connected in series

or parallel and form a stage, and a combination of stages is called a cascade. In membrane process design, the primary focus is on selecting the appropriate module configuration, membrane material selection, and determining the required membrane area for each module, as well as the compression or vacuum work needed to operate the system [179].

Modeling and simulating the membrane gas separation process is a cost-effective approach to gathering valuable data related to the economics, design, and operation of the separation process. Various aspects of membrane gas separation, such as economic evaluation, permeation analysis, and module design, could be studied through process modeling and simulation. However, most of the existing models primarily focus on binary gas systems and steady operation without considering pressure drop and temperature changes [180,181], with only a limited number of models considering multicomponent systems and unsteady operation [182,183]. The development of a comprehensive model for hollow fiber membrane modules, coupled with a robust and flexible solution method, can offer valuable insights into achieving the effective separation of multicomponent gas mixtures. Such a model can be a useful tool for guiding the design process and optimizing membrane-based gas separation systems.

Considering the existing membrane properties and other technical limitations, the development and improvement of membrane process design and optimization of system operating and design conditions can play an important role in improving the sustainability and viability of the membrane process for CCS application. Due to the low partial pressure of CO_2 and low driving force in flue gas, implementing a multi-stage membrane design and creating an internal gas recycling is essential to reach the high CO_2 recovery (90%) and high CO_2 purity (95 mole%) targets. The schematic of the single- and two-stage membrane process is illustrated in Fig. 2-14 [184]. To reach this separation target for post-combustion applications, previous authors suggested different approaches for generating higher driving forces for CO_2 permeation by a combination of feed compression, vacuum permeation, feed-air sweep system, retentate recycling, as well as enricher and stripper designs [127,185–188]. In this regard, various parametric studies have been implemented to study the effect of multiple designs, operating conditions, and membrane properties on the system's performance and economy [189].

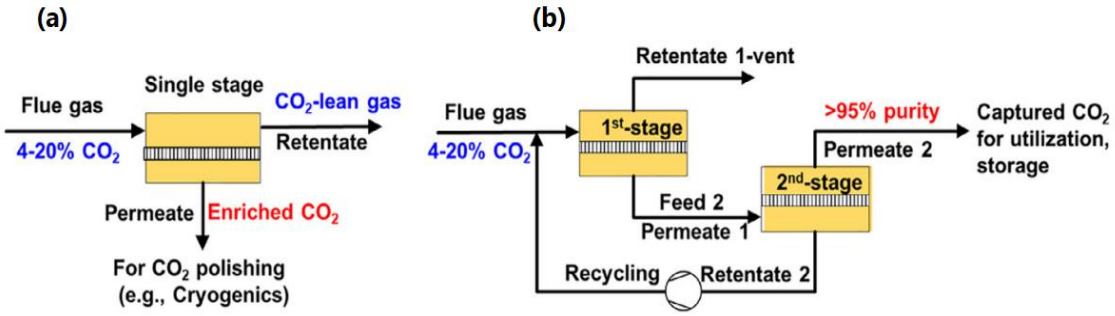

Fig. 2-14. Single (a) and two-stage (b) membrane process for CO_2 capturing [184]

Merkel et al. [127] examined the influence of membrane properties and design parameters on the required membrane area and the specific cost of a multi-stage membrane process. They concluded that improving membrane permeability is more beneficial than increasing CO_2/N_2 selectivity for reducing the CO_2 capturing cost. Zhao et al. [185] investigated the energy requirement and the capture cost of different designs of a two-stage membrane system using Polyactive membrane with a 70% CO_2 separation target and 95 mol% CO_2 purity. Zhang et al. [82] presented a thermo-economic analysis of a two-stage membrane system for post-combustion CCS in a coal-fired power plant. They simulated the membrane process using PRO/II software, and they resulted that selecting a membrane with high selectivity led to a reduction in energy consumption and an increment in the required membrane area. Brunetti et al. [187] focused on evaluating a two-stage co-current membrane process without sweep gas and recycling for CO_2 separation from flue gas. They analyzed the influence of the pressure ratio, mass transport properties, and feed composition on CO_2 recovery and permeate CO_2 purity. Giordano et al. [188] examined the energy demands and capture costs of single and double-stage membrane systems at different CO_2 permeate purity using Polyactive™1500 polymer as a membrane. Mores et al. [190] performed a superstructure optimization of the membrane process, considering up to four stages and various driving force generation technologies, to minimize the associate cost of CO_2 capture. They substantiated that in a membrane system with four stages and two recycles, the total annual cost of 99.53 M$/year can be reached by generating driving force using feed compression and permeate vacuum. Xu et al. [178] conducted a parametric study of a two-stage membrane with a crossflow configuration to find proper feed pressure and membrane selectivity, focusing on decreasing energy usage, required membrane area, and the cost of CO_2 capture. They suggested

that by considering a membrane with low CO_2/N_2 selectivity in the first stage and with high CO_2/N_2 selectivity in the second stage, the CO_2 capture cost significantly reduces. He et al. [184] conducted a sensitivity analysis to assess different types of membranes for capturing CO_2 from fossil fuel-fired power plants. They found the specific cost of capturing CO_2 at a rate below $20 per tonne using Polaris and PolyActive membranes where the concentration of CO_2 exceeds 13% by volume.

Using multi-objective optimization (MOO), it is possible to efficiently address the various trade-offs between operating and design parameters in membrane-based CCS to achieve the specified CO_2 removal target. In CCS processes, both evolutionary algorithms, such as NSGA (Non-dominated sorting genetic algorithm), and gradient-based methods, such as nonlinear programming, have been applied [191]. The optimal design and operation of solvent-based CCS have been widely studied [83,158,164]. For membrane-based CCS, multi-objective and superstructure-based optimization methods have also been applied [179,191–196]. For a multi-stage membrane process, Arias et al. [191] used a superstructure optimization approach to determine the optimal number of membrane stages and operating conditions for a range of CO_2 recovery objectives. According to Mat and Lipscomb [193], a global search of the decision variables space was used to find optimal membrane properties and operating conditions for minimizing levelized electricity costs for multi-stage hybrid membrane-cryogenic design. The cost function for a novel cryogenic carbon capture system below ambient temperature was minimized by Lee et al. [195]. To the best of our knowledge, most of the studies conducted on the optimization of membrane-based CCS have focused on the economic parameters' optimization of a specific membrane design with a fixed value of membrane properties. Furthermore, few publications [179,191,194] are available addressing multi-objective and superstructure optimization in two-stage membrane CCS systems for determining simultaneously and systematically the optimal configuration variables, operating conditions, and membrane properties for capturing CO_2 from coal-fired power plants to meet the separation target specified by the U.S. Department of Energy (90% CO_2 recovery).

Although some research is devoted to addressing these challenges, there are still many fundamental questions and gaps about the membrane-based CCS for flexible and optimal integration into fossil-fueled power plants. Table 2-5 presents the critical literature review on the membrane-based CCS and the identified research limitations and gaps.

Table 2-5. A critical review of recent publications in the field of membrane-based CCS

Ref	**Field of investigation**	**research founding**	**Limitations and gaps**
[185]	Parametric study of membrane-based CCS	A cascade arrangement makes it possible to reach high CO_2 Purity, and lead to a slight energetic advantage in comparison with MEA absorption was achieved	• A limited CO_2 Separation target (70%) is considered. • various membrane configurations are not studied • sweep gas and recirculation effect are ignored
[82]	Parametric study of membrane-based CCS, Thermodynamic analysis	The main energy bottleneck of membrane technology is located in the membrane unit operation, which has relatively low exergy efficiency. The optimal CO_2/N2 selectivity is 70−90.	• Various membrane configurations are not studied. • Sweep gas and recirculation effect is ignored • Economic evaluation is not complete. • The effect of the operating parameter on the required membrane area is not discussed.
[187]	Parametric study of membrane-based CCS	The influence of the pressure ratio, mass transport properties, and feed composition on CO_2 recovery and permeate CO_2 purity are reported.	• They only focused on a two-stage co-current membrane process without sweep gas and recycling. • The effect of operating conditions on CO_2 capture cost is ignored.
[188]	Techno-economic study of membrane process	The effect of CO_2 permeate purity on the energy requirements and costs of Polyactive membrane-based CCS are reported.	• The simulated process is without sweep gas and recycling, and various membrane flow configurations. • The effect of operating conditions on CO_2 capture cost is ignored • The separation target is not fixed, which in some cases leads to low CO_2 separation
[190]	optimization study of membrane-based separation systems	They substantiated that a membrane system with four stages and two recycles is the optimum design for the membrane system.	• Fixed membrane properties are considered. • The effect of operating conditions on CO_2 capture cost is ignored • Various design and membrane module flow regime is not evaluated in their super-structure model • Validation has not been reported
[178]	Performance analysis of membrane-based CCS	Proper feed pressure and membrane selectivity have been found with a focus on decreasing energy usage, required membrane area, and the cost of CO_2 capture.	• The focus is on the cross-flow membrane module • Various design and membrane module flow regime is not evaluated • Fixed membrane properties are considered. • Unsteady state simulation is not performed • various compression methods are not investigated.
[197]	A new approach to using membrane in CCS application	An assessment of the feasibility of membrane-based direct air capture has been implemented. They showed that mixed-matrix membranes (MMMs) could reach both high CO_2 permeability and selectivity in the mDAC system.	• High CO_2 capture cost of this technology • It can be used in removing CO_2 from the atmosphere rather than large sources such as power plants. • More studies need to be done in order to evaluate the reliability and effectiveness of this technology.
[198]	Pilot-scale of membrane-based CCS for CO_2 separation from the power plant	They resulted that the membrane separation process is available on-demand, without the need for lengthy start-up and shut-down procedures or even the need to operate continuously regardless of flue gas availability. Membrane processes using PolyActive™ membranes seem to be well suited for post-combustion CO_2 separation.	• The dynamic performance and response of membrane-based CCS toward possible variations of operating parameters in partial load conditions have not been fully examined due to the limitation of the pilot plant. • Efficient polymer membranes such as Polaris have not been investigated. • Multi-stage membrane design has not been investigated.

[123]	Pilot-scale of membrane-based CCS for CO_2 separation from power plant	Long-term testing of pilot-scale membrane modules containing hybrid facilitated transport membranes in hollow fiber configuration is reported. Membrane modules showed long-term stability with negligible effects from impurities. Simulation studies revealed the high potential of the membranes for CO_2 capture.	• The effect of a step change in operating conditions has not been studied. • The effect of unsteady operation on the size of the system has not been investigated. • Multi-stage membrane design has not been investigated.
[199]	Dynamic simulation model for membrane module	They presented detailed dynamic modeling of a bore-side feed hollow fiber membrane module with a counter-current flow structure to separate CO_2 from coalbed methane.	• Focused on mathematical modeling of the membrane separation • The effect of step-change in operating conditions has not been studied. • The effect of unsteady operation on the size of the system has not been investigated. • Multi-stage membrane design has not been investigated • Constant membrane permeability and selectivity
[183]	Dynamic simulation model for membrane module	A model for the dynamics of an unsteady closed-mode membrane module operation was developed. The composition profile established over time was simulated with an axial mixing effect.	• The simulation is in closed mode (No product flow) • The effect of step-change in operating conditions has not been studied. • The effect of unsteady operation on the size of the system has not been investigated. • Multi-stage membrane design has not been investigated.

Even though valuable information about the performance and economy of carbon capture systems was provided by the above-described references, there are still many fundamental questions about flexible integration and designs as well as efficient process operation. Novel process designs such as multi-stage design, retentate recirculation, and sweep gas and their influence on the system performance and CO_2 capture cost are not thoroughly evaluated. Additionally, previous studies have not addressed the behavior of various membranes at different operating conditions as well as their potential effects on energy usage and system cost. In addition, a fixed membrane system layout for the techno-economic analysis is mainly used in the previous works, and various configurations of membrane-based CCS have not also been proposed and evaluated technically and economically. On the other hand, all of the dynamic simulation studies generally focused on mathematical modeling of the membrane separation process in an unsteady state, and the system's dynamic response toward variations in operating conditions, which reflects the flexible operation of the membrane system, has not been addressed. Additionally, many mathematical models usually rely on several fixed assumptions, such as constant membrane permeability and selectivity, which can reduce the accuracy of the dynamic model.

To the best of our knowledge, a detailed study on the flexible design and operation of membrane-based CCS has not been performed. Moreover, the dynamic behavior of membrane modules under various step-changes in operating variables has not yet been analyzed in the open literature. Accordingly, investigating the optimal design of the membrane separation process for integration into the power plant through a comprehensive techno-economic analysis and dynamic behavior analysis is among the research goals of this dissertation.

2.5 Flexible design and operation of CO_2 capture systems

Fossil-fueled power plants, responsible for a significant amount of GHG emissions, are expected to be integrated with CCS and the increasing share of variable renewable energy (VRE) sources such as solar and wind energy, as shown in Fig. 2-15 [34]. To achieve the desired low-carbon energy systems, different components of the energy systems need to operate in a flexible manner at different operating conditions [200]. The flexibility of CCS corresponds to the capability of CCS to respond to changes produced by the connected power generation systems (renewable and thermal power plants) and is also responsive to external factors such as carbon price, electricity demand, and electricity price [201]. The high penetration of intermittent renewable energy in the energy systems requires the CCS integrated with power plants to respond promptly to variations of seasonal and daily demands so that overall CO_2 emissions from the power plant can be

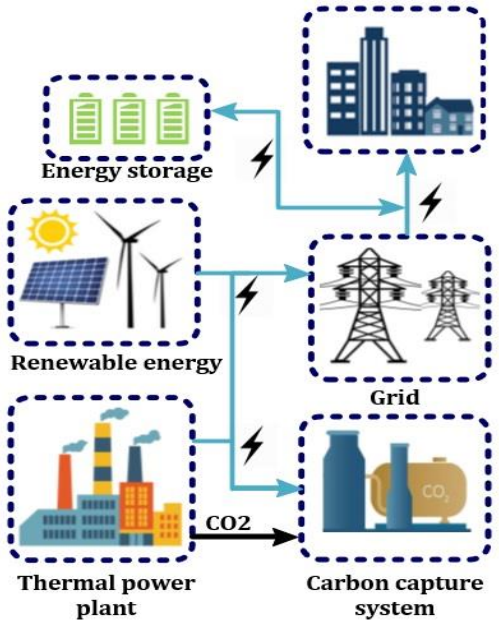

Fig. 2-15. Schematic of the future low carbon energy system

maintained at low levels [202]. Furthermore, most CCS technologies consume a considerable amount of energy, which underlines the necessity of their flexible operation as a way to balance the electricity supply during peak and off-peak periods [203].

Thus, selecting an appropriate CCS technology and reducing its energy penalty have a great influence on the flexible operation of future energy systems. Furthermore, the integration of fossil-fueled power plants with VRE leads to additional costs associated with load balancing, additional power capacity, and energy storage [203]. The load of thermal power plants changes due to the intermittent nature of VRE. Consequently, fossil-fueled power plants are exposed to cycling operations at various partial loads, and the CCS technology requires to follow [204]. Fig. 2-16

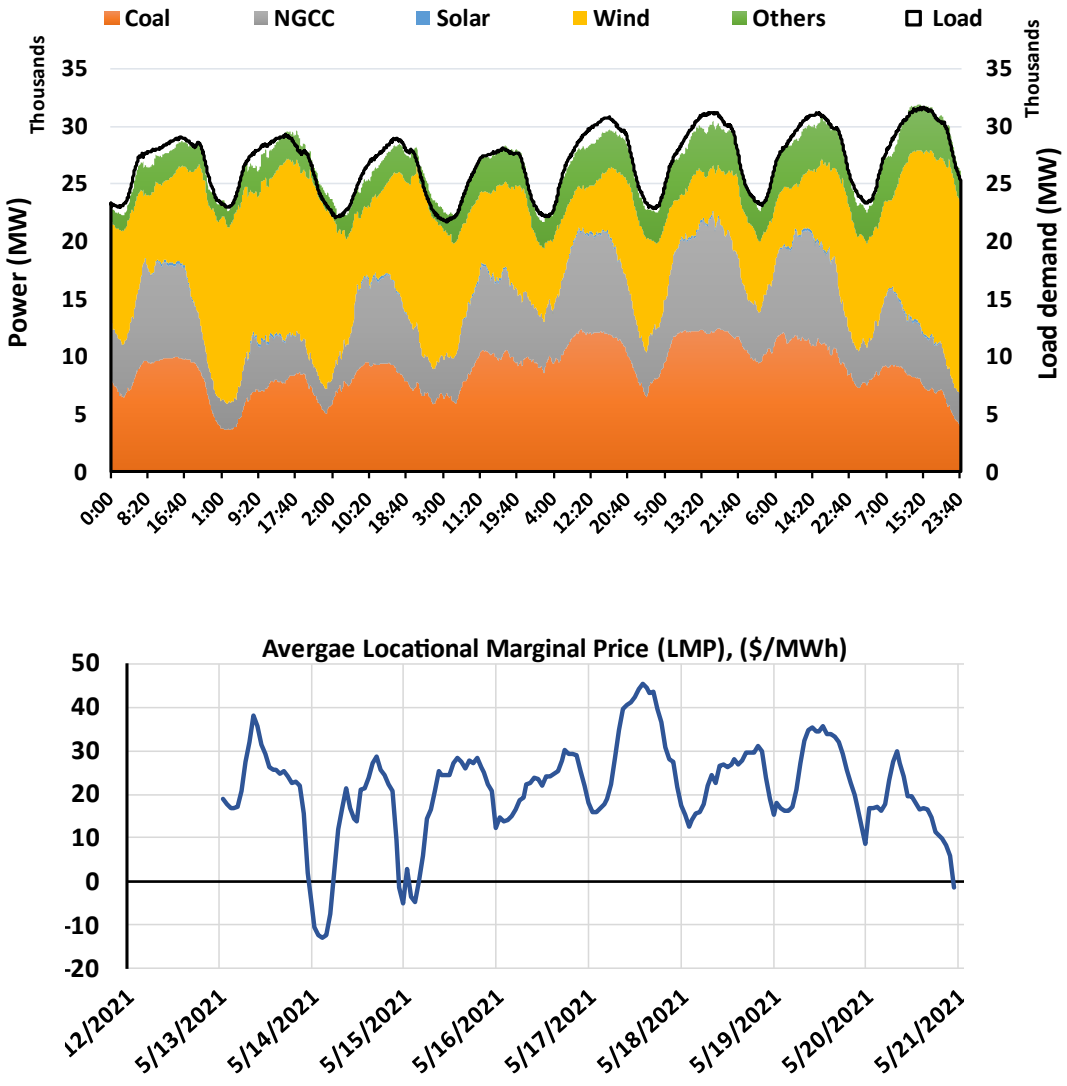

Fig. 2-16. variations of fossil-fueled power plants Load and LMP high share of renewable sources in grid

presents a schematic of a sample power generation mix in several days based on the renewable energy share in Oklahoma state, US, as well as the locational marginal price ($/MWh) of electricity. According to this figure, the load of coal-fired power plants NGCC power plants varies in response to the grid demand and LMP, as well as is required to respond to the high share of wind and solar energy during specific hours of the day.

As shown in Fig. 2-16, the price of electricity sold to consumers typically fluctuates based on the demand-side response, meaning that electricity prices are lower during off-peak hours when demand is lower compared to peak hours. Introducing a CCS plant into the power generation process will inevitably increase the cost of producing electricity. This additional cost becomes more noticeable during periods when electricity prices are already naturally high. As a result, there is an opportunity to mitigate the high electricity prices during peak hours by leveraging the inherent flexibility in the operation of CCS technology.

Generally, the flexible operation of CCS integrated with fossil fuel power plants depends on the transient behavior of the core technology used for CO_2 separation. The transient response of CCS at various operating conditions establishes requirements for the safe and efficient operation of the whole system. It identifies the limit that should be considered by designing and integrating various energy sources. Accordingly, it is crucially important to examine the capability of the CO_2 capture system for flexible operation, which can facilitate efficient technology development and implementation [200].

Besides the impact of VRE on power plant operation, there are other common scenarios that power plants encounter throughout their lifespan, leading to variations of flue gas properties and available energy for CCS [205]. These include:

- Quick start-up/shutdown: The ability to rapidly initiate or halt power generation in response to changing demand or operational requirements.
- Quick change in output (load variation): The capability to adjust the power plant's output rapidly, accommodating fluctuations in electricity demand.
- Increase in maximum output: The capacity to operate the power plant at its highest output level for extended periods.

- Decrease in the minimum output: The flexibility to reduce the power plant's output level to meet lower electricity demand efficiently.
- Fuel switchover: The ability to switch between different fuel sources seamlessly, enabling the power plant to adapt to fuel availability, cost, or environmental considerations.
- Bypass operation (in cases where the steam turbine fails to operate): A backup operation mode that allows the power plant to continue generating power by bypassing the steam turbine, ensuring uninterrupted electricity supply during turbine maintenance or failures.

Regarding the dynamic performance of power plants, the minimum load is typically limited to 40% of its full load in modern gas turbines due to factors such as the combustion stability of the fuel and associated emissions. This limitation prevents gas turbine-based power plants, which contribute significantly to the total power capacity of natural gas combined cycles, from reducing their power generation below this threshold. On the other hand, coal power plants can operate at a minimum compliant load of around 25% of their full load [206]. Modern gas turbines have fast load ramps and dominant dynamics in the order of seconds. In contrast, steam cycles have slower dynamics in the order of minutes due to the heat capacitance of the steam generator. Fig. 2-17 demonstrates the flexibility of a natural gas combined cycle, where the gas turbine responds faster to load changes while the steam cycle determines the time required to reach a steady-state [206]. Coal power plants lack a gas turbine for load control, relying on governor valves at the steam turbine inlet to control the load. Thus, their slower dynamics due to the slow performance steam

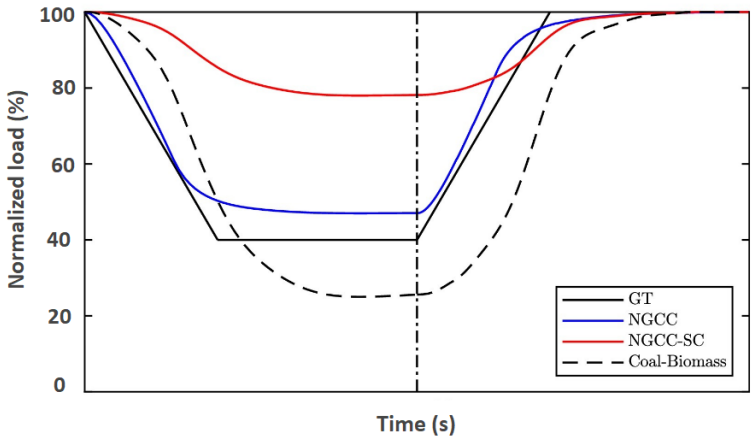

Fig. 2-17. Flexibility of various thermal power plants GT: gas turbine, NGCC: natural gas combined cycle, SC: steam cycle [206].

cycle make them less suitable for flexible operation compared to modern natural gas combined cycles [207].

Accordingly, the flexible operation of both the power plant and CCS plays a crucial role in optimizing the performance, efficiency, and reliability of future power generation systems. Most research on combining capture plants and power plants focuses on analyzing a single design point under stable conditions [154,173,208]. However, relying solely on steady-state models is inadequate for fully understanding the system's behavior during operation or optimizing its efficiency. Therefore, it is crucial to consider and analyze the flexible operation of power plants with integrated post-combustion capture, paying particular attention to their dynamic performance in fluctuating conditions.

The flexibility of amine-based CO_2 absorption technology has been widely investigated in current pilot capture plants by studying the effect of flue gas flow rate, liquid absorbent flow rate, and steam pressure [209–212]. To achieve flexible operation in amine-based CCS, several operating modes and process configuration modifications have been suggested as follows [213]:

1. Flue gas venting: This method is the most common and involves releasing a portion of the flue gas without undergoing the capture process. By selectively venting the flue gas, the capture system's capacity and energy requirements can be adjusted based on the current demand or operating conditions, as presented in Fig. 2-18 [214].

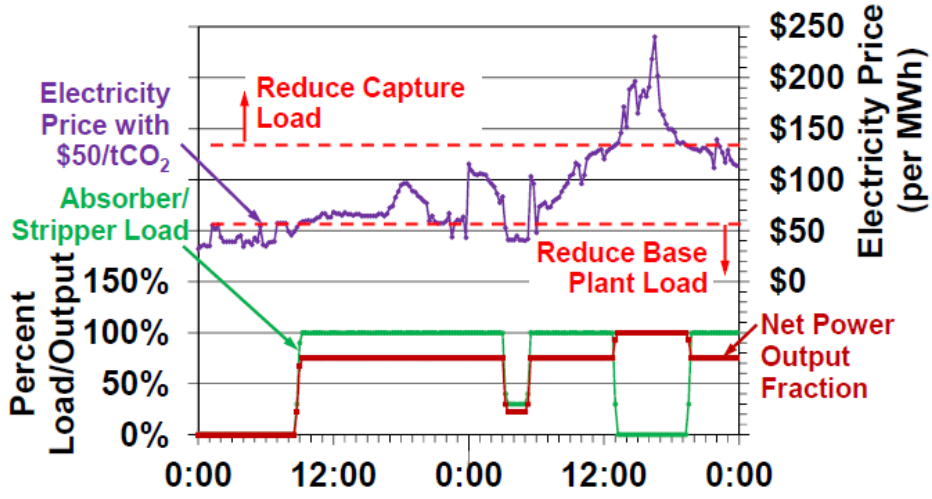

Fig. 2-18. Flue gas venting (bypassing CCS) for flexible operation in conventional amine-based CCS [214]

2. Varying degree of solvent regeneration: The process of regenerating the solvent used in the capture system can be adjusted to different levels. By varying the extent of solvent regeneration, the energy consumption and capture efficiency can be optimized based on the specific operating requirements.

3. Lean/rich solvent storage: The storage of capture solvent can be managed in a lean or rich state. Lean solvent refers to a solvent with a lower concentration of the captured CO_2, while rich solvent has a higher CO_2 concentration. By storing and utilizing solvents with varying CO_2 content, the capture system can adapt to different operating conditions and demands.

The dynamics of absorption-based CCS are inherently slow due to the complex interactions involved in the process, such as mass transfer, heat transfer, and chemical reactions between gas and liquid phases. Lawal et al. [215] demonstrated that when there is a decrease in the re-boiler heat duty, it takes more than two hours for the system to reach a new steady state. This response time is significantly longer compared to the upstream coal-fired power plant, which experiences faster dynamics. Additionally, certain components of the system, such as the absorber, stripper sumps, and lean MEA tanks, act as buffers for solvent flow rate, further contributing to the slow response of the system [33,210,211]. These slow dynamics pose challenges in terms of system control, particularly when it comes to responding to rapid changes in operating conditions or electricity demand. Moreover, due to the complexity of the absorption-based CCS, control of this process at various changes in flue gas conditions is challenging and imposes other drawbacks for this technology regarding the flexible operation [216].

On the other hand, membrane-based CCS is considered a flexible alternative for integration with power plants due to lower energy consumption and modular design of parallel units, which allows bypassing some units in order to respond efficiently to the load variation meanwhile capturing 90% of CO_2 emissions. In membrane contactors, the gas and liquid phases are effectively separated into distinct compartments (shell and tube sides), facilitating efficient mass transfer through the membrane pores. Also, it is expected that this process will respond rapidly to the change in flue gas conditions. For a deep understanding of the effect of flexible operation on the performance of membrane-based CO_2 capture systems, dynamic pilot plants, as well as dynamic and steady-state simulation, are fundamental.

Several membrane gas separation pilot plant studies have been conducted to investigate the long-term separation performance of the membrane system [123,135,198,217]. However, the dynamic performance and response of membrane-based CCS toward possible variations of operating parameters in partial load conditions have not been examined in pilot-scale studies since it may be challenging in pilot plants, specifically when performed frequently. Limited knowledge of the flexible design and operation of membrane-based CCS and difficulties of experimental studies are the primary motivations for using dynamic and steady-state simulation of membrane modules as a beneficial approach for analyzing the system's flexibility. Many studies are available concerning the steady-state modeling and techno-economic analysis of membrane-based CCS processes to analyze and improve the flexibility of the process [189,196,218]. Although this approach provides valuable information about membrane performance at different operating conditions, it cannot consider various time-dependent operating variables which can significantly affect the design and operation of the system. Dynamic modeling is necessary for the realistic design of the membrane gas separation process since it can estimate transient behaviors at start-up, shut-down and the system transient behavior toward disturbances in the process.

Several methods and tools for the dynamic modeling of membrane modules for gas separation have been developed to analyze the system's dynamic performance. Bouton and Luyben [219] developed a transient model for both cross-flow and counter-flow membrane configurations using differential equations for gas mole fractions. They assumed steady-state conditions in the formulation and used the flow resistance parameter and pressure drop to calculate the total molar flowrates of the product streams. Tanks in-series approach for multicomponent gas separation in membrane module was implemented by Katoh et al. [220]. They have considered nonideal mixing flows in the retentate and permeate sides, and the governing ordinary differential equations are simultaneously solved using a relaxation method that uses steady-state solutions based on the steady profiles of pressures and component concentration to calculate the time-dependent variables of the model. Daeho Ko [199] provided detailed dynamic modeling of a bore-side feed hollow fiber membrane module with a counter-current flow structure to separate CO_2 from coalbed methane. Scholz et al. [221] proposed a dynamic simulation of a hollow fiber gas separation module for biogas upgrading processes to study control schemes for maintaining a required constant product purity. Also, the non-retentate flow withdrawal operation of a cross-flow gas

separation membrane module has been studied by Trubyanov et al. [183] by developing unsteady-state modeling to optimize a pulsed-retentate separation technique.

All of the studies above generally focused on mathematical modeling of the membrane separation process in an unsteady state, and the system's dynamic response toward variations in operating conditions, which reflects the flexible operation of the membrane system, has not been investigated. Additionally, many mathematical models usually rely on several fixed assumptions, such as constant membrane permeability and selectivity. Also, most of the proposed models have been formulated for simulating the steady-state operation of the membrane system rather than the unsteady state condition. However, as mentioned before, due to strong interactions between membrane-based CCS with other components of a low carbon energy system, flexible operation of the membrane process is of great importance to attain satisfactory control performance. In this regard, studying the dynamic behavior of the membrane process can provide practical information for rational system design, process start-up and shut-down, the transition between two steady states, control, and operational strategies for flexible operation and response to the variation of fossil-fueled power plant operation.

2.6 Process integration and hybridization of CCS

Among the fossil-fueled power plant options, NGCC power plants are favored due to their moderate capital costs, lower emissions, shorter construction times, and high efficiency and flexibility [222]. These characteristics make NGCC power plants attractive for integrating CCS technologies, enabling effective reduction of CO_2 emissions while maintaining efficient and reliable electricity generation. Currently, the average carbon intensity of global power plants stands at approximately 475 gCO_2/kWh, which is still far from the required global average of 100 gCO_2/kWh by 2050 to align with the climate goals [223]. To achieve the designated emissions reduction targets, CCS implementation is necessary. However, as mentioned before, integrating carbon capture technologies with power plants faces several challenges, as this integration results in a considerable energy penalty and increased electricity costs. Particularly in NGCC power plants, where the CO_2 concentration is much lower (around 4 mol.% compared to 15 mol.% in coal-fired power plants), the specific regeneration heat for amine-based CCS is higher since the energy penalty associated with CO_2 capture increases as the CO_2 concentration in the feed decreases [30,70]. Specifically, by integrating amine-based CCS with the NGCC plant, the power

plant net efficiency reduces by 7%, and the cost of electricity could increase from 57.1 to 84.3 $/MWh, resulting in a capture cost of 86.6 $/ton of CO_2 [13,49]. Therefore, developing CO_2 separation technologies along with optimal process design and integration is crucial to minimize the thermal energy demand and the capture cost of the post-combustion carbon capture process.

The thermal energy required for operating a post-combustion carbon capture system in a power plant is often met by extracting low-pressure steam from the turbine, which reduces the overall energy efficiency of the power plant [224]. Additionally, in this process, the thermal energy requirement for CO_2 removal is typically fulfilled by burning extra fossil-fuel, resulting in further CO_2 emissions. One potential solution to mitigate the energy penalty associated with PCC plants in fossil-fueled power plants is integrating solar thermal energy with the carbon capture system [225]. The schematic of this integration is presented in Fig. 2-19 [154]. This approach not only reduces the reliance on the power plant for thermal energy but also helps to increase the overall efficiency and sustainability of the carbon-capturing system.

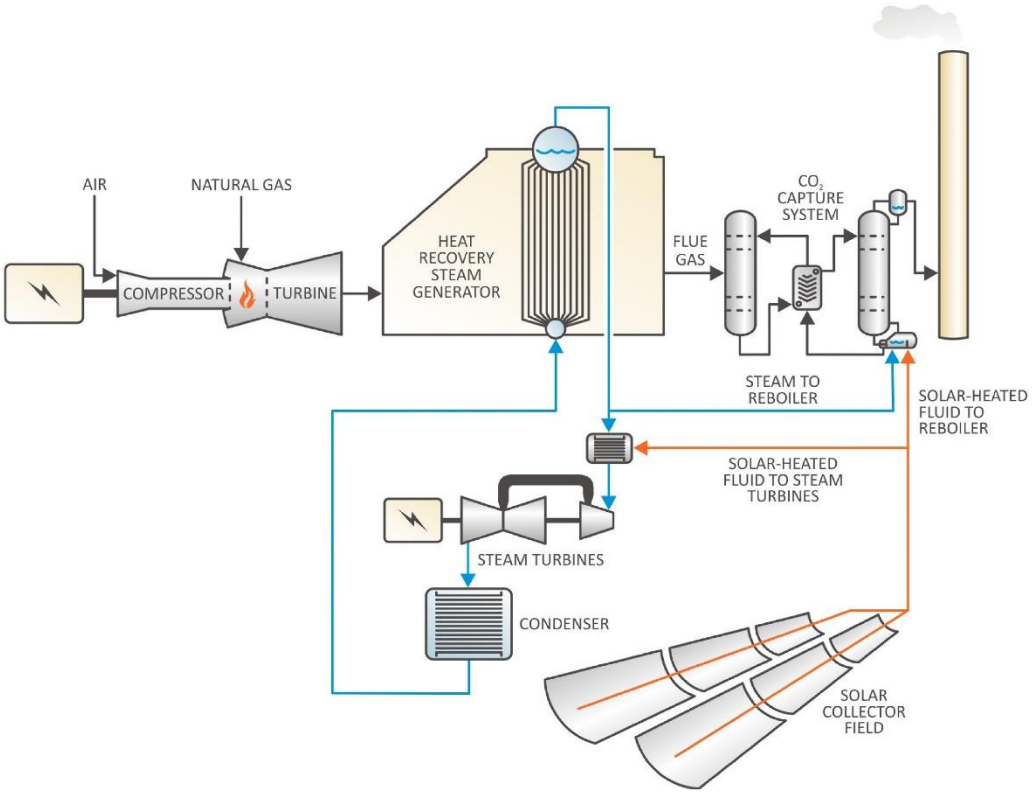

Fig. 2-19. Integration of solar collectors with stripper reboiler duty

Integrating Concentrated Solar Power (CSP) with Thermal Energy Storage (TES) for providing heat to the PCC systems, as presented in Fig. 2-20, offers a particularly suitable solution [226]. This integrated system has the potential to play a crucial role in transitioning to a sustainable power generation system, reducing energy penalties from the integration of CCS with power and industrial sectors [227]. Despite potential investment requirements, the cost of solar energy equipment has decreased in recent years, and the limitations of relying on sunlight can be mitigated by considering thermal energy storage [228]. Concentrated solar power (CSP) is particularly well-suited to being integrated with PCC, as the temperature needed in the reboiler is typically around 120°C, and commercially available CSP systems can supply this required temperature [229,230]. Various studies have explored the feasibility and benefits of integrating solar energy into carbon-capturing systems, aiming to enhance the performance and environmental impact of coal-fired power plants [230–232]. In a study conducted by Bravo et al. [154], parabolic trough collectors (PTC) were integrated into an NGCC (Natural Gas Combined Cycle) power plant and CO_2 capture system in two different scenarios: integration with the PCC reboiler and LP steam heating. The results indicated that utilizing solar thermal steam generation for the PCC reboiler was more efficient compared to LP steam heating. Moreover, if the solar PTC field could fully meet the reboiler duty requirements, around 5.5% increase in the net efficiency of the power plant could

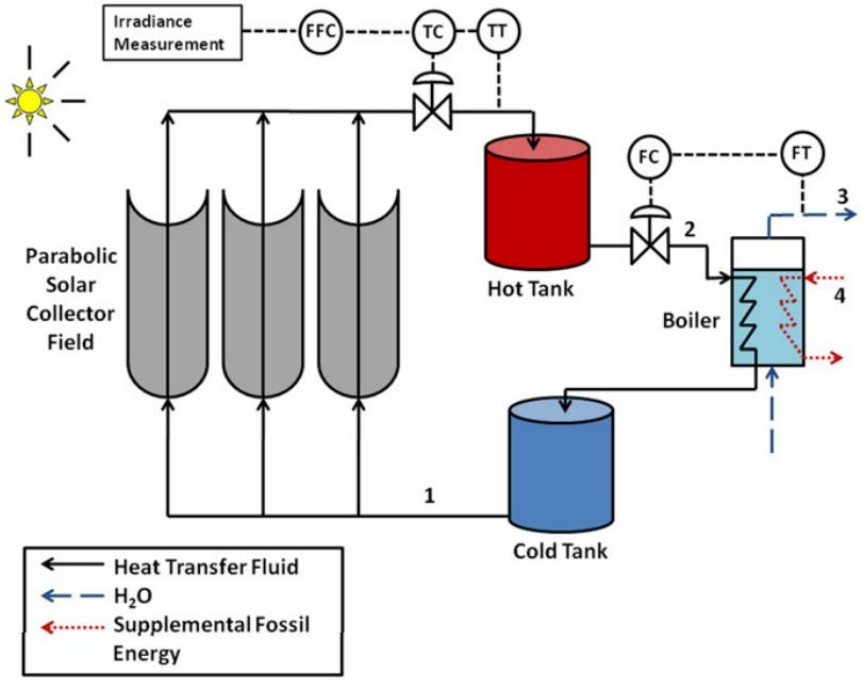

Fig. 2-20. Integration of solar collector with thermal energy storage tanks [226]

potentially be achieved. However, the economic performance of the integrated system and the potential impact of thermal energy storage to address the intermittency of solar energy has not been evaluated.

On the other hand, several studies have focused on optimizing the design, integration, and operation of the CO_2 capture plant, enhancing the energy efficiency and cost-effectiveness of the integrated NGCC with CCS technology, making it more viable and attractive for widescale implementation [66,152,216,233]. Although NGCC plants are considered potential candidates for implementing CCS technologies, the high flow rate of exhaust gas with low CO_2 concentrations presents challenges for integrating post-combustion CCS [234]. This requires large CO_2 capture reactors to accommodate the high flowrates, operating at low CO_2 separation driving forces that increase the energy needed for separating CO_2 and the size of the PCC plant [235]. In this regard, new process modifications such as exhaust gas recirculation (EGR) have been suggested to address the limitations of low CO_2 concentration and optimize CO_2 capture processes in NGCC power plants. This process involves recycling a portion of the exhaust gas exiting the heat recovery steam generator (HRSG) system. This recycled flue gas is cooled and then introduced into the inlet of the compressor, thereby replacing a portion of the air that enters the compressor [63,236–238]. It has been reported that recycling 30–40% of the exhaust gas to the inlet air stream could raise the CO_2 concentration in the flue gas to approximately 7 vol.%, meanwhile decreasing the volumetric flowrate of the flue gas, which resulted in the reduction of energy penalty and capital cost of PCC [32,239–241]. Li et al. [242] found that applying 50% recirculation ratio can raise the CO_2 concentration to 7.9% while simultaneously reducing the inlet flow rate of the absorber by 51%. This modification led to 8% reduction in reboiler energy consumption, from 4 to 3.7 MJ/kg CO_2. Biliyok and Yeung [238] also reported that at a 40% EGR ratio, the CO_2 concentration can be increased from 4% to 6.6%, resulting in 7.5% reduction of the reboiler duty. Also, the volume of absorber packing is decreased by increasing the ratio of flue gas recirculation. Nonetheless, the extent to which Exhaust Gas Recirculation (EGR) can be implemented is constrained by the need to maintain a certain oxygen concentration, typically around 16% vol, in the air stream of the gas turbine compressor. This precaution is essential to avoid issues related to flame stability and combustion efficiency [243].

Additionally, It has been reported that the Levelized Cost of Electricity (LCOE) of the power plant integrated with EGR and CCS could be decreased by 2-4% [32]. The extent to which

Exhaust Gas Recirculation (EGR) can be implemented is constrained by the need to maintain a certain oxygen concentration, typically around 16% vol, in the air stream of the gas turbine compressor, as this precaution is essential to avoid issues related to flame stability and combustion efficiency [244]. To overcome this limitation, hybrid carbon capture systems have been proposed, mainly by integration of the conventional amine-based CCS with CO_2 selective membrane modules for Selective Exhaust Gas Recirculation (SEGR) in NGCC flue gas [165,192,245]. Hybrid membrane-solvent processes have the potential to significantly enhance the performance of post-combustion carbon capture by leveraging the advantages of both absorption and membrane technologies in a synergistic manner [186,246]. Merkel et al. [235] suggested integrating a CO_2 selective membrane process into the power plant to achieve higher CO_2 concentration in the flue gas (potential above 15 mole%) without affecting the oxygen concentration in the inlet air. Herraiz et al. [165] proposed the technology of selective CO_2 recirculation using physical adsorption in a rotary wheel configuration. The configuration utilizes a rotary wheel with selective porous material for CO_2 adsorption. Flue gas contacts the solid material for CO_2 absorption at a lower rotational velocity, and the separated CO_2 is directed into a counter-current air flow. Diego et al. [239,247] conducted a techno-economic analysis of CO_2 selective membrane and amine-based CCS (Carbon Capture and Storage) plants, considering parallel and hybrid parallel/series designs. They demonstrated that a parallel design with a SEGR recycle ratio of 53% could achieve 90% CO_2 recovery and raise the CO_2 concentration in NGCC exhaust gas to 18%vol by hybrid parallel and series design. They reported that the power plant net efficiency and thermal requirement of the capture plant are improved compared to the baseline case. However, they reported that the cost of electricity and the cost of CO_2 avoided considerably increased by almost 10% and 25%, respectively. Considering the minimum oxygen requirement in the gas turbine inlet air stream, in the case of stand-alone SEGR, it has been reported that the flue gas CO_2 concentration significantly increases from less than 4 mole% in the baseline case to about 18 mole% at 76 percent SEGR ratio. In contrast, in the stand-alone EGR where 40% of flue gas is recycled back, the concentration in the flue gas is about 6.5 mole%. The EGR strategy is more favorable in terms of capital cost requirement, while the SEGR design is capable of significantly increasing the CO_2 concentration leading to lower energy specific reboiler duty and capital cost PCC plant, but it requires considerable capital investment for the membrane-based system [247]. Qureshi et al. [248] analyzed the part load performance of parallel, series, and hybrid configurations of SEGR systems integrated with an NGCC plant. Their study showed that the NGCC power plant with SEGR

presents stable operation with a slight decrease in efficiency at partial loads. However, they have assumed a hypothetical simple component splitter model in Aspen Plus for modeling selective exhaust CO_2 separation. Baker et al. [233] investigated the post-combustion CO_2 capturing from the NGCC power plant equipped with multi-stage membrane separation and selective exhaust gas recirculation. It has been reported that although membrane-based CCS with SEGR leads to a significant reduction in the energy requirement of CO_2 capture, the large membrane area required by this process is a key issue that needs to be addressed.

By optimal design and hybridization of both amin-based and membrane-based CCS, it is possible to harness their complementary strengths and overcome their individual limitations. On the other hand, it is critical to study and analyze the performance of the integrated system both in terms of economic and technical indicators to ensure the viability of the developed process for commercialization. Besides the importance of the techno-economic performance of the integrated NGCC plant with CO_2 capture, the other crucial aspect of the system is flexible operation, which includes both steady-state design and part-load off-design performance [201]. As mentioned before, by increasing share of intermittent renewable energy sources in the energy mix and lack of commercially available energy storage systems, fossil fuel-based power plants will continue to play a crucial role in providing balancing energy by operating at part load conditions to adapt to fluctuating energy demands [200]. Accordingly, evaluating and ensuring operational flexibility of new alternative designs for the decarbonization of the NGCC plant is vital for its successful implementation and long-term sustainability in the electricity market. Literature is scarce on the analysis of the part-load operation of NGCC plants with CO_2 capture, specifically for novel designs and integration. Rezazadeh et al. [150] studied the part-load performance of the conventional integration of NGCC with PCC. Alcaraz-Calderon et al. [249] assess the part-load performance of an NGCC power plant that incorporates exhaust gas recirculation and an amine-based CO_2 capture plant. Ven der Spek et al. [218] compared the part-load techno-economic performance of the NGCC plant with selective exhaust gas recirculation with the conventional process. They reported that the electricity costs are higher in partial loads compared to full-load operation. Also, Qureshi et al. [248] examined the part-load performance of the NGCC plant integrated with various CO_2 concentrating schemes using a hypothetical simple component splitter model in Aspen Plus software. Their findings demonstrated that the integrated system maintained stable operation even at partial loads, albeit with a slight decrease in efficiency. However, the impact of high CO_2

concentration and altered air properties resulting from selective exhaust recirculation on the full load and partial load performance of the NGCC plant is still a subject of discussion and needs to be addressed.

2.7 Chapter Summary

In this chapter, a detailed literature review in the field of CO_2 capture system and power plant decarbonization is performed to address the first research question (RQ1) by providing an overview of the recent progress, developments, and challenges in CO_2 capture technologies. In this regard, the available CO_2 capture technologies for power plants can be categorized as post-combustion, pre-combustion, and oxy-fuel combustion methods. Depending on the specific characteristics of the gas stream requiring CO_2 separation, multiple technologies can be utilized, such as adsorption, physical/chemical absorption, membrane separation, and cryogenic separation. Previous studies contributed to an enhanced understanding of process improvements and modifications that makes CO_2 capturing from the NGCC power plant more efficient and viable. Despite significant advancements, there are ongoing challenges in the sustainable design and flexible operation and integration of carbon capture systems with fossil-fueled power plants. These challenges primarily revolve around reducing costs, minimizing energy penalties, and enhancing the flexible operation of solar-integrated systems. Addressing these gaps is essential as it enhances the efficiency and viability of these integrated systems for large-scale deployment, making a valuable contribution to global efforts in combating climate change.

Chapter 3. Multi-Stage Membrane-Based Process for Power Plant Decarbonization

- ? **Research questions: RQ2-** How can the technical performance of membrane-based carbon capture technologies be improved to enhance their efficiency and effectiveness in capturing and storing carbon dioxide?
- ➢ **Objective:** Component and system-level simulations and techno-economic investigation of the membrane-based CCS
- ✓ **New knowledge:** The technical performance and cost of membrane technologies in various designs scenarios and operation conditions imposed by upstream power plants

In this chapter, a comprehensive techno-economic assessment of several membrane separation processes is performed to investigate the potential and viability of such systems as a flexible CCS technology for integrating into future low-carbon power plants. The technical model combines lumped system models integrated with a distributed and mechanistic membrane model that can predict the spatial distributions of all species along the membrane length in different configurations. The economic model comprises different cost factors for the capital cost, energy cost, and operation cost of the system components. Both models are employed to evaluate four system designs with three membrane types. The impacts of several decision-making parameters, such as the feed pressure and membrane properties, are fully investigated.

3.1 Introduction

As a breakthrough step toward developing an optimal system for decarbonizing the future grid involving flexible CCS, energy storage, renewable resources, and fossil fuel power plants, this chapter discusses a comprehensive techno-economic analysis of membrane separation systems for post-combustion CCS. The objective of this chapter is to determine and evaluate the performance, cost impacts, and flexibility of membrane-based CCS systems by varying operating parameters and membrane properties to simultaneously obtain 90% CO_2 recovery and 95 mole% CO_2 purity in the permeate gas. Accordingly, three potential CO_2-selective polymeric membranes

are selected, and the effects of key process parameters, including feed pressure, feed CO_2 concentration, recycle ratio, sweep gas flowrate, and CO_2 recovery ratio, on the process performance and cost of membrane-based CCS are examined. Moreover, further investigations are performed to study the effects of membrane properties, selectivity, and permeability on the system energy consumption and capture cost. Finally, different designs of the membrane separation process, including various compression strategies and membrane flow patterns, are compared from technical and economic viewpoints to find an appropriate design for improving the flexibility of the membrane-based CO_2 capture system.

3.2 Method

3.2.1 Membrane-based CCS in a low-carbon energy system

A membrane-based post-combustion CCS can be easily retrofitted to fossil fuel power plants to significantly reduce the CO_2 emissions produced by the gasification process or combustion. However, there are several challenges, such as energy-intensive operation and the high cost of the CO_2 separation system, which affect the reliability and the cost of electricity generation. A coal-fired power plant with 600 MW gross power capacity releases approximately 500 m^3/s of flue gas, significantly larger than the input of a typical CO_2 absorption unit in natural gas refineries [127]. Besides, the CO_2 partial pressure in typical power plants is lower than 0.15 bar, which implies a very low available driving force for separation and the need for creating an artificial CO_2 partial pressure difference. Also, the power plant's flue gas requires to be treated to remove contaminants, including ash, SO_x, NO_x, and water, which further increases the cost of CO_2 separation from flue gas with available technologies.

The schematic of a basic two-stage membrane system integrated with a 600 MW coal-fired power plant is presented in Fig. 3-1. The 500 m^3/s of flue gas generated in the power plant is sent to the particulate and water removal units in order to separate its contaminants before entering the CCS unit. In the membrane-based CCS process, the flue gas with almost atmospheric pressure and temperature of 50 ℃ enters the compression section (outlet pressure: 5 bar) to provide the required driving force for CO_2 separation. The compressed gas enters into a series of heat exchangers to be cooled to 50 ℃, then enters the first stage of the membrane separation system. The required energy for the equipment operation in the CCS units is provided by the power plant. The permeate stream exits the first membrane at 1 bar and enters to compressor and heat exchangers to be prepared for

the next stage of the membrane. In the second stage, the permeate stream is enriched from CO_2, and the retentate stream, enriched from N_2, is mixed with the first-stage retentate and enters the turboexpander for the partial recovery of energy used by the compressors. The captured CO_2 exits the CCS units in order to be utilized in other processes or transported to safe storage to retain it for long periods.

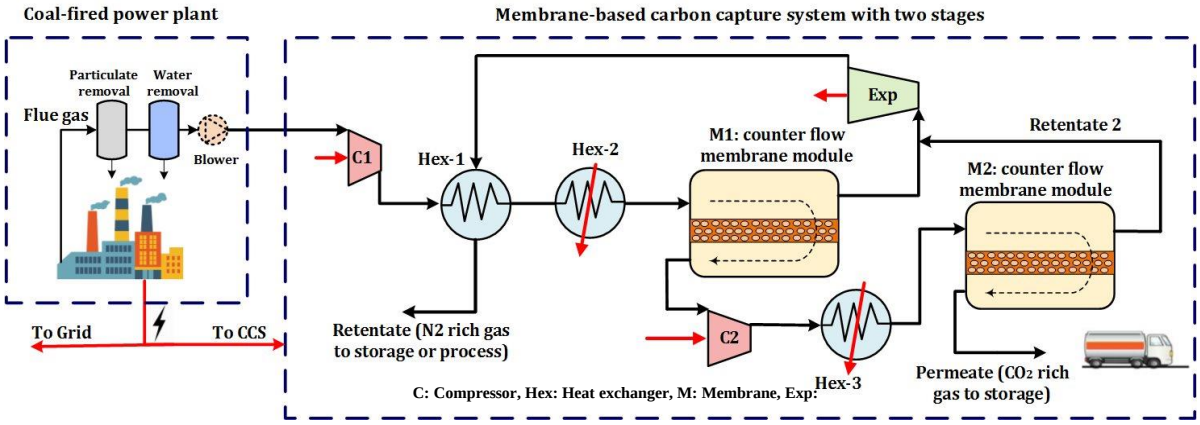

Fig. 3-1. The base case of a two-stage membrane separation unit integrated with a coal-fired power plant

3.2.2 Mathematical modeling of the membrane system

There are two types of gas permeation modules suitable for the CCS application, i.e., spiral wound and hollow fiber. For the modeling of CO_2 separation by the membrane system, a hollow fiber module is beneficial since the permeate pressure drop effects can be described by basic principles, and the flow patterns can be considered as one dimension. Accordingly, in this study, the mathematical model for both counter-current and crossflow for the hollow fiber membrane is considered using the modeling strategy reported by Shindo et al. [250], which was widely adopted in previous works [251,252]. Fig. 3-2 represents a schematic of the gas permeation in a counter-current hollow fiber membrane module. The flue gas enters the shell side of the module and permeates to the fiber's bore, and the retentate stream (N_2 enriched) exits from the end of the module. On the other hand, the permeate stream enriched from CO_2 exists from the feed side with the assist of sweep gas (optional), which enters the fiber bore side in the opposite direction of the feed.

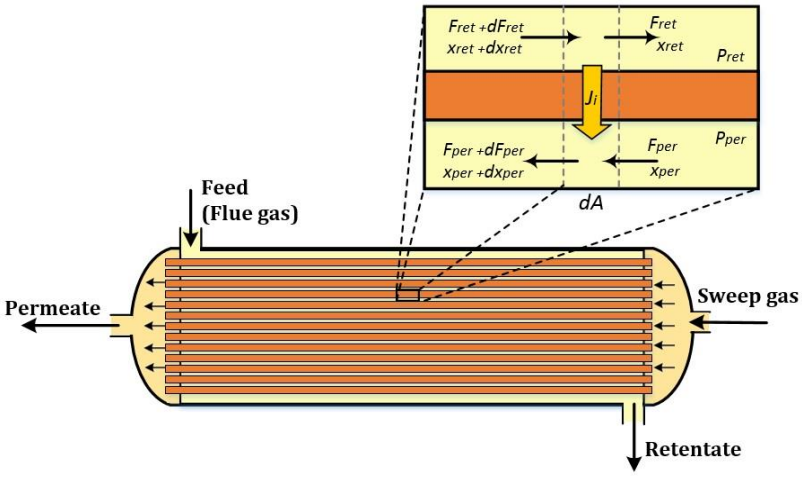

Fig. 3-2. Gas permeation in a counter-flow membrane

The considered assumptions to derive the mathematical formulations are as follows:

- The fibers are identical and straight with a uniform thickness.
- The variation of concentration and pressure in the radial axis is negligible.
- Membrane permeability is independent of pressure and temperature.
- The gas mixtures are assumed to be ideal gas.
- The pressure drop is calculated by the Hagen-Poiseuille equation.
- The effect of concentration polarization is neglected.
- The membrane model is isothermal and steady-state.

The gas separation across the selective membrane is assumed to follow the solution-diffusion mechanism, in which the permeance is the controlling parameter. Referring to Fig. 3-2, the permeation of a multi-component gas mixture can be described as follows:

$$J_i = 2\pi r_{FO} n_F \frac{Q_{CO_2}}{\alpha_i}\left(P_{ret} y_{ret,i} - P_{per} y_{per,i}\right) \qquad (1)$$

$$J_t = \sum_{j}^{n} J_j \quad (2)$$

$$\alpha_i = \frac{Q_{CO_2}}{Q_i} \quad (3)$$

where J_i is the permeation rate of component *i*, Q_i is the permeance of component *i* (permeability of component *i* divided by the thickness), α_i is the selectivity of component *i*, r_{FO} is the fiber outer radius, n_F is the number of fibers, *P* is the pressure, $y_{ret,i}$ is the mole concentration of component *i* in the shell side, and $y_{per,i}$ is the bulk composition of component *i* in the bore side.

The total molar balance of fiber bore can be described by Eq. 4 as follows:

$$\frac{dF_{per}}{dx} = -J_t \quad (4)$$

The pressure drop in the bore side can be calculated by the Hagen-Poiseuille equation [253]:

$$P_{per}\frac{dP_{per}}{dx} = \frac{16RT\mu F_{per}}{\pi r_{FI}^4 n_F} \quad (5)$$

The components' molar balance in the fiber bore is:

$$\frac{d(F_{per}y_{per,i})}{dx} = J_t\, y_{per,i} - J_i \quad (6)$$

The total molar balance in the shell side of the membrane module is:

$$\frac{dF_{ret}}{dx} = -J_t \quad (7)$$

The pressure drop of retentate that exits from the shell side is calculated as:

$$\frac{dP_{ret}}{dx} = \frac{8\mu}{r_H^2} V_{ret} \quad (8)$$

The components *i* molar balance in the shell side is presented in Eq. 9.

$$\frac{d(F_{ret} y_{ret,i})}{dx} = J_t \, y_{ret,i} \, - J_i \quad (9)$$

The above system of differential equations, as well as boundary conditions, physical properties of components, and other equations, are programmed in the Aspen Custom Modeler. The axial domain has been discretized by a 2nd-order central finite difference method, and it is found that considering 400 divisions is acceptable to achieve reliable and valid results. The set of equations is solved using Aspen Custom Modeler built-in DMO solver, which is very robust and generates results within almost one minute using a typical laptop with Intel Core i7-10510U CPU@1.80-2.30 GHz and 16 GB RAM. Furthermore, the membrane length is assumed to be 1 m, and the inner and outer diameter of the membrane is 400 and 600 µm, respectively. Two versions of mathematical modeling are considered for counter-current flow patterns, including with and without a sweep stream inlet.

For modeling the crossflow case, the direction of the permeate stream is vertical to the direction of the feed stream over the membrane surface area. In this flow pattern, the local concentration of a component on the permeate side is equal to the portion of gas that passes through a specific point of the membrane. More details of crossflow membrane modeling are provided in references [250,254].

3.2.3 Simulation of two-stage membrane-based CCS

After modeling the counter-flow membrane in Aspen Custom Modeler, the membrane module is used as a user-defined model in the Aspen Plus software for simulation of the whole CO_2 separation process. For modeling the general equipment such as compressor, expander, and heat exchanger, the built-in models available in the Aspen Plus model library have been used. The

detailed mathematical modeling of this equipment can be found in the user manual of Aspen Plus software as well as Ref. [255].

The Peng-Robinson thermodynamic model is considered for the modeling of gas behavior in the process. The efficiency of all rotary equipment is assumed to be 85%. It is assumed that after passing from the particulate and water removal units, the input flue gas of the CCS system is a binary gas consisting of CO_2 and N_2. This assumption and system modeling hypotheses are widely justified in previous studies [256–258].

Regarding the simulation results for the base case of CO_2 separation by a two-stage membrane system (as shown in Fig. 2), it is considered that the overall CO_2 recovery of the system is fixed at 90%. As a result, the permeate gas is enriched from CO_2 with a purity of 73.5 mole%, and the retentate gas is enriched from N_2 with a purity of 98.4 mole%. Also, the total membrane area of 1.807 million m^2 is required 111.7 MW of power plant capacity consumed by compressors to reach the mentioned performance of the base case system for 500 m^3/s of flue gas, including 13 mole% of CO_2.

In the simulation of the membrane CO_2 separation process, the separation targets can be defined for the membrane module in the Aspen Plus software. Accordingly, it is possible to fix the purity of products or CO_2 recovery of each membrane stage, and the required area of the membrane is adjusted at each trial-and-error step until reaching the specified targets. Using this approach gives the opportunity to perform a comprehensive evaluation of membrane-based CCS.

3.2.4 Various membrane process designs and CO_2-selective membranes

As discussed before, the driving force for CO_2 permeation in a gas separation membrane is the difference in the partial pressure of the feed and permeate side. Due to the low CO_2 partial pressure in the post-combustion flue gas, great effort should be placed to achieve an adequate driving force with lower energy consumption. In this regard, various modifications can be proposed to address the driving force challenge, considering a compressor at the membrane feed inlet, using a vacuum pump at the membrane permeate outlet, increasing the feed CO_2 concentration by recirculation, and reducing the CO_2 concentration in permeate by a sweep gas. At a specified CO_2 recovery and product purity, considering each of these designs can significantly affect the system cost and process energy consumption. On the other hand, different flow

configurations of the membrane impact the performance and required membrane area. Therefore, for evaluating and comparing different designs of membrane separation systems for CO_2 capture from a power plant flue gas, four different concepts are considered to cover various designs of membrane-based CCS. Concept A: feed compression and crossflow membrane modules. Concept B: feed compression, counter-flow membrane module, and sweep gas. Concept C: vacuum pump and crossflow module. Concept D: vacuum pump and counter-flow module. The schematic of the proposed concepts is demonstrated in Fig. 3-3.

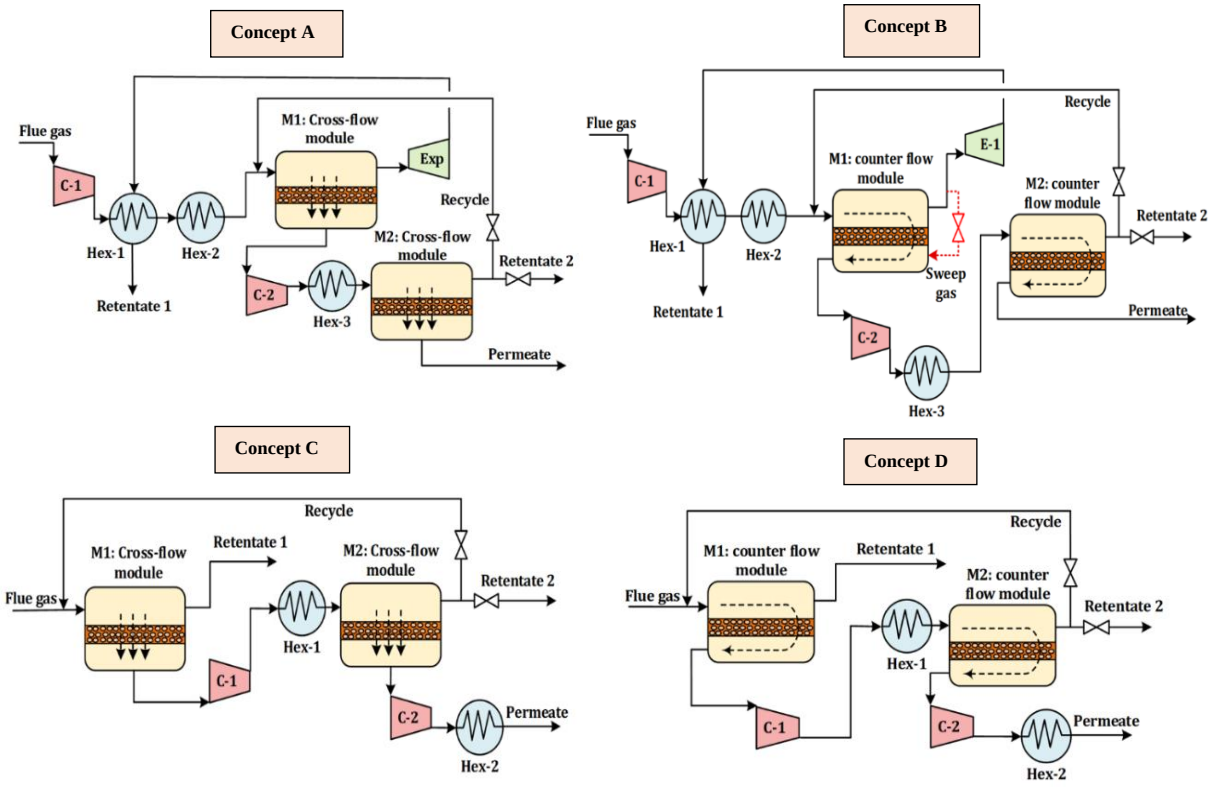

Fig. 3-3. Various designs for membrane-based CO_2 capture

The selection of a membrane with appropriate CO_2 selectivity and permeability can lead to an improvement in the performance of membrane-based CCS. Accordingly, the effect of membrane properties (selectivity and permeability) on the performance of the system, as well as the behavior of various membranes at different operating conditions, are investigated by considering three polymeric membranes. The considered membranes cover a wide range of selectivity and permeability, from existing polymeric membranes with CO_2/N_2 selectivity of about 50 and high permeability to more CO_2-selective membranes such as facilitated transport polymeric

membranes with CO_2/N_2 selectivity of more than 100. In this regard, the first generation of Polaris™ membrane (Polaris gen1) and the second generation of Polaris™ membrane (Polaris gen2) are considered, which have high CO_2 permeance equal to 1000 and 2000 GPU, respectively [126]. Besides this high CO_2 permeance, the first and second generation of Polaris membranes has a moderate CO_2/N_2 selectivity of 50 and 49, respectively. Also, the PVAm/PG as a facilitated transport polymeric membrane is considered, which demonstrates a high CO_2/N_2 selectivity of 148 and good CO_2 permeance equal to 735 GPU at pilot-scale tests [129].

To analyze the techno-economic performance of the CCS with various membranes, the membrane degradation over time is not considered due to the lack of experimental data, and it is assumed the membranes are chemically and thermally stable during the operation. More information regarding membrane degradation and stability is provided in the references [217,259].

It is worth noting that although the PVAm/PG, as a facilitated transport membrane, follows the reaction-diffusion mechanism and CO_2 partial pressure has a considerable effect on its permeability, the separation process can be simplified by considering the solution-diffusion mechanism, which neglects the mass transfer by the carrier effect [260,261]. In other words, the PVAm/PG membrane is modeled as a common polymeric membrane that follows the solution-diffusion mechanism and has constant CO_2 permeance and CO_2/N_2 selectivity equal to 735 GPU and 148, respectively. This assumption is considered in the modeling since the research goal of this chapter is to study the techno-economic performance of membrane-based CCS at various values of membrane selectivity and permeability rather than to study the influence of different transport mechanisms and membrane types that generally needs experimental data.

3.2.5 Cost evaluation

To perform an economic analysis of membrane-based CCS, different cost factors are considered for the capital cost (membrane and its frame, compressor, vacuum pump, heat exchanger, and turboexpander), energy cost, and O&M (operation and maintenance) cost. The procedure to calculate the CO_2 capturing cost by membrane process is presented in Table 3-1, which is comparable to those reported by previous works.

Table 3-1. Assumption and equipment cost for economic evaluation [16,31,45]

Category	Value
Membrane module cost ($/m^2)	50
Total membrane cost ($)	$I_{mb} = A_{mb,tot} \times 50$
Membrane frame cost ($)	$I_{mb\ frame} = 238 \times 10^3 \times \left(\frac{A_{mb,tot}}{2000}\right)^{0.7} \times \left(\frac{P_{mb}}{55}\right)^{0.88}$
Compressor cost ($)	$I_c = F_c \times 0.0224 \times 1.8 \times 96 \times 10^3$
Vacuum pump cost ($)	$I_{vp} = F_{vp} \times 0.0224 \times 1.8 \times 4 \times 96 \times 10^3$
Expander cost ($)	$I_{exp} = W_{exp} \times 0.5 \times 1.8$
Heat exchanger cost ($)	$I_{hex} = F_{hex} \times \frac{3.5}{440} \times 10^6$
Depreciation factor (25 years)	$\mathrm{DF} = 0.064$
Membrane depreciation factor (5 years)	$\mathrm{DF}_{mb} = 0.225$
Total annual capital cost ($)	$I_{TC} = \left(I_{mbf} + I_c + I_{vp} + I_{ex} + I_{hex}\right) \times DF + I_{mb} \times \mathrm{DF}_{mb}$
Total annual operation and maintenance cost ($)	$I_{O\&M} = 0.01 \times \left(I_{mb} + I_{mb\ frame}\right) + 0.036 \times \left(I_c + I_{vp} + I_{exp} + I_{hex}\right)$
Operational time (hr/year)	$t_{op} = 8000$
Electricity cost ($/kW h^{-1})	$EC = 0.04$
Cooling water cost ($/GJ)	$CWC = 0.354$
Total annual energy cost ($)	$I_{EN} = t_{op} \times \left(EC \times \left(W_c + W_{vp} - W_{exp}\right) + CWC \times Q_{hex}\right)$
Total annual cost ($)	$I_{Total} = I_{TC} + I_{O\&M} + I_{EN}$
Total operational cost ($)	$OPEX = I_{EN} + I_{O\&M}$
Compressor and vacuum compressor efficiency	0.85
CO_2 capture cost ($/ton$CO_2$)	$I_{CO_2} = \frac{I_{Total}}{Annual\ seprated\ CO_2}$

There are several uncertainties about the power cost and the cost of various polymeric membranes. For instance, membrane degradation and durability over a long operational time is an uncertainty in the economic analysis. In this study, the average cost of 50 $/m^2 has been considered, which is widely used in previous works [178,191]. Even though the cost estimation of a large-scale membrane-based CCS may involve substantial uncertainties (−15% to −30% on the low side

and +20% to +50% on the high side [262]), the relative cost comparison of various system designs and different operating conditions using the specified assumptions and cost functions are still valid and notable.

3.2.6 The framework of techno-economic analysis

The proposed framework for the techno-economic analysis of membrane-based carbon capture is presented in Fig. 3-4. The framework of techno-economic analysis is divided into three steps. First, the membrane system for different flow patterns is modeled in the Aspen Custom Modeler. Afterward, four different designs of membrane processes for CO_2 separation are considered and simulated in the Aspen Plus software. Also, three potential membranes covering a wide range of selectivity and permeability are considered to comprehensively evaluate the system performance. In the second step, process parameters' effects on the required area of various membranes as well as the required energy, are investigated at a given separation target. The main variables influencing the process performances are:

- The concentration of CO_2 in flue gas
- The pressure of the feed stream to the membrane module
- Recycle ratio, which indicates the amount of second-stage retentate which recycle to the feed of the first stage
- CO_2 permeance and selectivity of the membrane
- The CO_2 recovery ratio.
- Sweep gas flowrate

In the third step, the modeling of process costs, including capital cost, O&M cost, and energy cost, is implemented to examine the influence of the variation of process parameters on the CO_2 capture cost. Finally, the various designs of CO_2 separation by the membrane are compared and evaluated from the techno-economic point of view.

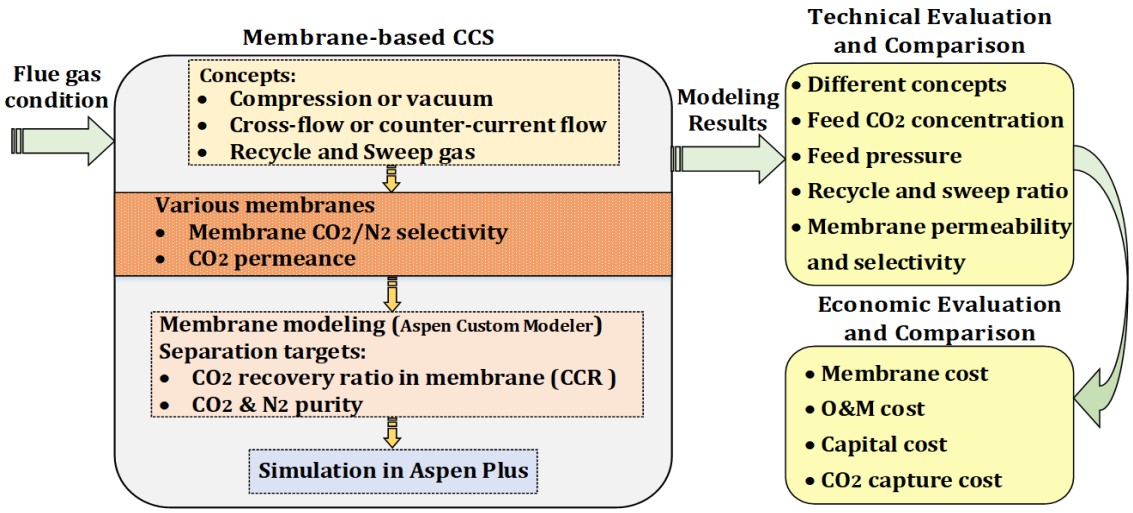

Fig. 3-4. Schematic of proposed framework for techno-economic analysis of membrane-based CCS

Throughout the system techno-economic analysis, the separation target has been considered as achieving 90% CO_2 capture ratio and 95 mole% CO_2 purity in the second stage permeate stream. Since the single-stage membrane process cannot reach the separation goal, a two-stage membrane process needs to be considered for techno-economic analysis. Among the proposed concepts, Concept B with counter-current flow pattern and retentate recycling has been considered for analyzing the effect of various designs and operating conditions since this membrane configuration has been suggested by previous works as a promising design, and the effect of sweep gas can be studied in this case. Finally, the techno-economic performance of all proposed concepts is compared at specific operating conditions.

3.3 Results and Discussion

3.3.1 Model validation

The developed mathematical model for calculating the performance of both counter-current and crossflow membrane processes is validated with the model presented by Merkel et al. [127], and the results are shown in Table 3-2. The flue gas conditions are assumed to be 500 m^3/s, 1.1 bar, 50 °C, and 13 mole% of CO_2. Also, the CO_2 recovery ratio and permeate pressure are fixed at 0.9 and 0.22, respectively. The validation results show an excellent agreement with the

maximum absolute percentage error of less than 1%. The small error is attributed to the numerical approach, solver, and the number of discretization elements.

Table 3-2. Validation of membrane modeling with the work by Merkel et al. [16]

	Counter-current flow		**Crossflow**	
Membrane module properties	**Modeling results**	**The work by Merkel (2010)**	**Modeling results**	**The work by Merkel (2010)**
Membrane area (m^2)	6.77×10^6	6.80×10^6	10.91×10^6	11.00×10^6
CO_2 mole% in permeate	40.57	40.60	28.86	28.90
CO_2 mole% in retentate	2.09	2.10	2.08	2.10
Abs. Maximum error	0.47 %		0.95%	

3.3.2 Technical analysis of the membrane process

In the following sections, we analyze and discuss important operational parameters and process design considerations of a two-stage counter-current membrane process for CO_2 separation. Furthermore, it has been discussed how this chapter's findings can be reconciled to develop an efficient and cost-effective CO_2 separation system.

3.3.3 Effect of retentate recirculation

The recycle ratio is defined as the ratio of the retentate stream flowrate that is recycled to the first stage feed. For analyzing the influence of the recycle ratio on the performance of a two-stage membrane system (Concept B), the overall CO_2 recovery of the system is fixed at 90%, the Polaris gen1 is considered as a membrane, and the feed pressure and permeate pressure are fixed at 5 bar and 1 bar, respectively. It should be noted that in a two-stage membrane system with high CO_2 recovery, permeate enriching by recycling second-stage retentate gas is required to achieve a high CO_2 purity in the gas permeate [185]. Accordingly, to cover a wide range of recycle ratios and to study the effect of retentate recycling on the CO_2 purity of permeate stream, the separation target of 95 mole% permeate CO_2 purity is not taken into account. Also, it should be noted that the unrecycled amount of retentate stream is sent to the turboexpander for energy recovery. It means that at zero recycle ratio all the second-stage retentate gas is sent to the expander, which represents the base case design.

Fig. 3-5(a) shows the variation of the required membrane area and second membrane CO_2 recovery (CCR) at different recycle ratios. By increasing the recycle ratio to 0.8, the inlet flowrate of the first membrane module increases. This brings about an increment in the required membrane area to meet the target of 0.95% CO_2 recovery. However, at high recycle ratios (greater than 0.8), the loss of CO_2 in the system decreases, and the required membrane area of the second module to maintain the total CO_2 recovery at 90% reduces considerably. This can be observed from the reduction of second membrane CCR at high recycle ratios.

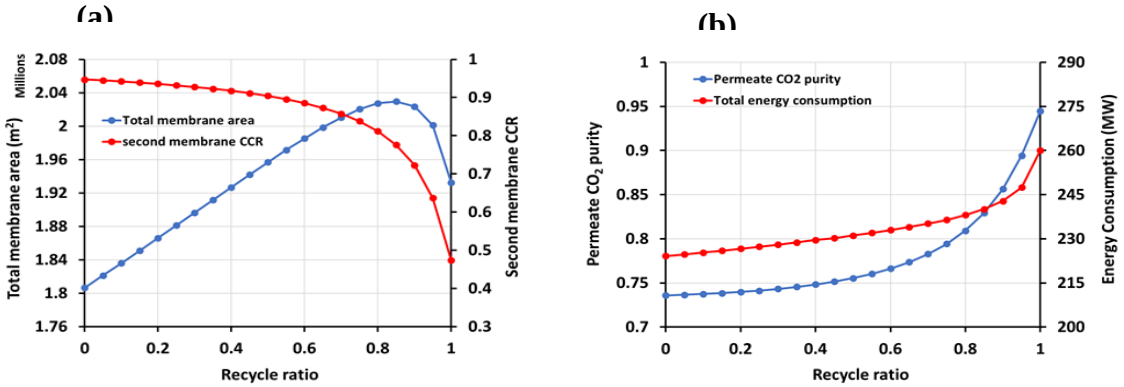

Fig. 3-5. The effect of recycle ratio on the membrane-based CCS performance

Fig. 3-5(b) presents the effect of the recycle ratio on the permeate CO_2 purity and process energy consumption (total auxiliary power consumption). As can be seen, increasing the retentate recirculation boosts the permeate CO_2 purity and increase energy consumption, specifically at high recycle ratios. Because more driving force is generated due to the increased CO_2 concentration at the membrane feed, it is possible to achieve a higher purity of CO_2 after the separation. On the other hand, retentate recirculation requires higher energy usage, which is mainly associated with a higher flow rate in compressors. Moreover, at a high recycle ratio, the increase of the retentate flowrate of the second stage due to lower CCR is coincident with the raise of retentate recycling, leading to a sharp increase in the input flowrate of the compressor and cooler. Consequently, the system energy consumption significantly increases at high recycle ratios. As shown here, recycling the second stage retentate gas to the first stage is required to ensure a higher purity of CO_2 in the permeate gas, although both energy consumption and required membrane area increase compared to a design without retentate recirculation.

3.3.4 Effect of feed pressure

The pressure ratio is a very crucial parameter for system performance and economy. For evaluating this operating parameter, Concept B with full retentate recirculation is considered, and the permeate pressure is fixed at 1 bar. Also, as a separation target, the overall CO_2 capture ratio and the permeate CO_2 purity are fixed at 90% and 95 mole%, respectively.

Fig. 3-6(a) illustrates the effect of the feed pressure on the system performance and the behavior of various membranes. It can be noticed from Fig. 3-6(a) that the increment of feed pressure leads to a decrease in the required area of the membrane, although the rate of reduction decreases at high feed pressures (i.e., P >7 bar). Because by increasing the pressure difference across the membrane, a more driving force is generated for the CO_2 separation, leading to a decrease in the required membrane area to reach the specified separation target. This pressure difference can be generated by considering a vacuum pump at the permeate side or a compressor at the feed side. The required area of the Polaris gen2 membrane is slightly affected by the variation of feed pressure compared to other membrane types, which is mainly due to its high CO_2 permeance.

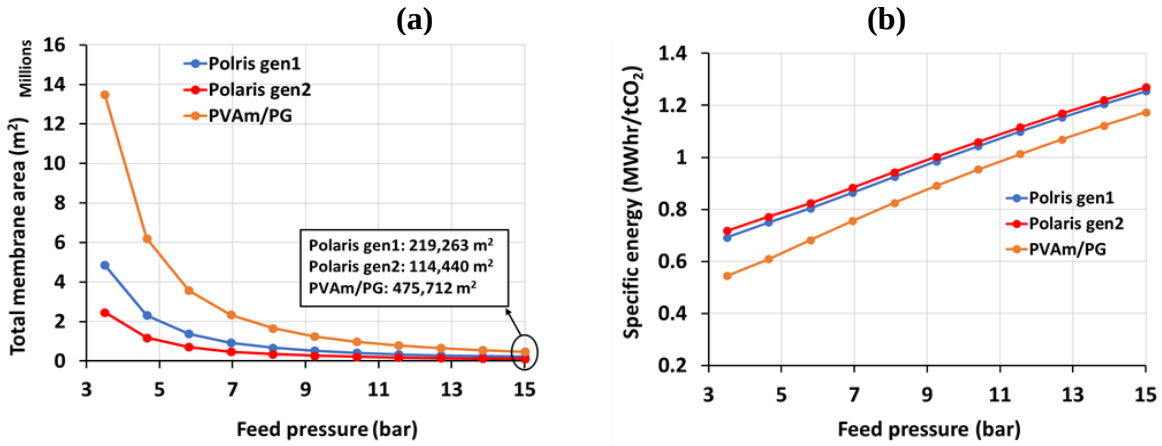

Fig. 3-6. Effect of feed pressure on the membrane

Fig. 3-6(b) shows the specific energy (total required auxiliary power for capturing one tonne of CO_2) versus feed pressure. As can be seen, by increasing the feed pressure, the specific energy for CO_2 capturing increases due to the additional power required by compressors. In

addition, utilizing the PVAm/PG membrane leads to lower specific energy at various feed pressures, which is mainly because of its high selectivity.

It can be concluded that at a low feed pressure, the difference between the performance of various membranes is more remarkable, and both Polaris membranes are better choices than PVAm/PG, although they require more energy to separate a specific amount of CO_2. The effect of membrane properties is discussed in detail in another section. Also, an interesting trade-off is observed by changing the pressure ratio; by increasing feed pressure, the required membrane area reduces, while the system consumes more power for compression. Economic analysis of feed compression is discussed in the next section, which guides the selection of the most cost-effective option.

3.3.5 Effect of CO_2 recovery ratio

The CO_2 recovery ratio corresponds to the CO_2 molar flowrate in the permeate to feed the CO_2 molar flowrate, which shows the efficiency of the separation system. The effect of CO_2 recovery on the total required membrane area and permeate CO_2 purity is depicted in Fig. 3-7 by considering feed pressure equal to 5 bar. The first membrane capture ratio is fixed at 90%, and the second module capture ratio is variable to change the total CO_2 recovery ratio of the system.

The results disclose that by increasing the CO_2 recovery ratio, the product purity decreases, and the required membrane area increases, representing a trade-off between the CO_2 recovery of the system, the CO_2 purity, and the required membrane area. This effect can be described by the fact that for increasing the flowrate of CO_2 in the permeate side, more membrane area is required, and consequently, the other components can permeate through the membrane, and the CO_2 purity in the permeate side decreases. Also, the PVAm/PG membrane demonstrates a preferable performance to achieve satisfactory permeate compositions and recovery ratios since it has higher CO_2/N_2 selectivity. However, the required membrane area to reach high CO_2 separation increases more significantly in the PVAm/PG membrane compared to the Polaris membranes, which can be described by the lower CO_2 permeance of this membrane.

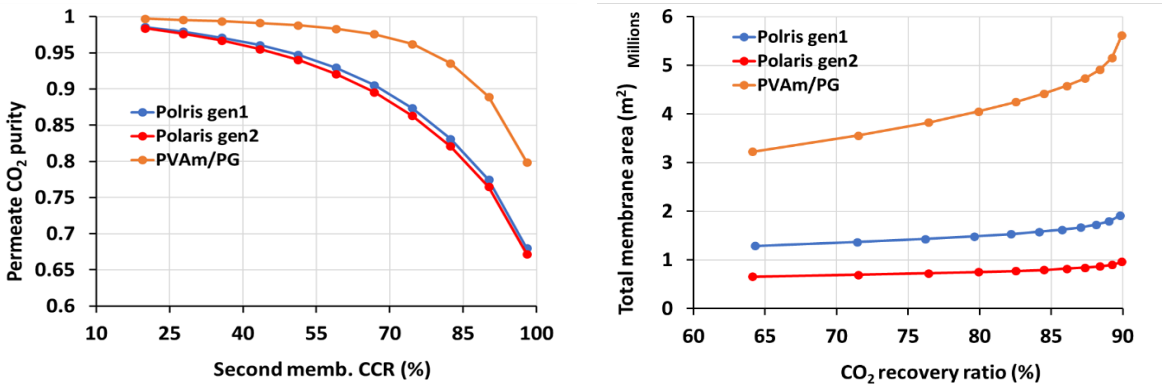

Fig. 3-7. Effect of CO_2 recovery ratio on the membrane area and permeate CO_2 purity

3.3.6 Effect of membrane permeability and selectivity

CO_2/N_2 selectivity and permeability of the membrane are two important parameters in a membrane-based CCS system. This can significantly affect system performance. Thus, the membrane selectivity and CO_2 permeance are investigated for concept B at a feed pressure of 5 bar with the aim of 90% CO_2 recovery and 95 mole% permeate CO_2 purity.

Fig. 3-8 illustrates the effect of membrane selectivity on the specific energy and the required membrane area. It can be observed from Fig. 3-8(a) that by improving membrane CO_2/N_2 selectivity, the energy consumption of the process decreases. Importantly, this influence on the specific energy is more significant at lower CO_2/N_2 selectivity since the compressor and cooler before the second membrane module should handle higher flowrates. Moreover, from the variation of specific energy with respect to selectivity at various values of membrane CO_2 permeance, it can be concluded that the effect of membrane permeability on the specific energy is insignificant in comparison to the effect of membrane selectivity, specifically at high values of membrane CO_2/N_2 selectivity.

Fig. 3-8(b) illustrates the required membrane area versus the CO_2/N_2 selectivity at three different CO_2 permeance values (500, 1000, and 2000 GPU). The required membrane area increases by the increment of membrane selectivity, and this increasing tendency in the required membrane area is more intense at low CO_2 permeance (500 GPU). This behavior is due to the fact that as CO_2/N_2 selectivity increases, the purity of CO_2 in the permeate increases, and the N_2

permeation decreases, which implies that the total permeate flowrate decreases and a larger membrane area is needed to reach the target of separation.

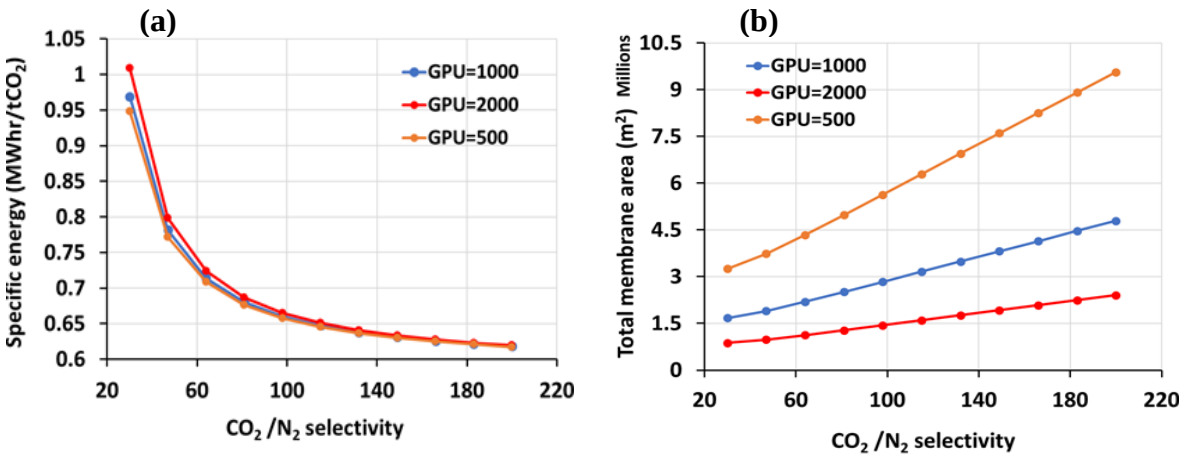

Fig. 3-8. Effect of membrane selectivity on the membrane performance

The influence of membrane permeability on the total required membrane area and specific energy is investigated for a membrane with the CO_2/N_2 selectivity of 50, and the results are presented in Fig. 3-9. It shows that by increasing the CO_2 permeance, the required membrane area decreases, and the specific energy slightly increases because the available driving force and permeate flow rate increase by improving the membrane CO_2 permeance.

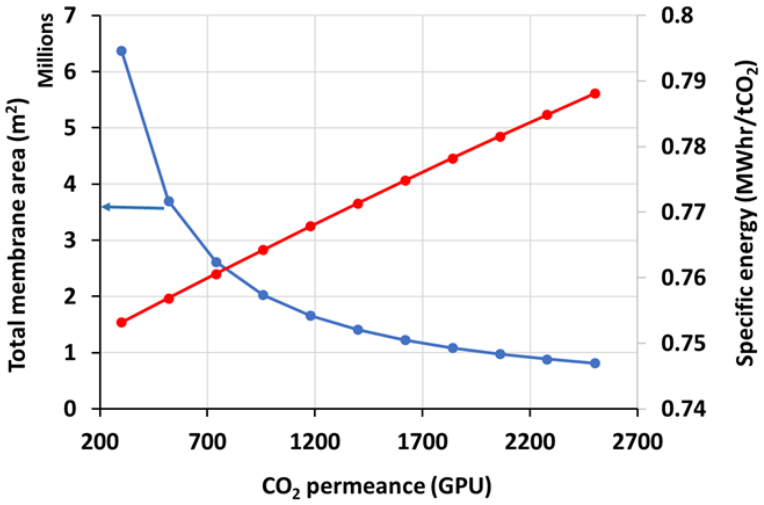

Fig. 3-9. The effect of CO_2 permeance on the total membrane area and specific energy

Therefore, although a membrane with high selectivity decreases the specific energy, its undesirable effect on the required membrane area clearly proves that a membrane with moderate selectivity and high permeability is more beneficial for membrane-based CCS.

3.3.7 Effect of CO_2 feed concentration

The CO_2 concentration of the flue gas exiting power plants can fluctuate considerably depending on the operational conditions forced by the grid. Also, different types of power plants produce flue gas with varying levels of CO_2. The flue gas of natural gas power plants includes about 5 mole% CO_2, and the coal-fired power plant produces flue gas with 10-15 mole% CO_2 [263]. In this regard, the investigation of feed CO_2 concentration influence on the membrane-based CCS is performed for Concept B at a feed pressure of 5 bar with the target of 95 mole% permeate CO_2 purity and 90% CO_2 capture ratio.

Fig. 3-10 shows the effect of CO_2 feed concentration on the system performance indicators. According to Fig. 3-10(a), by increasing the feed CO_2 concentration, the specific energy consumption for membrane separation decreases. This can be described by the definition of specific energy consumption, the required energy for capturing one ton of CO_2. With the increase of permeate flowrate, resulting from the rise of CO_2 level in feed, the energy consumption of the compressor and cooler (C-2 and Hex-3) increases. However, the permeate flow rate is the denominator of specific energy, and its increment aggregately leads to a decrease in the specific energy.

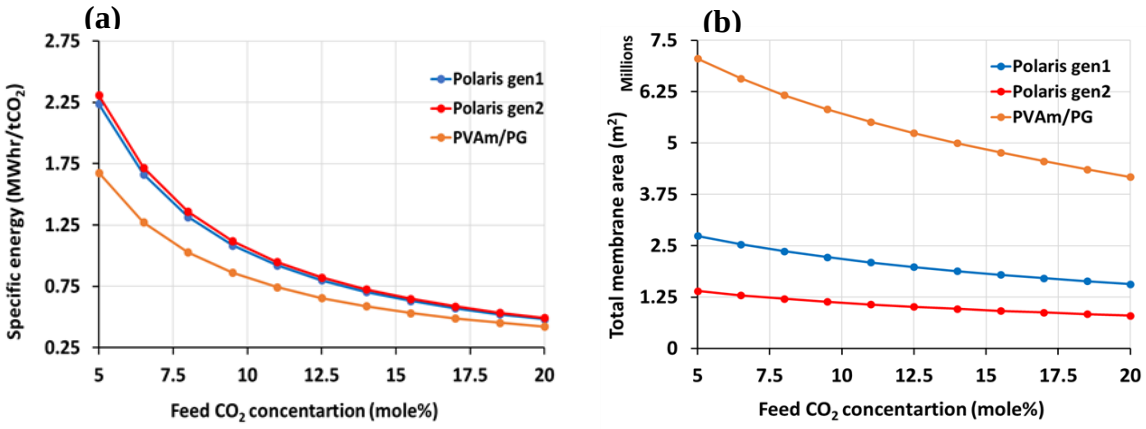

Fig. 3-10. Effect of different level of CO_2 in the feed on membrane system performance

As depicted in Fig. 3-10(b), the required membrane area decreases with the increment of CO_2 concentration in the feed gas. This is primarily because by increasing the feed CO_2 concentration, the available driving force for CO_2 separation improves, and the membrane achieves the specified separation target with a lower total required membrane area. Furthermore, this decreasing trend in the membrane area becomes more considerable when a membrane with a higher CO_2/N_2 selectivity, such as PVAm/PG is considered, owning to applying an extra driving force to the membrane system.

It can be concluded that the increase of CO_2 level in the flue gas generally improves the performance of membrane-based CCS. In this context, different approaches are suggested to increase the level of CO_2 in flue gas, such as flue gas recycling and combustion using oxygen-enhanced air [264].

3.3.8 Effect of sweep gas

Using sweep gas in the permeate side of the counter-flow membrane modules is suggested as a promising way to produce a larger driving force for the separation of CO_2 [265]. To analyze the sweep gas effects on the membrane-based CCS, the performance of concept B with and without sweep gas is compared, and the process information is presented in Fig. 3-11. The flowrate of sweep gas is equal to five percent of the flue gas flowrate, taken from the first module retentate stream. Also, the separation target has been fixed at 90% CO_2 capture ratio and 95 mole% CO_2 purity in the second stage permeate gas. The results show that considering sweep gas can significantly decrease the required membrane area (~16%) compared to the case without sweep gas, although the energy consumption has a slight increase in the case with sweep gas. It can be concluded that using a small portion of the retentate stream as a sweep gas in the counter-flow membrane system leads to a remarkable decrease in the required membrane area owing to the creation of a larger driving force that facilitates CO_2 permeation.

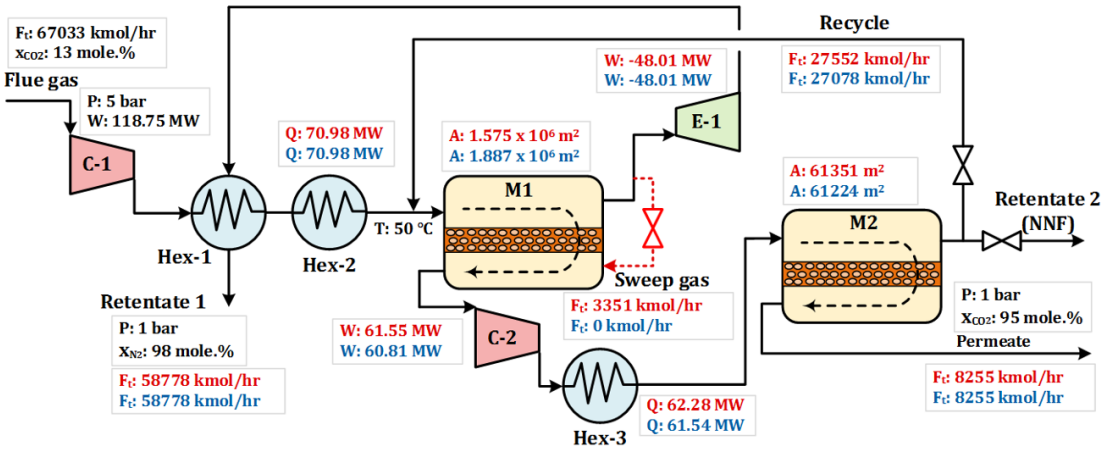

	With sweep gas	Without sweep gas
CO_2 recovery	90%	90%
Total membrane area (m^2)	1.636×10^6	1.948×10^6
Energy consumption (MW)	265.55	264.07

Fig. 3-11. Operation and design information of two-stage membrane-based CCS with and without sweep gas

The required membrane area and specific energy in terms of various amounts of sweep gas using different membranes are depicted in Fig. 3-12. It is notable that the decreasing trend in the required membrane area abates at a higher ratio of sweep gas, as shown in Fig. 3-12(a). Furthermore, the decreasing trend in the required membrane area is more notable for the PVAm/PG membrane in comparison with Polaris gen1 and gen2. The other interesting result is that at high ratios of sweep gas, the required membrane area of the considered membrane becomes closer, which is due to the availability of a significant driving force for each of the membranes. Also, as shown in Fig. 3-12(b), the specific energy escalates by increasing the sweep gas to the flue gas ratio, mainly due to the increase of flowrate in the second compressor and cooler. Also, the increasing trend of specific energy intensifies at a higher flowrate of sweep gas. Accordingly,

recycling a portion of the retentate stream as a sweep gas design improves the partial pressure of CO_2 in the system and in turn, remarkably decreases the required membrane area.

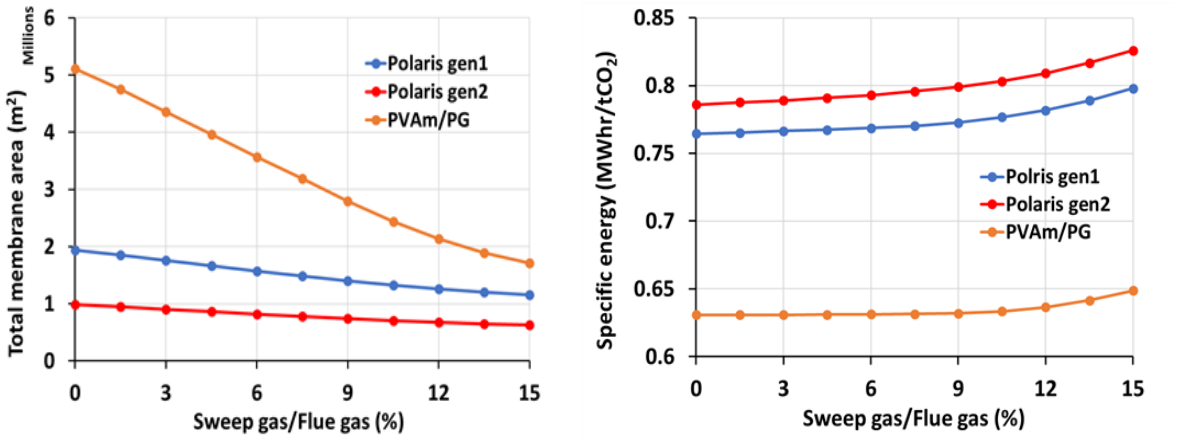

Fig. 3-12. Effect of sweep gas on required membrane area and specific energy for various membranes

3.3.9 Effects of compression strategies and membrane flow pattern

The driving force for CO_2 permeation in the membrane process can be provided by the pressure ratio created by two strategies: feed compression and permeate vacuum. Since using each of the approaches may have a significant influence on the process energy consumption and system performance, these two different approaches are compared for the membrane-based CCS process with the separation target of 90% CO_2 capture ratio and 95 mole% CO_2 purity in the second stage permeate gas. The comparison results of two compression strategies are presented in Table 3-3 for a two-stage counter-flow membrane system. It should be noted that the pressure ratio of both strategies is identical and equal to 5.

The results of Table 3-3 demonstrate that the using feed compression approach brings about a substantial decrease (about 82%) in the total required membrane area in comparison with the permeate vacuum. This is mainly because the pressure difference (ΔP) in the vacuum strategy is lower than the feed compression, which resulted in a lower driving force and higher required membrane area, as shown in Eq. 1. On the other hand, the permeate vacuum is a more energy-efficient approach compared to the feed compression; it needs 35.7% lower energy for separating one tonne of CO_2 because the vacuum approach only pumps the permeate stream rather than the feed stream that is mostly nitrogen. It should be noted that the turboexpander in the feed

compression strategy recovers a part of the energy used by compressors, while it is not possible in the permeate vacuum approach.

Table 3-3. Comparison of CCS performance with different compression strategies and membrane flow patterns

	Compression strategies		**Membrane flow pattern**	
	Feed compression	**Vacuum pump**	**Counter-flow**	**Crossflow**
Total required memb. area (m2)	1.948×10^6	10.850×10^6	1.948×10^6	5.451×10^6
Total energy consumption (MW)	264.7	169.83	264.07	421.47
Specific energy (MWhr/ton capture CO_2)	0.765	0.492	0.765	1.221
Permeate flowrate (kmol/hr)	8255	8255	8255	8255
CO_2 recovery (%)	90	90	90	90

It can be concluded that using the vacuum pump in the membrane separation process increases the flexibility of the CCS system because it reduces the system energy penalty resulting from the integrating of CCS with existing power plants. However, the practicality of such a vacuum pump in large-scale membrane-based CCS is questionable. The economic evaluations of these two compression strategies are discussed in the following sections.

The membrane flow pattern is another design aspect of the membrane-based CCS, which is expected to affect the performance of the system. Among different membrane flow patterns (cross flow, countercurrent, co-current, perfect-mixing, and one-side mixing), the crossflow and counter-flow are more practical and efficient for CO_2 separation [111,266]. Thus, the comparison between the performance of counter-flow and crossflow modules for a two-stage membrane system at the abovementioned separation targets is performed in this study, and the results are presented in Table 3. The results substantiate the counter-flow design is more advantageous since this design requires about 64% lower membrane area and about 37% lower required energy to separate one tonne of CO_2. Also, Merkel et al. [127] proved that the permeate stream from the counter-flow membrane has a higher CO_2 purity at a fixed recovery ratio compared with the permeate stream from the crossflow membrane.

From a practical viewpoint, although the performance of the counter-flow pattern is superior to that of the crossflow pattern, it has not been widely applied in the industry due to some drawbacks, such as complexity and concentration polarization on the permeate side. Accordingly,

further research to address these issues and to enhance the applicability of counter-flow membranes in the carbon capture system can contribute to effective and flexible carbon capture systems.

3.3.10 Economic analysis of membrane-based CCS

This section is devoted to the economic analysis of a two-stage counter-flow membrane-based CCS to have a better understanding of the various operating parameters effects and different membranes on the cost of CO_2 capture. For this purpose, the assumed process conditions for studying the effect of each operating parameter are identical to those considered in the technical analysis sections. Also, the CO_2 capture cost ($/t$CO_2$) is defined as the total annual cost of the system per annual tonne of captured CO_2. Thus, this economic indicator can represent all associated costs of CO_2 capturing, including the annual capital cost, energy cost, and O&M cost.

Fig. 3-13 illustrates the influence of feed pressure on the CO_2 capture cost. It can be observed that there is an optimum feed pressure range (5.8 to 8 bar) at which the CO_2 capture cost for Polaris gen 1 and Polaris gen 2 is as minimum as 23.85 $/t$CO_2$ and 25.36 $/t$CO_2$. Also, this optimum feed pressure for the PVAm/PG membrane is 8.1 bar, which leads to the CO_2 capture cost of 27.35 $/t$CO_2$. At low feed pressures (lower than 5.8 and 7 bar for Polaris and PVAm/PG membranes, respectively), the declining trend of CO_2 capture cost is mainly due to the decreasing trend of the required membrane area, which is more significant at lower pressure range, as it is

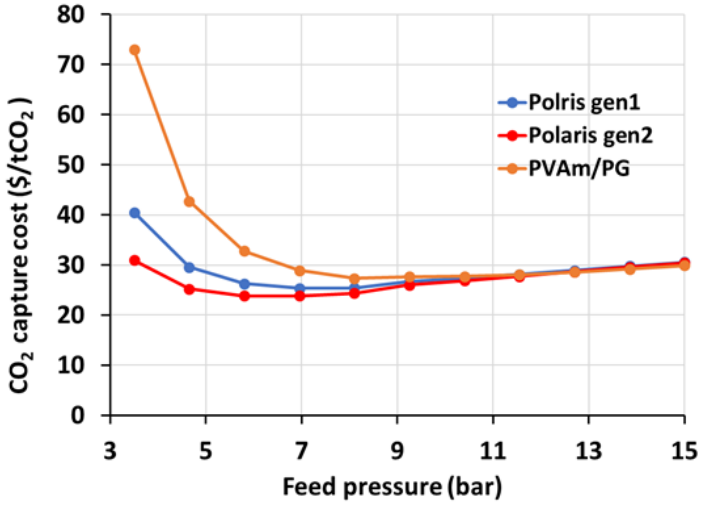

Fig. 3-13. Effect of feed pressure on CO_2 capture cost for different membrane types

shown in Fig. 3-6. However, at a feed pressure greater than 5.8 bar, the increasing cost of energy is the primary reason for the increasing cost of CO_2 capture.

The recovery ratio effect on CO_2 separation cost is presented in Fig. 3-14. Increasing the CO_2 recovery, the cost of CO_2 capturing decreases due to a higher amount of CO_2 at the permeate flowrate. However, this decreasing trend in the CO_2 capture cost slows down at higher CO_2 recovery, mainly because of an increment in the required membrane area at high CO_2 recovery. This behavior is more intense for PVAm/PG membrane, and it leads to a minimum value in CO_2 capture cost, which can be described by a significant increase in the required PVAm/PG membrane area at high CO_2 recovery rates.

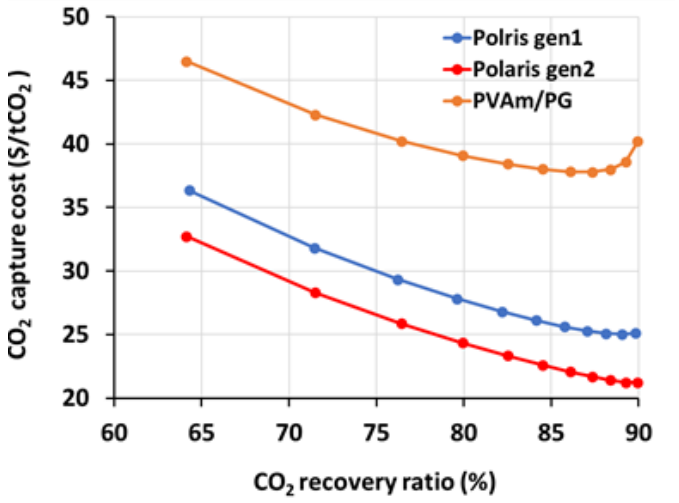

Fig. 3-14. Effect of CO_2 recovery on CO_2 capture cost for different membrane types

The variation of CO_2 capture cost by the feed CO_2 concentration is presented in Fig. 3-15. By increasing the concentration of CO_2 in the feed gas, the CO_2 capture cost decreases considerably, which is mainly due to the reduction of energy consumption and required membrane area. Also, for the flue gas with low CO_2 concentration, the CO_2 capture cost by PVAm/PG membrane is considerably higher than others, which substantiates that using membranes with higher CO_2 permeance is more cost-effective in this case.

The variation of CO_2 capture cost versus CO_2/N_2 selectivity at different CO_2 permeance rates is presented in Fig. 3-16(a). The result indicates for membranes with the CO_2 permeance of 1000 and 2000 GPU (such as Polaris gen1 and gen2), the optimum value of CO_2/N_2 selectivity, which leads to a minimum value of CO_2 capture cost, is 64 and 81, respectively. Also, it can be seen that improving the selectivity of membranes does not always offer a cost-saving process. On the other hand, a higher value of selectivity decreases the specific energy of the system (as shown in Fig. 3-8(a)), which is of great importance for the flexible operation of the membrane-based CCSs. The other interesting point is that at higher CO_2 permeance, not only the value of CO_2 capture cost is lower, but also the negative influence of increasing the selectivity on the capture cost becomes insignificant.

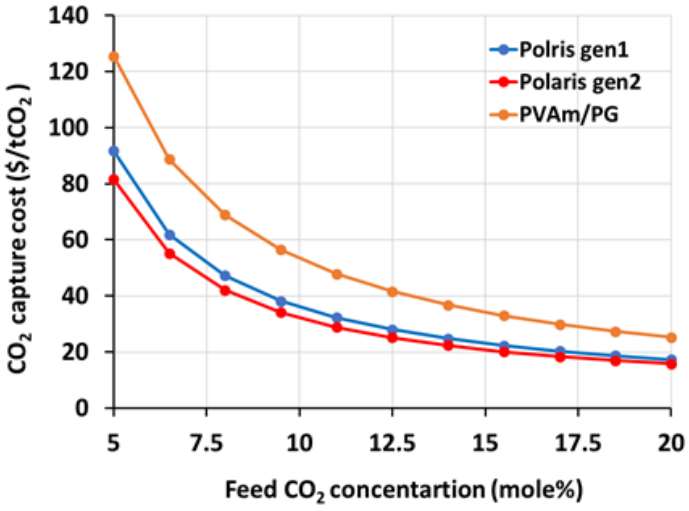

Fig. 3-15. Effect of feed CO_2 concentration on CO_2 capture cost for different membrane type

Fig. 3-16(b) clearly illustrates the influence of membrane permeability and selectivity on the CO_2 capture cost. As can be seen, improving the membrane CO_2 permeance is by far more important than the selectivity parameter to achieve a cost-effective membrane-based CCS. Also, a further increment of the membrane selectivity after the optimum point increases the CO_2 capture cost. Furthermore, this three-dimensional curve could be useful for developing new membranes to reach the desired level of CO_2 capture cost or evaluate the economic feasibility of available membranes.

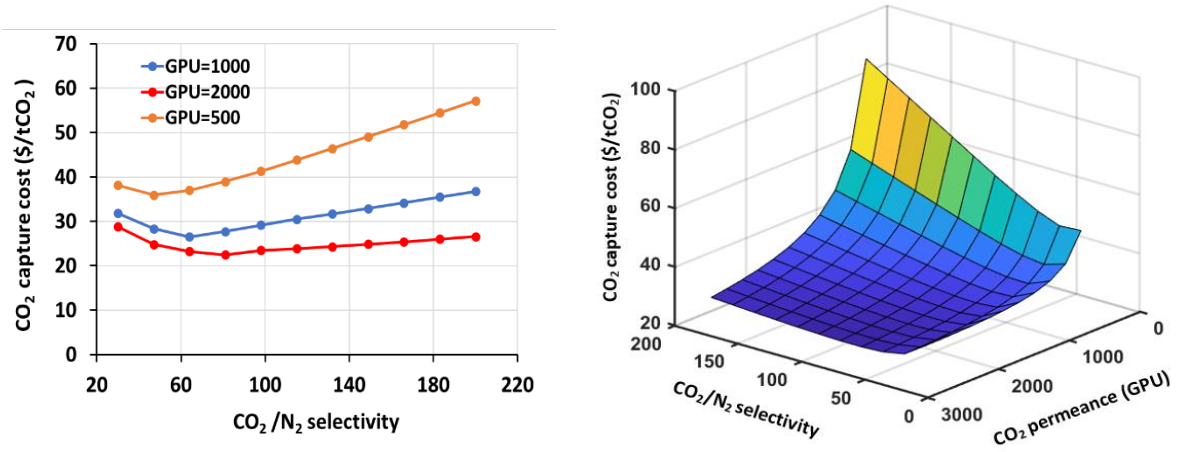

Fig. 3-16. Effect of selectivity and CO_2 permeance on the CO_2 capture cost

3.3.11 Economic comparison of different designs of membrane-based CCS

In this section, the four designs of the two-stage membrane process are compared economically using the cost function presented in Table 2. In this regard, the four considered concepts are simulated in the Aspen Plus software with the separation target of 90% total CO_2 recovery and 95 mole% of CO_2 purity in the final permeate gas. Also, the properties of the Polaris gen1 membrane are considered, and the pressure ratio of compressors and vacuum pump are identical and equal to 8. Furthermore, due to the beneficial effect of sweep gas on the system performance, five percent of the flue gas flowrate is considered as a sweep gas in concept B. It should be noted that the base case is not compared with other concepts since it cannot meet the separation target.

Fig. 3-17 shows the total annual energy cost and capital cost in different concepts. It is obvious from this figure that the case of using a vacuum system with a counter-current flow membrane (concept D) leads to the lowest amount of annual energy cost compared with other concepts. Even though the lower energy cost of vacuum operation is advantageous for the flexible operation of membrane-based CCS, there are other challenges that need to be addressed when using this approach, such as the possibility of working at low vacuum pressure, large-scale application, and leakage. On the other hand, concept C (permeate vacuum and crossflow membrane module) requires the highest capital cost, followed by concept D. This is mainly

because of the higher cost of the vacuum system compared with typical compressors and higher membrane module cost due to higher required membrane area to reach the specified separation target. Overall, concept B has the lowest capital cost and a moderate energy cost in comparison to other concepts.

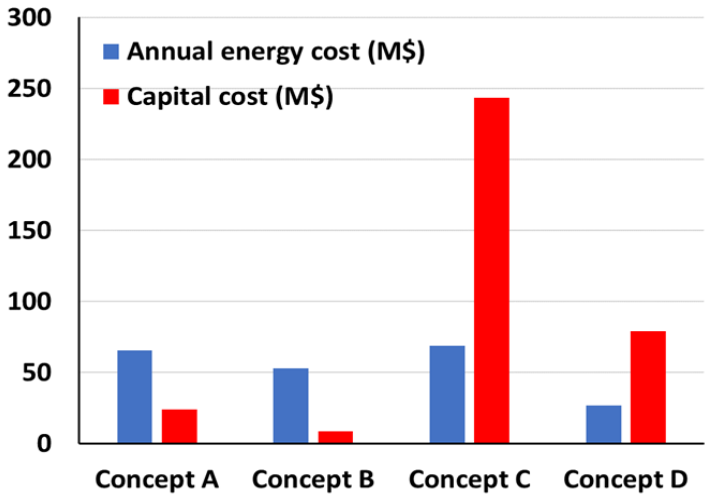

Fig. 3-17. Comparison of different concepts with respect to annual energy cost and capital cost

Fig. 3-18 presents the comparison between different concepts in terms of the required membrane area and CO_2 capture cost. As can be seen, using a vacuum compressor in the configuration significantly increases the required membrane area, which may affect the cost of the membrane module. Similarly, the concepts with a crossflow membrane module (concepts A and C) suffer from a larger membrane area and a greater CO_2 capture cost compared with the counter-flow module. On the other hand, the concepts equipped with a feed gas compression system (concepts A and B) need a lower membrane area, leading to a lower CO_2 capture cost. It can be concluded that the feed compression approach by counter-current membrane module and sweep gas (concept B) is the most cost-effective design (22.76\$/tCO_2) since it has the lowest capital cost and CO_2 capture cost. Moreover, concept C (vacuum system with crossflow module) is the most expensive design (118.9 \$/tCO_2), although it can be considered a potential option when the energy penalty of the power plant is of great importance.

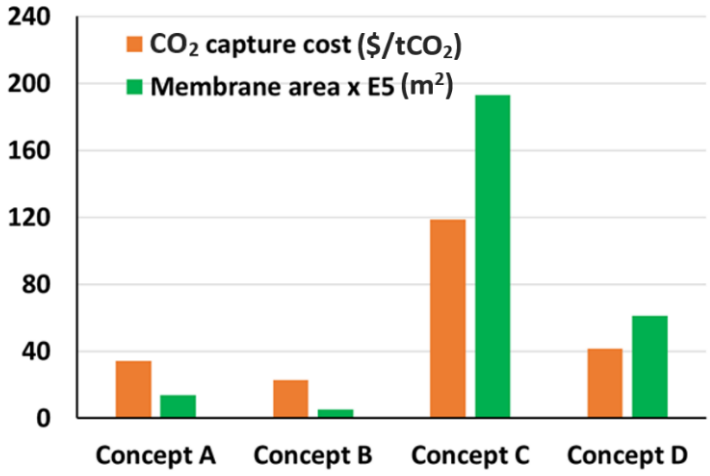

Fig. 3-18. Required membrane area and CO_2 capture cost for different concepts

The results of the economic analysis presented here can help process developers select the appropriate design for membrane-based carbon capture systems. The total cost of a CO_2 capture system varies by separation targets, process design, operating parameters, and membrane properties. The incorporation of a counter-current membrane module with a sweep gas as well as a feed compression approach into a membrane-based capture process can considerably enhance the cost-effectiveness of the post-combustion carbon capture system. Also, generating driving force via the vacuum system at permeate side is a more energy-efficient approach, which can improve the flexibility of the system.

3.4 Chapter Summary

The objective of this chapter is to address the second research question (RQ2) focuses on possible solutions to enhance the technical performance of membrane-based carbon capture technologies to improve their efficiency and effectiveness in capturing and storing carbon dioxide. To achieve this objective, the study employs component and system-level simulations and conducts a thorough techno-economic investigation of membrane-based CCS. Through this research, new knowledge regarding the technical aspects and cost implications associated with various membrane technology designs under different operational conditions has been acquired and presented in this chapter. These contributions provide valuable insights into how membrane

technologies can be optimized to achieve better performance and cost-effectiveness, leading to the advancement of carbon capture and storage solutions.

A fossil fuel power plant will soon need to work in an integrated and fully connected grid that involves components such as renewable sources and energy storage. In such a complex energy system, a carbon capture system needs to satisfy other requirements to be effectively integrated with other components. As the operational parameters of fossil fuel power plants change due to intermittent renewable sources, the energy consumption and operating expenses of carbon capture technologies are important decision parameters. To evaluate these parameters, a comprehensive techno-economic analysis of membrane separation systems for post-combustion CCS was conducted in this chapter to identify the opportunities and find limitations of membrane processes to be considered as a flexible carbon capture system in power plants.

The main goal of this chapter is how various designs and operating parameters of the membrane-based CCS can improve the techno-economic performance and flexibility of the system to be considered as a potential option for integrating into the future low-carbon energy system. To this end, four designs of the double-stage membrane process and three polymeric membranes with various transport properties were considered, and the influence of the feed pressure, feed CO_2 concentration, retentate recycling, sweep gas, and membrane properties on their techno-economic performance have been investigated with the separation target of 90% of CO_2 recovery and 95 mole% CO_2 purity. The results revealed that by increasing the feed pressure, the required membrane area significantly decreases, although the specific energy increases due to the additional power required by compressors. Also, using a membrane with higher CO_2/N_2 selectivity, such as PVAm/PG membrane, leads to lower specific energy. Also, analyzing the effect of retentate recycling showed that at full retentate recycling, although higher CO_2 purity of the permeate gas can be achieved, the system energy consumption and required membrane area increase compared with the case of zero retentate recycling. Furthermore, considering a portion of the retentate stream as a sweep gas remarkably reduces the required membrane area, although the specific energy of the system increases. Moreover, the increase of the CO_2 level in the flue gas improves the performance and economy of the membrane-based CCS. The other notable result is that enhancing the selectivity of membranes does not always offer a cost-saving process. On the other hand, a higher value of selectivity decreases the specific energy of the system, which is of great importance for the flexible operation of membrane-based CCSs.

The economic comparison of different designs proved that considering the feed compression approach by counter-current membrane module and sweep gas is the most cost-effective design (22.76$/t$CO_2$) since it has the lowest capital cost and CO_2 capture cost. On the other hand, the vacuum system with a counter-flow module design is the most energy-efficient option, which decreases the energy penalty of the power plant and may lead to the flexible operation of the system. The techno-economic analysis results demonstrated that among the various designs of membrane-based CCS, selecting a counter-flow membrane module equipped with a membrane with moderate selectivity and high permeability is the optimal design for reducing CO_2 capture cost and energy consumption and improving the system flexibility. Also, second-stage retentate recirculation, moderate sweep gas flowrate, high CO_2 concentration of feed, and moderate pressure ratio are other operating considerations that can contribute to system flexibility improvement.

The results of this research can be used by policymakers and process designers in the field of carbon capture system design and operation. Also, the presented results can be considered in the experimental research to develop new membranes with optimum selectivity and permeability, which can lead to a cost-effective and flexible membrane-based CCS. Future studies can be performed to investigate the following points: the performance of the system using other membrane types by considering the dependency of membrane properties on system pressure and temperature, uncertainties impact on the design and cost of the membrane-based CCS, multi-objective and superstructure optimization of the system.

Chapter 4. Optimal Design and Dynamic Behavior of Membrane-based CCS

- ? **Research questions: RQ3-** What are the key factors influencing the economic and energy performance of membrane-based carbon capture systems, and how can they be optimized to reduce costs and increase energy effectiveness? **RQ4-** How is the dynamic performance of membrane-based integrated with load-following power plants, and how can the flexibility of membrane-based carbon capture systems be enhanced to accommodate different industrial processes and varying carbon capture requirements?
- ➢ **Objective:** Development of an economically viable design of multi-stage membrane-based CCS with a flexible operation for integration with power plant under load following operation
- ✓ **New knowledge:** Optimal multi-stage membrane-based CCS process and possible trade-offs for energy and cost penalty - Flexible operation and transient behavior of membrane process for integration with power plant under load following operation

The objective of this chapter is to develop optimal membrane-based carbon capture systems to enhance the sustainability of fossil-fuel power plants by reducing their energy consumption and operating costs. The multi-stage membrane process is numerically modeled using Aspen Custom Modeler based on the solution-diffusion mechanism, and the effects of important operating and design parameters are investigated. A multi-objective process optimization is then carried out by linking Aspen Plus with MATLAB and using an evolutionary technique to determine optimal operating and design conditions by calculating the best possible trade-offs between objective functions. Furthermore, this chapter aims to improve the flexibility of membrane-based CCS units as a promising technology for CO_2 capturing by analyzing the system's transient behavior. A rigorous dynamic model for a membrane separation system is developed, which includes differential equations of transport phenomena across the membrane, mass balances, and pressure distributions. The model is utilized to investigate the dynamic performance of a single-stage counter-current membrane module for separating CO_2 from the flue

gas of a power plant. Step-changes in feed pressure, feed flow rate, feed composition, and retentate recycling are considered for the analysis.

4.1 Introduction

Both the industrial and scientific communities have shown increasing interest in membrane-based CO_2 separation in recent years due to several advantages over the amine-based post-combustion capture method. However, this process is still under development and requires a significant amount of energy to generate enough driving force in the membrane module for separating CO_2 from other components of flue gas. Accordingly, the optimal design and operation of membrane-based CCS could pave the way for optimal integration and improving sustainability of fossil-fueled power plants. In the following sections, the potential of a two-stage membrane process for optimal CO_2 capturing from a 600 MW coal-fired power plant is discussed and investigated. In this chapter, based on a mathematical model developed in Aspen Custom Modeler for the hollow-fiber membrane module, multi-objective optimization of membrane-based CCS is performed, considering sustainability criteria as objective functions. To this end, first, a sensitivity analysis was conducted to determine which operating and design parameters affect energy consumption, capital, and operating costs of the multi-stage membrane process. Afterward, an evolutionary algorithm is utilized to perform a comprehensive multi-objective superstructure optimization for a two-stage membrane-based CCS with the goal of achieving a sustainable and flexible membrane-based CCS that can integrate with fossil-fueled power plants. This is aimed at identifying the optimal system design, operating conditions, and membrane transport properties.

As mentioned before, due to strong interactions between membrane-based CCS with other components of a low carbon energy system, flexible operation of the membrane process is of great importance to attain satisfactory control performance. In this regard, studying the dynamic behavior of the membrane process can provide practical information for rational system design, process start-up and shut-down, the transition between two steady states, control, and operational strategies. To the best of our knowledge, the dynamic behavior of membrane modules under various step-changes in operating variables has not yet been analyzed in the open literature. Also, the dependency of pressure and temperature on the membrane transport properties and its effect on the dynamic behavior of the membrane process is another critical concern that needs to be investigated. Accordingly, this chapter aims to investigate the flexibility of the membrane

separation process by analyzing the dynamic behavior of hollow fiber membrane gas separation. To this end, the dynamic model of the process is developed and programmed in gPROMS software to analyze the transient response of the membrane process. Thus, the purposes of the present study are (1) to study the capability of the membrane-based CCS for flexible operation by developing a rigorous dynamic model of the system, (2) to investigate the response of membrane module at a sudden step-change in the process and feed conditions, and (3) to estimate the required time of the membrane module to reach steady-state after step changes.

4.2 Superstructure for two-stage membrane-based CCS process

For an optimal membrane separation process, it is necessary to develop a superstructure that includes various potential designs and all the required components (e.g., compressors, heat exchangers, splitters, membranes, vacuum pumps, etc.). Fig. 1 illustrates the general superstructure for a two-stage membrane process for separating CO_2 from flue gases of a 600 MW coal-fired power plant. Gasification or combustion exhaust flue gas must be treated before entering the membrane module in order to remove contaminants like ash, SOx, NOx, and water. A membrane-based CCS feed gas primarily contains N_2 and CO_2, and the fraction of CO_2 is commonly below 15 mole%. Because the CO_2 partial pressure in flue gas is low, an additional driving force is needed to separate the gas, which can be supplied by either compressor at the membrane feed side or by a vacuum pump at the permeate side. Flue gas conditions and other fixed parameters used in this study are presented in Table 4-1.

Table 4-1. Flue gas condition and fixed membrane parameters

Parameter	Value
Flue gas flowrate	500 m^3/s
Flue gas mole fraction	CO_2: 13 mole%, N_2: 87 mole%
Flue gas temperature and pressure	50 ℃ and 1 bar
Membrane operating temperature	50 ℃
Membrane inner and outer diameter	400 and 600 μm
Membrane length	1 m
Membrane packing density	0.8
Rotary equipment efficiency	0.85
Pressure drop in pipes	0

Fig. 4-1 shows how exhaust flue gas entering the membrane CCS unit can follow a variety of process pathways, which are determined by various splitters (SP) in the superstructure. To generate the driving force, two methods have been considered: feed compression and permeate vacuum. The blue and green lines depict these approaches, respectively. In this regard, the splitter can be seen as a binary variable that determines the method of generating the driving force. Each method has the same main pipelines, which are represented by black lines. System performance and separation efficiency can be affected by retentate recycling and sweep gas, so different valves need to be considered in the system model, which specifies the flowrate ratio of the recycling process. In addition, the proposed superstructure considers two common membrane flow configurations, including cross-current and counter-current flow. The membrane modules can also incorporate different polymeric membranes with a wide range of transport properties. So, several commercially available membranes are considered for the superstructure. In order to optimize and analyze the proposed model, a mathematical programming model including both discrete and continuous variables is developed based on the proposed superstructure.

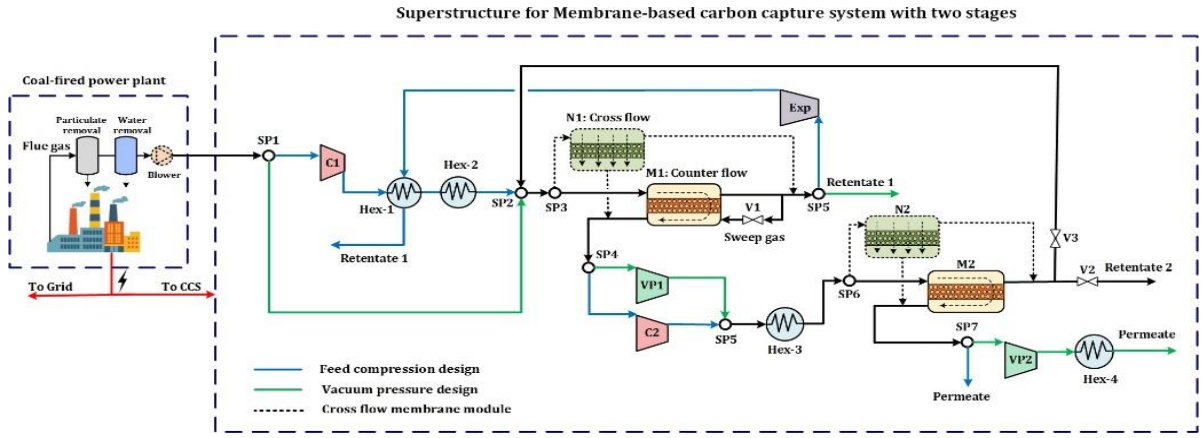

Fig. 4-1. Proposed superstructure of two stage membrane process for CCS application

4.3 Mathematical formulation and optimization problem

On the basis of a solution-diffusion mechanism, mathematical models for counter-current and cross-flow hollow fiber membranes are developed. Same schematic of a counter-current hollow fiber membrane module, as presented in the previous chapter, with the inlet gas flowing to the module shell side and permeating to the fiber bore side. Gas enriched with N_2 (retentate stream) exits from the shell side of the module, whereas CO_2-enriched gas (permeate stream) exits from

the bore side in the opposite direction. For the mathematical modeling of a membrane stage, the same assumptions mentioned in the previous chapter have been taken into account:

The summary of the mathematical formulation of a membrane stage is shown in Table 4-2, assuming solution-diffusion is the primary mechanism for CO_2 permeation. As for the crossflow membrane module, the local concentration of each component on the permeate side is equal to the fraction of gas passing through the membrane at a given point. Detailed mathematical modeling of a crossflow membrane module is presented by [254]. The membrane model is also validated in the previous chapter.

By utilizing the 2nd-order central finite discretization method with 200 elements, we have programmed and solved the mentioned differential equations using the Aspen Custom Modeler and DMO solver. Following the creation of the membrane models, the user-defined models are imported into Aspen PLUS for further analysis and optimization.

The power plant flue gas condition and membrane process parameters are presented in Table 4-1. Although it is more realistic to consider oxygen and water contents in the flue gas, it is assumed that the flue gas entering the membrane-based CCS is binary gas, including CO_2 and N_2 with the atmospheric pressure as justified in previous works [189,267]. The thermodynamic properties and gas behavior are modeled using the Peng-Robinson thermodynamic package. Compressors and vacuum pumps are modeled as single-stage with fixed efficiency of 85%, and heat exchangers are utilized after a feed or permeate compression to cool down the gas streams to the process operating temperature. Despite the fact that oxygen and water are more realistically present in flue gases, it is assumed that the flue gas entering membrane-based CCS is binary gas, including CO_2 and N_2. This is in line with previous works [189,267]. Also, single-stage compressors and vacuum pumps are assumed with a fixed efficiency of 85%, and heat exchangers are used to cooling down the gas streams to process operational temperatures after feed or permeate compression.

Table 4-2. Mathematical equations for modeling membrane stage

1	Permeation rate of component *i*	$J_i = 2\pi r_{FO} n_F \frac{Q_{CO_2}}{\alpha_i}\left(P_{ret} y_{ret,i} - P_{per} y_{per,i}\right)$
2	Selectivity of component *i*	$\alpha_i = \frac{Q_{CO_2}}{Q_i}$

3	Total permeation rate of component *i*	$J_t = \sum_j^n J_j$
4	Total molar balance of bore and shell side	$\frac{dF_{per}}{dx} = -J_t$ and $\frac{dF_{ret}}{dx} = -J_t$
5	Components molar balance in fiber bore	$\frac{d(F_{per} y_{per,i})}{dx} = J_t\, y_{per,i} - J_i$
6	Components molar balance in shell side	$\frac{d(F_{ret} y_{ret,i})}{dx} = J_t\, y_{ret,i} - J_i$
7	Pressure drop in bore side	$P_{per} \frac{dP_{per}}{dx} = \frac{128 RT \mu F_{per}}{\pi D_{FI}^4 n_F}$
8	Pressure drop in shell side	$\frac{dP_{ret}}{dx} = \frac{32\mu}{D_H^2} V_{ret}$

Moreover, the economic evaluation and cost functions are based on Table 2 presented in chapter 3. These equations include fixed operating and maintenance (O&M) costs, annual capital costs, equipment purchase costs, and utility costs.

4.3.1 System optimization procedure

Optimization of membrane-based CCS system design and operating parameters requires a rigorous optimization procedure that simultaneously optimizes conflicting objective functions with both continuous and discrete decision variables. As there can be no single optimal solution to the multi-objective optimization (MOO) problem because the objective functions compete with each other, the optimization solution leads to a Pareto frontier containing a set of optimal points [268]. As a consequence, the Pareto solutions represent the optimal trade-off between objective functions, which is critical for the design and operation of systems.

Mixed Integer Nonlinear Programming (MINLP) has been formulated to describe the best design and operation of a membrane-based CCS, which can be solved both with heuristics and deterministic methods[179]. For optimization, the heuristic optimization algorithms were selected due to their robustness and capability of generating Pareto solution sets. Additionally, the Multi Leader Multi-Objective Particle Swarm Optimization algorithm (MLMOPSO) as a heuristic algorithm proposed by [269] has been employed, which is capable of handling and optimizing constrained MINLP problems efficiently. An innovative approach to updating particle positions

by multiple leaders is employed based on this algorithm, which allows particles to use the information of several non-dominated solutions rather than just the closest. Additionally, there is a parameter called the Social Influence Factor (SIF) that controls the influence of leaders on velocity vectors [269]. In previous works [270–272], this method has proven successful in maintaining the diversity and quality of Pareto solution sets.

The membrane-based CCS optimization problem can be expressed as MINLP as follows:

$$Minimize\ F_i(x) \quad \forall_i = 1,2,\dots,n_{obj}$$

Subjected to:

$$\begin{cases} h_m(x) = 0, & \forall_m \\ g_n(x) \le 0, & \forall_n \end{cases}$$

where F represents the vector of objective functions, x represents the vector of model decision variables, $h_m(x)$ is the vector of equality constraints and $g_n(x)$ is to the vector of inequality constraints.

The objective functions vector includes the following performance indicators:

- CO_2 capture cost: an economic indicator that shows the required cost to capture one tonne of CO_2 from flue gas ($/t$CO_2$).
- CCS energy penalty: this indicator shows the energy consumption of the CCS process per power plant net capacity
- CO_2 removal percentage: this indicator shows the removal efficiency of CCS, which can calculate as the flowrate of CO_2 in permeate gas per the flowrate of CO_2 in the flue gas.

In order to generate the best possible trade-offs for enhancing the sustainability and flexibility of membrane-based CCS, the CO_2 capture cost and the total energy consumption and CO_2 capture cost need to be minimized, and CO_2 removal should be maximized.

Continuous decision variables are composed of critical process parameters that affect system performance and economic indicators. These variables include feed gas pressure, CO_2 concentration in the feed gas, and retentate recycling ratio, which are considered a vector of continuous decision variables. As discrete decision variables, we consider three membranes with

varying selectivity and permeability (first- and second-generation Polaris membranes and PVAM/PG membrane). Also, various layouts of the process in the superstructure model are represented through the value of nodes (splitter) as binary variables in the MINLP problem. The SP3 and SP7 splitters value indicate whether the membrane module is counter flow (SP3 = SP7 = 1) or crossflow (SP3 = SP7 = 0). The values of other splitters also determine whether the compression strategy is feed compression (SP1, SP2, SP4, SP5, SP6, SP8 = 1) or permeate vacuum (SP1, SP2, SP4, SP5, SP6, SP8 = 0). The process simulator applies mass and energy balance constraints along with other design specifications automatically. The programmed MINLP has inequalities constraints involving the range of decision variables as well as the CO_2 removal objective function, which according to previous studies, must be above 70%. The lower and upper range of decision variables are shown in Table 4-3.

Table 4-3. The range of decision variables

Variable	**bound**
Compressor pressure ratio	4-14
Vacuum ratio	2-8
CO_2 concentration in flue gas	5 – 20 (mole.%)
Retentate recycling ratio	0 – 1
Sweep gas ratio	0 – 0.1
Polaris gen 1	α: 50, Q_{CO_2}: 1000 GPU
Polaris gen 2	α: 50, Q_{CO_2}: 2000 GPU
PVAM/PG	α: 148, Q_{CO_2}: 735 GPU

It should be mentioned that a higher vacuum level is not achievable at an industrial scale (< 0.2 bar) [194]. The steady-state simulation of the process was performed in Aspen Plus, and the MINLP problem and MLMOPSO optimization algorithm were implemented in MATLAB 2021a. Aspen Plus and MATLAB are then linked using the Actxserver function in MATLAB through a Component Object Model (COM) server, which enables information about equipment and streams to be exchanged between the two software.

4.4 Optimal design results and discussion

4.4.1 Parametric study of membrane-based CCS

Prior to performing process optimization, it is beneficial to have an understanding of the process behavior under different operating conditions. In our previous work [189], a detailed technical evaluation of the two-stage membrane process has been performed considering fixed CO_2 recovery (90%) and fixed CO_2 purity in the permeate gas (95 mole%). In this study, we have considered a fixed membrane area in the module.

Here, a parametric study for counter flow configuration has been discussed in this subsection, where the membrane areas of the modules are fixed, and the CO_2 recovery varies.

Considering the first generation of Polaris™ membrane (CO_2/N_2 selectivity: 50, CO_2 permeance: 1000 GPU) in the first and second module membrane with a fixed area equal to 6.6×10^5 m^2 and 3.5×10^4, respectively, the effect of various operating parameters on the system performance has been analyzed. It should be noted that at the considered membrane areas, the compressors discharge pressure of 8 bar, zero sweep gas, and full retentate recycling, the CCS unit leads to 90% CO_2 recovery and 95 mole% CO_2 purity.

The influence of the compressor outlet pressure on the membrane separation performance as well as the economic and energy indicators, is illustrated in Fig.4-2. The result shows that when the feed pressure is increased, the total energy requirement of the CCS unit increases because of the extra power required by the compressors. Also, there is an optimum compressor discharge pressure (~7 bar) at which the CO_2 capture cost of the system is minimum (~ 25.2 \$/tCO_2). Also, since there is a low driving force for CO_2 separation at lower pressures, lower CO_2 flowrates at permeate stream can be obtained, leading to a declining trend in CO_2 capturing cost. However, by further increasing the compressor discharge pressure, although CO_2 recovery increases, the increasing slope becomes slow at high pressures and negatively impacts CO_2 capture cost.

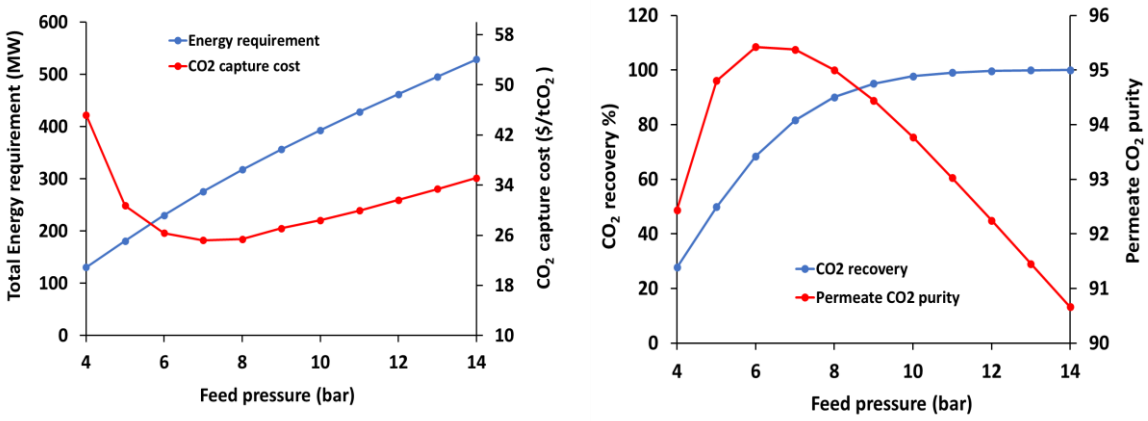

Fig.4-2. Effect of feed pressure on the membrane performance indicators

Depending on the operational conditions imposed by the grid and power plant fuel type, the CO_2 concentration of flue gas can fluctuate considerably. Accordingly, the influence of CO_2 fraction of flue gas on the CCS unit performance has been analyzed, and the results are presented in Fig.4-3. It is shown that by raising the feed CO_2 concentration, the total energy requirement for membrane-based CCS unit increases, which can be described by the higher energy consumption of the compressor and cooler upstream of the second membrane module. Also, the increment of feed CO_2 concentration increases the CO_2 recovery of process and CO_2 purity of permeate gas due to the availability of extra driving force. The higher increasing slope of CO_2 purity compared with CO_2 recovery is associated with the influence of membrane selectivity to improve the permeate purity at low availability of driving force. Although increasing the CO_2 concentration in the feed

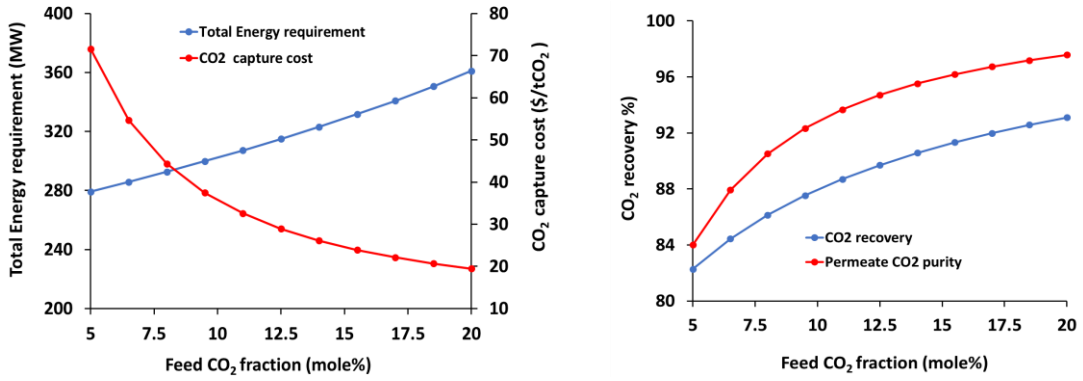

Fig.4-3. Effect of CO_2 fraction of flue gas on the CCS unit performance

gas increases the energy cost, the CO_2 capture cost significantly decreases due to the higher flowrate of CO_2 in permeate gas, which is the denominator of the economic indicator.

The influence of retentate recycling on the system performance indicator is illustrated in Fig.4-4. It can be concluded that by increasing the retentate recycling, the permeate CO_2 purity and CO_2 recovery improve due to the recirculation concept and high availability of driving force. Although recycling the second stage retentate stream increases the process energy consumption since a higher flow rate enters the compressors, it improves the economic indicator of the membrane CCS unit as the system can capture a larger amount of CO_2. It is shown here that it is necessary to recirculate the retentate gas from the second stage back to the first stage in order to guarantee high CO_2 purity in the permeate, although the energy consumption increases compared with a design without retentate recirculation.

According to the above parametric study of membrane-based CCS, along with the results provided in our previous work [189], there are various conflicts between the effect of operating and design variables of the CCS unit on the system performance, which need to be addressed for flexible and sustainable operation and design. In this regard, multi-objective optimization of the system has been performed, and the results are presented in the following section.

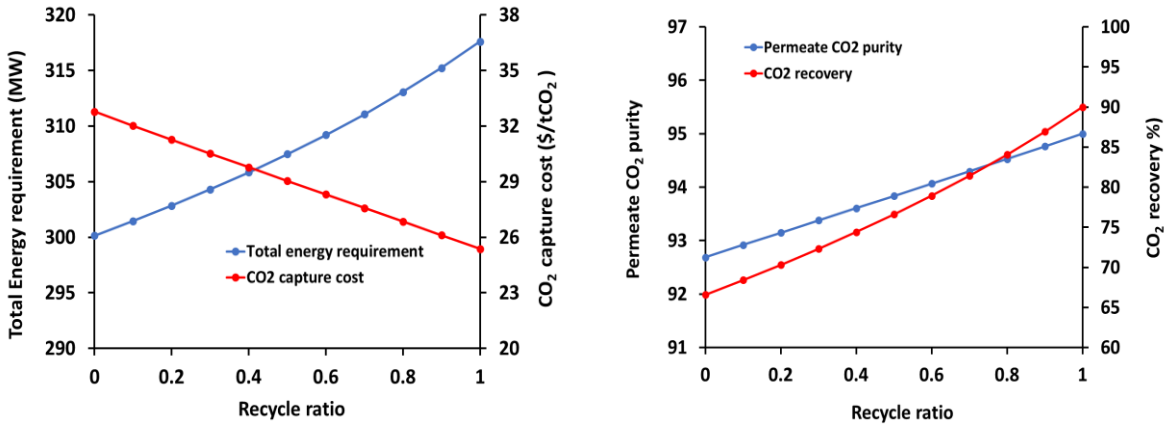

Fig.4-4. Effect of retentate recycling on the system performance

4.4.2 Process optimization

The multi-objective optimization of the two-stage membrane CCS process has been implemented by linking Aspen Plus and MATLAB using the MLMOPSO technique. As mentioned before, the membrane area is considered to be fixed, and their values for various membrane types are considered as the system reaches 90% CO_2 recovery and 95mole% CO_2 purity at the pressure of 8 bar, 13 mole% CO_2 in the feed gas, and full recycling. For the case of the Polaris gen1 membrane, the first and second module membrane areas are fixed at 6.6×10^5 m^2 and 3.5×10^4 m^2, respectively. These values are 3.41×10^5 and 1.79×10^4 for the case of the Polaris gen2 membrane.

To reach acceptable Pareto solution sets, several algorithm parameters are evaluated, and it has been concluded to consider maximum archive size = 200, swarm size = 50, number of leaders = 5, maximum iteration = 100, SIF = 2, global learning coefficient = 2.8, and personal learning coefficient = 1.2. The stopping criteria were met at the iteration number of 64, and 73 Pareto optimal solutions are found, as shown in Figure 6.

Fig.4-5 (a) presents the Pareto optimum solutions for the CO_2 capture cost and energy penalty of the process. Two Pareto points of A and B are marked, corresponding to the minimum total power requirement and the minimum CO_2 capture cost, respectively. Based on point (A), using the PVAM/PG membrane in the counter flow module and permeate vacuum approach led to the most energy-saving approach compared to the other designs, leading to the minimum energy penalty equal to 10.02%. Although turboexpander is unavailable in the vacuum design, since this design handles the permeate stream with a lower flowrate compared to the feed stream, which mostly consists of nitrogen, it requires a lower amount of power for recovering more than 70% of CO_2. However, the CO_2 capture cost at point (A) is the maximum (194 \$/tCO_2), which is mainly due to the higher capital cost as the prespecified required area of vacuum design (1.3×10^7 m^2) is significantly higher than feed compression to reach the separation target. The minimum CO_2 capture cost (point B) is equal to 13.1 \$/tCO_2 resulting from using the feed compression method and Polaris gen2 in the counter flow membrane module, which can be related to low required membrane area resulting from using a membrane with high permeance and efficient design. It should be noted that at this point, the values of energy penalty and CO_2 recovery are relatively high (35.5% and 92%, respectively), which is because of the high discharge pressure of compressors.

The Pareto optimum solutions for the CO_2 recovery and total power requirement of the process are shown in Fig.4-5 (b), in which Point C represents the highest achievable CO_2 removal of the system (99.99%). Considering a fixed membrane area, using feed compression and a counter flow module equipped with Polaris gen1 leads to the highest separation efficiency in the Pareto

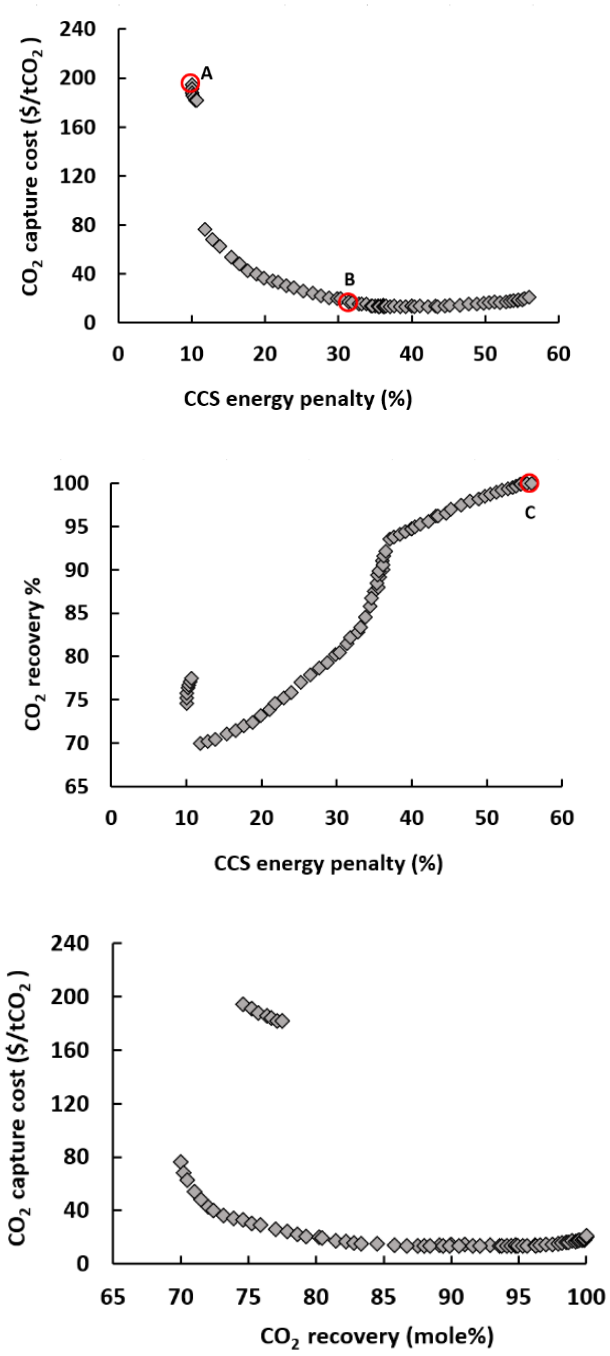

Fig.4-5. Pareto solutions set obtained from process optimization

solution set. At this point, the second stage is fully recycled, and flue gas CO_2 concentration and feed pressure are 20 mole% and 10.57 bar, respectively.

Accordingly, through the integration of a counter-current membrane module and feed compression approach, a post-combustion carbon capture process can be considerably improved in terms of sustainability. Additionally, generating driving force by means of permeate vacuum is more energy-efficient, improving the flexibility of the system. The results of the process analysis and optimization presented here can help process developers, and decision-makers select the sustainable design and operating conditions for the membrane-based carbon capture systems.

4.5 Dynamic modeling of a membrane module

Fig. 4-6 shows the schematic of a two-dimensional section of the hollow fiber membrane module corresponding to the geometry of the model considered in this study. For a hollow fiber membrane module, the basic principles for pressure drop calculation in permeate side and one-dimension flow patterns are valid.

In the membrane-based CO_2 separation, the post-combustion flue gas as the feed is supplied into the shell side, and carbon dioxide is separated via diffusion in the membrane and is exited from the end of the bore side as permeate gas. Also, the retentate gas, which mainly includes N_2, is exited from the outlet side of the shell.

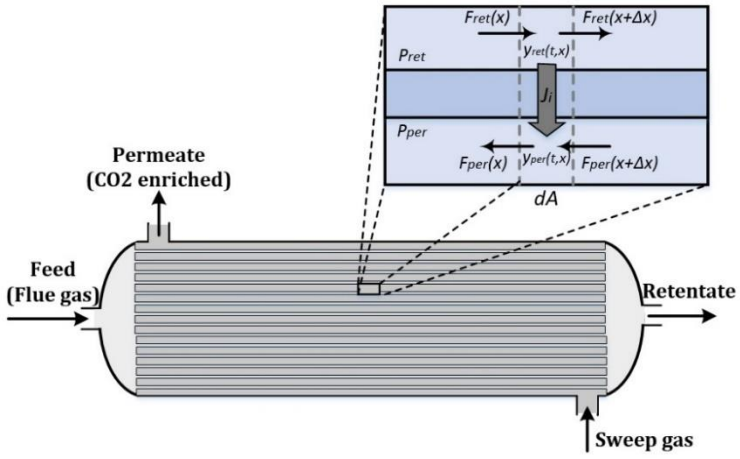

Fig. 4-6. Schematic of a hollow-fiber membrane in the counter-current flow design

The mathematical modeling of the membrane module proposed in this study allows the simulation of co-current and counter-current flow configurations. Also, it is possible to consider the shell-side of the membrane module as a feed inlet or its bore-side as a feed inlet. The considered assumptions in the mathematical formulation are listed below.

- The geometry of the hollow fibers is unaffected by high pressures.
- All fibers have identical inner and outer radiuses. This assumption allows modeling one fiber instead of various fibers with different diameters.
- The membrane module is under isothermal conditions because the temperature change of flue gas due to the Joule-Thompson effect is neglected in the studied range of feed pressure.
- There is a negligible pressure change in the feed side of the hollow fiber (shell side) because of constant bulk flow in the axial direction.
- The pressure drop in the bore side is described by the Hagen–Poiseuille equation.
- The plug flow model has been assumed in both bore and shell sides, which means that radial gradient in pressure and concentrations can be neglected. This leads to one-dimensional modeling of the membrane module in the direction of flow.
- Compressibility factor and pressure are considered to be steady for stable numerical solutions.
- Concentration polarization is negligible since it has a minor effect on the system performance.
- The gases behave as an ideal gas.

Transport through dense membranes can be described via the solution-diffusion mechanism [131]. The gas molecules diffuse through the membrane after being dissolved in the dense polymer membrane based on this method. Gas permeability is referred to the product of solubility and diffusivity. The rate of gas permeation through a dense membrane is described by Fick's law, where the partial pressure difference over the membrane is the driving force.

$$J_i = Q_i \pi D_o n_f \left(P_{ret} y_{ret,i} - P_{per} y_{per,i}\right) \qquad (1)$$

Where Q_i is permeance of *i* component in the membrane, P_{ret} and P_{per} are the retentate and permeate pressures, $x_{ret,i}$ and $y_{per,i}$ are the mole fraction of *i* component at the retentate and permeate, D_o is the fiber outer diameter, and n_f is the number of the fibers.

To write the overall mass balances, a differential area is selected, and the change of molar fraction for a certain period $[t\,;t+\Delta t]$ can be described as follows:

$$F_{per}(x+\Delta x)-F_{per}(x)=-\Delta x\sum_{i=1}^{n}J_i \qquad (2)$$

$$\left[F_{per}(x+\Delta x)y_{per,i}(t,x+\Delta x)-F_{per}(x)y_{per,i}(t,x)\right]\Delta t+\ J_i\Delta x\Delta t=\rho_{per}A_{per}\Delta x\left[y_{per,i}(t+\Delta t,x)-y_{per,i}(t,x)\right] \qquad (3)$$

Dividing the right and left sides of Equations (2) and (3) by Δx and $\Delta x\Delta t$, respectively, and tending Δx and Δt to zero, the following ordinary and partial derivatives equations are obtained:

$$\frac{dF_{per}}{dx}=-J_t \qquad (4)$$

$$\frac{d(F_{per}y_{per,i})}{dx}+J_i=\rho_{per}A_{per}\frac{dy_{per,i}}{dt} \qquad (5)$$

Applying the product rule to the first term of Equation 2 leads to:

$$F_{per}\frac{d(y_{per,i})}{dx}+\ y_{per,i}\frac{d(F_{per})}{dx}+J_i=\rho_{per}A_{per}\frac{dy_{per,i}}{dt} \qquad (6)$$

By substituting equation 4 in equation 6, the rate of change in component concentration can be calculated as follows:

$$F_{per}\frac{d(y_{per,i})}{dx}+J_i-J_t\,y_{per,i}\ =\ \rho_{per}A_{per}\frac{dy_{per,i}}{dt} \qquad (7)$$

Considering the same approach for the shell side, the following equations can be derived for the retentate flow rate and rate of changes in component concentration of the retentate side.

$$\frac{dF_{ret}}{dx} = -J_t \qquad (8)$$

$$\rho_{ret} A_{ret} \frac{dy_{ret,i}}{dt} = F_{ret} \frac{d(y_{ret,i})}{dx} + J_i - J_t \, y_{ret,i} \qquad (9)$$

Besides the equation for gas flowrate, the model needs to calculate the pressure on both shell and bore sides. Therefore, the permeate side and retentate side pressure changes are calculated as follows:

$$p_{per} \frac{dp_{per}}{dx} = \frac{128 \mu R T F_{per}}{n_p \pi D^4} \qquad (10)$$

$$\frac{dp_{ret}}{dx} = \frac{32 V_{ret}}{D_h^2} \qquad (11)$$

$$V_{ret} = \frac{F_{ret}}{\rho_{ret} S_{sh}} \qquad (12)$$

Where D_h is the hydraulic diameter of the shell side, and S_{sh} is the cross-sectional flow area of the shell side.

For polymer membranes, the solution–diffusion mechanism describes the gas permeation. Based on this mechanism and physiochemical interactions between the membrane and gas components, the separation of gas components can occur by both diffusions through the membrane and the solubility of gas molecules in the membrane. The gas permeability (*P*) is defined as the product of the diffusivity coefficient (*D*) and the solubility coefficient (*S*):

$$P = D \times S \qquad (13)$$

In the membrane module, the gas separation is described by the sorption of the permeant components in the membrane at the high-pressure side (feed side), diffusion through the membrane due to the gradient of partial pressure, and finally, the gas components desorption at the low-pressure side (permeate side). The penetrant solubility measures the gas amount sorbed by the membrane in an equilibrium state at a specific gas temperature and pressure, which commonly increases as the gas condensability and interactions with the polymer increase (thermodynamic parameter). On the other hand, diffusivity is a kinetic measurement of the permeate gas transport

rate through the membrane, which depends on penetrant size, membrane free-volume, and polymer chain flexibility.

The membrane selectivity toward a specific gas component is defined as the capability of the gas to permeate through the membrane. The permselectivity is the ratio of the permeability coefficient of two gases, A and B, as follows:

$$\alpha_{A/B} = \frac{P_A}{P_B} = \left[\frac{D_A}{D_B}\right] \times \left[\frac{S_A}{S_B}\right] \qquad (14)$$

The dependency of transport properties on the pressure and temperature of rubbery polymeric membranes is considered using a modified form of the Van't Hoff-Arrhenius model developed by Maghami et al. [181]. Based on this model, the following equations describe the effect of temperature and pressure on membrane permeability.

$$P_i = a_p p^{b_p} exp\left(\frac{-\left(c_p \ln p + d_p\right)}{RT}\right) \qquad (15)$$

where *a*, *b*, *c*, and *d* are modifiable parameters, and *p* is the feed pressure. This study considers the adjustable parameters suggested by Maghami et al. (2019) for the 6FDA-DAM membrane.

The boundary conditions for the above equation can be written as follows:

At x=0: $F_{ret} = F_{feed}$, $p_{ret} = p_{feed}$, $F_{per} = F_{feed} - F_{ret}(x = L)$

At x=L: $p_{per} = 1.1\ bar$

The initial condition for the simulation is considered the steady-state condition, which means that the time derivative of all variables at t=0 is equal to zero.

The resulting solution of the above equations allows modeling the concentration profile along the membrane in the counter flow hollow fiber membrane gas separation under unsteady operation. Accordingly, the model is programmed using the Academic license of gPROMS v1.5.0 custom process modeling software, and all PDEs and ODEs are solved using the default gPROMS solver considering a variable time step. The second-order centered finite difference method is used for discretizing the spatial domain, and 400 elements are used as a default. The Peng-Robinson equation of state model is considered using the Multiflash thermodynamic package to model the

gas behavior in the membrane separation process. The gas inlets and outlets are defined using the built-in gPROMS mole fraction port. Finally, all differential equations pertaining to the membrane module are solved using the central finite difference and default solver in gPROMS software.

It should be noted that before the flue gas is delivered to a membrane module, other impurities in the flue gas, such as CO, H_2S, NO_x, and SO_x, need to be removed to prevent corrosion of the pipeline and improve the process operation. Also, due to possible interactions of sorbed water with the membrane, analyzing the impact of water vapors on membrane system performance is complex and challenging. Accordingly, it is assumed that the power plant flue gas passes from the particulate and water removal units, and the input gas to the CCS unit can be considered as a binary gas consisting of CO_2 and N_2 (87 mole% N_2 and 13 mole% CO_2). The membrane length is assumed to be 1 *m*, and the membrane's outer and inner diameters are 600 and 400 µm, respectively. Also, the selectivity of N_2 (α) and CO_2 permeance (p_{CO2}) is assumed to be 50 and 1000 GPU, respectively, which are similar to the properties of the first generation of Polaris^{TM} membrane developed by Membrane Technology Research Inc [126]. CCR is a custom variable corresponding to the fraction (mol basis) of CO_2 that leaves in the permeate outlet stream with respect to the CO_2 at the feed inlet, fixed at 0.8. Furthermore, It has been assumed that the membrane system is working under isothermal conditions, and the energy balance equations are ignored. The inputs and outputs of the dynamic model of the membrane are presented in Table 1.

Table 4-4. Inputs and outputs of the system model

Model	Input	Output
Fiber bundle	Feed flow rate: 67033 kmol/hr	Tube side partial pressure
	Feed composition: 0.13 mole% CO_2	
	Feed pressure: 5 bar	
Shell	Sweep flow rate: 13% of retentate	Shell side partial pressure
	Sweep composition: same as retentate	
	Sweep pressure: 1 bar	
Membrane	Permeance: 1000 GPU	Component flux
	CO_2 Selectivity: 50	
	Tube side pressure: 5 bar	
	Shell side pressure: 1 bar	
	CO_2 recovery: 80%	
Membrane module	Size specifications	Permeation area,

	• Fiber bundle length: 1 m • Fiber inner diameter: 0.4 m • Fiber outer diameter: 0.6 m • module Packing density: 0.8	Retentate composition, Retentate pressure, Permeate composition, Permeate pressure

The steady-state simulation of membrane-based CCS showed that system energy consumption, CO_2 separation cost, membrane size, and system cost significantly vary by a change in feed condition. For investigating the transient response of the membrane process system, step changes in the process feed conditions have been applied, and the response of system operating and design variables such as permeate concentration, permeate flowrate, retentate concentration, and the total required membrane area have been evaluated. To this end, we have utilized the Schedule feature of gPROMS to impose the dynamic membrane model to step-change at a specified time in feed pressure, feed flow rate, feed concentration, and retentate recycling ratio.

4.6 Transient behavior results and discussion

The proposed model of the membrane module is first validated using the results of membrane gas separation processes reported by Merkel et al. [127], as shown in Table 4-5. The flue gas flow rate is assumed to be 500 m^3/s with 13 mole.% of CO_2, and the feed pressure and temperature are considered to be 1.1 bar and 50 ℃, respectively. The permeate side pressure and the recovery ratio of CO_2 are constant and equal to 0.22 and 0.9, respectively. Considering the same membrane geometry and modeling methodology, there is an excellent agreement between the modeling results and the results provided by Merkel et al. [127]. According to Table 2, the absolute maximum error is less than 1% which is related to the solver, numerical approach, and the size of discretization elements.

Table 4-5. Model validation using the reported data by Merkel et al. (2010).

	Counter-current flow configuration	
process specification	**Modeling results**	**The work by Merkel (2010)**
Membrane area (m^2)	6.77×10^6	6.80×10^6
CO_2 mole% in permeate	40.57	40.60

CO_2 mole% in retentate	2.09	2.10
Abs. Maximum error	0.47 %	

4.6.1 Dynamic behavior of CCS system to step-change in membrane feed pressure

The pressure ratio available in the membrane module is an essential parameter for the performance of the membrane system, which is supplied from compressors upstream of the membrane. The compressor outlet pressure is mainly controlled to be fixed at a specified pressure; however, at partial operating conditions with the aim of changing compressor energy consumption, the compressor outlet pressure may suddenly change, which affects the performance of membrane CCS. Moreover, the inlet pressure of the membrane module is considered an operational parameter that can highly affect the performance and energy requirement of the membrane module. Therefore, the change in membrane module feed pressure plays an important role in improving the flexibility of the membrane module. In this section, the transient behavior of the membrane module is investigated as the feed pressure suddenly decreases from 8 to 5 barg at t =20 s. Also, the effect of a sudden increment in inlet pressure on the transient behavior of the membrane module (from 5 to 8 barg at t =20 s) is analyzed. In all process analyses, the total CO_2 recovery ratio is considered to be constant and equal to 80%, which is a typical recovery ratio for single-stage membrane-based CCS. The dynamic behavior of stream flowrate, permeate and retentate concentration, and required membrane area are presented in this section for two cases: constant membrane permeability and variable membrane permeability as a function of operating pressure and temperature.

Constant membrane transport properties

As common assumptions in membrane separation modeling, the membrane permeability can be considered to be constant and independent of operating parameters. For this case, the effect of step-change in feed pressure on the transient behavior of permeate and retentate flowrate is presented in Fig. 4-7. Generally, considering a fixed CO_2 recovery, the decrease of feed pressure leads to a lower permeate gas CO_2 concentration and a higher permeate gas flow rate. Therefore, by a step decrease of feed pressure from 8 to 5 barg, the permeate flowrate exhibits an overshoot; it quickly reaches a new steady-state condition after 11 seconds. In contrast, the retentate molar flowrate shows an undershoot by a step-change in feed pressure, and it goes to a new steady-state after 11 seconds. The undershoot and overshoot behavior of the molar flowrate response are

attributed to the jump in the rate of permeation (Eq. 1), which decreases proportionally to the step-decrease in the feed pressure. This causes a significant change in the membrane permeation resistance, leading to overshoot and undershoot in the molar flow rate of permeate and retentate, respectively. Moreover, by increasing the feed pressure from 5 to 8 barg, the permeate flowrate exhibits an undershoot; it quickly reaches a new steady-state condition after 7 seconds. It can be concluded that the transient response of the membrane module toward the step decrease in feed pressure is faster than that of the step increase in feed pressure.

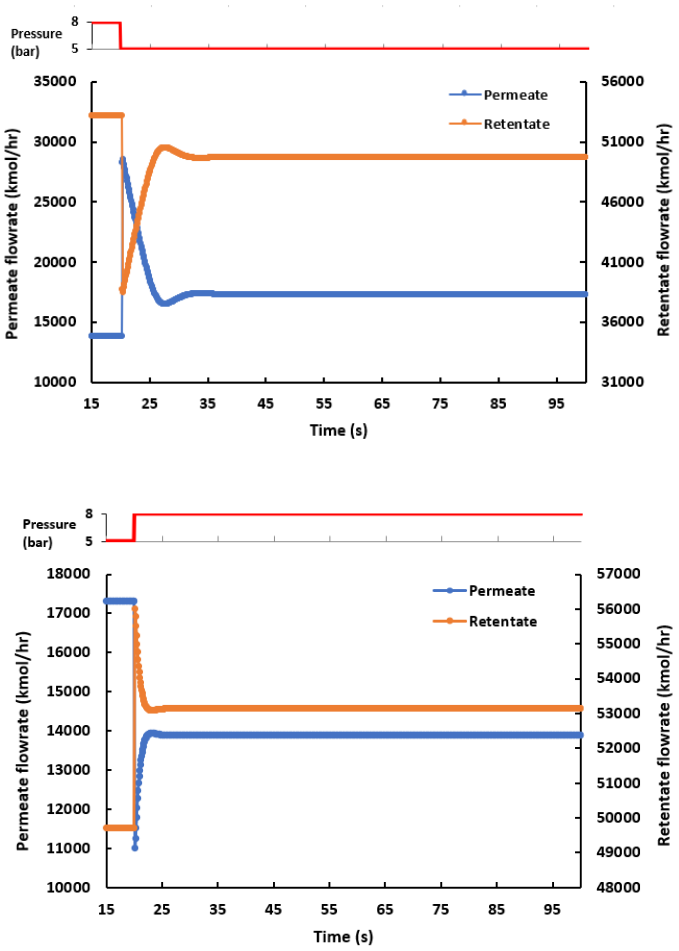

Fig. 4-7. Transient behavior of membrane system flowrate to step-change in pressure.

The effect of step decrease in feed pressure on the CO_2 purity of permeate stream and N_2 purity of the retentate stream is depicted in Fig. 4-8. Generally, the permeate stream has a higher purity of CO_2 at the higher feed pressure since more driving force is available in the system, and

the membrane separation performance improves, as described by the solution diffusion mechanism. As shown in Fig. 4-8, the transient behavior of permeate and retentate concentration due to step-change in the feed pressure is very fast, and the system can reach to steady state in less than 13 seconds. Also, the transient behavior of N_2 purity in the retentate and CO_2 purity in the permeate stream shows an undershoot by applying a step decrease in the feed pressure due to the jump in the rate of CO_2 permeation. After a time delay of 13 seconds due to the overshoot and undershoot, the system becomes steady at the new feed pressure conditions. Also, the transient behavior of permeate and retentate concentration due to step-increase in the feed pressure is faster than the stem decrease condition. As a result, the system can reach a steady state in less than 5 seconds. Also, the transient behavior of N_2 purity in the retentate and CO_2 purity in the permeate stream shows a slight overshoot. After a time delay of 5 seconds due to the overshoot, the system becomes steady at the new feed pressure conditions.

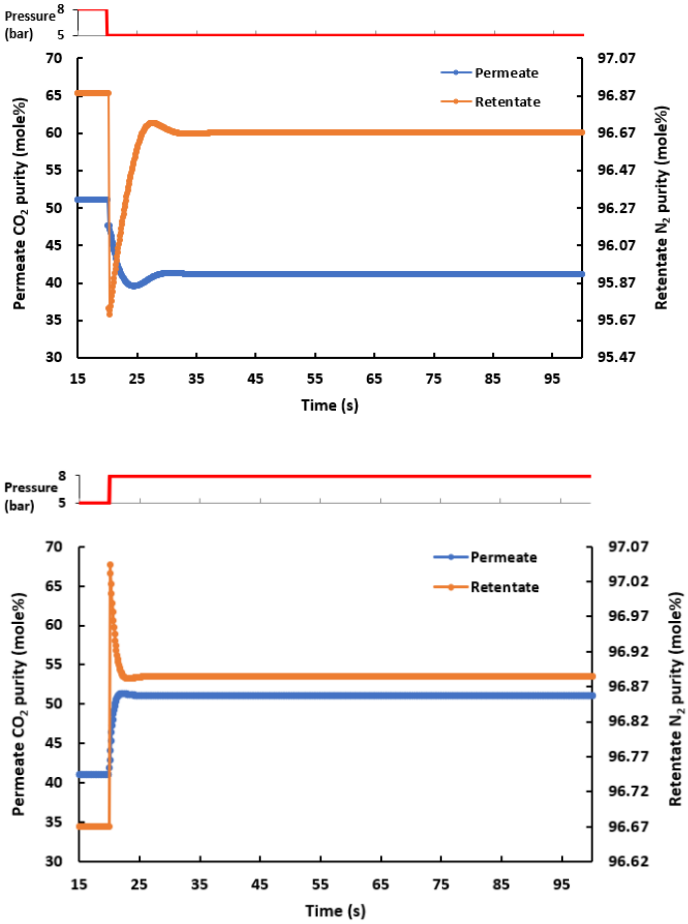

Fig. 4-8. Transient behavior of membrane system concentration to step-change in pressure

Understanding the required membrane area at various times and operations can help process engineers design a membrane module that can operate flexibly and tolerate unexpected operating conditions. Also, it shows the membrane's flexible operation at different operating conditions as the membrane design is modular and parallel and can bypass some modules to reduce the available contact area. Therefore, the effect of a step decrease of the feed pressure on the total membrane area required to meet 80% CO_2 recovery is illustrated in Fig. 4-9. It can be noticed that decreasing the membrane feed pressure causes an increase in the required membrane area. Because by decreasing the pressure difference between the inlet and outlet of the membrane, the available driving force for the CO_2 separation decreases, which leads to an increase in the required area of the membrane. Furthermore, an undershoot in the dynamic response of the membrane area can be seen due to a sudden increase in the feed pressure, and there is an overshoot in the required membrane area with a step decrease in feed pressure, which needs to be considered by process designers.

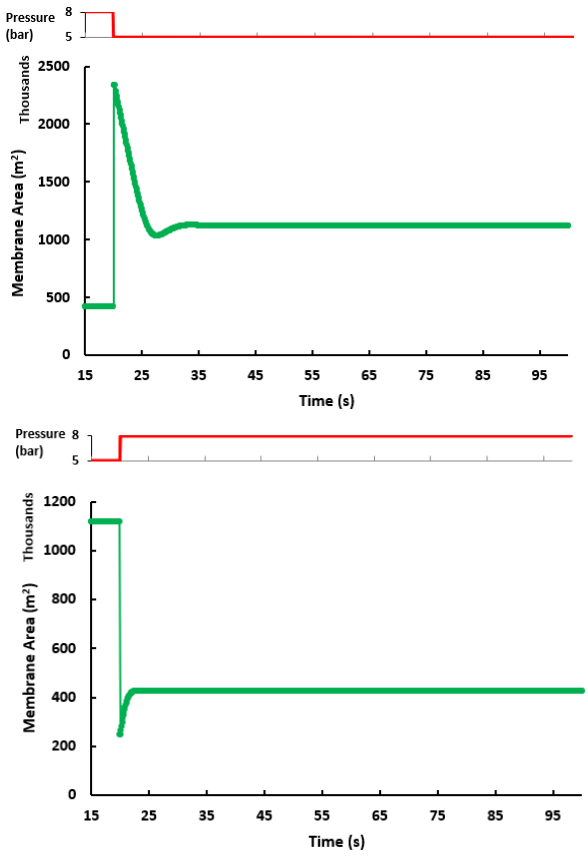

Fig. 4-9. Transient behavior of membrane system area to step change in pressure

Accordingly, it can be concluded that by reducing the feed pressure, the available driving force for permeation is decreased, leading to a higher required membrane area to achieve the separation target (80% CO_2 recovery). The higher area of the membrane in the module leads to a higher flowrate of permeate stream with a lower concentration of CO_2, as shown in Fig. 4-8. Therefore, considering a fixed CO_2 recovery, by decreasing the feed pressure, the required membrane area and permeate flowrate increases, however, the purity of CO_2 in the permeate gas decreases.

Variable membrane transport properties

To thoroughly analyze the effect of step pressure reduction and temperature change on the transient behavior of the membrane separation process, it is required to consider the variation of membrane permeability and selectivity with pressure and temperature. Accordingly, based on the modified form of the Van't Hoff-Arrhenius model, by applying a step decrease in feed pressure from 8 bar to 5 bar at t= 20s, the variation of permeability and selectivity of membrane versus operation time at two different temperatures are presented in Table 4-6.

Table 4-6. Effect of pressure and temperature on the membrane permeability and selectivity at T= 35 ℃ and 40 ℃

Membrane properties	Constant value	Time: 0-20s (inlet pressure: 8 bar)		Time: 20-100s (inlet pressure: 5 bar)	
		T= 35 ℃	T= 45 ℃	T= 35 ℃	T= 45 ℃
Permeability (GPU)	1000	900	1000	927	980
Selectivity	50	34.9	50	29.7	42.5

As shown in Table 4-6, the permeability of CO_2 through the membrane is increased upon the decrease of the membrane feed pressure from 8 to 5 bar at t=20s. However, it is reported that the permeability of N_2 slightly decreases by increasing the membrane feed pressure. Also, the permeability of CO_2 is much higher than N_2 in all cases. In principle, this behavior corresponds to the variation of the polymer's physical properties like density, molecular weight, and free volume, and plasticization is not expected to play a role in the considered pressure range [181]. Also, the observed increase in CO_2 permeability with pressure can be explained by Eq. 15. On the other hand, the CO_2 permeance of the membrane declines with increasing the operating temperature. Because, contrary to diffusivity, the solubility generally reduces at lower temperatures, and as shown in Eq. 13, the combination of these parameters leads to a decrease in CO_2 permeability.

Consequently, as shown in Table 4-6, decreasing the feed pressure from 8 to 5 bar increases the selectivity of CO_2/N_2, and the selectivity of CO_2/N_2 decreases by increasing the temperature from 35 to 45 °C. The effects of membrane permeability and selectivity variations -resulting from pressure and temperature changes- on the transient behavior of the separation process are presented in Fig. 4-10. As mentioned, in the case with a variable permeability and selectivity, the values of membrane transport coefficients are lower at various times compared to the case with fixed transport coefficients, which leads to a lower CO_2 mole fraction in the permeate. Furthermore, more membrane area is required at a higher membrane selectivity since the higher value of CO_2/N_2 selectivity results in higher CO_2 purity in the permeate and lower N_2 permeation. Therefore, this reduction in the total flow rate of permeate resulted in a larger required membrane area to obtain the specified CO_2 recovery ratio. The other interesting result is that in the case of variable permeability and selectivity, the length of overshooting and undershooting in the membrane transient response becomes lower, which is attributed to the lower membrane transport coefficients. Accordingly, it can be concluded that the higher selectivity and permeability of the membrane, the larger the length of overshooting and undershooting in the transient response of the membrane module.

4.6.2 Dynamic behavior of the system to step-change in feed flow rate

The fossil-fueled power plant is coupled with a carbon capture system and renewable energy sources in a flexible and sustainable power generation system. This integration requires all components to operate in a flexible manner which necessitates their partial load operation. When a power plant is working in partial capacity, the amount of produced flow gas varies at different operating conditions, which can be interpreted as a step change of flow rate in the downstream unit, membrane-based carbon capture system. To analyze the dynamic behavior of a membrane module toward step-change in feed flow rate, we have imposed a step increase of 30000 kmol/hr in feed flow rate after 20 seconds of steady operation at 67033 kmol/hr. Accordingly, the transient behavior of the membrane module as the feed flowrate suddenly changes from 67033 kmol/hr to 97033 kmol/hr at t = 20 has been investigated by assuming the total CO_2 recovery of the system is equal to 80%.

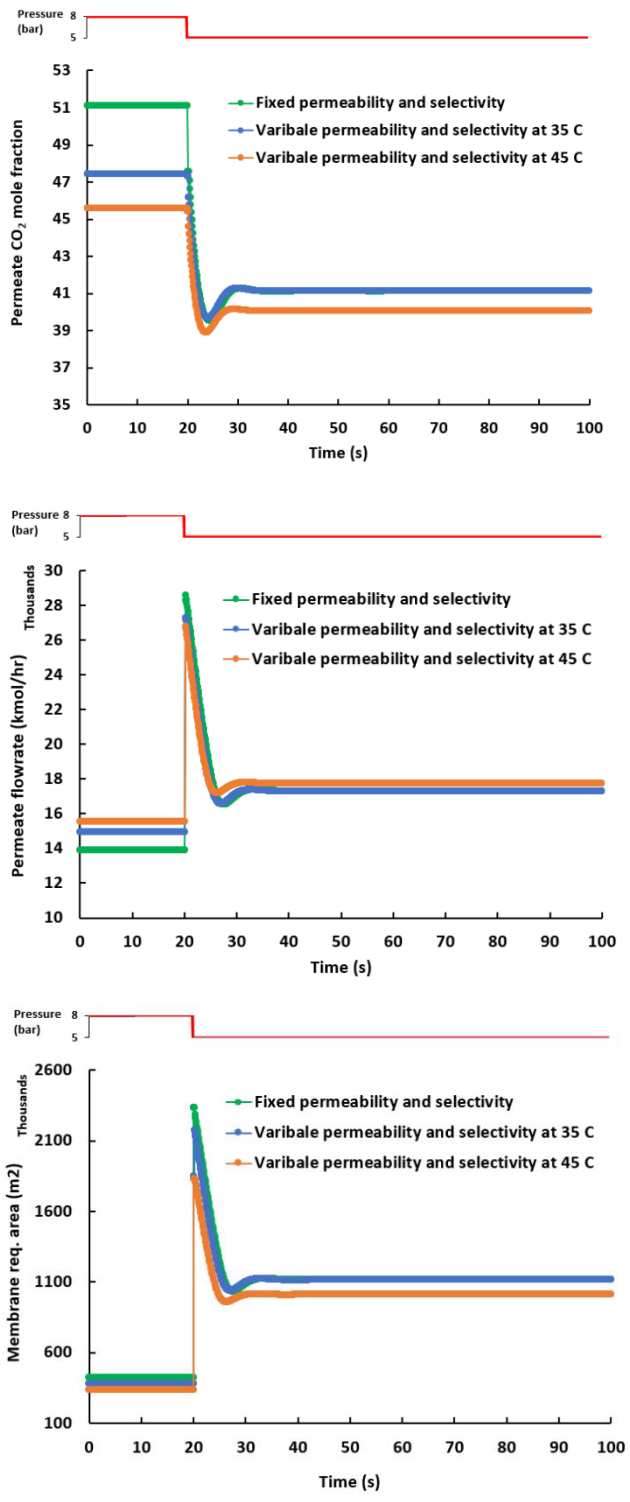

Fig. 4-10. Comparison the transient behavior of membrane system to step increase in the feed pressure at two cases: Constant and Variable permeability and selectivity

Fig. 4-11 presents the transient behavior of the membrane system toward step increase in the feed flowrate as described above. An increment of the feed flowrate proportionally increases the permeate and retentate flowrate. Also, it shows that by applying a step increase in the feed flowrate, the molar flow rate of permeate and retentate respond very fast and without time delay to reach a new steady state. Therefore, The fast dynamic behavior of the membrane system by step change at feed flowrate makes this system a good alternative for future flexible carbon capture systems, in which the membrane system needs to operate in partial load conditions typically.

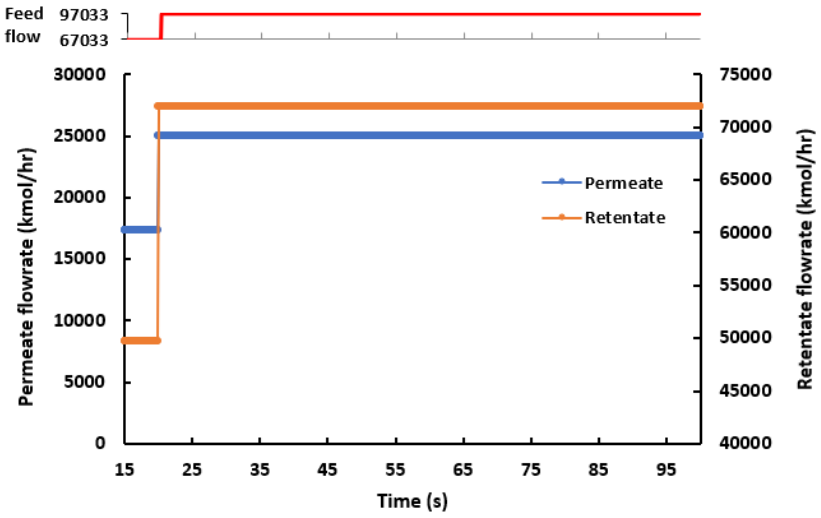

Fig. 4-11. Transient behavior of membrane system flowrate to step change in feed flowrate

Fig. 4-12 presents the transient behavior of product purity towards step increase in the feed flowrate. Since the CO_2 recovery ratio of the membrane module is constant (80%), product purities in both permeate and retentate streams do not change by any disturbance in feed flowrate.

Fig. 4-13 depicts the transient behavior of the required membrane area by applying a step increase in feed flowrate after 20 seconds of steady operation. Generally, by increasing the feed flowrate in the membrane module, more membrane area is required to separate the required amount of CO_2. Based on the result of Fig. 4-13, the required membrane area quickly increases by applying a step increase in feed flow rate. It should be noted that since our goal is to improve the design of membrane-based CCS for flexible operation, the membrane area is not considered to be fixed. Accordingly, by increasing the feed flowrate, both outlets' flowrate and the membrane area

required to achieve the specified CO_2 recovery ratio increase. This increase in membrane area improves the permeate rate of components through the membrane so that the product purities in both permeate and retentate streams do not change by any disturbance in feed flowrate.

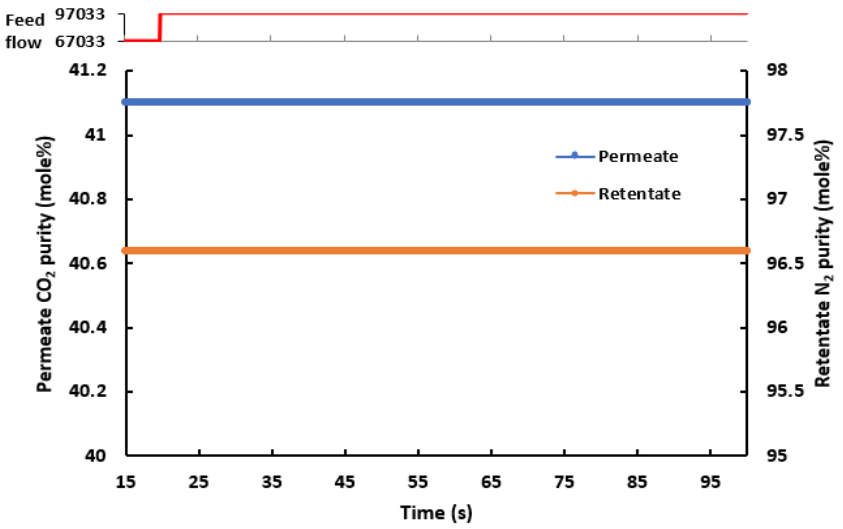

Fig. 4-12 Transient behavior of membrane system concentration to step change in feed flowrate

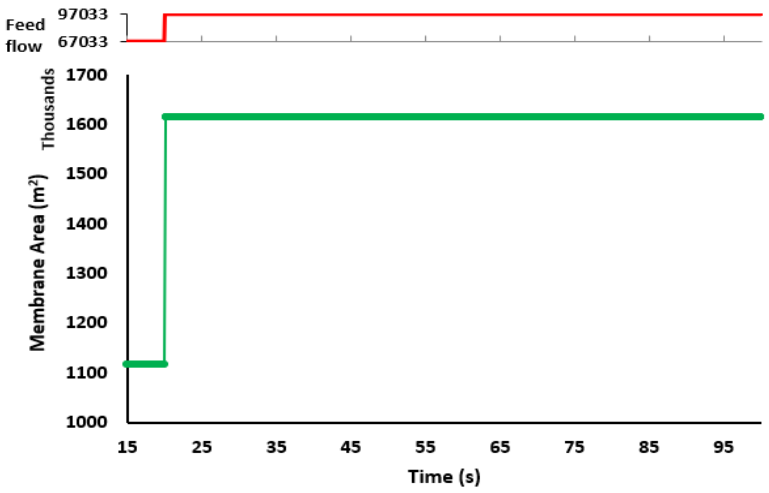

Fig. 4-13 Transient behavior of membrane system area to step change in feed flowrate

Overall, it can be concluded that the dynamic performance of the membrane toward a step-change in feed flowrate is very fast, which implies that membrane-based carbon capture can respond quickly and operate in a flexible manner in the future low-carbon energy system.

4.6.3 Dynamic behavior of the system to step change in feed composition

The concentration of CO_2 in the post-combustion flue gas is not constant, and it can change at various operating conditions, particularly when the power plant is integrated with renewable energy sources and a carbon capture system. Moreover, some power plants can operate with various fossil fuels, which leads to the generation of flue gas with different concentrations of CO_2. For instance, natural gas power plants produce a flue gas with about 5 mole% CO_2, while the flue gas released from coal-fired power plants includes 10-15 mole% CO_2 [263]. Accordingly, investigating the transient behavior of membrane systems toward changes in feed composition is of great importance. In this section, the transient behavior of the membrane module is investigated as the CO_2 concentration of feed suddenly decreases from 13 mole% to 5 mole% after 20 seconds of steady operation, considering the fixed CO_2 recovery of the membrane module equal to 80%.

The effects of step decrease in feed CO_2 concentration on the transient behavior of permeate and retentate flowrate are presented in Fig. 4-14. As can be seen, the membrane system response to a step-change in feed CO_2 concentration is slow compared to other step changes in feed pressure and feed flow rate. It can be seen that when the feed CO_2 concentration reduces from 13 mole% to 5 mole% after 20 seconds of operation, the permeate and retentate flowrate slowly reach steady-state condition, approximately after 17 seconds.

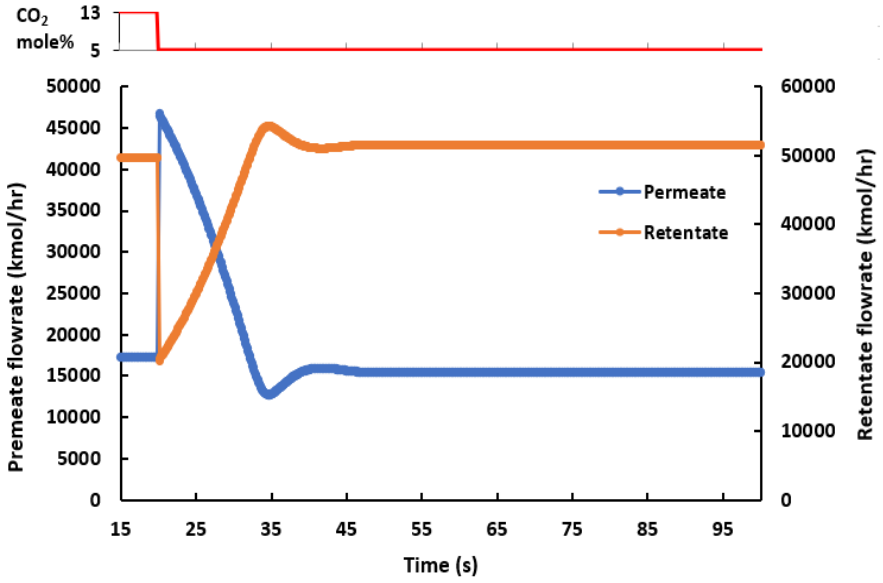

Fig. 4-14 Transient behavior of membrane system flowrate to step change in feed concentration

Fig. 4-15 presents the transient behavior of product purity in permeate and retentate toward step-change in feed CO_2 concentration. Similar behavior to product flowrate can be seen for permeate and retentate concentrations, in which by decreasing the CO_2 concentration in the feed, the permeate CO_2 concentration decreases and retentate N_2 concentration increases. The reason for this slow response is due to the rate of permeation and its dependence on the components mole fraction, which make the membrane module respond slowly to a step-change in feed concentration.

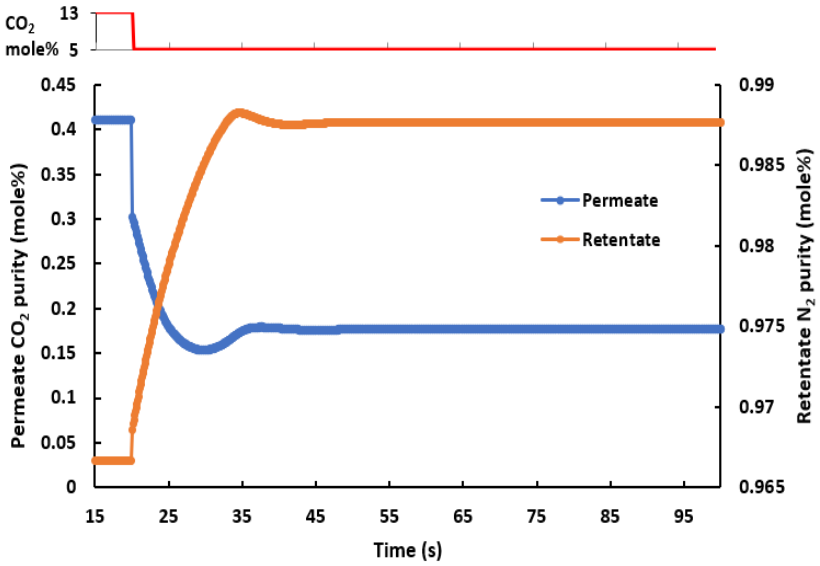

Fig. 4-15 Transient behavior of membrane system concentration to step change in feed concentration

The dynamic behavior of the required membrane area toward step-change in the CO_2 concentration of the feed stream is shown in Fig. 4-16. According to this figure, the required membrane area slowly changes with the step decrease of feed gas CO_2 concentration after 20 seconds. This is mainly because by increasing the permeate gas flow rate, a larger membrane area is required for separating a certain purity of CO_2. Also, this increasing trend in membrane area is more intense in the case of a step decrease in the feed CO_2 concentration applied to the membrane system.

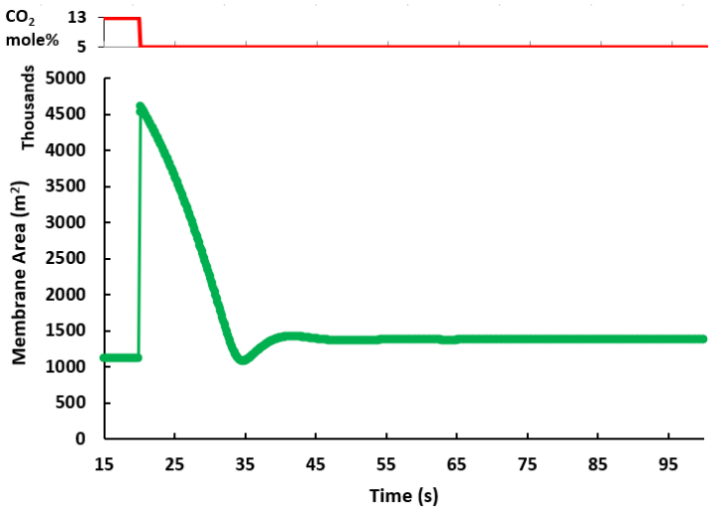

Fig. 4-16 Transient behavior of membrane system area to step change in feed concentration

4.6.4 Dynamic behavior of the system to step change retentate recycling

Considering recycling in the membrane-based carbon capture has a significant influence on the system performance, and since the recycling is from the retentate stream, it is not fixed and can vary at different operating conditions. To analyze the dynamic behavior of the membrane module toward step-change in retentate recycling, we have imposed a step increase of 20% of retentate flowrate to be recycled after 20 seconds of steady operation without recycling by assuming the fixed total CO_2 recovery of the membrane module.

Fig. 4-17 and Fig. 4-18 present the transient behavior of molar flowrate and product purities toward step-change in the amount of retentate recycling ratio. Based on Fig. 4-17, applying step increase in retentate recycling, undershoot the permeate flow rate, and the system needs 22 seconds to reach a new steady-state condition. The reason for undershooting in the permeate flow rate is that by increasing the retentate recycling, an additional driving force will be generated in the system, which leads to improving the system performance. Therefore, it can be concluded that at a fixed CO_2 recovery ratio, a lower permeate flow rate is required to capture a specific amount of CO_2, which is represented by a higher purity of permeate stream.

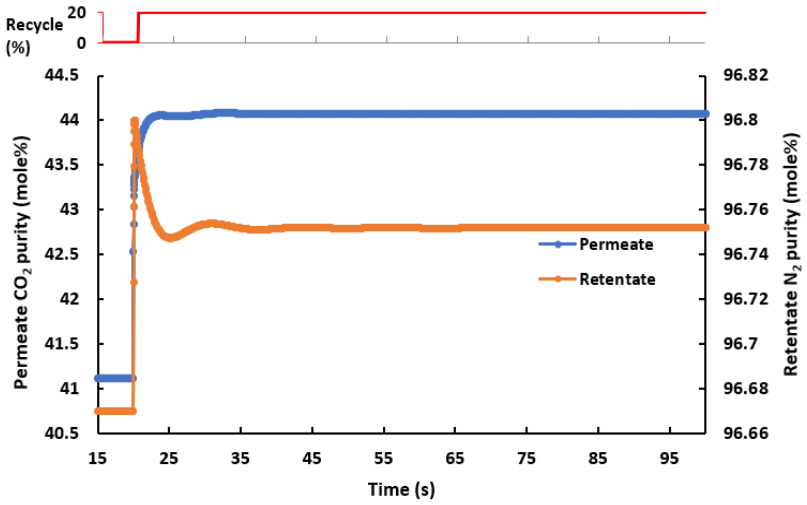

Fig. 4-18 Transient behavior of membrane system concentration to step change in retentate recycling

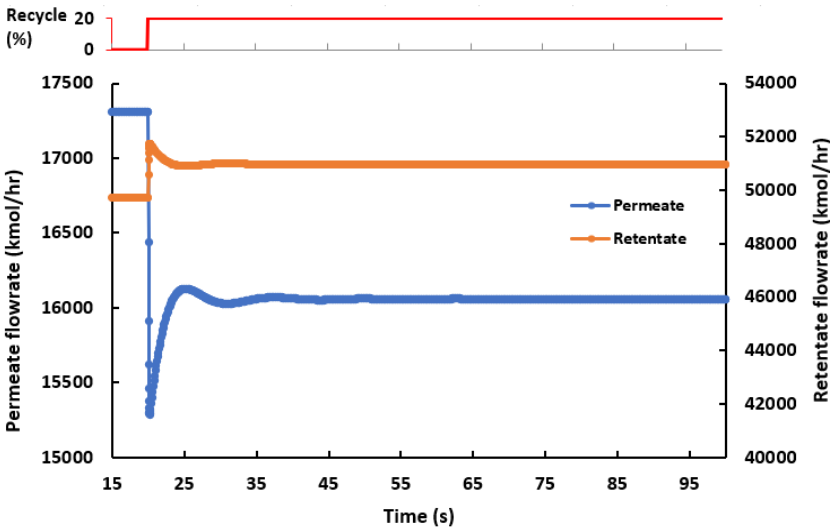

Fig. 4-17 Transient behavior of membrane system flowrate to step change in retentate recycling

As shown in Fig. 4-19, by increasing the recycling percentage, the inlet flow rate of the membrane system elevates, leading to an increment in the required membrane area to meet the separation target. Accordingly, considering 20% of the retentate stream as a step-change in the recycling flowrate, the membrane area required to capture 80% of CO_2 suddenly increases due to the availability of more flowrate in the membrane module. Moreover, the time delay of the

membrane area to reach a new steady-state is small, and the system experiences a steady-state condition after almost 6 seconds.

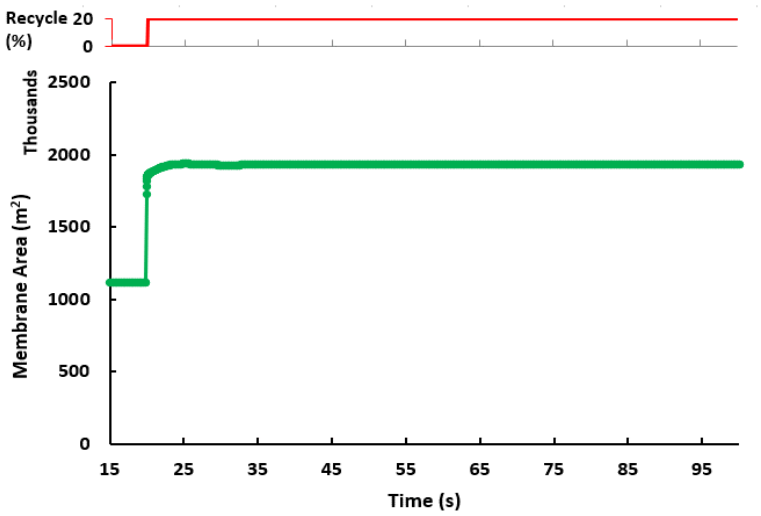

Fig. 4-19. Transient behavior of membrane system area to step change in retentate recycling

4.7 Chapter Summary

The objective of this chapter is to tackle the third and fourth research questions (RQ3 and RQ4) since the design and operation of membrane-based CCS in a sustainable and optimal manner are crucial to their large-scale deployment. It aims to achieve this by devising an economically feasible design for a multi-stage membrane-based CCS system that can operate flexibly alongside a power plant engaged in load-following operations. The chapter presents novel findings pertaining to these research questions. Specifically, it discusses the optimized multi-stage membrane-based CCS process and explores the potential trade-offs between energy consumption and cost implications (addressing RQ3). Additionally, it examines the flexible operation and transient behavior of the membrane process when integrated with a power plant that follows load fluctuations (addressing RQ4).

The unsteady model of the membrane is programmed in Aspen Custom Modeler and imported into Aspen Plus to examine the effects of feed pressure, CO_2 concentration, retentate recycling, and membrane properties on separation efficiency, power consumption, and economic performance of a double-stage membrane process. Following that, Aspen Plus and MATLAB are

linked to determine the optimal operating and design conditions of the process using the MLMOPSO technique. With increasing CO_2 concentration in the feed gas, CO_2 removal improves, and CO_2 capture costs decrease significantly, although the process energy requirement increases slightly. Analyzing the best possible trade-offs between objective functions confirms that there is significant potential to improve the sustainability of the process.

Since the membrane technology for gas separation is a promising alternative for capturing CO_2 from the flue of gas power plants, it is of great importance to study the transient behavior of membrane gas separations at various operating conditions. In this regard, the flexibility of the membrane process is discussed in this paper by developing a rigorous dynamic model for the membrane module and analyzing the system's transient response. The transient behavior of membrane-based CCS by applying step change in the process parameters such as membrane pressure, feed flow rate, feed CO_2 concentration, and recycling percentage is then investigated using gPROMS custom modeling software.

The results show that the response of the membrane module to a step-change in pressure is relatively fast; the membrane module requires 11 seconds to reach a steady-state, while the system response to a step-change in feed composition is slower and goes to a steady-state after 20 seconds. The permeate and retentate concentration present a fast response to step-change in the feed pressure, and the system reaches to steady state in less than 13 seconds. Also, the results show that the higher selectivity and permeability of the membrane, the larger the length of overshooting and undershooting in the transient response of the membrane module. Furthermore, the fast dynamic behavior of the membrane system by step change at feed flowrate makes this system a good alternative for future flexible carbon capture systems, in which the membrane system needs to operate in partial load conditions typically. The results of this work can be helpful for process designers and decision-makers to understand better the optimal and flexible design and operation of CO_2 capture systems.

Chapter 5. A Novel Solar-assisted Hybrid Design of CCS Process for Flexible Integration

- ? **Research question: RQ5-** What novel process design and integration can be developed to overcome the limitations of the current carbon capture systems? How can the integration of power plants with renewable energy sources and membrane-based CCS be optimized to create a hybrid system that combines efficient carbon capture with sustainable power generation?
- ➢ **Objective:** Development of a novel solar-assisted hybrid membrane-amine carbon capture system for flexible and sustainable decarbonization of natural gas-fired combined cycle power plant
- ✓ **New knowledge:** Efficient and robust design of a CCS process by hybridization of membrane-amine process and solar heating field for flexible and sustainable decarbonization of NGCC power plant

In this chapter, a flexible and sustainable design is proposed for decarbonizing a Natural Gas-fired Combined Cycle (NGCC) power plant using a solar-assisted hybrid membrane-amine carbon capture and storage (CCS) system. The design incorporates a multi-stage CO_2 selective membrane module for Selective Exhaust Gas Recirculation (SEGR) combined with exhaust gas recirculation (EGR) to increase the concentration of CO_2 in the flue gas. Additionally, a solar PTC field with thermal energy storage is integrated with the CCS reboiler to provide the necessary thermal energy for capturing 90% of the generated CO_2. A comprehensive process modeling and simulation framework is developed and validated by results provided by the National Energy Technology Laboratory (NETL) to accurately investigate the interactions between different components of the integrated proposed designs. The proposed designs and analysis have the potential to contribute significantly to the decarbonization of fossil-fueled power plants and enhance the sustainability and flexibility of the power sector.

5.1 Introduction

Previous studies contributed to an enhanced understanding of process improvements and sustainable integrations that makes CO_2 capturing from the NGCC power plant more efficient and viable. Despite significant advancements, there are ongoing challenges in the sustainable design and integration of carbon capture systems with fossil-fueled power plants. These challenges primarily revolve around reducing costs, minimizing energy penalties, and enhancing the flexible operation of solar-integrated systems. Addressing these gaps is crucial for maximizing the efficiency and viability of these integrated systems. In this context, it is hypothesized that the optimal hybridization of the membrane process with amine-based CCS for selective and non-selective exhaust gas recirculation, along with the integration of solar thermal collectors with thermal energy storage, could be a sustainable and flexible option for the decarbonization of NGCC power plant. Accordingly, this work proposed a novel design that consists of the combination of EGR and SEGR with the integration of PTC solar energy that provides 100% of the reboiler steam requirement and presents a detailed study on the design and performance of this integrated system. Furthermore, in order to improve the flexibility of the integrated system, thermal storage tanks have been modeled and integrated with solar energy fields to offset solar energy intermittency. In this regard, a 650 MW NGCC power plant has been simulated in Thermoflex software, and the carbon capture system, including both amine and membrane processes has been designed and modeled in Aspen Plus software in order to capture 90% of CO_2 produced by the power plant. The PTC solar field, with a capacity of 240 MW located in Oklahoma City, US, is simulated in System Advisor Model software. The simulations of various components are soft-linked through Excel in off-design mode to study the performance of the integrated system.

5.2 Process description

5.2.1 Baseline natural gas combined cycle (NGCC) power plant

Fig. 5-1 illustrates the NGCC power plant, which comprises two GE 7FA.05 gas turbines, each producing 420.6 MWe of power. Additionally, the plant includes two HRSG units and a steam turbine that generates 185.9 MWe. The NGCC plant generates a net power output of 634 MW with net plant efficiency of 57.4%. The design and configuration of the reference plant are based on a typical NGCC plant defined by DoE/NETL (National Energy Technology Laboratory)

[13]. The process begins with air at ISO conditions (15 °C) being compressed in a gas turbine compressor with a pressure ration of 17 and then mixed with natural gas in a combustor to create a mixture of air and fuel for combustion and further expansion in a turbine with inlet temperature at 1357 °C to generate power. The exhaust gas from the turbine at 604 °C then enters the two HRSGs, where the remaining heat is recovered to produce steam.

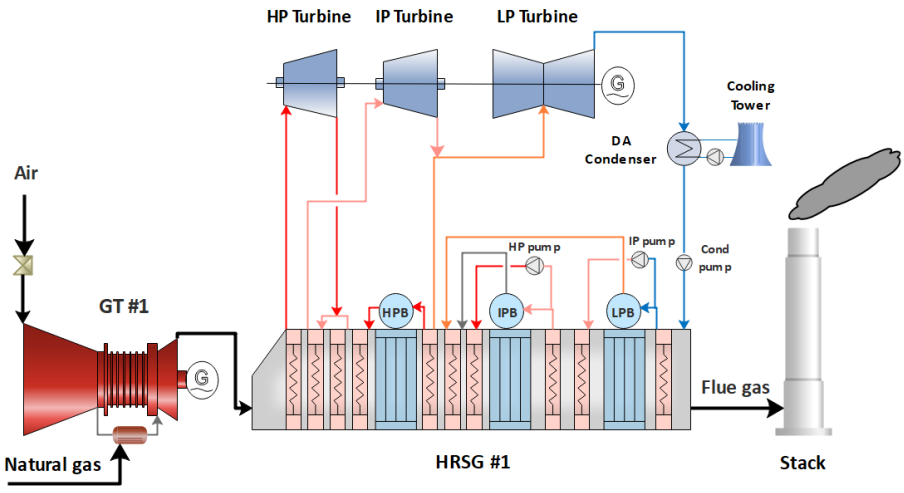

Fig. 5-1. Schematic of the baseline NGCC plant

The steam generation section consists of two identical HRSGs with triple-pressure and reheat configurations. Each HRSG is composed of HP, IP, and LP steam drums, as well as economizers, superheaters, and reheat sections. Within each HRSG, there are evaporators that produce steam at three different pressure levels, namely 175/28/3.8 bar. The high-pressure steam, after expansion in the HP turbine, combines with the IP steam, and the combined steam is then directed through a reheater before entering the IP turbine for further expansion. The low-pressure steam, after expansion in the LP turbine, is sent to the condenser and subsequently pumped back to the economizer using the LP pump.

The gas turbine exhaust gas exits each HRSG at 88 °C and passes to stacks. The considered baseline NGCC power plant releases 224 tonnes of CO_2 per hour with a concentration of 3.9%.

The gas turbines in the NGCC plant operate with surplus air, resulting in much lower concentrations of CO_2 in the turbine exhaust gas compared to a coal-fired power plant. The flue gas from the NGCC plant typically contains only 3-4 vol% of CO_2, significantly less than the 10-

14 vol% found in the flue gas of coal-fired power plants. Consequently, the CO_2 capture plant integrated into the NGCC plant needs to efficiently separate CO_2 from a larger exhaust gas volume, which contains approximately 30% of the CO_2 partial pressure found in coal-fired power plant flue gas. The main technical challenges for CCS wide-scale CCS application in NGCC power plants are the high energy penalty and cost of conventional MEA-based CCS. To address these challenges, a novel design based on the solar-assisted hybrid CCS has been proposed in this paper and discussed in the following sections.

5.2.2 Solar-assisted hybrid CO_2 capture system

The proposed solar-assisted hybrid CCS process is depicted in Fig. 5-2, which comprises an NGCC plant, the combination of exhaust gas recirculation (EGR) and selective exhaust gas recirculation (SEGR) by CO_2 selective membrane, an amine-based carbon capture unit powered by a solar collector field and a thermal storage system. This integration serves to raise the CO_2 concentration and reduce the flow rate of flue gas delivered to the post-combustion MEA-based CCS plant. Additionally, the stripper reboiler of the CO_2 capture plant is integrated with parabolic trough solar collectors (PTC) to generate the necessary heat during daylight hours instead of relying on steam extraction from the power plant IP/LP crossover. Accordingly, the aim of this design is to increase the concentration of CO_2 and decrease the flow rate of flue gas from the

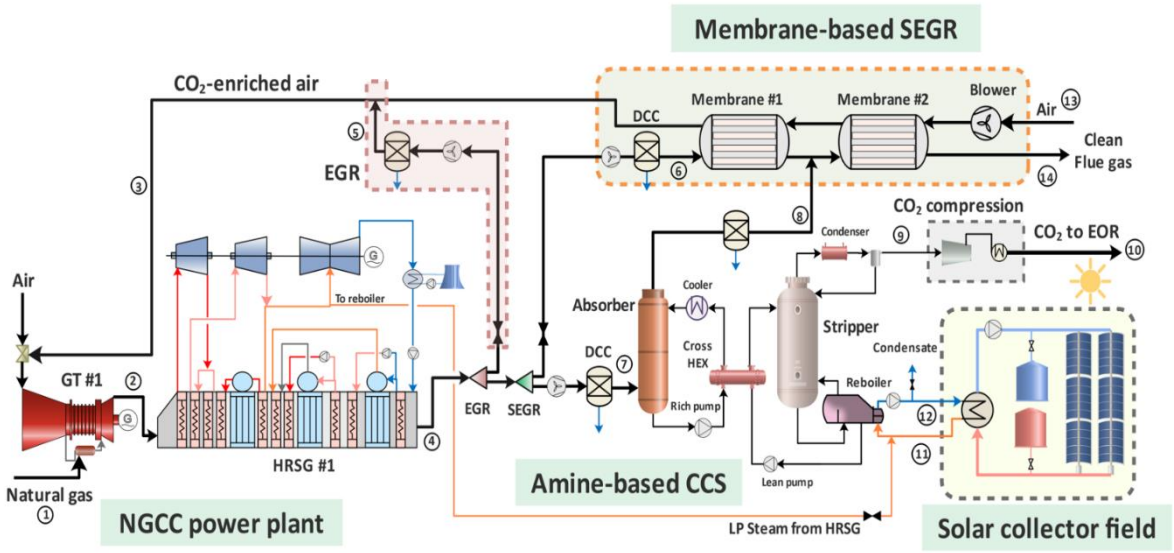

Fig. 5-2. NGCC integrated with exhaust gas recirculation strategies and solar-assisted amine-based CCS.

NGCC plant by utilizing a combination of EGR and SEGR while also reducing the power penalty of the NGCC plant by incorporating renewable energy sources.

In the proposed design, the amine-based CCS plant is integrated with a membrane-based SEGR process as a combination of parallel and serries configurations, as suggested by [247], in order to decrease flue gas flowrate in amine-based CO_2 capture plant (achieved by parallel integration) and avoid high CO_2 recovery in the absorber (achieved by series integration). Additionally, the proposed design incorporates an EGR strategy, where a portion of the flue gas leaving HRSG is recycled and mixed with the air stream, leaving the SEGR process to optimize and reduce the membrane area required for the SEGR purpose. Accordingly, a two-stage membrane-based SEGR is considered in the proposed design, where a portion of exhaust gas from the HRSG is cooled to 30 °C using a direct contact cooler (DCC) and then directed to the first CO_2 selective membrane module, in parallel to the amine-based CCS plant. In this first stage, the flue gas and a CO_2-lean air stream are brought into counter-current contact across the membrane, allowing CO_2 to permeate through the membrane and generate CO_2-enriched air that is fed to the GT compressor. The partially depleted flue gas from the retentate side of the first membrane stage is then mixed with the stream leaving the top of the absorber and is directed to the second membrane stage, in series with amine plant, in order to satisfy 90% CO_2 capturing from the NGCC plant. The portion of the exhaust gas that is directed to EGR passes from a DCC to reduce its temperature to 30 °C and then mixes with the CO_2-rich air stream from the membrane SEGR and finally enters the gas turbine. In this design, the inlet air of the GT compressor acts as a sweep gas in the counter-current membrane module configuration and generates the driving force required for separating CO_2 without the need to utilize a huge compressor [189,233].

It is important to note that maintaining an adequate oxygen concentration in the entering air stream to the GT is crucial for stable operation and to avoid significant modifications in gas turbine design since any significant changes to gas turbine engines would require a long time and considerable cost for development, testing, and optimization. Therefore, the proposed design assumes that the concentration of oxygen in the air stream entering the gas turbine should not be lower than 16 mol% [32,249]. Although the EGR strategy is more favorable in terms of capital cost requirement, the limitation of the NGCC equipped with only EGR is that the maximum achievable CO_2 concentration in the flue gas is about 6.5%vol with approximately a 40% EGR ratio [273,274]. On the other hand, the SEGR design is capable of significantly increasing the CO_2

concentration to about 18%vol., but it requires considerable capital investment for the membrane-based system [233,247]. Therefore, to take advantage of the benefits of both configurations, the proposed design combines both EGR and SEGR. In this regard, two dedicated splitters to define the recirculation ratio in EGR and SEGR are considered so that the ratios change in a way that satisfies the minimum oxygen purity requirement in the gas turbine inlet air stream. This allows to analyze multiple designs for the achievement of higher CO_2 concentrations in the flue gas while minimizing the capital cost requirement. By utilizing both EGR and SEGR, it is expected the proposed design offers an optimal solution for sustainable and flexing CO_2 capturing from NGCC power plants. The properties of main streams and composition for the case of EGR+SEGR are presented in the next sections.

Typically, steam from the turbine cycle is utilized to fulfill the thermal energy requirements of the PCC reboiler, approximately 120 °C, but this results in reduced power generation and lower electrical efficiency [275]. Accordingly, in the proposed design, a concentrated solar energy plant is integrated with the reboiler of the amine regeneration process to provide the required thermal duty from solar energy and avoid efficiency penalty due to steam extraction from the LP turbine. Also, thermal energy storage is considered to compensate for the solar energy intermittency. As a result, the heating demand of the reboiler can be met using solar energy, or steam extraction can be used as a backup during periods when an ample amount of solar energy is unavailable. Overall, the proposed design presents a promising approach to enhancing the efficiency of the CCS plant while also reducing the energy penalty of the power plant.

5.3 Model development

5.3.1 **NGCC power plant**

The simulation of the NGCC power plant has been carried out in Thermoflex V30 [276] and Aspen Plus V12.1 based on the design parameters of the baseline NGCC plant reported by DOE/NETL [13] presented in Table 5-1. The Thermoflex suite includes specialized equipment utilized in power generation plants designed to ensure the efficient and optimal convergence of thermal power cycles. This comprehensive suite is further enhanced by an extensive database consisting of several gas turbines, which are characterized by their performance maps.

To evaluate the influence of the proposed design on the performance of the Class F gas turbine, the simulation of the gas turbine is performed for the baseline plant at ISO ambient conditions using Thermoflex software in the design mode. Afterward, for the integration of the gas turbine with EGR and SEGR, it has been considered that the gas turbine operates at off-design conditions to evaluate the variation in the composition and properties of the inlet air. For the off-design operation of the gas turbines, it has been assumed that the turbine inlet temperature (TIT) is fixed at the design condition temperature, so the compressor pressure ratio and inlet flowrates change in order to maintain the TIT at 1357 °C, which is a typical temperature for GE 7FA.05 gas turbine engine [13]. Moreover, the impact of variation in inlet air properties on the gas turbine performance is described by constant swallowing capacity at different sections of the gas turbine operating at choked conditions [277]:

$$\frac{\dot{m}_{in}}{P_{in}}.\sqrt{\frac{Z.T_{in}}{\gamma.MW}\left(\frac{\gamma+1}{2}\right)^{\frac{\gamma+1}{\gamma-1}}} = constant \qquad (1)$$

where $\dot{m}$ is combustion gases flow rate, T and P are given temperature and pressure, γ is isentropic exponents ($\gamma = \frac{C_p}{C_v}$), Z and MW are compressibility factors and the gas molecular weight. By utilizing Thermoflex software at off-design mode for the gas turbine, the new operating condition of the gas turbine at various inlet air properties could be calculated based on the mapped performance curve.

The downstream equipment, including HRSGs and feedwater system, are simulated in design mode to suit the gas turbine exhaust gas flow rate and temperature, using a similar configuration of heat exchangers, steam pressure, and temperature levels to the baseline design. However, to account for differences between configurations, steam flow rates and heat transfer areas are calculated using the design criteria provided in DOE/NETL reports [13,49]. By doing so, the overall impact on the power output and thermal performance of the combined cycle can be investigated.

Table 5-1. Operating parameters for the simulation of the NGCC power plant based on the DOE/NETL report [47]

Parameter	Value
Inlet air temperature [°C]	15
Inlet air flow rate [tonne/h]	3623
Fuel inlet pressure [bar]	27.56
Fuel inlet temperature [°C]	38
Fuel composition [vol.%]	
Methane (CH_4)	93.1
Ethane (C_2H_6)	3.2
Propane(C_3H_8)	0.7
n-Butane (C_4H_{10})	0.4
Carbon Dioxide (CO_2)	1.0
Nitrogen (N_2)	1.6
Fuel lower heating value @ 25°C [kJ/kg]	47216
Gas turbine inlet temperature [°C]	1357
Compressor pressure ratio	17
Compressor polytrophic efficiency [%]	85
Steam turbine efficiency HP/IP [%]	88–92.4
Steam turbine efficiency LP [%]	93.7
Condenser pressure [kPa]	4.8
HRSG pressure drop[kPa]	3.6
HP/IP steam temperature [°C]	567
Flue gas composition [mol.%]	
N_2	74.398
O_2	12.389
CO_2	3.898
H_2O	8.420
Ar	0.895

For the solvent regeneration in the stripper of the downstream CO_2 capture plant, the required steam is originally obtained from the IP/LP crossover, where the steam is at optimal pressure for being supplied to the reboiler. Considering all pressure drops in pipes and equipment (~0.5 bar), a throttle valve has been considered on the IP/LP crossover to maintain the pressure at 3 bar in different cases, including solar energy integration. Also, to prevent solvent degradation

due to high temperature (degradation threshold is 120 °C), the steam must be cooled down to slightly above saturation temperature using a de-superheating system. To recover the waste heat and reduce the steam extraction, a fraction of the condensate generated in the reboiler is recycled back into the de-superheater.

5.3.2 Amine-based CO_2 capture system

The implementation of post-combustion CO_2 capture (PCC) is the most preferred option for retrofitting existing NGCC power plants as it requires minimal modifications to the original cycle. As shown in Figure 2, the considered PCC process is based on a standard chemical absorption process that uses Monoethanolamine (MEA) solvent, which is capable of achieving a 90% capture rate with high purity of CO_2. This process has been widely described in previous works [103,278]. The power plant and capture plant are primarily interconnected through the following main connections: flue gas pre-processing (blower and DCC to cool the exhaust gas temperature to 40 °C), steam extraction from the inlet steam to the LP turbine or from PTC solar field to feed the reboiler, and the recycled condensate from the PCC to the HRSG water system. In the mentioned integration, the first two operations lead to a reduction in the net electricity output.

The simulation of MEA-based PCC is implemented in Aspen Plus software using the rate-based approach for both absorber and stripper modeling. The thermodynamic properties are determined using the unsymmetric electrolyte Non-Random-Two-Liquid (e-NRTL) activity coefficient model to consider the non-ideal behavior of the liquid phase. Additionally, the vapor phase is described using the Redlich-Kwong (RK) equation of state, which has been recommended in previous studies and validated against experimental data in previous works [162,279]. The absorber and stripper model incorporates multiple equilibrium and kinetic reactions. The aqueous phase chemical equilibrium reactions among the MEA–H_2O–CO_2 system are as follows:

$$MEAH^+ + H_2O \leftrightarrow MEA + H_3O^+ \quad (1)$$

$$MEACOO^- + H_2O \leftrightarrow MEA + HCO_3^- \quad (2)$$

$$2H_2O \leftrightarrow H_3O^+ + OH^- \quad (3)$$

$$HCO_3^- + H_2O \leftrightarrow H_3O^+ + CO_3^{-2} \quad (4)$$

$$CO_2 + 2H_2O \leftrightarrow H_3O^+ + HCO_3^- \quad (5)$$

The equilibrium constants (K) for the mentioned reactions are determined by calculating the standard Gibbs free energy for each component involved in the reactions:

$$-RT\ln K_j = \Delta G_j^0 \quad (6)$$

where, R represents the universal gas constant, T denotes the system temperature, and ΔG_j^0 represents the standard Gibbs energy change for reaction j.

The rate of formation of carbamate and bicarbonate is constrained by kinetics, and the forward and reverse kinetic reactions are presented below.

$$MEA + CO_2 + H_2O \rightarrow MEACOO^- + H_3O^+ \quad (7)$$

$$MEACOO^- + H3O^+ \rightarrow MEA + CO_2 + H_2O \quad (8)$$

$$HCO_3^- \rightarrow CO_2 + OH^- \quad (9)$$

$$CO_2 + OH^- \rightarrow HCO_3 \quad (10)$$

The details of the kinetic reaction rate equations and related parameters are available in [39,98]. To use the Aspen rate-based model for estimating mass transfer, heat transfer, interfacial area, pressure drop, and liquid holdup, it is crucial to have quantitative values and accurate calculation of transport properties like density, viscosity, thermal conductivity, surface tension, and binary diffusivity. The details of models considered to calculate transport properties are presented in references [39,162,279].

The amine-based PCC plant is designed to remove 90% of CO_2 released by the NGCC power plant, using the Mellapak 250Y structured packing and an aqueous solvent with 30 wt.% MEA and an optimal CO_2 lean loading of 0.2 (mol CO_2/mol MEA) in all cases. The considered

optimum value for lean loading is considered based on the recommendation of previous works. Specifically, the optimization study conducted by Agbonghae et al. [39] showed that the considered lean CO_2 loading is the optimal value for MEA-based PCC integrating with commercial-scale fossil-fueled power plants.

Considering the optimal design and required flexibility of the PCC, it has been suggested to consider two similar absorber columns along with one stripper column [280]. For designing absorber and stripper columns, the columns' diameter is determined based on the velocity of flue gas that equals 75% of the velocity at which flooding occurs, and pressure drop along the column to be in the ranges from 147 to 490 Pa per meter packing. At a fixed absorber diameter and design spec of 90% CO_2 recovery, the absorber packing height gradually increases, leading to better contact area and residence time and improving the CO_2 absorption rate and rich CO_2 loading at the bottom of the absorber. Accordingly, by increasing absorber height, the liquid-to-gas (L/G) ratio decreases, which leads to a reduction in reboiler energy requirement. The optimum absorber height and L/G are then selected at a point where further increasing absorber height (higher capital cost requirement) leads to a minor reduction in the reboiler duty. A similar design procedure is used to estimate the optimum stripper height; the stripper height gradually increases to the level that the reduction in reboiler duty becomes insignificant. The constant parameters and design specs for the simulation of MEA-based PCC in Aspen Plus is presented in Table 5-2, which are selected based on several studies on large-scale capture plant [39,150,278,281].

Table 5-2. constant parameters and design specs for MEA-based PCC simulation

Parameter	**Value**
Absorbent	MEA
Column packing type	MellaPack 250Y
Absorbent concentration [wt.%]	30
Number of Absorber columns	2
Number of Stripper column	1
CO_2 capture efficiency	90%
Absorber column pressure (top stage) [kPa]	104
Gas temperature at absorber exit [°C]	35
Inlet solvent temperature [°C]	40

Inlet flue gas temperature [°C]	40
Flue gas pressure at absorber inlet [bar]	1.137
Solvent lean loading (mol CO_2/mol MEA)	0.2
Stripper column pressure (top stage) [bar]	1.62
Stripper condenser temperature [°C]	35
Approach temperature in cross heat exchanger [°C]	10
Approach temperature in reboiler [°C]	10
Rich/lean pumps outlet pressure [bar]	3
Solvent pumps efficiency [%]	75
Blower efficiency [%]	85

5.3.3 Membrane-based SEGR

To hybridize amine-based PCC and membrane process in the proposed design, a two-stage counter-current flow membrane module equipped with sweep gas and CO_2 selective polymeric membrane has been considered. The gas separation process across the CO_2 selective membrane is assumed to be described by the solution diffusion mechanism, where the controlling parameter is the gas permeance, and the permeation rate of gas components can be described as follows:

$$J_i = 2\pi r_{FO} n_F \frac{Q_{CO_2}}{\alpha_i}\left(P_{ret} y_{ret,i} - P_{per} y_{per,i}\right) \qquad (11)$$

where J_i represents the rate of permeation for component *i*, Q_{CO_2} is the CO_2permeability, α_i denotes the component *i* selectivity, r_{FO} is the outer radius of fiber, n_F is the total number of fibers, and *P* represents the pressure on permeate and retentate side. Also, the mole concentration of component *i* in the shell side and the bulk composition of component *i* in the bore side are represented by $y_{ret,i}$ and $y_{per,i}$, respectively.

Details of considered modeling assumptions as well as mass balance, energy balance, and pressure drop equations involved in membrane gas separation modeling, have been widely discussed and validated in our previous works [176,189].

The resulting system of differential equations, along with boundary conditions, are programed in the Aspen Custom Modeler software and exported to Aspen Plus for integration with amine-based PCC. All equations for the membrane model are solved using the built-in DMO solver

considering the second-order central finite difference method using 40 elements in the axial domain.

For the purpose of SEGR, the second generation of Polaris membrane [142] is considered as it offers high CO_2 permeability, 2200 GPU, along with moderate CO_2/N_2 selectivity of 50. The selectivity of other components, including H_2O and Ar is 0.7 and 50, respectively [126]. Furthermore, the CO_2 recovery of the first membrane module is constant at 90%, while the recovery of the second membrane module is adjusted to ensure an overall 90% CO_2 recovery in the integrated processes.

5.3.4 Parabolic trough solar collector with thermal storage

One of the most economical and sustainable options for providing industrial process heat is a parabolic through collector field, which primarily comprises two subsystems: the solar collector and thermal energy storage. In the proposed design, the solar heat collected via parabolic through collectors is utilized to replace the steam extraction from the LP turbine for the PCC reboiler by providing the required thermal energy through the oil-water heat exchanger. In this design, a heat transfer fluid (HTF) heated up to 300 °C by the concentrated sunlight in the collector tube and is used to generate the required steam for the PCC reboiler, raising the return condensate temperature to 128.4 °C (1°C above the saturation temperature at 2.5 bar). After rejecting its thermal energy, the HTF is pumped back to the PTC field at 150 °C. Steam at 128.4 °C enters the reboiler, where it condenses to 127.4 °C (1°C below its saturation temperature), releasing its heat. After condensation, the condensate is pumped to compensate for pressure losses before being recirculated back to the main HTF heat exchanger.

Furthermore, a thermal energy storage (TES) subsystem (including hot and cold tanks) with the capacity of 4 hours of energy storage has been considered to provide better flexibility for the power plant and to overcome the intermittency of the solar energy by supporting the stripper reboiler energy requirement for some extra hours. In situations where solar irradiance is insufficient, the thermal storage subsystem releases stored energy. Additionally, if there is a lack of solar energy to fulfill the heating demands of the reboiler, the extracted steam from the LP turbine can be utilized as an additional heat source.

The System Advisor Model (SAM) from the National Renewable Energy Laboratory (NREL) [282] is used to model the parabolic trough solar heating plant for the duration of one year located in Oklahoma City, US. The model in SAM software is then linked with the Aspen Plus using Excel for integration with the reboiler. For the simulation of the PTC field, the typical metrological year (TMY), direct normal irradiance (DNI), and other climate data for the considered location are extracted from the NREL database. The hourly DNI-cosine product irradiance for the PTC field located in Oklahoma City is presented in Fig. 5-3, which shows approximate peaks at 950 W/m^2 during hours of maximum direct sunlight. Accordingly, the design of the PTC field is performed for operation at maximum irradiance [154].

Based on the required HTF temperature, Therminol VP-1 is considered the HTF for the PTC field. The flow rate in the single loop ranges from 1 to 12 kg/s, and the design flow velocity of the headers is aimed to be between 2 and 3 m/s [228]. A Siemens SunField 6 is selected as a collector type, and the Siemens UVAC 2010 is considered as the receiver model. Solar multiple, which is the ratio of the thermal capacity of the solar field at the design point to the required thermal power, is selected to be two for the design of the PTC system, which is a typical value for the system with thermal energy storage [283,284], and the design thermal power generation of the parabolic trough collector is fixed at 240 MW in all cases, by considering 15% thermal loss in the heat exchanger and reboiler [154].

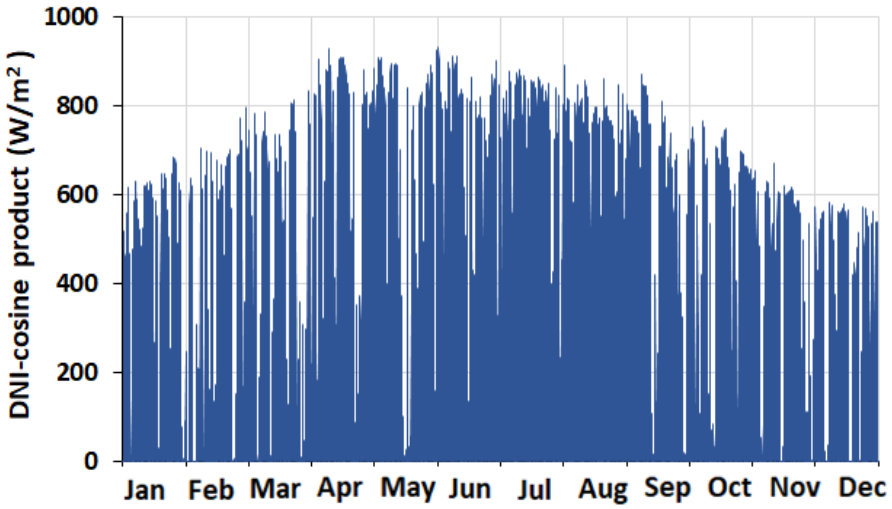

Fig. 5-3. Hourly DNI-Cosine Product Irradiance for Parabolic Trough Collector at Oklahoma City

5.3.5 CO_2 compression and storage

The recovered CO_2 stream, after leaving the stripper condenser at 35 ºC and 1.62 bar with a CO_2 purity of 96 vol%, requires conditioning before being transported or stored/utilized. The multi-stage compression train consists of five compression stages with an intercooler that increases the captured CO_2 pressure to 150 bar with a purity of more than 99%. The CO_2 compression is simulated in Aspen Plus, considering the intercooler temperature of 37 ºC, pressure ratio of 2.52, and compressor with an isentropic efficiency of 85%.

5.4 Framework and model validation

5.4.1 Modeling framework

In order to design and analyze the performance of the proposed system, various simulation software, including Thermoflex, Aspen Plus, Aspen Custom Modeler, and SAM, have been utilized due to their accuracy and advantages for the simulation of the specific components. Fig. 5-4 presents the hierarchical structure that has been utilized for the modeling of the proposed hybrid solar SEGR process for flexible decarbonization of the NGCC power plant. It should be noted that in the proposed framework, all data transfer and soft linking between software have been implemented in Excel using Thermoflex and Aspen Plus Add-in in Excel software.

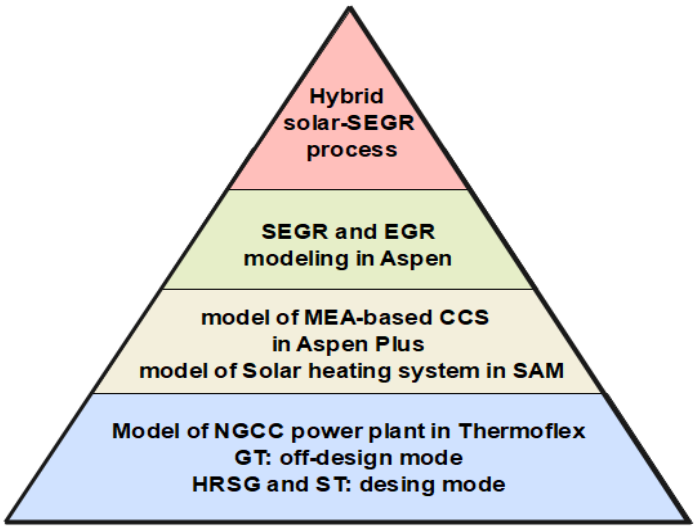

Fig. 5-4. Hierarchical diagram for the simulation of proposed system

To analyze the system performance, several indicators are considered, as described in Table 5-3

Table 5-3. Performance indicator considered for system analysis.

Performance indicator	Equation	
Gas turbine power output [MW]	$W_{GT} = \left(\frac{W_t - W_c}{\eta_{mech}}\right) \times \eta_{gen}$	(12)
Steam turbine power output [MW]	$W_{ST} = (W_{HP} + W_{IP} + W_{LP}) \times \eta_{gen}$	(13)
Total Gross power [MW]	$W_{gross} = W_{GT} + W_{ST}$	(14)
GT efficiency [%]	$\eta_{GT} = W_{GT}/Fuel\ input\ (LHV)$	(15)
Auxiliary power [MW]	$W_{aux} = W_{CCS} + W_{fans} + W_{pumps} + W_{CT} + W_{misc}$	(16)
Net power [MW]	$W_{net} = W_{gross} - W_{aux}$	(17)
HRSG efficiency [%]	$\eta_{HRSG} = Q_{recovered}/Q_{input\ from\ exhaust}$	(18)
Specific reboiler duty [MJ/kgCO_2]	$SRD = Q_{reb}/m_{CO_2}$	(19)
Carbon intensity [kgCO_2/MWh]	$CI = m_{CO_2}/Net\ power$	(20)
CO_2 capture efficiency [%]	$\frac{CO_2\ mole\ flow\ to\ compression}{CO_2\ mole\ flow\ generated\ in\ GT}$	(21)

To analyze and compare the performance of the proposed solar-assisted hybrid CCS with the baseline system, various cases have been considered as follows:

- Baseline: Air-combustion NGCC with conventional MEA-based CCS
- EGR: NGCC with MEA-based CCS equipped with EGR
- SEGR: NGCC with MEA-based CCS equipped with membrane-based SEGR
- EGR+SEGR: NGCC with MEA-based CCS equipped with a combination of EGR and SEGR

The flow splitters considered on the SEGR and EGR stream control the amount of flowrate that is directed to each process. In this study, the SEGR ratio is the fraction of flue gas relative to the total flow of flue gas diverted to the membrane-based SEGR. Also, the ratio of EGR is determined to provide maximum CO_2 recirculation while maintaining the minimum required O_2 concertation in the GT air inlet stream at various SEGR ratios.

The overall CO_2 recovery in all analyses is fixed at 90%, and a parabolic through solar collector field with a fixed thermal capacity of 240 MW and 4 hours of thermal storage is integrated into all systems. The design of the gas turbine is fixed the same as the baseline case, while downstream components, including HRSGs, feedwater system, MEA-based CCS, and membrane-based SEGR, are designed based on the properties of their inlet streams while considering the same design criteria.

5.4.2 Model validation

To verify the NGCC modeling results, important operating parameters of the system are compared with those reported in NETL/DOE report case-1a, as presented in Table 5-4. The difference between simulation results and reported values is less than 2.5%, which shows the high accuracy of the developed model for the NGCC power plant.

Table 5-4. Validation of NGCC simulation by DOE-NETL report [13]

Parameters	**NETL report**	**Model**	**Error %**
Gas turbine power [MW_e]	420.8	420.8	0.005
Steam turbine power [MW_e]	229.6	229.3	0.135
Total gross power [MW_e]	650.4	650.1	0.045
Total Auxiliary loads [MWe]	16.5	16.9	2.182
Total net power [MWe]	633.9	633.2	0.104
Cooling tower duty [MWt]	358.6	358.8	0.053
Total process pumps load [MW_e]	7.33	7.2	1.438
Turbine inlet temperature [°C]	1359.4	1357.2	0.162
Turbine exhaust temperature [°C]	604.4	603.3	0.182
Thermal Input (LHV) [MWt]	1103.9	1101.7	0.199
GT efficiency (LHV)	38.1	38.2	0.262
Net electric Efficiency (LHV)	57.4	57.5	0.139
HP steam flowrate [tonne/h]	400.1	398.5	0.400
IP steam flowrate [tonne/h]	498.7	487.2	2.306
LP steam flowrate [tonne/h]	575.3	573.5	0.313
HRSG outlet temperature [°C]	87.7	87.8	0.114
Flue gas flow rate [tonne/h]	3706.9	3706.8	0.003
CO_2	3.91	3.90	0.256

O_2	12.37	12.39	0.162
N_2	74.39	74.4	0.013
Ar	0.9	0.89	1.111
H_2O	8.44	8.42	0.237

The validation of MEA-based CCS simulation was conducted based on a set of pilot plant experiments published by Notz et al. [285]. The accuracy of the developed model is confirmed through eight experiments, and the differences between the obtained results and the reported experimental data are below 5%. Table 5-5 outlines the simulation results compared with the pilot plant results. The process description of the pilot plant as well as additional information about the experiments design specification are available in the reference [285].

Table 5-5. Validation of MEA-based CCS with pilot plant data provided by [285]

Pilot plant experiment	**Captured CO_2 flow (kg/hr)**			**SRD (MJ/kg CO_2)**			**Rich loading (mol CO_2/mol MEA)**		
	Exp	Sim	Error %	Exp	Sim	Error %	Exp	Sim	Error %
1	4.67	4.74	1.50	5.01	5.09	1.60	0.386	0.385	0.26
4	4.83	4.98	3.11	5.05	5.12	1.39	0.397	0.397	0.00
34	4.41	4.62	4.76	4.85	4.71	2.89	0.417	0.426	2.16
35	4.57	4.71	3.06	4.27	4.35	1.87	0.411	0.419	1.95
36	4.46	4.68	4.93	4.68	4.51	3.63	0.393	0.408	3.82
37	4.41	4.39	0.45	5.11	4.91	3.91	0.398	0.411	3.27
38	4.52	4.5	0.44	5.4	5.18	4.07	0.385	0.401	4.16
39	4.48	4.42	1.34	5.23	4.98	4.78	0.4	0.405	1.25

Regarding the validity of the developed model for the counter-current membrane module, a detailed validation has been performed in our previous works [176,189].

5.5 Results and discussion

This section describes the behavior and performance of the proposed configurations, specifically focusing on the behavior of the various parts of the studied design and their interfaces.

The schematic of the proposed design is illustrated in Fig. 5-2, and the properties and composition of the main streams for the case of EGR+SEGR are presented in Table 5-6. In the EGR+SEGR case, it has been considered that the same flowrate enters the PCC and membrane-

based SEGR (SEGR ratio is equal to 50%). Afterward, the flow fraction that is sent to EGR is controlled in a way that a further increase in the CO_2 concentration of the GT air inlet stream could be achieved while meeting the minimum requirement for oxygen concentration (16 mole%) in the compressor inlet air stream. As presented in Table 5-6, 25.6% of the HRSGs exit stream (stream 4) is directed to the EGR (stream 5) after cooling down and condensing out water in DCC). The remaining amount of flue gas goes to the SEGR splitter, where 50% of flue gas is directed to the membrane-based SEGR process, where the gas is cooled to 30 °C in DCC (stream 6) and is passed through the first membrane module with CO_2 recovery of 90%. The absorber top stream at 30 °C (stream 8) is then mixed with the first membrane retentate stream at a similar CO_2 concentration (1.3 mole%) and enters the second membrane module for further CO_2 separation and ensuring the overall 90% CO_2 recovery of the integrated system. The results show the proposed method recycles about 107.6 kg/s CO_2 (63.9 kg/s CO_2 via SEGR and 43.7 kg/s CO_2 via EGR) to GT inlet air stream, leading to a concentration of 10.87 mole% CO_2 in the GT flue gas. The portion of flue gas that enters the PCC is cooled to 40 °C at the absorber inlet (stream 7), and finally, the captured CO_2 at 35 °C with a purity of 96% enters the CO_2 compression process where it is compressed to 150 bar (stream 9) through the multi-stage compressor with intercooler. The required thermal duty of the reboiler is provided by the solar collector field. Steam from HTF heat exchangers (stream 11) at 2.5 bar with 1 degree superheated enters the reboiler, where the steam is condensed to released heat for amine regeneration. The condensate then is pumped back to the HTF heat exchangers (stream 12), where the heat is transferred from the HTF at 300 °C to the condensate, and steam produces for being sent to the reboiler.

Table 5-6. Properties of streams in EGR+SEGR design

Stream parameter	**1**	**2**	**3**	**4**	**5**	**6**	**7**	**8**	**9**	**10**	**11**	**12**	**13**	**14**
Mass flow [kg/s]	24	1038	1015	1038	254	369	375	310	58	57	93	93	687	607
Temperature [°C]	38	628	28	82	30	30	40	30	35	38	128	127	15	19
Pressure [bar]	27.56	1.05	1.01	1.01	1.01	1.05	1.14	1.03	1.62	150	2.5	2.6	1.01	1.01
Mole Fraction [mole%]														
CO_2		10.87	7.13	10.87	11.70	11.71	11.41	1.30	96.33	100	0	0	0.03	0.68
O_2		7.51	16	7.51	8.08	8.09	7.87	9.10	0.02	0	0	0	20.74	9.99
N_2	NG fuel	69.81	72.63	69.81	75.13	75.21	73.28	84.69	0.12	0	0	0	77.29	86.44
H_2O		10.97	3.36	10.97	4.19	4.09	6.56	3.96	3.52	0	100	100	1.01	1.86
Ar		0.84	0.87	0.84	0.90	0.9	0.88	0.95	0.00	0	0	0	0.94	1

As can be seen from Table 5-6, the properties (temperature and composition) of the inlet air to the gas turbine (stream 3) in the proposed design changes compared to the air stream (stream 13) that is utilized in the conventional baseline case without any recirculation. The next sections provide a detailed discussion of how these variations impact the NGCC plant operation.

The effect of the SEGR ratio on the flue gas CO_2 concentration is presented in Fig. 5-5. As it can be seen, by raising the SEGR ratio, the flue gas CO_2 concentration significantly increases from less than 4 mole% in the baseline case to about 18.1 mole% at 76.4 percent SEGR ratio (SEGR case). The limit on the quantity of CO_2 that can be recycled back is determined by the concentration of oxygen at the combustor inlet air, which must remain constant at 16 mole%. In the SEGR case that represents the highest CO_2 concentration in the flue gas, a negligible amount of flue gas is sent to EGR since the air oxygen concentration is already at its minimum requirement. Furthermore, the required EGR ratio decreases more significantly at a higher SEGR ratio which is mainly due to high CO_2 transfer between the flue gas and air in the membrane modules. At a medium level of SEGR ratio, the combination of EGR and SEGR could still lead to a high level of CO_2 concentration compared to the baseline and EGR case. In the EGR+SEGR case, where 50% of flue gas is sent to the membrane-based SEGR, 25.6% EGR ratio has resulted in achieving a higher CO_2 concentration in the flue gas while maintaining oxygen requirement in the air stream. In this design, the achievable CO_2 concentration in the exhaust gas is 10.87 mole% which is still considerably higher than the value in the EGR case (6.4 mole%).

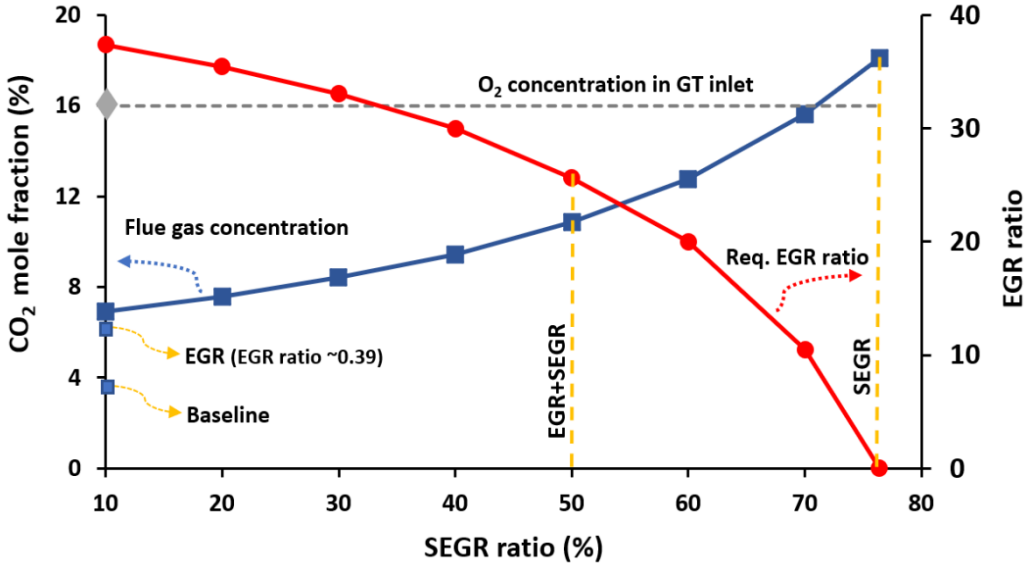

Fig. 5-5. Variation of flue gas CO_2 concentration and EGR ratio at different SEGR ratios

5.5.1 Performance analysis of the NGCC plant

Increasing the CO_2 content of the air stream by SEGR and EGR has several effects on the performance of the gas turbine, specifically affecting the swallowed mass flow rate by the compressor as well as the turbine outlet temperature. As previously mentioned, the gas turbine is typically operating at a constant turbine inlet temperature (TIT) determined by the materials used in constructing and the cooling system employed in the expansion section. Accordingly, by variation of inlet air stream properties due to recirculation, the fuel gas and excess air flowrates are varied in order to maintain the TIT at 1357 °C for the GE 7FA.05 gas turbine engine. In this section, it has been assumed the solar energy is unavailable, and LP steam is extracted from the IP/LP crossover to supply the required thermal energy of the PCC reboiler. The integration of solar field is studied in the next sections.

Table 5-7 presents the operating conditions at the inlets and outlet of the gas turbine (one train) for three different cases, including EGR, EGR+SEGR, and SEGR. As shown in Table 5-7, by implementing CO_2 recirculation via EGR or SEGR, the temperature of the inlet air stream increases from 15 °C at ISO conditions to 30 °C in the SEGR case, primarily resulting from the transfer of sensible heat from the flue gas to the air stream. However, this temperature rise is lower in the EGR case compared to the EGR+SEGR and SEGR case due to lower sensible heat transfer. Also, it can be observed that the turbine exhaust gas temperature escalates from 602.8 °C in the baseline case to 627.6 and 646.4 °C in EGR+SEGR and SEGR cases, respectively. Because the molecular wight, density, and the specific heat of the inlet air by implementing EGR and SEGR considerably increases since the mentioned properties in CO_2 are higher than the rest of the components, leading to a reduction in the compressor outlet temperature and increment of the turbine exhaust temperature (as it can be described by Eq.1). Consequently, the air and fuel flowrate increase to keep the TIT in the gas turbine at its design value for EGR+SEGR and SEGR cases, resulted in a higher exhaust gas flowrate in EGR+SEGR (519.2 kg/s) and SEGR cases (535.4 kg/s). However, the exhaust gas flowrate in the EGR case does not change considerably compared to the baseline case. It is mainly because, at a lower CO_2 concentration, the influence of temperature increase on reducing gas air density is more significant than the influence of CO_2 concentration on increasing gas density. Therefore, the overall effect is a reduction of the gas density in the EGR case, leading to a lower mass flow rate through the air compressor. A similar

trend in the gas turbine performance at off-design conditions has also been reported by other references [63,165,286].

Table 5-7. Properties and composition of gas turbine inlet air and exhaust gas for considered designs (one train).

	Baseline	**EGR**	**EGR+SEGR**	**SEGR**
EGR ratio [%]	-	38.6	25.6	-
SEGR ratio [%]	-	-	50	76.4
GT inlet air stream				
Air temperature [°C]	15	20.8	28.3	30
Pressure [bar]	1.01	1.01	1.01	1.01
Mass flow [kg/s]	503.2	502.7	507.3	522.8
CO_2 concentration [mole%]	0.03	2.59	7.13	14.44
O_2 concentration [mole%]	20.74	16	16	16
Density [kg/m]	1.220	1.201	1.195	1.234
GT exhaust gas stream				
Temperature [°C]	603.3	612	627.6	645
Pressure [bar]	1.05	1.05	1.05	1.05
Mass flow [kg/s]	514.8	514.5	519.2	535.4
CO_2 concentration [mole%]	3.90	6.40	10.87	18.08
H_2O concentration [mole%]	8.42	9.66	10.97	11.63
O_2 concentration [mole%]	12.39	7.74	7.51	7.04

The variations in inlet air stream properties and subsequent changes in stream flowrate and properties to maintain TIT at its design value affect the performance of gas turbines and downstream equipment, including HRSGs and steam turbines. The influence of different designs on the performance of the NGCC plant is presented in Table 5-8.

The greater mass flow through the gas turbine caused by increased air density leads to a rise in the net power output from the gas turbine. Accordingly, the gas turbine power output is boosted by 2.5 MW in the SEGR design, while the power output is reduced by 2.9 MW in the EGR+SEGR design compared to the baseline configuration. Achieving a greater power output is attainable by introducing the rich CO_2 inlet air into the compressor at a decreased temperature since it leads to a higher inlet air density and higher swallowed mass flowrate by the compressor. On the other hand, the elevated temperature and increased flow rate of the exhaust gases contribute to greater availability of heat and efficiency in the HRSGs and a substantial boost in the power output of the steam turbines. Accordingly, compared to the baseline case, the steam turbine power

output demonstrates a notable boost of around 41.5 MW and 21 MW in the SEGR and EGR+SEGR cases, respectively.

Table 5-8. Performance indicators of the NGCC plant for the considered designs

	Baseline	EGR	EGR+ SEGR	SEGR
Gas turbine net power [MWe] × 2	210.4	208.7	207.5	212.9
Steam turbine Power [MWe]	175.2	180.8	195.9	216.76
Gross power [MWe]	596.1	598.3	610.98	642.58
Gross electric efficiency (LHV) [%]	54.1	53.96	54.14	54.23
Net power [MWe]	537.8	545.22	557.84	588.13
Plant auxiliary [MWe]	58.26	53.05	53.14	54.46
HRSG efficiency [%]	82.9	83.89	84.91	86
Stack gas exit temperature [°C]	116.7	112.5	109.5	106.4
Fuel LHV [kJ/kg]	47180	47180	47180	47180
Fuel input [kg/s] × 2	11.67	11.74	11.95	12.55
Carbon intensity [kgCO_2/MWh]	416.5	412.2	409.7	408.8

The overall effect of the proposed designs on the NGCC performance indicators and power outputs is presented in Fig. 5-6. It can be observed that the net electric efficiency in SEGR and EGR+SEGR cases is increased by 1.7 and 1.3%, respectively, compared to the baseline case. The main reason for this is the higher power outputs from the steam turbine train and lower plant auxiliary, which leads to higher net power output from the NGCC plant. Furthermore, the carbon intensity reduces by -1.8% in the SEGR cases and by -1.6% in the EGR+SEGR cases.

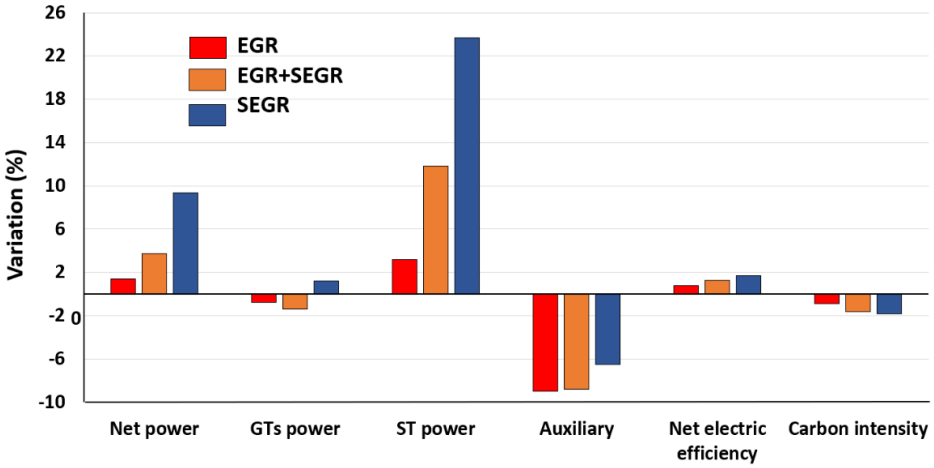

Fig. 5-6. Variation of performance indicators and power output of NGCC in different designs compared to the baseline case

It is worth highlighting that the plant auxiliary power consumption for the SEGR design is higher than that of EGR+SEGR as well as EGR designs, while all considered designs offer lower auxiliary power consumption compared to the baseline case. This can be described by analyzing the share of different components in the total auxiliary power consumption of the plants, as presented in Fig. 5-7. According to this figure, the SEGR case has notably a higher required power of fans for pushing air through the membrane modules since fan need to handle about 76% of flue gas. Also, higher required power for circulating water pumps and cooling tower fans is demonstrated for the SEGR case, which is due to the higher availability of heat in this case and leads to higher circulating water in the steam cycle compared to other cases. Among the considered designs, the EGR case shows the lowest auxiliary power, although the EGR+SEGR case is competitive with the EGR. Importantly, in terms of required power for CO_2 capture and compression, the SEGR case has the lowest power consumption, followed by the EGR+SEGR case, which is mainly because of higher CO_2 concentrations of the flue gas entering the amine-based CCS. The impact of selective exhaust gas recirculation on the performance of the capture plant is studied in the next section.

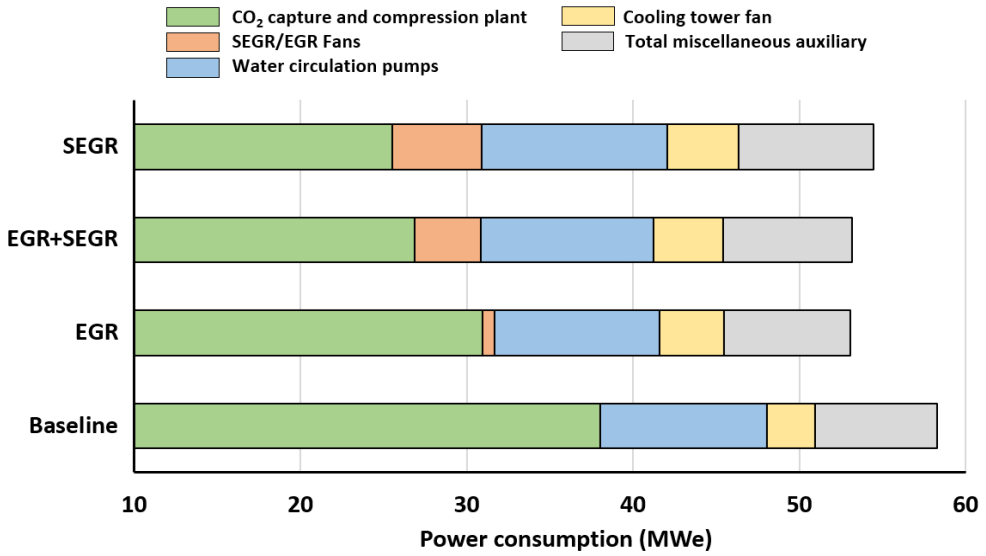

Fig. 5-7. Share of various components in the total auxiliary power consumption of the plant

Overall, the performance indicator of the NGCC plant designed for integrating with selective exhaust gas recirculation is superior compared to the conventional case, although the

associated costs of larger HRSGs and steam turbines, as well as the cost of equipment related to SEGR and EGR+SEGR designs need to be considered.

5.5.2 Performance Analysis of CO_2 capture plant and membrane-based SEGR

The effect of selective exhaust gas recirculation on the performance and design of PCC plants is investigated with the aim of 90% overall CO_2 capturing. For all considered cases, the packing volume of the absorber and stripper is optimized based on the procedure presented in section 5.3.2.

The design and operation parameters of PCC and membrane modules for considered designs are presented in Table 5-9. For the SEGR case where 76.4% of the exhaust gas is directed to the membrane modules for selective CO_2 recirculation, the PCC plant needs to handle only 23.6% of the NGCC flue gas flowrate, leading to a reduction of absorbers diameter by about 38% compared to the baseline case. However, the membrane-based SEGR needs to handle a higher flow rate and separate huge amounts of CO_2, leading to a high required membrane area (about 3 million square meters).

On the other hand, in the EGR+SEGR design, after recycling 25.6% of the flue gas through the EGR, 37% of total flue gas from gas turbines is directed to each membrane-based SEGR and PCC plants, leading to moderate size of membrane modules and PCC. Accordingly, although the diameter of the absorber in the EGR+SEGR case increases by 15% compared to the SEGR case, the membrane required area significantly reduces by 71% in the EGR+SEGR case.

Table 5-9. Design and operating input data for MEA-based PCC simulation

Configuration/Case	Baseline	EGR	EGR+SEGR	SEGR
Absorber efficiency [%]	90	90	90	90
Inlet mass flow rate [kg/s]	1030	632	386	253
Rich solvent loading [mol CO_2/ mol MEA]	0.479	0.486	0.497	0.510
Solvent capacity [mol CO_2/ mol MEA]	0.279	0.286	0.297	0.310
Lean solvent flow rate [kg/s]	970	948	930	936
Liquid / Gas ratio [kg/kg]	0.954	1.53	2.48	3.83
Absorber diameter [m]	14.80	12.60	10.45	9.11
Absorber height [m]	18.3	17.2	20.2	24.8
Stripper diameter [m]	9	9	9	9

Stripper height [m]	28	26	23	20
Total packing Volume [m^3]	8073	5940	4927	4508
Stripper pressure [bar]	1.62	1.62	1.62	1.62
Specific Reboiler Duty [MJ/ $kgCO_2$]	3.822	3.751	3.658	3.559
First membrane CO_2 recovery [%]	0	0	90	90
Second membrane CO_2 recovery [%]	0	0	50	76
Total required membrane area [Mm^2]	0	0	0.892	3.079
CO_2 to storage [kg/s]	56.00	56.18	57.13	60.11

Furthermore, the elevated concentration of CO_2 in the absorber inlet gas significantly improves the absorption rate of CO_2 by increasing the mass transfer driving force and shifting the thermodynamic equilibrium towards higher CO_2 loadings of the rich solvent stream. As can be seen from Table 5-9, the rich solvent CO_2 loading and the solvent capacity increase in the cases with higher CO_2 concentration. This accelerated rate of CO_2 absorption brings about several benefits, including a notable decrease in the required volume of the packing material and smaller energy requirements for regenerating the solvent. The specific reboiler duty decreases because of the lower amount of solvent required to separate 90% of the CO_2 amount. Similarly, achieving a specific CO_2 absorption efficiency requires a smaller surface contact area in the packing material, leading to a decrease in the required packing volume. It should be noted that due to the operation of the upstream power plant in the cases equipped with selective recirculation, the PCC plant needs to capture more CO_2 from the flue gas to fulfill 90% CO_2 recovery, which could result in higher reboiler duty and required packing volume. However, the performance of the PCC plant in EGR+SEGR and SEGR cases is considerably superior to the conventional design by having lower specific reboiler duty and a smaller volume of packing material.

Fig. 5-8 highlights the effect of exhaust gas recirculation designs on the required packing volume and specific reboiler duty of the PCC unit. The specific reboiler duty and total packing volume in the case of SEGR have been reduced by 6.9% and 44%, respectively, compared to the baseline case, which affects the steam requirement for the stripper reboiler. Also, in the EGR+SEGR case, the required thermal energy for capturing one tonne of CO_2 decreases by 4.3%, and the total packing volume decreases by 39% compared to the baseline case. Moreover, it can be seen from Fig. 8 that the rate of reduction of packing volume is decreasing at higher flue gas CO_2 concentrations, as the required packing volume in the SEGR case is lower only by 8.5%

compared to the EGR+SEGR case. Accordingly, it can be inferred that a further increase in the CO_2 concentration of the flue gas would not lead to a considerable reduction in packing volume.

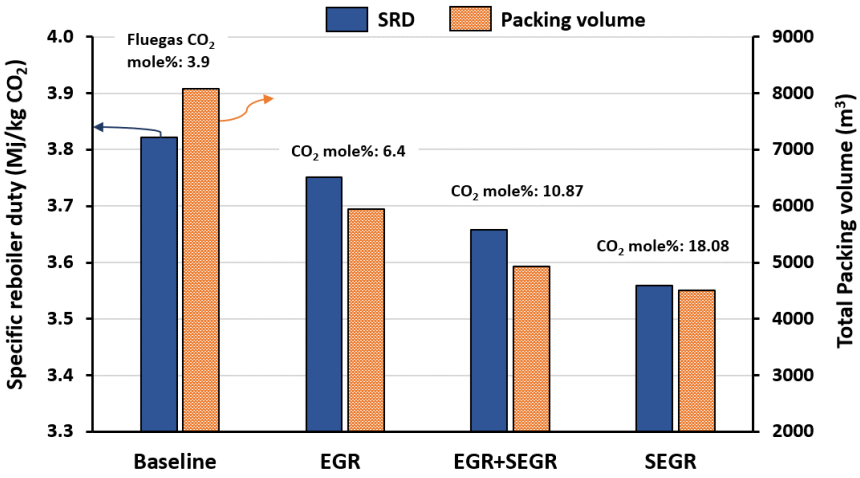

Fig. 5-8. Variation of SRD and packing volume for different designs

Regarding the results of the optimal sizing of the absorber and stripper column, it should be noted that the diameter of the stripper column does not vary in different cases since the flowrate of the stream entering the stripper does not change. Also, the reduction in specific reboiler duty with increasing stripper height becomes negligible at lower heights for the cases with higher CO_2 concentration, which is mainly due to the higher rich loading value of solvent that enters the stripper column. A similar trend in stripper height has also been reported in reference [39].

The optimal sizing results of the absorber column in different cases are illustrated in Fig. 5-9. It is clear that in a specific case, the specific reboiler duty increases at a higher level of L/G since the reboiler needs to vaporize and strip higher solvent flow. According to Fig. 9, it is observed that in the cases with lower CO_2 concentration (baseline and EGR), increasing the absorber height above a certain value leads to a negligible reduction in L/G and, subsequently, the specific reboiler duty. This is mainly because when the ratio of L/G is decreased below the optimal value, the ability to achieve the required CO_2 loading necessary for a 90% CO_2 recovery becomes increasingly challenging. However, for the cases with higher CO_2 concentration, it is easier to achieve a lower value of L/G and specific reboiler duty by increasing the absorber height, which is mainly due to the improved CO_2 separation driving force at higher CO_2 concentration. A comparable pattern has

also been observed in previous studies comparing design results of PCC for NGCC and coal-fired power plants [39,287]. It should be noted that although the optimum value of L/G leads to a higher absorber height in the EGR+SEGR and SEGR cases compared to the baseline case, the overall packing volume has been significantly reduced in those cases, leading to more compact PCC with a lower capital cost requirement.

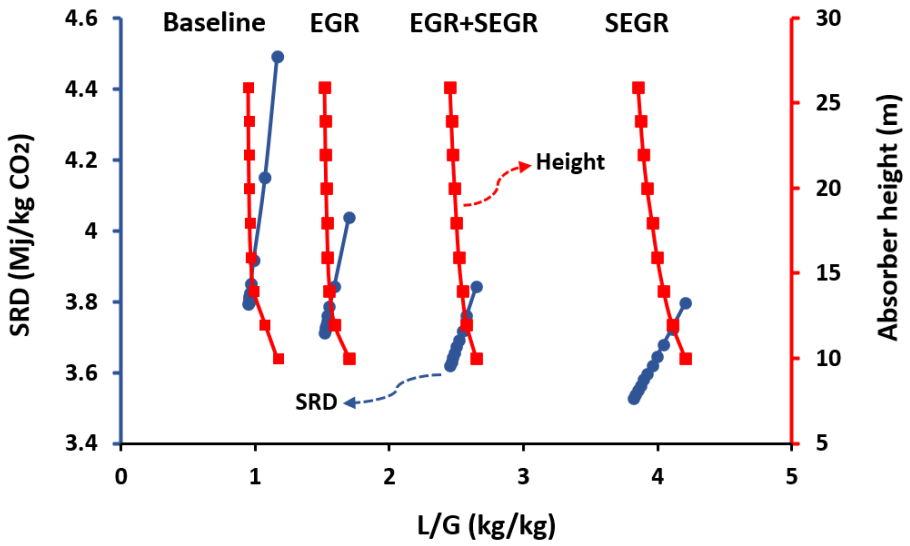

Fig. 5-9. Design results for the absorber of MEA-based PCC in EGR, full SEGR, and EGR+SEGR cases

Overall, the elevated CO_2 concentration within the flue gas in the EGR+SEGR and SEGR case has a beneficial effect on the required flow rate of solvent in the capture stage, reducing the amount of steam needed for regenerating the solvent and subsequently resulting in a lower reboiler duty compared to the conventional case.

Regarding the design of membrane modules in the cases equipped with membrane-based SEGR, the SEGR case required about 3.1 Mm^2 of Polaris 2nd generation membrane (CO_2 permeance = 2200 GPU) in order to selectively recycle CO_2, while the required membrane area for the EGR+SEGR case is about 0.9 Mm^2. The required membrane area would substantially affect the capital and operating cost of the SEGR cases. Accordingly, improvement and commercialization of the high CO_2 permeance are exceptionally vital for this design.

Fig. 5-10 depicts the variation of the required membrane area for both cases at different values of CO_2 permeance ranging from 1000 GPU (first generation of Polaris membrane) to 10000 GPU (ultra-thin composite membrane and rubbery polymers). According to this figure, the required membrane area for both cases is significantly reduced by increasing CO_2 permeance, specifically between 1000 and 5000 GPU. Currently, membranes with high CO_2 permeance are being tested and developed at a laboratory scale, that includes the third generation of Polaris membrane with CO_2 permeance of 3000 GPU [142], and PDMS/PAN thin film composite membrane exhibits an excellent CO_2 permeance equal to 5000 GPU [288,289]. According to Fig. 10, utilizing the third generation of Polaris membrane in the EGR+SEGR case leads to the reduction of membrane area by 27% compared to the second generation of Polaris membrane with 2200 GPU. This reduction in membrane area would be 56% and 78% by utilizing thin film composite membranes with CO_2 permeance equal to 5000 and 10000 GPU, respectively.

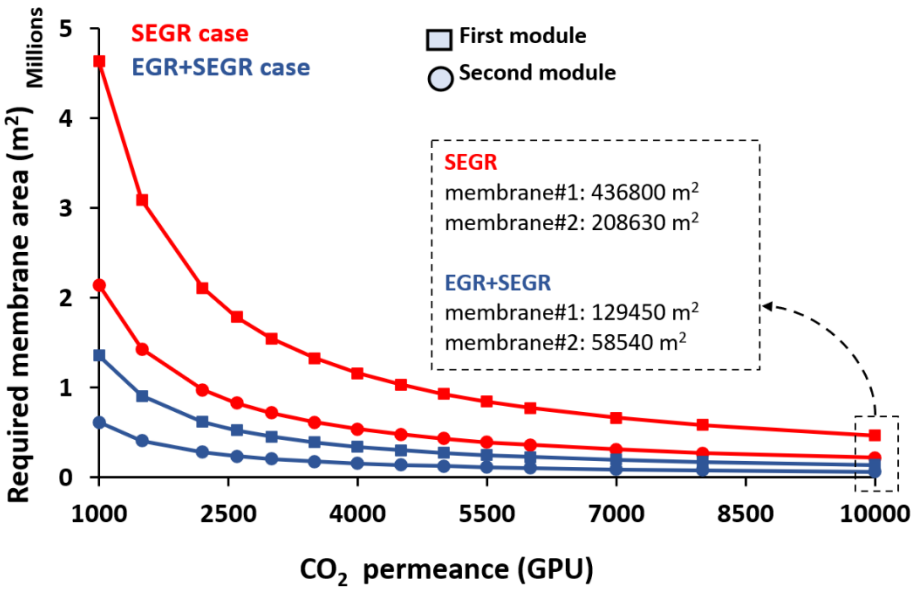

Fig. 5-10. The effect of CO_2 permeance on the total membrane area

5.5.3 Performance analysis of the solar-assisted hybrid CCS

In this section, the results of EGR+SEGR and SEGR cases integrated with a parabolic trough collector (PTC) field designed for generating 240 MW thermal energy are provided and discussed. Due to the intermittency of solar energy, thermal energy storage with 4 hours capacity is considered, and during the time that insufficient availability of solar energy, the necessary thermal load for the reboiler is provided from IP/LP crossover. Specifically, during nighttime when

solar energy is unavailable, all the required thermal load for the reboiler is sourced from LP steam. Furthermore, considering 15% heat transfer loss in the HTF heat exchangers and reboiler, the maximum thermal duty delivered to the PCC reboiler would be 204 MW in all cases.

Fig. 5-11 illustrates the variation of annual thermal energy production by the PTC field through the year. It is evident that peak thermal energy generation occurs from 9 am to 10 pm, taking into account the inclusion of a 4-hour energy storage capacity. Also, it can be seen in the first two months (Jan and Feb) and the las two months (Nov and Dec) of the year, the solar energy availability is limited, and the duration of providing thermal energy to PCC reboiler is shorter compared to other months. This is mainly because of the fluctuation in direct normal irradiance of different seasons in Oklahoma City, which greatly impact the availability of solar thermal energy (See Fig. 5-3).

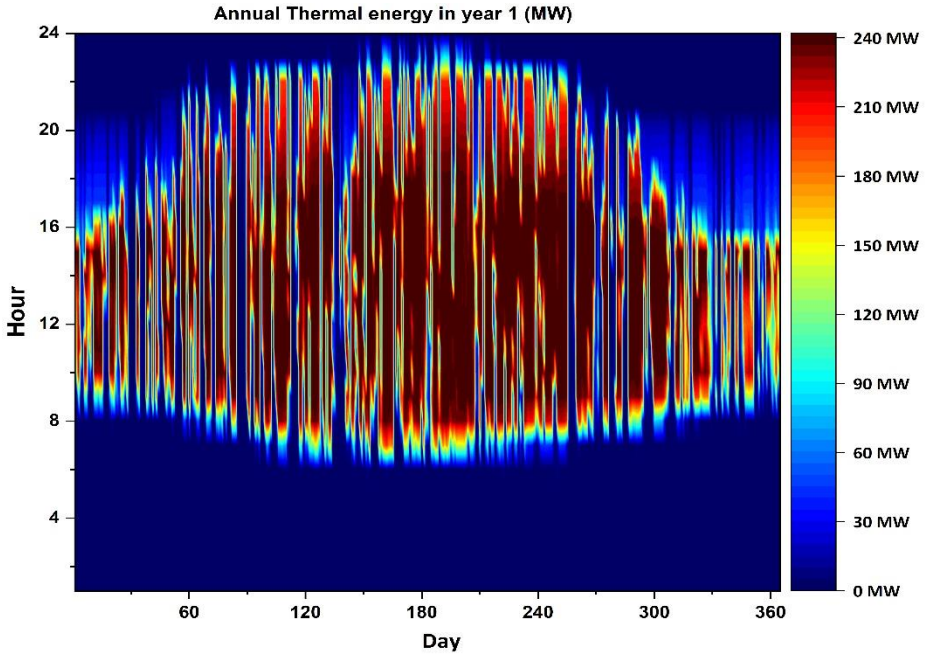

Fig. 5-11. Annual energy production as function of time (MWt).

The hourly net thermal energy delivered to the PCC reboiler by the solar system and the hourly net power generated by NGCC integrated with solar-assisted hybrid CCS (EGR+SEGR case) for the entire year is depicted in Fig. 5-12. It is evident that while the desired solar thermal capacity of 204 MW is often delivered during the entire year, it is maintained for a short duration. Certain days exhibit a mix of both high and zero solar irradiance, while some days have moderate

conditions. Additionally, there are days when solar irradiance is absent due to adverse weather conditions for the PTC field. Also, the maximum net generated power by the integrated NGCC power plant is about 612 MWe at 100% of solar energy availability (240 MWt), which shows 54.2 MWe increases compared to the absence of solar energy. Accordingly, it can be concluded that the solar thermal energy to electricity conversion efficiency in the proposed system is about 22.6% (54.2 MWe divided by 240 MWt), which is commendable considering the relatively low operating temperature of solar HTF.

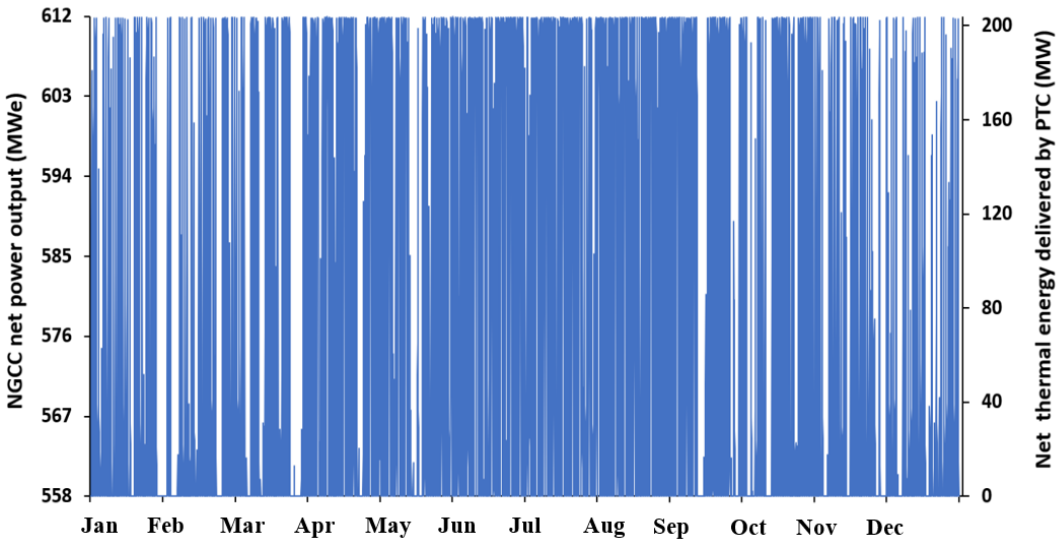

Fig. 5-12. Net output of the integrated NGCC plant and the net solar thermal energy delivered to PCC over the year

Fig. 5-13 presents the average net power output of NGCC and the variation of net thermal efficiency in proposed designs compared to the baseline case in four representative months, including January, April, July, and October. It can be observed that the net power output and electric efficiency considerably increase in all considered months as the required thermal energy of the reboiler is supplied by the solar field, leading to lower steam extraction from IP/LP crossover and higher power output form the LP steam turbine. The average net power output of the NGCC equipped with SEGR and EGR+SEGR case during July is higher than in other months, demonstrating 14.4% and 8.8% increase compared to the baseline case, respectively. This increase in the generated power is mainly due to higher power generated in the LP turbine since negligible

steam is extracted for the PCC reboiler when there is a high share of solar energy. Furthermore, during July, the average increase in net electric efficiency for these cases compared to the baseline case is 6.37% and 6.22%, respectively. However, the average performance of the proposed designs in January is notably lower than in the summer months, which is due to the lower efficiency of the PTC field this month, as described in the next figure.

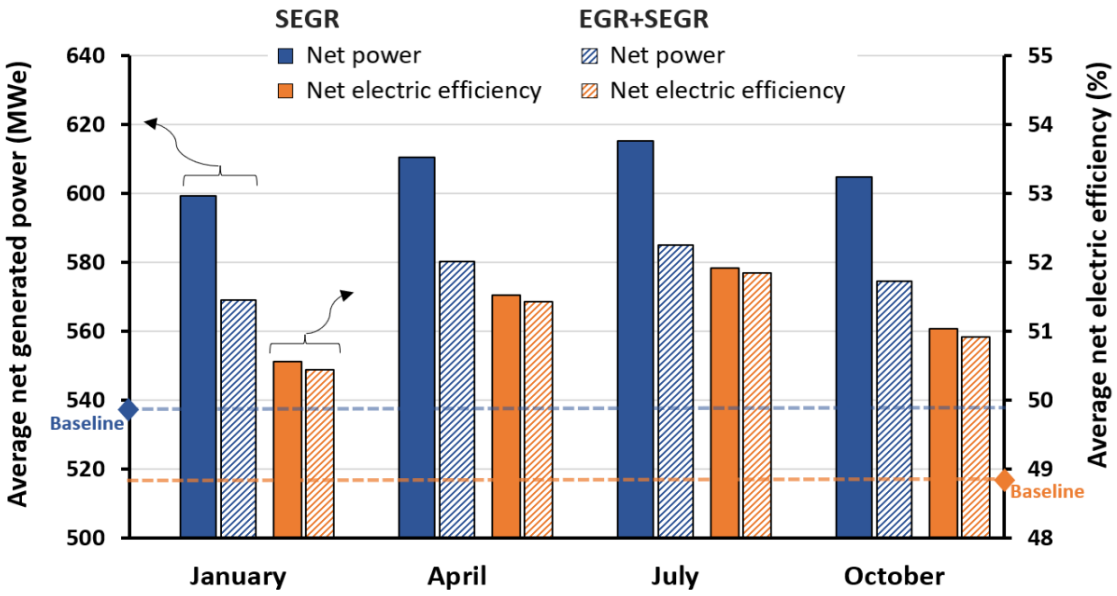

Fig. 5-13. Average net power output of NGCC and net thermal efficiency variation in proposed designs

The average hourly value of solar field operating parameters for four considered months is presented in Fig. 5-14. The findings indicate that the thermal power received from the PTC field in July surpasses that of other months, resulting in an extended supply of solar energy to the PCC reboiler. This figure shows the charging and discharging states of thermal energy storage (orange and green lines), which is more pronounced in April and July due to the higher thermal power incident. Therefore, it leads to the effective utilization of thermal energy storage, which is adequately charged during the daytime in April and July. With the aid of 4 hours of thermal energy storage, the flexibility of the system for responding to the variability of solar irradiance has been improved, and the thermal energy could be supplied even after sunshine hours. In contrast, during January, there is an insignificant surplus of solar energy available for charging the thermal energy storage. Accordingly, the 4 hours of thermal energy storage contributes to the more flexible

operation of the integrated system by reducing the period of ramp-up and ramp-down of the steam turbine and providing more stable operation.

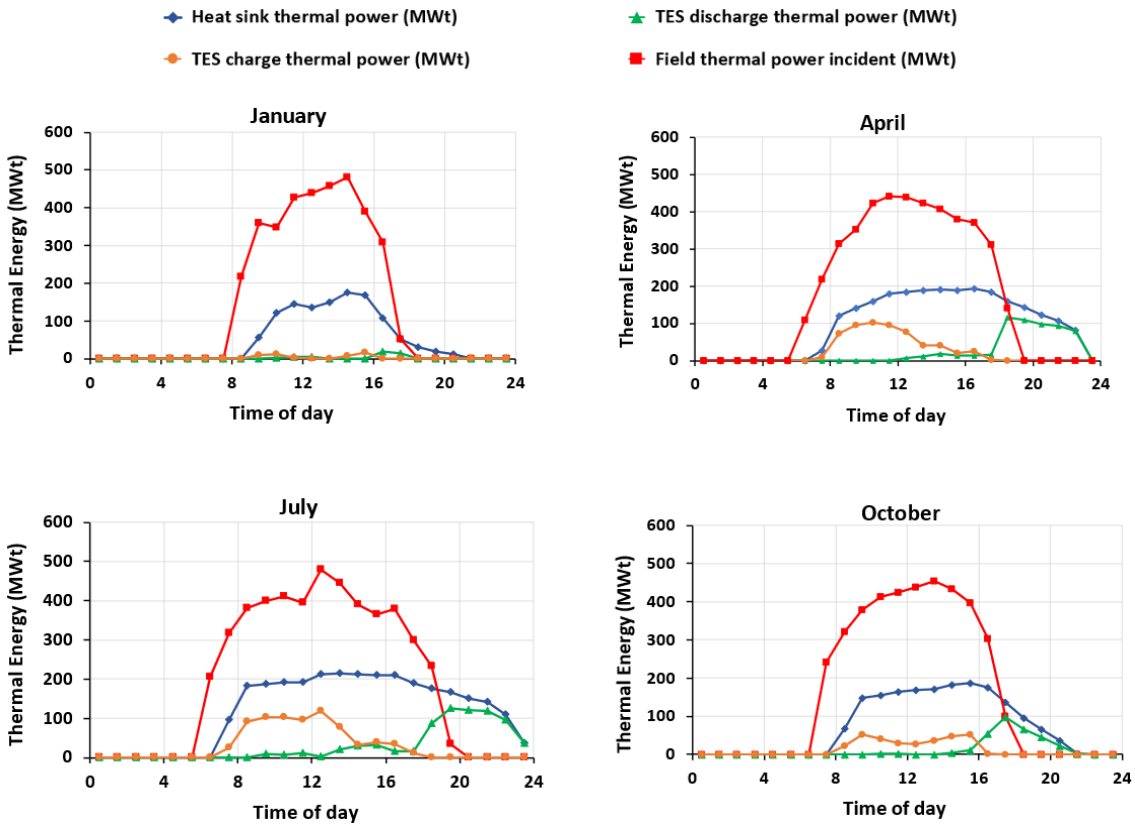

Fig. 5-14. Average value of generated thermal power, thermal power incident, and thermal energy storage charge and discharge for four various months in a year

5.5.4 Comparative analysis of the proposed designs

Table 5-10 presents the overall performance of proposed designs at different shares of solar energy delivered by the integrated PTC field, including 0% solar, 100% solar (204 MW delivered to PCC reboiler), and maximum annual average share. According to the observed results for the solar irradiance in Oklahoma City, the maximum annual average supply of solar thermal energy to the PCC reboiler is 180.8 MW at 2 pm, which is about 11.4% lower than the designed heat sink power for the PTC field.

Table 5-10. performance of EGR+SEGR and SEGR designs compared to the baseline case

		EGR+SEGR			SEGR		
	Baseline	0% solar	100% solar	Annual average @ 2 pm	0% solar	100% solar	Annual average @ 2 pm
Delivered solar thermal power [MWt]	0.0	0.0	204.0	180.8	0.0	204.0	180.8
Net power [MW]	537.8	557.8	612.0	606.0	588.1	642.1	636.0
Net electric efficiency (LHV) [%]	48.81	49.43	54.22	53.69	49.63	54.18	53.67
Net fuel input (LHV) [MW]	1101.8	1128.6	1128.6	1128.6	11850.0	11850.0	11850.0
Gas turbine power output [MW]	210.4	207.5	207.5	207.5	212.9	212.9	212.9
Steam turbine total power output [MW]	175.2	195.9	250.1	244.1	216.8	270.8	264.7
HPS Turbine power [MW]	47.8	56.8	56.8	56.8	63.8	63.8	63.8
IPS Turbine power [MW]	82.4	90.4	90.5	90.5	98.2	98.3	98.3
LPS Turbine power [MW]	48.6	53.0	108.0	101.8	59.4	114.2	108.1
Plant Total auxiliary [MW]	58.3	53	53	53	54.5	54.5	54.5
CO_2 capture & compression power consumption [MW]	38.0	26.9	26.9	26.9	25.5	25.5	25.5
CO_2 compression power consumption [MW]	19.0	19.3	19.3	19.3	20.3	20.3	20.3
Steam generated by PTC field [kg/s]	0.0	0.0	93.5	82.8	0.0	93.5	82.8
LPS turbine inlet flowrate [kg/s]	73.5	86.9	169.3	159.9	96.9	179.4	170.0
Specific reboiler duty [MJ/ kg_{CO2}]	3.822	3.658	3.658	3.658	3.559	3.559	3.559
Total required membrane area (m^2)	0	0.892	0.892	0.892	3.079	3.079	3.079
Annual generated electricity [GWh]	4711.3	4886.7	5361.4	5308.6	5152.0	5624.4	5571.6
NGCC carbon intensity [$kgCO_2$/MWh]	416.5	409.7	373.4	377.1	408.8	374.5	378.0

As can be seen from Table 10, during the time that there was high availability of solar energy (100% solar), the EGR+SEGR design annually generated 13.8% more electricity than the baseline with 11.1% higher electric efficiency. The annual generated electricity for the SEGR case is even higher by 19.4% compared to the baseline case, although this case needs considerable investment in membrane modules as it requires 71% more membrane area compared to the EGR+SEGR case. Also, due to variability in solar incidence at different times, the annual average value of net generated power is lower by 6 MWe compared to the 100% solar case. Furthermore, the NGCC plant carbon intensity in the proposed design is about 374 $kgCO_2$/MWh, 90% of which is captured and stored by the CCS plant, resulting in the maximum reduction achieved in the power plant carbon intensity to be 10.3 % for the proposed solar-assisted hybrid CCS design.

Overall, it can be concluded that a significant improvement in the flexibility and sustainability of the power generation system could be achieved by designing an NGCC power plant integrated with solar-assisted hybrid CCS.

5.6 Chapter Summary

This chapter deals with the fifth research question (RQ5), focuses on overcoming the limitations of existing carbon capture systems, and explores the possibilities for developing novel process designs and integrations. With this objective in mind, this chapter aims to propose a solar-assisted hybrid membrane-amine carbon capture system that can effectively and sustainably decarbonize natural gas-fired combined cycle power plants. The research endeavors to contribute new knowledge by successfully designing a novel CCS process through the integration of membrane-amine technology with a solar heating field. This innovative solution enables flexible and sustainable decarbonization of NGCC power plants and represents a significant step forward in addressing carbon emissions and promoting environmentally friendly energy generation.

In this regard, a multi-stage CO_2 selective membrane module with the aid of exhaust gas recirculation (EGR) is used to selectively recirculate CO_2 to the turbine inlet air and increase the CO_2 concentration of flue gas. Furthermore, the solar PTC field with 4-hour thermal energy storage is integrated with the MEA-based CCS reboiler to provide the required thermal energy for capturing 90% of generated CO_2. A comprehensive process modeling and simulation framework was created to analyze the interactions among different components in the proposed hybrid systems. This framework has utilized several simulator software, including Aspen Plus, Thermoflex, and SAM, to provide a thorough comprehension of the design and accurate simulation of components involving the gas. Afterward, a sensitivity and comparative analysis of key design variables were performed, which supported the investigation of the proposed designs.

The CO_2 concentration of the NGCC plant flue gas increases from 3.9 mole% in conventional design to 10.87 mole% in the EGR+SEGR case (26% EGR and 50% SEGR), while the SEGR case (76% SEGR) demonstrates 18.08 CO_2 mole% in the flue gas. Due to the change in the inlet air properties and integration of the solar PTC field, the output power of the system in SEGR and EGR+SEGR cases could be increased by 19.4% and 13.8% in comparison to the baseline case. Furthermore, due to the higher driving force in the PCC plant, resulting from high CO_2 concentration, along with lower flue gas flowrate entering MEA-based PCC in the proposed

designs, the specific reboiler duty and required packing material volume in the absorber and stripper considerably improves. Also, the power plant carbon intensity in the proposed solar-assisted hybrid design could be reduced by 10.3% based on the solar irradiance data in Oklahoma City, US.

The comparative analysis results showed that for a fixed gas turbine design (GE 7FA.05), the SEGR case could generate more power compared to the EGR+SEGR case (approximately 5%), and the reboiler duty and columns size of the PCC plant is slightly smaller in the SEGR case compared the EGR+SEGR case. However, the EGR+SEGR case offers an optimal solution as it requires a significantly smaller membrane area compared to the SEGR case (reduced by approximately 71%). Sensitivity analysis of the membrane-based SEGR system showed that improving membrane CO_2 permeation is an important factor affecting the required membrane area and cost of the system.

The proposed designs and analysis conducted in this chapter have the potential to significantly contribute to the decarbonization of fossil-fueled power plants and enhance the sustainability of the power sector. In order to fully comprehend the sustainable and flexible designs proposed in this study, it is crucial to undertake comprehensive multi-objective optimization, part-load analysis, and detailed economic analysis. These analytical approaches would offer valuable insights and support informed decision-making, ultimately advancing the development of environmentally sustainable energy solutions.

Chapter 6. Off-design Operation and Economic Viability of the Integrated System

- ❓ **Research questions: RQ6-** What are the impacts of commercial-scale deployment of the proposed hybrid design on the capital cost, operational costs, equipment size, capture cost, and electricity cost of the system? **RQ7-** How is the performance of the proposed novel hybrid system in the case of off-design and partial load performance?
- ➢ **Objective:** Investigation of part load performance and economic viability of the natural gas combined cycle power plant integrated with solar-assisted hybrid carbon capture system
- ✓ **New knowledge:** Insight into part load performance and economic viability of the natural gas combined cycle power plant integrated with the proposed design

The objective of this chapter is to assess the economic performance and load-driven operation of solar-assisted hybrid membrane-amine carbon capture and storage (CCS) systems for the decarbonization of Natural Gas-fired Combined Cycle (NGCC) power plants. The proposed post-combustion CO_2 capture process involves two configurations for enhancing the CO_2 separation driving force in the conventional amine-based CCS: a multi-stage membrane module for selective exhaust gas recirculation (SEGR case) and the combination of turbine exhaust gas recirculation with SEGR (EGR+SEGR case). Furthermore, the stripper reboiler in both configurations is integrated with a parabolic trough solar collector field with 4-hour thermal energy storage to provide the required thermal duty for solvent regeneration. Various system components are designed and simulated in commercial software and integrated to perform a comprehensive evaluation of the system's behavior and efficiency across a wide range of power plant loads. Furthermore, an economic model based on National Energy Technology Laboratory (NETL) procedure is developed to estimate the costs of electricity generation and CO_2 mitigation by considering cost factors such as capital investment, operational expenses, and maintenance costs. Furthermore, a sensitivity analysis is performed to assess the impact of key process and design parameters on the economic viability and feasibility of the system. The analysis of this study demonstrates the potential of the proposed hybrid system to contribute significantly to the

decarbonization of fossil-fueled power plants and enhance the sustainability and flexibility of the power sector.

6.1 Introduction

In the present chapter, the focus is on the economic performance as well as part-load operation of the particular case of an NGCC power plant with a solar-assisted amine-based CO_2 capture plant designed for integration with the combination of EGR and membrane-based SEGR system. The primary novelty of this paper lies in the examination of the flexible operation of the previously proposed NGCC plant with solar-assisted hybrid CCS and the investigation of part-load operation on the technical performance of various system components, including NGCC plant, amine-based CCS, membrane-based SEGR, PTC solar collectors and energy storage. Additionally, the study includes a detailed analysis of the economic aspects of the proposed system and a sensitivity analysis of various system parameters on the electricity and CO_2 avoided cost. By addressing these research gaps, the study aims to provide valuable insights into the flexible and sustainable decarbonization of NGCC power plants.

6.2 Standard NGCC plant with conventional amine-based CCS

The design and configuration of the reference plant are based on a nominal 650 MWNGCC plant defined by DoE/NETL (United States Department of Energy's National Energy Technology Laboratory). [13]. The process begins with air at ISO conditions (15 °C) being compressed in a gas turbine compressor with a pressure ration of 17 and then mixed with natural gas in a combustor to create a mixture of air and fuel for combustion and further expansion in a turbine with inlet temperature at 1357 °C to generate power. The NGCC plant comprises two GE 7FA.05 gas turbines, generating 420.6 MWe of power. The exhaust gas from the turbine at 604 °C then enters the two HRSGs, where the remaining heat is recovered to produce steam. The steam cycle includes two HRSG units with a triple pressure level single reheat cycle with a condensing steam turbine that generates 185.9 MWe. Each HRSG is composed of economizers, superheaters, and reheat sections, as well as HP, IP, and LP evaporators that produce steam at three different pressure levels, namely 175/28/3.8 bar. The high-pressure steam, after expansion in the HP turbine, combines with the IP steam, and the combined steam is then directed through a reheater before entering the IP turbine for further expansion. The low-pressure steam, after expansion in the LP turbine, is sent to

the condenser and subsequently pumped back to the economizer using the LP pump. The NGCC plant generates a net power output of 634 MW with net plant efficiency of 57.4% without the operation of a CO_2 capture plant.

The considered baseline NGCC power plant releases 224 tonnes of CO_2 per hour with a concentration of 3.9%. The post-combustion CO_2 capture (PCC) plant with the conventional chemical absorption process that uses Monoethanolamine (MEA) solvent has been integrated to the NGCC plant, which is capable of capturing a 90% of the generated CO_2. This is achieved by considering two similar absorber columns and one stripper column utilizing the Mellapak 250Y structured packing and an aqueous solvent containing 30% weight percent of MEA. The optimal CO_2 lean loading, which refers to the ratio of moles of CO_2 to moles of MEA, is set at 0.2 in all operating conditions. This particular value for lean loading is chosen based on recommendations from previous studies and research in the field [39,290]. Furthermore, for solvent regeneration in the PCC stripper, the required steam is extracted from the IP/LP crossover, where the steam is at optimal pressure for being supplied to the reboiler. Since the MEA solvent is degraded at temperatures higher than 120 °C, a de-superheating system based on the condensate recirculation is considered to slightly cool the extracted steam down to above saturation temperature using. Table 6-1 presents the considered design and operating parameters of the standard NGCC as well as conventional MEA-based CCS plant data at design load. It should be noted that the design parameters mentioned in Table 6-1 have been considered to be fixed in the rest of the paper.

Table 6-1. Operating and design parameters of the standard NGCC plant and MEA-based PCC

NGCC plant parameters	**Value**	**MEA-based CCS parameters**	**Value**
Inlet air temperature [°C]	15	Absorbent	MEA
Inlet air flow rate [tonne/hr]	3623	Column packing type	MellaPack 250Y
Fuel inlet pressure [bar]	27.56	Absorbent concentration [wt.%]	30
Fuel inlet temperature [°C]	38	Number of Absorber columns	2
Fuel composition [vol.%]		Number of Stripper column	1
Methane (CH_4)	93.1	CO_2 capture efficiency	90%
Ethane (C_2H_6)	3.2	Absorber pressure (top stage) [kPa]	104
Propane(C_3H_8)	0.7	Gas temperature at absorber exit [°C]	35
n-Butane (C_4H_{10})	0.4	Inlet solvent temperature [°C]	40
Carbon Dioxide (CO_2)	1.0	Inlet flue gas temperature [°C]	40
Nitrogen (N_2)	1.6	absorber inlet pressure [bar]	1.137

Fuel LHV @ 25°C [kJ/kg]	47216	Solvent lean loading	0.2
Gas turbine inlet temperature [°C]	1357	Stripper top stage pressure [bar]	1.62
Compressor pressure ratio	17	Stripper condenser temperature [°C]	35
Compressor polytrophic efficiency [%]	85	Approach temperature in cross heat exchanger [°C]	10
Steam turbine efficiency HP/IP [%]	88–92.4	Reboiler approach temperature [°C]	10
Steam turbine efficiency LP [%]	93.7	Rich/lean pumps outlet pressure [bar]	3
Condenser pressure [kPa]	4.8	Solvent pumps efficiency [%]	75
Pump efficiency [%]	75	Blower efficiency [%]	85
HP/IP steam temperature [°C]	567	CO_2 compression pressure [bar]	150
Flue gas composition [mol.%]	N_2: 74.398	O_2:12.389	CO_2:3.898	H_2O:8.420	Ar:0.895

6.3 Solar-assisted hybrid CO_2 capture system

The considered NGCC plant integrated with a solar-assisted hybrid CCS process is based on the design depicted in Fig. 6-1. This integrated system comprises of NGCC plant, the combination of EGR and membrane-based SEGR, MEA-based carbon capture unit equipped with a PTC solar collector field, and thermal energy storage. In order to integrate the amine-based PCC plant and membrane-based SEGR in the suggested design, a two-stage counter-current flow membrane module with a sweep gas and a CO_2-selective polymeric membrane has been considered. The primary objective of this design is to enhance the CO_2 concentration and flow rate of flue gas entering amine-based CCS, which is achieved through a combination of EGR and SEGR techniques. Additionally, the design aims to minimize the power penalty associated with CO_2 capture and increase the flexibility of the system by integrating PTC solar collector field with thermal energy sources.

In the EGR+SEGR integration, after splitting a specific amount of flue gas for EGR purposes, 50% of flue gas flow enters the ME-based PCC, and the other 50% enters membrane-based SEGR system that is integrated into the PCC plant in both parallel and serries configurations for selective CO_2 recirculation. The percentage of EGR is controlled in a way that a further increase in EGR ratio leads to a lower oxygen concentration in the GT air inlet stream than the minimum requirement (16 mole%). Considering this constraint, 25.6% of the flue gas stream enters the EGR and is recycled back after cooling down to 40 °C and condensing out water in DCC. The remaining amount of flue gas flows to the SEGR splitter, where 50% of flue gas is directed to the membrane-based SEGR process, where the gas is cooled to 30 °C in DCC and is passed through the first membrane module with CO_2 recovery of 90%. The absorber top stream at 30 °C is then mixed

with the first membrane retentate stream at a similar CO_2 concentration and enters the second membrane module for further CO_2 separation and ensuring the overall 90% CO_2 recovery of the integrated system. The results showed that this design, known as the EGR+SEGR case, led to a concentration of 10.87 mole% CO_2 in the GT flue gas, and only 37% of the flue gas entered the PCC plant. In the SEGR case, where 76.4% of the exhaust gas is directed to the membrane modules for selective CO_2 recirculation, the PCC plant needs to handle 23.6% of the NGCC flue gas flowrate with a CO_2 concentration of 18.08%mole.

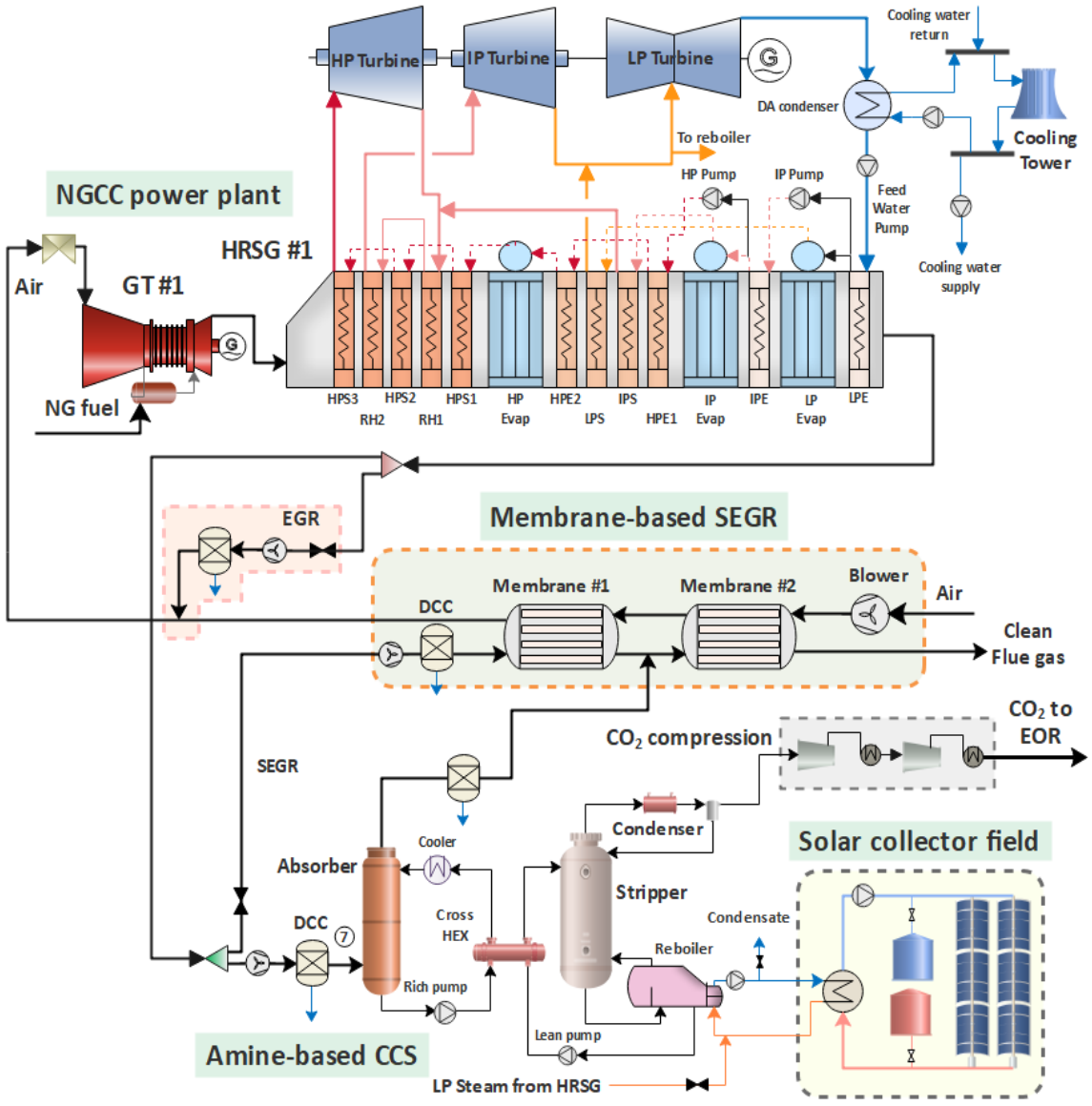

Fig. 6-1. The considered integration of NGCC plant with exhaust gas recirculation strategies (EGR+SEGR case) and solar-assisted amine-based CCS.

Furthermore, to provide the thermal energy requirement of the reboiler, a solar collector filed with 240 MW design capacity is considered that increase the HTF temperature to 300 °C for producing steam required for solvent regeneration in the HTF heat exchanger. Moreover, to enhance the power plant's flexibility and address the intermittent nature of solar energy, a TES subsystem has been incorporated, consisting of hot and cold tanks with 4 hours storage capacity. It serves the purpose of supporting the energy requirement for the stripper reboiler when solar irradiance is insufficient. Additionally, if the solar energy is inadequate to meet the reboiler heating demands, the steam extracted from the LP turbine can be utilized. Detail description of the process design and performance of this system is presented in our previous work. Table 6-2 presents the design specs and operating parameters of this integrated system.

Table 6-2. Constant parameters and design specs for membrane-based SEGR and PTS solar field

Membrane-based SEGR		**PTC solar field**	
Flow configuration	Counter-current	Location	Oklahoma City, US
Membrane type	Polaris 2nd generation	Design point DNI [W/m^2]	950
CO_2 permeance [GPU]	2200	Heat sink power [MW]	240
CO_2/N_2 selectivity	50	Solar multiple	2
CO_2/H_2O selectivity	0.7	Thermal energy storage capacity [hour]	4
CO_2/O_2 selectivity	50	HTF fluid	Therminol VP-1
CO_2/Ar selectivity	50	Collector type	Siemens SunField 6
Inlet temperature [°C]	30	Receiver type	Siemens UVAC 2010
Inlet pressure [bar]	1.05	Inlet HTF temperature [°C]	150
First module CO_2 recovery [%]	90	Inlet HTF temperature [°C]	300
Second module CO_2 recovery	variable	HTF heat exchanger loss [%]	15

6.4 Process modeling of the integrated system

6.4.1 NGCC power plant

The NGCC power plant simulation was conducted using Thermoflex V30 [276] and Aspen Plus V12.1 software, utilizing the design parameters from the DOE/NETL baseline NGCC plant, as outlined in Table 6-1. The Thermoflex suite includes an extensive database of several gas turbines, which are characterized by their performance maps and enable the performance of the

gas turbine at off-design mode. To study the performance of the integrated NGCC plant, first the NGCC power plant gas turbine models based on the GE Class F gas turbine at ISO ambient conditions using Thermoflex software in the design mode at 100% load, which replicates the standard NGCC case. Second, the gas turbine model is fixed at off-design mode for evaluating the part-load operation as well as the variation of inlet air composition and properties imposed by the integration of EGR and SEGR. The impact of off-design conditions on the performance of the gas turbine could be described by constant swallowing capacity at different sections of the gas turbine operating at choked conditions [277,291]:

$$\frac{\dot{m_{in}}}{P_{in}}.\sqrt{\frac{Z.T_{in}}{\gamma.MW}\left(\frac{\gamma+1}{2}\right)^{\frac{\gamma+1}{\gamma-1}}} = constant \qquad (1)$$

In this equation, T and P are given temperature and pressure, $\dot{m}$ is combustion gases flow rate, γ is isentropic exponents ($\gamma = \frac{C_p}{C_v}$), Z and MW are compressibility factors and the gas molecular weight. The efficiency of a gas turbine at off-design is estimated by a semi-empirical equation as follows [292]:

$$\frac{\eta_t}{\eta_{t,d}} = \frac{N}{N_d}\sqrt{\frac{T_{in.d}}{T_{in}}}K\left[Y-(Y-1)\frac{N}{N_d}\sqrt{\frac{T_{in.d}}{T_{in}}}\right] \qquad (2)$$

$$K = \frac{\sqrt{\left(\frac{P_{d,out}}{P_{d,in}}\right)^{\frac{\gamma-1}{\gamma}}-1}}{\sqrt{\left(\frac{P_{d,out}}{P_{d,in}}\right)^{\frac{\gamma-1}{\gamma}}-1}} \qquad (3)$$

The most commonly employed method to achieve optimal part-load performance in the modern gas turbine involves the utilization of Variable Inlet Guide Vanes (VIGVs) [293]. These vanes are positioned upstream of the first compressor stage and enable the generation of varying power levels by adjusting the position of the VIGVs to change the mass flow rate through the

compressor. Consequently, the VIGVs modify the effective flow area and the pressure ratio of the compressor, which would otherwise remain constant at a constant rotational speed [294]. During 100% load operation of the gas turbine, the VIGVs are fully open, while during part-load operation, the closure of the VIGVs results in a reduction in gas turbine efficiency, leading to an increase in outlet temperature. For gas turbine load management via VIGV, two practical control principals could be followed: constant turbine inlet temperature (TIT) or constant turbine exhaust temperature (TET) at the design value. The constant TIT principle offers superior efficiency compared to the alternative approach. However, as the load decreases, the constant TIT principle leads to an increase in the TET due to the declining expansion ratio, which is favorable in terms of higher heat availability in the downstream HRSG units [295]. However, an increased TET compared to the design temperature at part-load operation poses problems for the final uncooled stages of the turbine as well as the safe operation of downstream HRSG units [249]. Considering the material specification of gas turbine and downstream process units, the maximum allowable increase of TET compared to the nominal ISO base-load has been fixed by 50°C, as recommended in references [44,222]. The designed TIT and maximum allowable TET for the GE 7FA.05 gas turbine engine are 1357 °C and 645 °C, respectively.

Thermoflex software is able to perform off-design calculations and control the gas turbine based on the mapped performance curve and surge region. Accordingly, a macro is programmed in Thermoflex software by utilizing VIGV and control of fuel flow to maintain the designed TIT at part-load condition until the TET achieves its maximum allowable value. Below the minimum gas turbine load for TIT control, the TET control principles are employed, where air to fuel ratio increases in order to keep the TET at its maximum allowable value. A similar control procedure is recommended by other references for the efficient performance of gas turbines at partial loads [249,296,297].

The downstream process units of the NGCC plant, including HRSGs, feedwater system, and steam turbine, are designed for the 100% load of the gas turbine to suit the gas turbine exhaust gas flow rate and temperature, using a similar configuration of heat exchangers, steam pressure, and temperature levels to the baseline DOE/NETL design. During part-load operation of a gas turbine where the gas turbine exhaust gas flowrate and temperature changes, these units are in the rating mode in order to account for the performance variation during off-design at a fixed equipment size.

The heat transfer calculation procedure in part-load operation for various heat exchangers in the HRSG section is the same as the full load condition. However, the fluid pressure drop in the heat exchangers varies, and the overall heat transfer coefficient of heat exchangers at part-load operation is recalculated. Accordingly, the behavior of heat exchangers in the off-design conditions can be described as follows for the counter-flow exchangers:

$$Q = m_v\left(h_{v,out} - h_{v,in}\right) = m_g\left(h_{g,out} - h_{g,in}\right) \qquad (4)$$

$$Q = UA\frac{\left(T_{g,in} - T_{v,out}\right) - \left(T_{g,out} - T_{v,in}\right)}{ln\left(\frac{\left(T_{g,in} - T_{v,out}\right)}{\left(T_{g,out} - T_{v,in}\right)}\right)} \qquad (5)$$

where Q is the heat transfer, h_v and h_g are the enthalpy of vapor and gas sides, T_v and T_g are vapor and gas side temperatures, m_v and m_g are the vapor and gas mass flowrate, U is the overall heat transfer coefficient, and A is the heat transfer area. In the part-load operation heat transfer area is fixed, and the overall heat transfer coefficient is recalculated based on the following correlations [298]:

$$\frac{U}{U_d} = \left(\frac{m_g}{m_{g,d}}\right)^m \qquad (6)$$

$$\frac{U}{U_d} = \left(\frac{m_g}{m_{g,d}}\right)^m \left(\frac{m_v}{m_{v,d}}\right)^n \qquad (7)$$

Eq. 6 is used for calculating U in the off-design operation of economizers and evaporators, and Eq. 7 is used for superheaters. Suffix *d* denotes the value of parameters in the design condition. The empirical coefficients *m* and *n* are 0.6 and 0.8, which are estimated based on the Nusselt number equation for the gas and vapor sides [299].

$$\frac{h_v D_i}{k_v} = 0.023\left(\frac{G_v D_i}{\mu_v}\right)^{0.8} Pr_v^{0.33} \qquad (8)$$

$$\frac{h_g D}{k_g} = 0.4 \left(\frac{G_g D}{\mu_g}\right)^{0.8} Pr_g^{0.33} \qquad (9)$$

In these correlations, h denotes the heat transfer coefficient, G is the mass flux, k is the thermal conductivity, μ is the viscosity, Pr is the Prandtl number, D_i is the tube inside diameter, and D denotes the tube diameter. Suffix v and g denote the steam and gas side of the heat exchanger.

Stodala law of cones is used to describe the off-design performance of steam turbine at partial loads [293].

$$\frac{m_s}{m_{s,d}} = \sqrt{\frac{(P_{in}^2 - P_{out}^2)}{(P_{in,d}^2 - P_{out,d}^2)}} \sqrt{\frac{T_{in,d}}{T_{in}}} \qquad (10)$$

It has been assumed that at different part loads, the steam expansion in different sections of the steam turbine has a constant dry isentropic efficiency equal to the design conditions. This assumption is based on the fact that at different loads, the volumetric flow of the steam turbine is almost constant, which leads to a constant velocity triangle of the stages and unchanged efficiency [33]. The isentropic efficiency for the high-pressure, intermediate, and low-pressure sections of the steam turbine is considered to be 88.03, 92.37, and 93.67, respectively [13].

To regulate steam production in the HRSG during partial loads, a commonly used strategy is sliding pressure operation. This efficient control strategy is considered for high and intermediate turbines where the steam turbine's inlet control valves are fully opened, allowing the admittance pressure to slide or float [300]. Since the steam extraction for the amine-based CCS is from IP/LP crossover, a throttle valve is considered upstream of the LP turbine in order to maintain the extraction steam pressure high enough (3 bar) at partial loads where the pressure decreases compared to the full load.

6.4.2 Amine-based CO_2 capture and compression units

The simulation of amine-based PCC is implemented in Aspen Plus software V12.1 using the rate-based approach for both absorber and stripper modeling based on the 30 wt% MEA solvent. The unsymmetric electrolyte Non-Random-Two-Liquid (e-NRTL) activity coefficient model is considered the thermodynamic package to consider the non-ideal behavior of the liquid phase, while the Redlich-Kwong (RK) equation of state is utilized for describing the properties of vapor phase [162,279]. The detail of equilibrium and kinetic reactions, as well as the optimal design of amine-based CCS for capturing 90% of CO_2 at full load operation of both EGR+SEGR and SEGR designs, have been described and analyzed in our previous work. Table 6-3 presents the results of the MEA-based CCS process at optimal design and 100% load of NGCC.

During part load operation of the power plant where the flowrate of flue gas decreases and gas composition varies, the height and diameter of columns are fixed while maintaining the 90% CO_2 recovery by adjusting solvent recirculation flowrate (liquid to gas ratio). The flue gas at the absorber inlet was assumed to be cooled down to 40 ◦C by the DCC at various part loads. The heat transfer areas of all the heat exchangers in the plant remain constant, regardless of the load conditions, while the overall heat transfer coefficient is updated based on the correlation of the Nusselt number, similar to the Eq. 6. The stripper top stage pressure is kept constant at 1.62 bar, and the stripper reboiler duty is calculated based on the optimal lean solvent loading at the bottom stream.

Table 6-3. Design and operating results of MEA-based PCC at 100% load

Configuration/Case	Baseline	EGR+SEGR	SEGR
Absorber efficiency [%]	90	90	90
Inlet mass flow rate [kg/s]	1030	386	253
Rich solvent loading [mol CO_2/ mol MEA]	0.479	0.497	0.510
Solvent capacity [mol CO_2/ mol MEA]	0.279	0.297	0.310
Lean solvent flow rate [kg/s]	970	930	936
Liquid / Gas ratio [kg/kg]	0.954	2.48	3.83
Absorber diameter [m]	14.80	10.45	9.11
Absorber height [m]	18.3	20.2	24.8
Stripper diameter [m]	9	9	9
Stripper height [m]	28	23	20
Total packing Volume [m^3]	8073	4927	4508
Stripper pressure [bar]	1.62	1.62	1.62

Specific Reboiler Duty [MJ/ kgCO_2]	3.822	3.658	3.559
CO_2 to storage [kg/s]	56.00	57.13	60.11

The multi-stage compression plant, which consists of five compression stages with intercooling to 37 ºC increases the pressure of captured CO_2 to 150 bar with a purity of more than 99%. This plant is modeled in Aspen Plus, considering the same pressure ratio and compressor isentropic efficiency of 85%. During part-load operations, it has been assumed that the compression train is able to deliver CO_2 with a pressure of 150 bar by primarily using VIGV and flow recirculation.

6.4.3 Multi-stage membrane-based SEGR

Membrane modules are among flexible and scalable gas separation technologies with a fast response time and are ideal for part load operation [176]. Due to the modular and parallel design of the membrane gas separation plant, some membrane modules could be bypassed during part load operation in order that flue gas contacts with a lower membrane area, ensuring constant component recovery [196]. Accordingly, due to the variation of flue gas flowrate and composition, the required contact area of the membrane-based SEGR varies during partial loads to maintain the overall CO_2 recovery of the integrated system at 90%. Furthermore, since the proposed designs use air stream as a sweep gas for generation separation driving force and do not require huge compressors, the pressure ratio over the membrane is constant by utilizing blowers to overcome the pressure drop along the membrane modules.

The gas separation process is modeled based on the solution diffusion mechanism in the Aspen Custom Modeler software and exported to Aspen Plus for integration with amine-based PCC. Our previous work extensively discussed the modeling equations regarding mass balance, energy balance, and pressure drop involved in membrane gas separation modeling [189].

6.4.4 PTC solar field with thermal storage

As an economical and sustainable option for providing the required thermal energy of the CO_2 capture plant and reducing the power plant energy penalty, the PTC solar field with 240 MW design capacity and 4-hour thermal energy storage is integrated with a stripper reboiler in order to replace the steam extraction from the LP turbine during the sunshine time. This unit is designed and simulated using System Advisor Model (SAM) from the National Renewable Energy

Laboratory (NREL) [282], the detail of which is presented in our previous work. The PTC solar field model is then connected with the amine-based CCS model in Aspen Plus through the HTF heat exchanger, where the solar heat is transferred from the HTF at 300 °C to the return condensate to produce steam at 1°C above the saturation temperature at 2.5 bar. During part-load operations, the PTC solar field works under its design condition (same total aperture reflective area and target receiver thermal power), and the excess energy from the field is stored in the energy storage tank. In the case that the NGCC plant load reduces significantly and the energy storage tank is full, a fraction of solar collectors defocus in order to prevent the overproduction of steam. Additionally, if there is insufficient solar energy available to meet the heating requirements of the reboiler, the extracted steam from the LP turbine can be utilized as an additional heat source.

The thermal energy storage mass and energy balance calculations can be described as a function of time and inlet/outlet conditions as follows:

$$m_{f,in} = m_0 + \Delta t(\dot{m}_{in} - \dot{m}_{out}) \qquad (11)$$

Where $m_{f,in}$ is the mass of HTF in the storage tank at the end of the current time step.

$$\frac{\partial(u(t)m(t))}{\partial t} = -\dot{q}_L(t) + \dot{m}_{in}h(T_{in}) - \dot{m}_{out}\big(T(t)\big) \qquad (12)$$

In this energy balance equation, *u* is the internal energy, $\dot{q}_L$ is the heat loss in the storage tank, *h* is enthalpy, and *T* is the final HTF temperature. The obtained linear ODE can be solved for the HTF temperature as a function of time that results in the following expression:

$$T(t) = A_2 + \frac{1}{A_0}\left[\left(c_{htf}m_0\right)^{\left(-\frac{A_0}{A_1}\right)} \times \left(c_{htf}(m_0 + A_1 t)\right)^{\left(-\frac{A_0}{A_1}\right)} \times A_3\right] \qquad (13)$$

The constants in this equation are described as follows.

$$A_0 = \dot{m}_{in} + \frac{UA}{c_{htf}} \qquad (14)$$

$$A_1 = \dot{m}_{in} - \dot{m}_{out} \qquad (15)$$

$$A_2 = \frac{\dot{m}_{in}T_{in} + T_{amb}\dfrac{UA}{c_{htf}}}{A_0} \qquad (16)$$

$$A_3 = c_{htf}\dot{m}_{in}(T_0 - T_{in}) + UA(T_0 - T_{amb}) \qquad (17)$$

In the above equation, c is specific heat, T_0 is the initial temperature, and UA is the heat loss coefficient.

6.5 Economic analysis approach

6.5.1 Economic criteria

Developing an economic model aims to perform an economic analysis of the EGR+SRGR SEGR case and compare the results with the baseline case. The economic criteria used in this paper include the levelized cost of electricity (LCOE), the cost of CO_2 avoided (COA), and the cost of CO_2 captured (COC).

LCOE represents the specific price at which the power provider must charge for the generated electricity in order for the system to achieve break even by the end of its operational lifespan [301]. LOCE ($/MWh) is calculated using Eq. 18 by assuming all parameter values remain constant over the life of the plant (labor, material, fuel, among others).

$$LCOE = \frac{CCF \times TOC + FOM}{MW \times CF \times 8760} + VOM + FC \times HR + T\&S_{CO_2} \qquad (18)$$

Where TOC denotes the total overnight cost ($), CCF is the capital charge factor (1/year), FOM is the fixed operating and maintenance (O&M) costs ($), VOM is the variable O&M costs ($/MWh), FC is the fuel cost ($/MMBTU), HR is the net heat rate (HHV, MMBTU), MW is the net power output (MW), CF is the capacity factor (%), and $T\&S_{CO_2}$ is the transport and storage cost of CO_2 ($/MWh).

The cost of CO_2 avoided (COA) is the primary criterion for evaluating the economic effectiveness of the CCS system in reducing CO_2 emissions since it measures the average expense of preventing the release of one unit of CO_2 while generating a unit of electricity. COA ($/tonne CO_2) is expressed as follows:

$$COA = \frac{LCOE_{CCS} - LCOE_{ref}}{CO_2\ emission_{ref} - CO_2\ emission_{CCS}} \qquad (19)$$

Where $LCOE_{CCS}$ and $LCOE_{ref}$ represent the value of LCOE in the power plant with CCS and in the reference case without CCS, respectively. $CO_2\ emission$ is the mass flowrate of CO_2 emissions from each type of plant power per net plant power (tonne CO_2/MWh).

The Cost of CO_2 captured (COC) represent the production cost of CO_2 as it doesn't include the transport and storage cost of CO_2 in the LCOE calculation. This metric is calculated as follows:

$$COC = \frac{LCOE_{CCS} - LCOE_{ref}}{CO_2\ Captured} \qquad (20)$$

where the $CO_2\ Captured$ is the amount of captured CO_2 per unit of the net generated power

The economic method considered for calculating capital expenditure (CAPEX) and operating expenditure (OPEX) involved in these three economic criteria is provided below.

6.5.2 CAPEX and OPEX calculation

The economic analysis approach for the NGCC plant is based on the capital cost scaling guideline recommended by DOE/NETL for power plants [302]. The reference NGCC plant considered for scaling up is case 1b of the DOE/NETL report [13], and the capital cost is updated to US$ 2022 using the chemical engineering plant cost index (CEPCI) index. Eq. 21 shows the cost calculation for the year 2022 based on the CEPCI index, where the suffix *year* denoted the reference year for the cost calculation.

$$Cost_{2022} = Cost_{year} \times \frac{CEPCI_{2022}}{CEPCI_{year}} \qquad (21)$$

The process parameters required for estimating the costs of the target equipment are obtained through process design and simulation. The expenses associated with bare erected cost (BEC) of process equipment, including equipment costs, material costs, and labor costs for installation, were determined by scaling from similar items using the following equation and scaling parameters and exponents presented in Table 6-4. It should be noted that the capital cost

of the gas turbine remains the same as the reference case since an identical GE 7 series gas turbine type has been utilized in all cases.

$$BEC_d = BEC_{ref} \times \left(\frac{SP_d}{SP_{ref}}\right)^{SE} \qquad (22)$$

where SP and SE refer to the scaling parameter and scaling exponent, and suffixes d and ref denote to the design and reference cases.

Table 6-4. Scaling parameters used in this work [302].

Process equipment	Scaling parameter	Exponent
Feedwater system	Feedwater flowrate	0.72
Water makeup & Service water systems	Raw water withdrawal	0.73
HRSG/accessories	HRSG duty	0.7/1.4
Steam turbine generator & accessories	Steam turbine gross power	0.8
Condenser & auxiliaries	Condenser duty	0.8
Cooling towers	Cooling tower duty	0.73
Circulating water pumps	Circulating water flow rate	0.72
Generator equipment	Total plant gross power	0.59
Accessory electric plant	Auxiliary load	0.64
Instrumentation & control	Auxiliary load	0.16
Sire improvement	Total Plant Gross Power	0.46
Gas recycling system	Flue gas flowrate	0.70
CO_2 Compression & Drying	Compressor Auxiliary Load	0.41

Since the cost estimation of the CO_2 capture process in DOE/NETL reports is based on a particular solvent and process, the capital investment and operating costs associated with the conventional MEA-based capture processes are conducted using the costing approach suggested in references [65]. In this method, the capital cost correlation of equipment involves in the CO_2 capture cost is a function of the equipment size in the full load operation. This approach is more favorable and provides more accurate cost analysis accuracy since the size of capture cost significantly varies by the implementation of EGR and SEGR. The cost of the membrane module is preliminarily considered as 50 \$/$m^{2,}$ which is commonly reported in other techno-economic analyses of the membrane process [189,208,247,303]. The cost estimation of the PTC solar field, comprising solar collectors, HTF and hydraulic circuit, and thermal energy storage tank, is calculated based on the solar multiple of 2, and four hours of energy storage. Table 6-5 presents

the correlations for estimating the capital cost of components in the amine-based CCS, membrane-based SEGR, and PTC solar field.

Table 6-5. Equipment cost correlations for CO_2 capture process and PTC solar field

Equipment cost (US$)	Costing parameter	Equation	CEPCI
Absorber and stripper [304]	Diameter (D) and height (H), (m)	$H(10^{0.5633(logD)^2+1.0566(logD)+3.8057})$	2001: 397
Column packing [305]	Packing volume, (m^3)	$1700 \times Volume$	2009: 521.9
Heat exchanger [306]	Heat transfer area (m^2)	$94093 + 1127 \times Area^2$	2000: 391.1
Pump [304]	Volume flow rate (m^3/h)	$10^{0.2468(logF)^2-0.5966(logD)+3.9213}$	2001:397
Blower [65]	Volume flow rate (m^3/h)	$10^{0.6126(logF)+4.6614}$	2002: 395.6
Membrane [303]	Membrane area (m^2)	$50 \times Area$	2022: 813
CO_2 transport and storage [307]	Captured CO_2 (tonne CO_2)	$10 \times Captured\ CO_2$	2022: 813
Solar collector [308]	Aperture area (m^2)	$150 \times Area$	2022: 813
HTF and hydraulic circuit [309]	Aperture area (m^2)	$90 \times Area$	2022: 813
Thermal storage system [310]	Capacity ($kW_{th}h$)	$30 \times Capacity$	2022: 813

The total plant cost (TPC) of the integrated system is calculated by adding the costs associated with the engineering, procurement, and construction services (EPC) as well as project contingencies to the total determined BEC [301]. Finally, the total overnight cost (TOC) of the plant is calculated by adding the owner's costs, including financial cost, pre-production cost, and others, to the calculated value for TPC. The costs related to O&M costs include FOM and VOM. FOM cost is calculated per year and comprises labor expenses for operational, maintenance, administrative, and support functions, as well as property taxes and insurance costs. On the other hand, VOM cost is calculated based on $/MWh and consists of expenses for maintenance materials, consumables (such as cooling water, solvent, catalysts, and others), waste disposal costs, and fuel expenses. The details of the economic model and fundamental assumptions considered for the economic analysis of the integrated system are summarized in Table 6-6.

Table 6-6. Economic model parameters and assumptions.

	Parameters	References
	Capacity factor (85%)	
	Capital charge factor for NGCC plant with CCS (0.111)	[301]
	Capital charge factor for solar field (0.065) Interest rate (5%)	[311]

	Basis year of economic costing (2022)	
	CEPCI index in 2011 for NGCC plant (585.7)	
	Project lifetime (30 years)	[301]
	Membrane lifetime (5 years)	[312]
Total plant and overnight costs (TPC & TOC)	EPC and home office cost (8.4% of BEC)	[13]
	Project contingency of NGCC plant (17% of BEC_{NGCC})	[49]
	Project contingency of capture plant (20% of BEC_{CCS})	[13]
	Project contingency of solar field (10% of BEC_{solar})	[311]
	Process contingency of capture plant (20% of BEC_{CCS})	[13]
	Owner's costs [13]	
	Land cost for NGCC and CCS (0.3 M$)	
	6 months of all labor	
	1 month of maintenance materials	
	1 month of non-fuel consumables	
	25% of 1 month fuel cost	
	Miscellaneous (2% of TPC)	
	60 days of consumables	
	Spare parts (0.5 % of TPC)	
	Initial cost of chemicals (2.5$/kW)	
	Other owner's costs (15% of TPC)	
	Financing costs (2.7% of TPC)	
	Project, land, management of solar field (3.5% of BEC_{solar})	[311]
Fixed O&M costs (FOM) [13]	Total labor cost (50$ per hour)	
	3 shifts per day	
	6.3 operators per shift	
	Admin and support labor costs (25% of labor costs)	
	Taxes and insurance (2% of TPC)	
	Solar field FOM cost (1.5% of BEC_{solar})	[311]
Variable O&M costs (VOM)	Maintenance material cost (1.2% of TPC)	[13]
	Consumables cost (0.0012$/kWnet)	[13]
	Solvent cost (2.09 $/tonne)	[65]
	Membrane replacement cost (10 $/$m^2$)	[313]
	Solar filed VOM (0.001 $/kWh)	[154]
	Fuel cost (4$/MMBTU, HHV)	[314]

6.6 Results and discussion

In this section, the results of part-load operation and economic analysis for two designs, including the SEGR and EGR+SEGR cases have been provided and compared with the standard

case. It should be noted that the modeling and simulation of all subsystems have been validated in our previous work.

Table 6-7 presents the summary of operating conditions and stream properties at the maximum continuous rating (100% load) operation of each system. The observed trend reveals a notable enhancement in the concentration of CO_2 in the flue gas as the SEGR ratio is elevated. Specifically, the CO_2 concentration substantially increases from less than 4 mole% in the reference scenario to approximately 18.1 mole% when the SEGR ratio reaches 76.4 percent (SEGR case). In the scenario involving EGR+SEGR, where 50% of the flue gas is directed to the membrane-based SEGR, an EGR ratio of 25.6% has been found to yield a flue gas CO_2 concentration of 10.87 mole%, while simultaneously fulfilling the oxygen requirements within the air stream. The variation in the properties of the inlet air stream, along with the resulting adjustments in flow rates and properties of the streams to uphold the design value of the TIT, have an impact on the overall performance of gas turbines, as well as downstream equipment such as HRSGs and steam turbines. Compared to the baseline case, the net power output demonstrates a notable boost of around 50.33 MW and 20 MW in the SEGR and EGR+SEGR cases, respectively, while the net electric efficiency increases by 1.7% and 1.3% in the respective cases.

Table 6-7. Performance of NGCC plant at full load in EGR+SEGR and SEGR cases compared to the baseline case

	Baseline	**EGR+SEGR**	**SEGR**
EGR ratio [%]	-	25.6	-
SEGR ratio [%]	-	50	76.4
GT inlet air stream			
Air temperature [°C]	15	28.3	30
Pressure [bar]	1.01	1.01	1.01
Mass flow [kg/s]	503.2	507.3	522.8
CO_2 concentration [mole%]	0.03	7.13	14.44
O_2 concentration [mole%]	20.74	16	16
Density [kg/m]	1.220	1.195	1.234
GT exhaust gas stream			
Temperature [°C]	603.3	627.6	646.4
Pressure [bar]	1.05	1.05	1.05
Mass flow [kg/s]	514.8	519.2	535.4
CO_2 concentration [mole%]	3.90	10.87	18.08
H_2O concentration [mole%]	8.42	10.97	11.63
O_2 concentration [mole%]	12.39	7.51	7.04

NGCC plant performance			
Gas turbine net power [MWe]	420.9	415	425.8
Steam turbine Power [MWe]	175.2	196	216.8
Gross power [MWe]	596.1	611	642.6
Net power [MWe]	537.8	557.84	588.13
Net electric efficiency (LHV) [%]	48.81	49.43	49.63
Plant auxiliary [MWe]	58.26	53.14	54.46
HRSG efficiency [%]	82.9	84.91	86
Fuel LHV [kJ/kg]	47180	47180	47180
Fuel input [kg/s] × 2	11.67	11.95	12.55

A detailed discussion about the performance of the integrated system, including the NGCC power plant, amine-based CCS, membrane-based SEGR, and the solar PTC field at the design load, is provided in Chapter 5.

6.6.1 Part-load performance of the integrated system

NGCC plant

The part-load performance of the NGCC plant is evaluated by considering all equipment in the rating mode while the gas turbine load decreases from 100% to 50%, considering the control procedure presented in section 6.4.1. In the case of the NGCC plant integrated with selective exhaust gas recirculation, the gas turbine inlet air oxygen concentration remains constant at 16 mole% by controlling the recirculation ratio. Since this subsection focuses on the part load performance of the NGCC plant and the solar energy generation is typically intermittent, zero solar energy availability has been assumed. Accordingly, the part load performance of the NGCC plant in both EGR+SEGR and SEGR designs is evaluated and compared with the standard NGCC case with amine-based CCS. The summary of the part load performance of the NGCC plant integrated with PCC and EGR+SEGR is presented in Table 6-8. Also, a similar table for the reference case, as well as the SEGR case, is presented in Supporting Information.

Table 6-8. Part load performance of the EGR+SEGR case

Gas Turbine loading (%)	**100%**	**90%**	**80%**	**70%**	**60%**	**50%**
Gas turbines power (MW)	415.1	372.8	328.9	289.2	247.1	206.9
HP steam turbine power (MW)	56.8	56.7	54.6	52.1	47.5	44.8

IP steam turbine power (MW)	90.4	86.9	80.8	74.6	68.1	58.9
LP steam turbine power (MW)	53	52.6	51.2	49.7	48.2	46.6
Steam turbine power (MW)	195.9	192.1	182.6	172.5	160.1	146.7
Gross power (MW)	611	564.9	511.5	461.7	407.3	353.6
NGCC load (%)	100	92.45	83.71	75.56	66.66	57.88
Net power (MW)	557.8	515.1	465.2	418.4	367.2	316.5
Plant auxiliary (MW)	53.2	49.8	46.3	43.3	40.1	37.2
Net electric efficiency, LHV (%)	49.43	48.86	47.93	46.88	45.43	43.57
Net fuel input, LHV (MW)	1128.6	1054.4	970.6	892.5	808.3	726.3
Fuel flowrate change (%)	100.00	93.47	86.01	79.10	71.62	64.37
GT Exhaust flow (tonne/h)	3738.2	3483.4	3263.4	3071.4	2859.4	2649.4
Flue gas composition						
O_2 mol%	7.51	7.49	7.64	7.83	8.05	8.29
CO_2 mol%	10.87	10.88	10.76	10.60	10.42	10.23
H_2O mol%	10.97	10.99	10.86	10.70	10.51	10.31
N_2 mol%	69.81	69.80	69.90	70.03	70.17	70.33
Ar mol%	0.84	0.84	0.84	0.84	0.84	0.84

As it can be seen, by decreasing the gas turbine load from 100% to 50%, the NGCC load reduction is not proportional to the gas turbine load, which is mainly because of the steam turbine performance during part-load. Also, when the GT load decreases, the inlet fuel flowrate decreases by a lower percentage compared to the reduction in the GT load. This behavior could be described by analyzing the performance of gas turbines at partial loads. As mentioned before about the control procedure of the gas turbine during partial load, the turbine inlet temperature needs to be controlled at its design conditions while the turbine exhaust temperature keeps at its maximum allowable temperature of 645 °C to have an optimal operation of the gas turbine during load reduction.

The variation of air-to-fuel ratio and pressure ratio in the gas turbine of baseline, EGR+SEGR, and SEGR case to meet the partial loads by the control procedure is presented in Fig. 2. Also, the variation of TIT and TET during part load operation is presented in Fig. 6-3. During part-load operation, the gas turbine reduces the air flow and fuel flow to achieve the specified load, which results in the reduction of the pressure ratio from 17 to below 12 since less pressure is required to push the mixture through the turbine nozzles. The variation in the ratio of air to fuel depends on the TET and TIT at partial loads, while the pressure ratio decreases in all cases during partial loads. Furthermore, integrating the NGCC plant with SEGR and EGR caused an obvious deviation compared to the baseline case. This is mainly because of the utilization of EGR and

SEGR, which leads to an increase in the molecular weight, density, and specific heat of the incoming air. Therefore, according to Eq. 1-3, the inlet air and fuel flowrate, as well as pressure ratio, increases by CO_2 recirculation at 100% load. During partial loads, since the TET is higher in EGR+SEGR and SEGR case compared to the baseline case, the inlet air-to-fuel ratio increases more rapidly to keep the TET below the threshold. However, in the baseline case, because of the lower TET at design points, the air-to-fuel ratio is constant until 80% load, while at lower GT loads, the air-to-fuel ratio starts to increase.

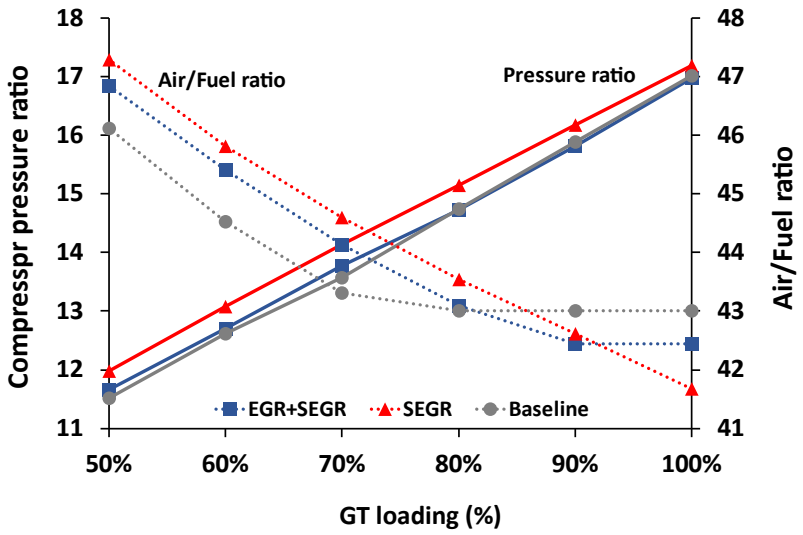

Fig. 6-2. Variation of compressor pressure ratio and air to fuel ratio at partial loads

The reduction in efficiency due to the lower pressure ratio at partial loads results in a higher turbine outlet temperature, as all cases achieve the maximum TET at the load of 70%. The air-to-fuel ratio, which was constant to keep the design TIT, increases in order to maintain the TET at the maximum allowable temperature leading to a reduction of TIT and efficiency, as presented in Fig. 6-3. For the baseline case, TIT is fixed at 1357.2 C from 100% to 80% GT loads, while in the EGR+SEGR case, the TIT is constant above 90% GT load. For the SEGR case, the TET is at its maximum value at its full load; thus, load reduction leads to a decrease in TIT.

Having a higher TET and mass flow with high specific heat in the exhaust gas is more favorable for the downstream HRSG and steam turbine system, and more power could be generated, as it is shown in Table 6-7 for the proposed cases.

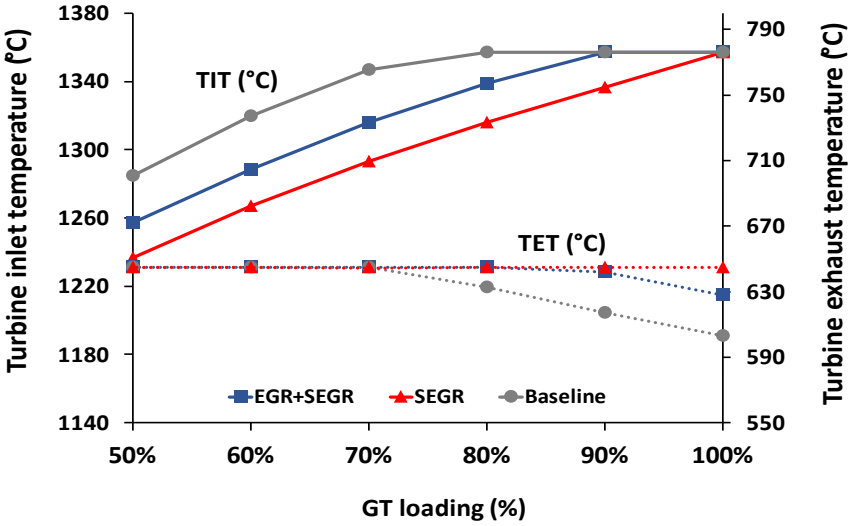

Fig. 6-3. Variation of TIT and TET at partial loads for different cases

The effect of part load operation on the NGCC gross power and efficiency is presented in Fig. 6-4. As can be seen, the NGCC gross efficiency drops by 5.45% and 4.84% for the EGR+SEGR and baseline cases, respectively. On the other hand, the total gross power in EGR+SEGR and SEGR case during part load operation is higher than the standard case,

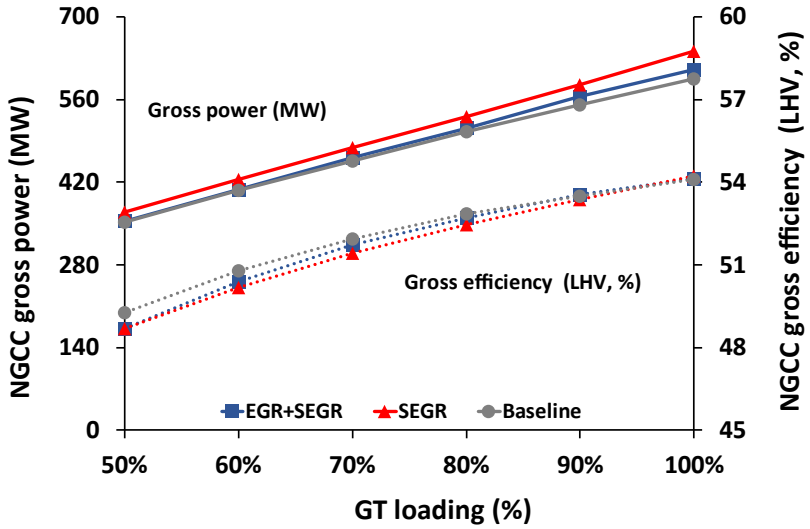

Fig. 6-4. Effect of part load operation on the NGCC gross power and efficiency

specifically at 100% load and higher partial loads where the NGCC efficiency is almost higher than the standard case. In the lower loads, since the high TET and air-to-fuel ratio leads to lower TIT, specifically for the SEGR case, it results in the reduction of efficiency of all cases.

Also, the NGCC gross power is not proportionally decreased by the gas turbine load reduction; as in the 50% gas turbine load, the NGCC combined cycle load is 57.88% of the full load operation. This is mainly because of the steam turbine performance that improves by the TET increment during part load. As depicted in Fig. 6-5, the steam turbine power generated in the SEGR and EGR+EGR cases is higher in all partial loads compared to the base case, specifically at higher loads where there is a considerable improvement for the proposed designs. Furthermore, by decreasing the gas turbine loads from 100% to 50%, the steam turbine power generated at 50% load is about 75% of the power generated in the full load. Also, comparing the reduction rate in the auxiliary power consumption of considered cases is notable for addressing. At high partial loads (100% to 80%), the auxiliary power consumption for both the EGR+SEGR case and SEGR case is lower than the baseline case, which is mainly because of the lower power requirement for the PCC case in the EGR+SEGR case compared to the baseline case. It can be seen that during NGCC load reduction from 100% to 50%, the auxiliary power consumption of the baseline case decreases by 37%, while this reduction in the SEGR case and EGR+SEGR case is 28.8% and 30%, respectively.

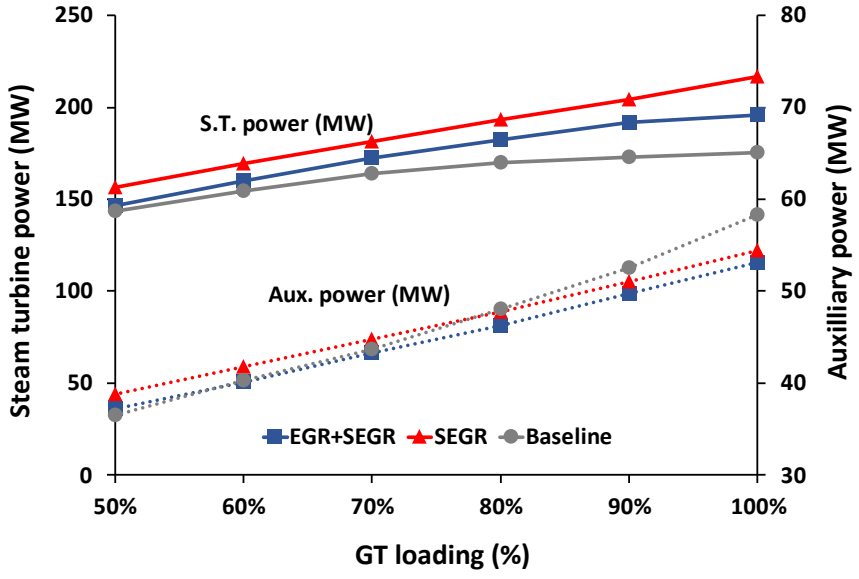

Fig. 6-5. Effect of part load operation on the steam turbine performance and auxiliary power consumption

The rate of reduction in auxiliary power due to partial load operation of the NGCC plant is faster in the baseline case as, in the partial load of 70%, the baseline case and EGR+SEGR case have the same auxiliary power consumption. As shown in Fig. 6-6, this is mainly due to higher PCC plant auxiliary power consumption in the baseline case, which decreases proportionally with the NGCC load reduction (as the flue gas flowrate decreases). However, for the SEGR case, the NGCC plant auxiliary consumption is dominant in partial loads and does not decrease proportionally with the NGCC load reduction. Accordingly, at full loads and higher partial loads, where the PCC plant auxiliary is dominant, the EGR+SEGR case, as well as the SEGR case, present lower auxiliary power consumption due to the improved performance of the PCC plant in these designs.

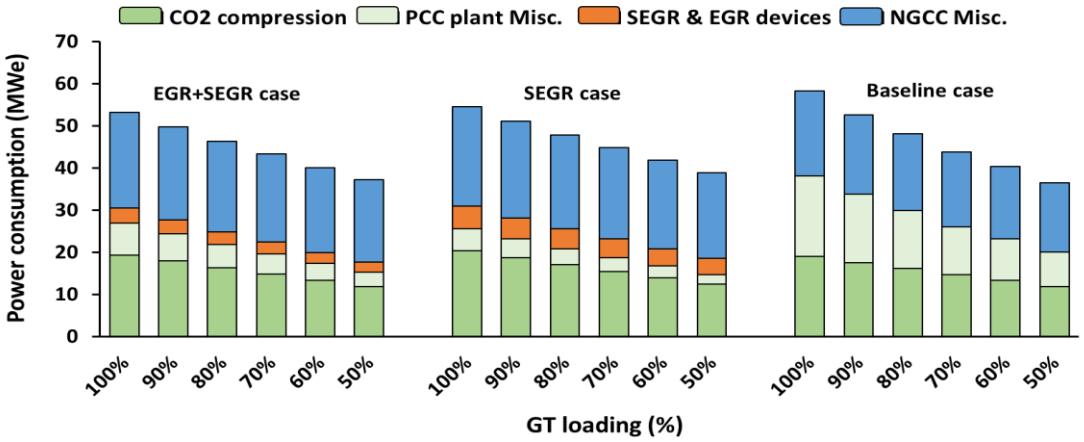

Fig. 6-6. Auxiliary power consumption at partial loads for the proposed cases

Regarding the condition of flue gas properties during the part-load operation of NGCC, the effects of the part-load operation on the flowrate and CO_2 concentration of the flue gas are demonstrated in Fig. 6-7. During partial loads, the CO_2 concentration in the flue gas slightly decreases from 10.87 mole% to 10.23 mole% during load reduction from 100% to 50% in the EGR+SEGR case mainly due to the higher air-to-fuel ratio, and exhaust flowrate decrease as well. Compared to the gas turbine load reduction, when the load is 50% of the design condition, the exhaust flowrate is approximately 64% of the flue gas flowrate at design condition for the EGR+SEGR case, which is mainly due to TET control of gas turbine by air to fuel ratio.

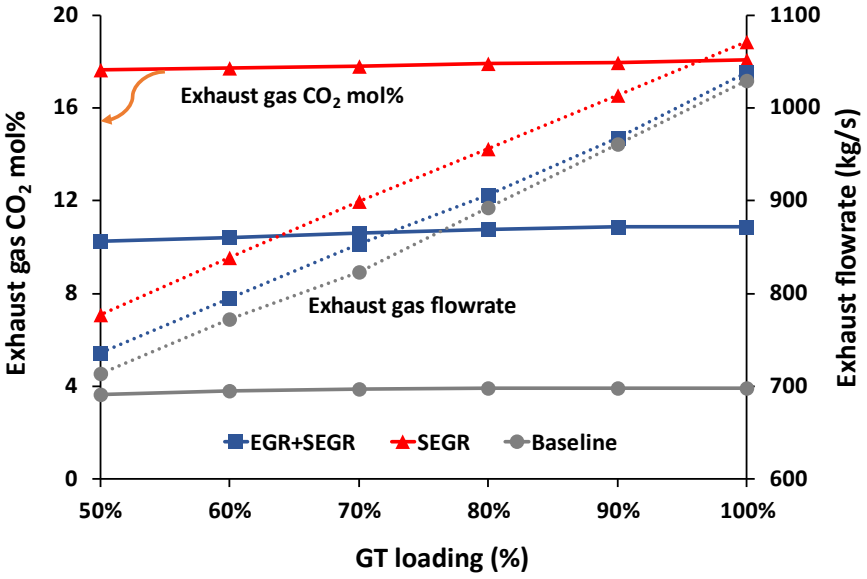

Fig. 6-7. Variation of CO_2 concentration and flowrate of flue gas during part load operation of NGCC

Overall, the results of NGCC plant performance at partial loads for the proposed designs revealed both SEGR and EGR+SEGR cases show acceptable performance, while the EGR+SEGR part load operation is slightly superior to the SEGR case. Furthermore, the results demonstrate that all cases perform considerably better at full load conditions. The efficiency reduction resulting from the gas turbine performance at partial loads needs to be addressed by the gas turbine manufacturer so that the gas turbine can handle higher TET during partial loads.

CO_2 capture plant

During part load operation of NGCC, since the flue gas properties and flowrate varies, the performance of the CO_2 capture plant is influenced. As mentioned before, the size of all equipment in the amine-based CCS plant is fixed, while the membrane-based SEGR operates at partial modes by varying the required membrane area due to its flexibility and parallel modular design. Accordingly, during partial loads, as the flowrate decreases, some of the membrane-based SEGR parallel modules are bypassed in order to achieve the separation target and specified requirement of O_2 concentration in the gas turbine inlet air. The summary of PCC plant performance during part load operation of the NGCC plant is presented in Table 6-9.

Table 6-9. PCC plant performance during part load operation of NGCC plant

Gas Turbine loading (%)	100%	90%	80%	70%	60%	50%
CO_2 recovery (%)	0.9	0.9	0.9	0.9	0.9	0.9
Flue gas flowrate to PCC (tonne/h)	1390.3	1297.1	1207.9	1127.4	1038.9	951
Reboiler duty (MW)	209.4	195.6	180.4	166.2	151.0	136.1
Absorber fraction to flooding (%)	75.0	69.9	64.8	60.1	55.0	50.0
Stripper fraction to flooding (%)	75.0	68.3	62.9	57.9	52.5	47.3
Specific reboiler duty (MJ/kgCO_2)	3.658	3.660	3.666	3.672	3.682	3.693
Liquid/Gas ratio (L/G, kg/kg)	2.481	2.476	2.445	2.401	2.356	2.309
Rich solvent CO_2 loading	0.497	0.498	0.498	0.499	0.499	0.499
Lean solvent CO_2 loading	0.2	0.2	0.2	0.2	0.2	0.2
Stripper inlet temperature (C)	106.9	106.6	106.3	106.0	105.5	105.1
Stripper bottom stage temperature (C)	117.6	117.6	117.6	117.6	117.6	117.6
Cross heat exchanger UA (kW/K)	19918	17899	15815	13892	11990	10222
Total required steam in reboiler (tonne/h)	344.6	89.58	297.5	274.1	248.9	224.4
Total extracted steam from NGCC (tonne/h)	303.6	281.268	257.4	235.5	211.7	188.7
Fraction of operating membrane module (%)	100	93.2	86.8	81.3	75.4	69.4

As shown in Table 6-9, the fraction of operating membrane modules decreases at partial loads; however, it is not proportionally reduced compared to the NGCC load reduction. This is mainly because of the variation of flue gas flowrate at partial loads and the ratio of EGR and SEGR in partial loads. In order to achieve the 90% separation target and minimum oxygen concentration

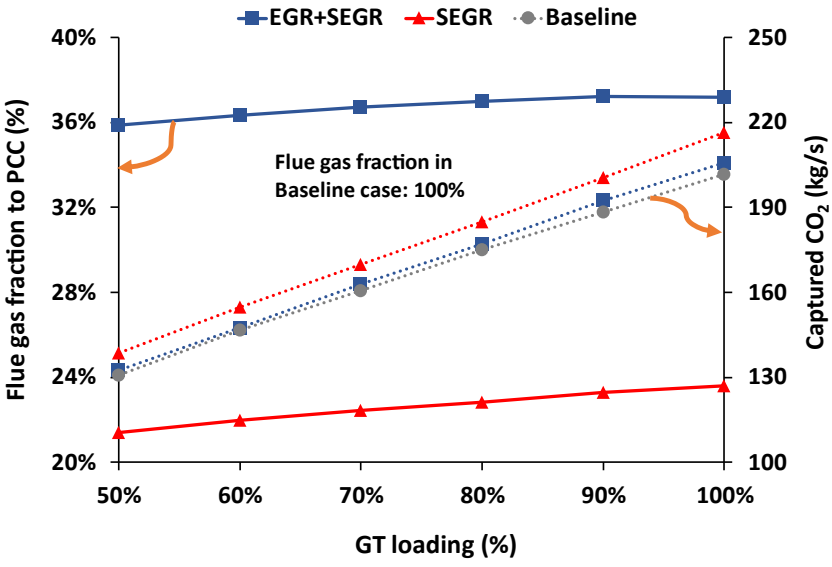

Fig. 6-8. Variation of flue gas fraction directed to the PCC plant and captured CO_2 in part load operation of considered cases

in the inlet air, the fraction of flue gas that is directed to the EGR and membrane-based SEGR is varied by the control valve, while in the baseline case, all the flue gas is directed to the amine-based CCS plant. As presented in Fig. 6-8, the fraction of flue gas directed to the PCC plant for the SEGR case decreases from 23.6% at full load to 21.5% at 50% gas turbine load, as the membrane-based SEGR could handle more flowrate to achieve the 16% mole% of oxygen in the partial loads. This reduction in the fraction of flue gas directed to the PCC plant for the EGR+SEGR case is from 37.2% to 35.9%. It should be noted that in the EGR+SEGR design, this variation in the PCC plant flue gas fraction is associated with the EGR split ratio since the SEGR ratio is fixed at 50%. Furthermore, the amount of captured CO_2 in the SEGR and EGR+SEGR cases is higher than the baseline case from full load to low partial loads, while the carbon intensity of these systems is lower than the baseline case considering the net power generated in these cases. The value of carbon intensity at full load is 408.8 and 409.7 $kgCO_2/MWh$ for the SEGR and EGR+SEGR case, respectively, while the carbon intensity of the baseline case is 416.5 $kgCO_2/MWh$.

During partial loads where the properties and flowrate of flue gas change, the required reboiler duty for capturing one tonne of CO_2 and the required solvent flow rate varies in order to achieve the 90% separation target. The influence of partial loads on the specific reboiler duty and L/G ratio is depicted in Fig. 6-9 to shed light on the PCC system behavior.

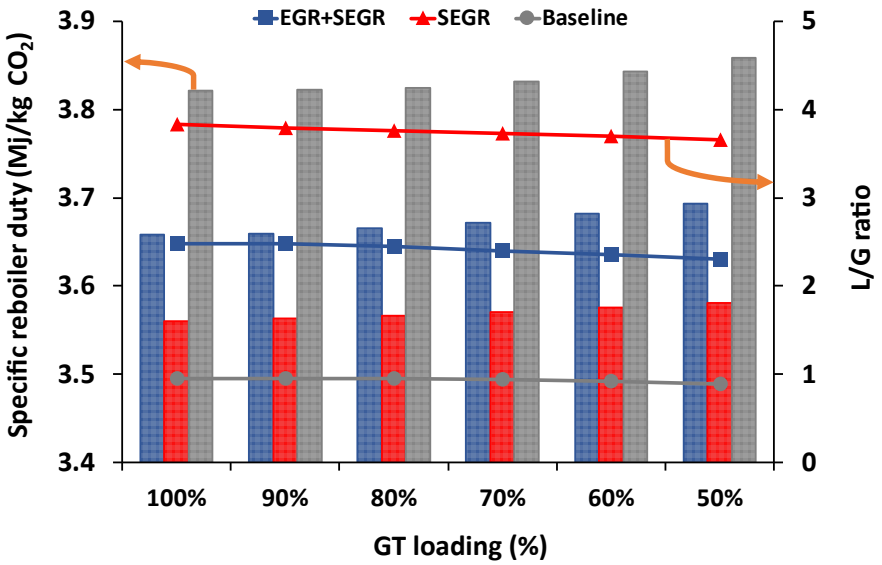

Fig. 6-9. Variation of the specific reboiler duty and L/G ratio during part load operation of gas turbine

As can be seen, during partial loads, the specific reboiler duty slightly increases, and the PCC plant deviates from its optimal operation in the full load conditions. This is mainly because of the lower CO_2 fraction in the flue gas that leads to the reduction of solvent recirculation (L/G ratio) in the process. The increase in the reboiler duty at partial loads is higher in the Baseline case compared to the EGR+SEGR case. More importantly, the lower efficiency of the cross-heat exchanger in partial loads, where the heat transfer coefficient decreases according to Eq. 6, resulted in lower stripper inlet temperature, as presented in Fig. 6-10. Subsequently, the required reboiler duty in the stripper and steam extraction from the NGCC plant increases. Also, the steam extraction for the PCC plant is always higher in the baseline case compared to the EGR+SEGR and SEGR case, which shows the improved performance of the PCC plant. Furthermore, the EGR+SEGR case extracts lower steam from the NGCC plant compared to the EGR+SEGR case mainly because of lower CO_2 generation in the NGCC plant. Regarding the stripper inlet temperature in the proposed design, the outlet temperature of the mixture from the absorber is higher in the EGR+SEGR and SEGR cases due to the release of heat absorption, resulting in lower cross-heat exchanger temperature to satisfy the specified 10 ℃ temperature approach in the cross-heat exchanger. Accordingly, if a lower temperature approach could be considered in the cross-heat exchanger, a lower reboiler duty could be achieved in the proposed designs.

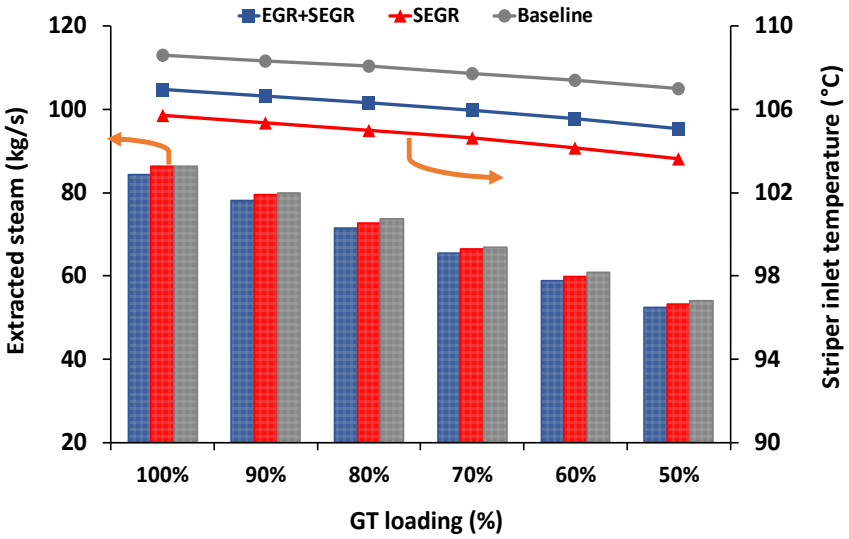

Fig. 6-10. Variation of steam extraction for the PCC plant reboiler and stripper inlet temperature in partial loads of gas turbine

The variation of the required membrane area to achieve the specified CO_2 separation and the oxygen requirement in the air stream during part load operation is presented in Fig. 6-11. As can be seen, the required membrane area for the SEGR case reduces from almost 3.1 Mm^2 to 2.56 Mm^2 during gas turbine load reduction from 100% to 50%. This value is considerably lower for the EGR+SEGR case as it decreases from 0.89 Mm^2 at full load to 0.62 Mm^2 in 50% load of the gas turbine. This lower reduction in required membrane area compared to the gas turbine load reduction is related to the flue gas fraction to SEGR during the part load operation as well as the flue gas flowrate that is achieved in partial loads that are not proportionally decreased compared to the gas turbine load reduction.

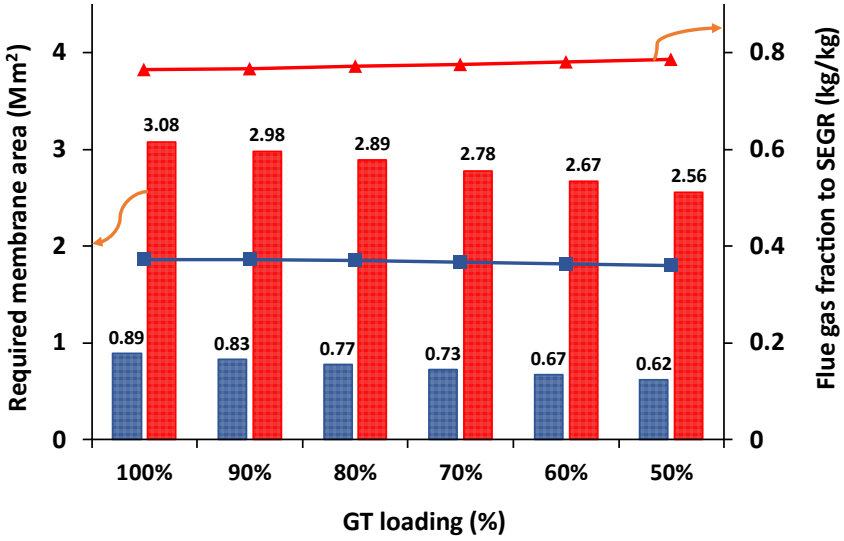

Fig. 6-11. Variation of required membrane area and SEGR ratio during part load operation of gas turbine

Solar PTC field

As mentioned in the previous section, the required reboiler duty of the capture plant reduces during the part load operation of the NGCC plant. Subsequently, the solar PTC field and energy storage heat delivery to the capture plant need to be adjusted based on the required reboiler duty to prevent overheating of the reboiler. Since the PTC solar field is designed for 240 MW capacity with 4-hour energy storage at 100% load of NGCC, during partial operation, the surplus solar energy could be stored, or in the case of the full capacity of thermal energy storage, a fraction of solar collectors are defocused.

Considering the solar PTC field located in Oklahoma City, US, a time-dependent simulation was conducted over 24 hours throughout the year to assess the hourly operation of the solar field and its integration with the PCC plant in full load and partial loads. The analysis is performed for the EGR+SEGR case as the design of the PTC field in all cases is similar. The result showed that the PTC solar field generates about 724164 MWh of thermal energy annually for the full load case and 638261 MWh in the 50% load of the gas turbine. Accordingly, while the reboiler duty has been decreased by 35% during the 50% load of gas turbine, the reduction in PTC field contribution to the PCC plant is decreased by 12% over the year, mainly due to the improved performance of thermal energy storage leading to a stable supply of thermal energy.

Fig. 6-12 presents the heat map of annual thermal energy delivered to the PCC reboiler via the PTC solar field in full and partial load conditions. In the full load operation, the period from 9 am to 7 pm shows a clear peak in thermal energy generation. Also, during the winter months (November, December, and January) of the year, the availability of solar energy is limited even by considering energy storge due to the fluctuations in direct normal irradiance across different seasons in Oklahoma City, which significantly affect the availability of solar thermal energy. Consequently, the duration of providing thermal energy to the PCC reboiler is shorter than in other months. In contrast, during part load operation of the gas turbine (50%), both the amount and duration of solar heat to the PCC reboiler increase significantly, and a more uniform supply of thermal energy to the reboiler is achieved. Even during the hours after sunset, a portion of the reboiler duty is fulfilled by solar thermal energy storage. This is mainly because of the reduced duty of the reboiler at 50% load of the gas turbine, which is 136.1 MW, 33% lower than the design capacity of the solar PTC field.

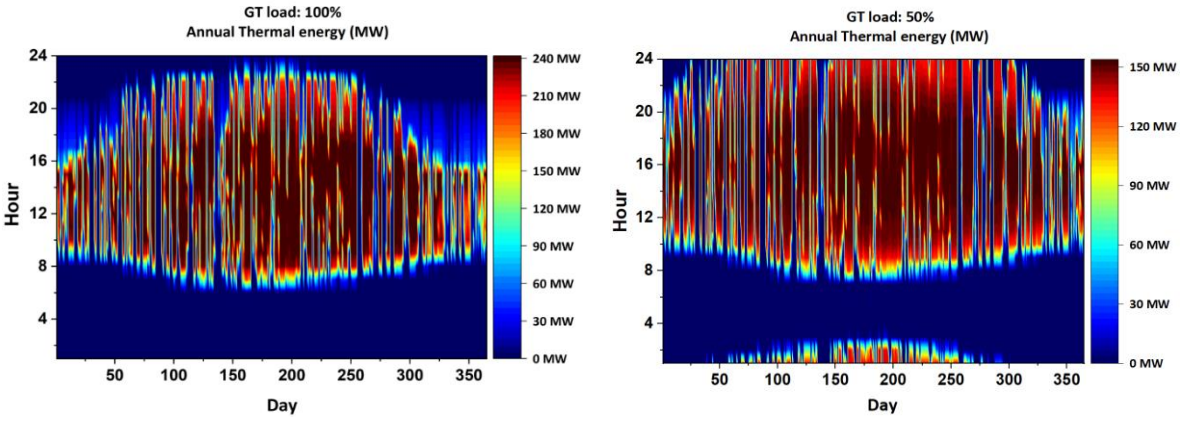

Fig. 6-12. Heat map of annual thermal energy delivered by the solar PTC field at full load and 50% load of gas turbine

Furthermore, due to the intermittent nature of the solar PTC field and the design criteria of the PTC field (solar multiple: 2 and design point DNI: 950 W/m^2), during some hours throughout the year, a portion of the solar collector is defocused even at the full load operation, as depicted in Fig. 6-13. During the 50% load of gas turbine, the fraction of unfocused solar collector increases since the reboiler steam requirement is reduced, and the thermal energy storage capacity is at its maximum value. Accordingly, the surplus generated solar energy needs to be utilized in other processes, such as in the HRSG system for heat recovery. Otherwise, some portion of the solar collector needs to be defocused.

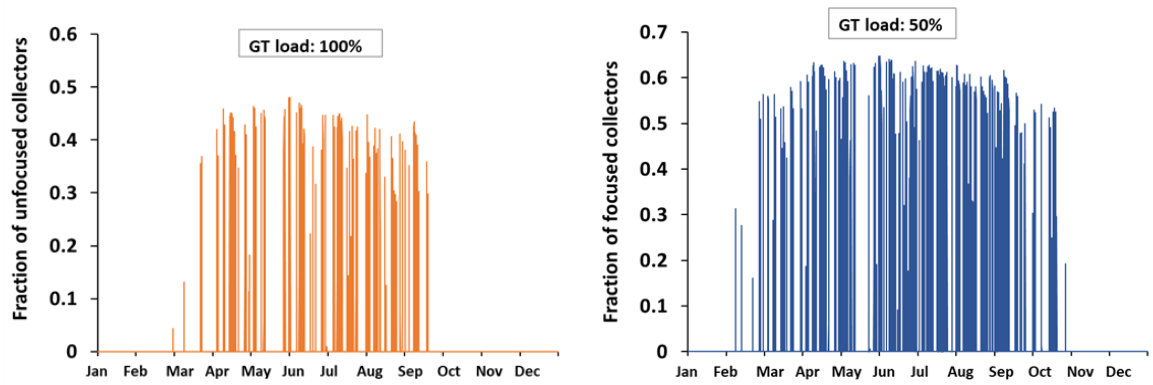

Fig. 6-13. Unfocused fraction of solar collector throughout the year at full load and partial load of NGCC plant

To analyze the detail of PTC field operation at full load and partial load, the performance of the system on two reference days representing winter and summer seasons (January 20th and July 20th) is analyzed using the weather and solar information for the target location. The hourly cosine product of direct normal irradiance (DNI), as well as the power incident for both reference days, is presented in Fig. 6-14, which shows how the fluctuations in solar radiation require ongoing adjustment of the heat transfer fluid (HTF) from the receivers and energy storage to ensure a consistent HTF outlet temperature and energy supply.

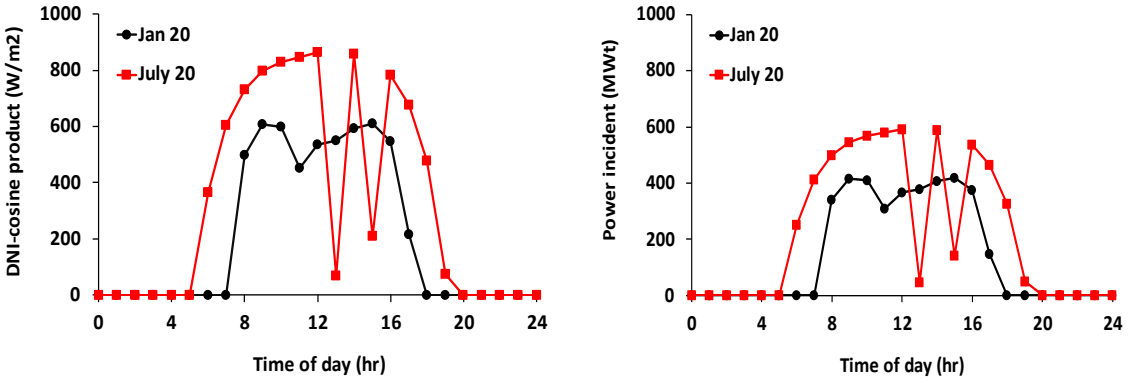

Fig. 6-14. Fluctuation of DNI-cosine product and power incident in the two reference days

Fig. 6-15 demonstrates the performance of the PTC field (generated thermal heat for the HTF heat exchanger) in the two reference days for full load and 50% load operation of the NGCC plant. As it can be seen, the PTC solar field, with the aid of thermal energy storage, shows a stable delivery of thermal energy to the PCC plant in both loads, specifically on July 20^{th,} due to the higher availability of solar irradiance compared to Jan 20th. Furthermore, the results prove the flexible operation of the system to respond to the variability of solar irradiance and the capability of thermal energy storage to supply thermal energy even after sunshine hours stably.

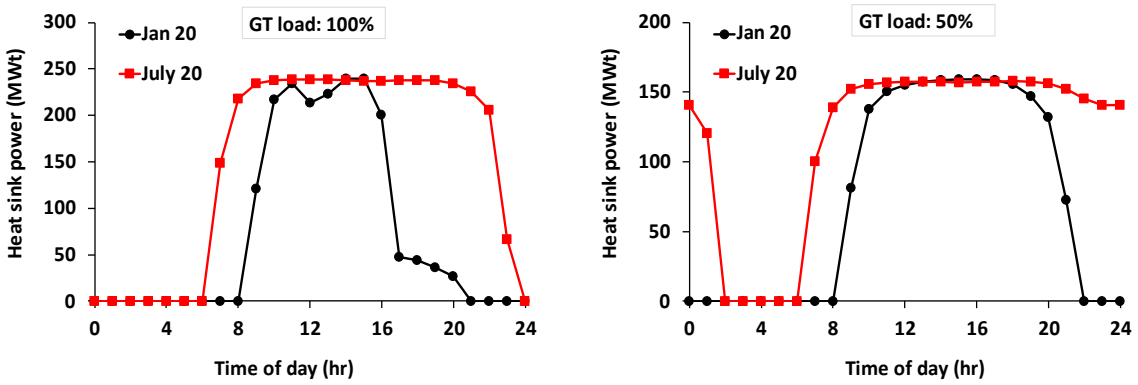

Fig. 6-15. Thermal power generation in the PTC field for two reference days

Notably, in the case of 50% gas turbine load, the PTC filed performance is more uniform and stable so that on July 20^{th,} a significant amount of solar energy provision continues even throughout the night. Also, a stable supply of thermal energy from the PTC field on Jan 20th.is

achieved with the aid of thermal energy storage that stores more energy during the part-load operation of the gas turbine.

The performance of thermal energy storage (TES) in the considered scenarios is presented in Fig. 6-16. The Thermal energy storage with a full capacity of 960 MWh is completely charged on July 20^{th,} specifically for the 50% load operation. The charging of TES starts at 8 am on Jan 20^{th,} while the charging starts at 6 am on July 20th with a faster rate of charging. Also, the TES experience full capacity in the case of 50% GT load on July 20^{th,} while the maximum charging state on Jan 20th is not more than 55% of its full load capacity. Additionally, the TES is charged slightly during the full load operation on Jan 20th due to the low DNI on this day.

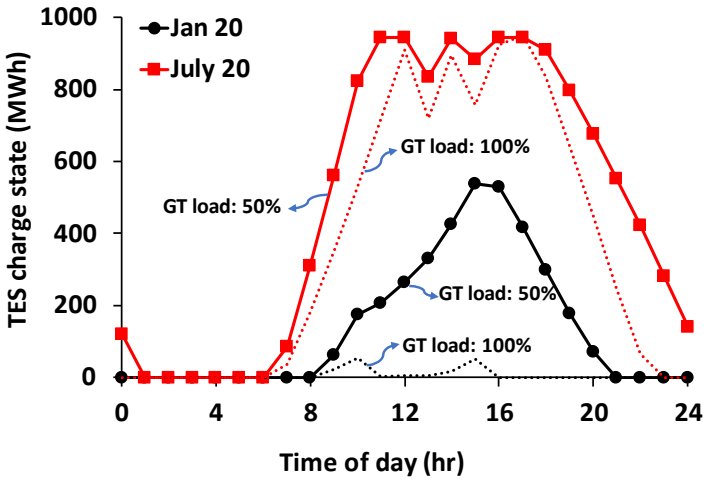

Fig. 6-16. Performance of thermal energy storage during full load and 50% load of gas turbine

Overall, the performance of the PTC solar field is intermittent and depends on the location and time. However, integrating solar energy with thermal energy storage that could offset the intermittent nature of solar irradiance is a potential option for integrating with a PCC reboiler. Integrating a 4-hour thermal energy storage system has significantly improved the system's flexibility in response to the variability of solar irradiance. This enhancement allows for the supply of thermal energy even after the end of sunshine hours. However, during the winter months, there is a negligible surplus of solar energy available for charging thermal energy storage. Nevertheless, the presence of the 4-hour thermal energy storage system contributes to a more flexible operation of the integrated system by reducing the ramp-up and ramp-down periods of the steam turbine and ensuring a more stable delivery of steam to the reboiler of the capture plant.

6.6.2 Economic analysis of the integrated system

The technical information obtained in the design and performance analysis, along with process design inputs of the integrated system, is considered as the input for the economic model to gain a better understanding of the feasibility and potential economic advantages of the EGR+SEGR and SEGR cases, which demonstrated a low energy requirement and acceptable part load performance. Two key economic indicators, LCOE ($/MWh) and COA ($/tCO_2 avoided), are used to evaluate the economic benefits of process modification. These parameters, along with the capital and operating costs, are calculated and compared with those of the conventional process to assess the economic viability and potential benefits of the proposed designs.

The details of capital and O&M cost estimation for the proposed designs and comparison of the results with the baseline case as well as with the NGCC plant without CO_2 capture are provided in Table 6-10. In this table, the EGR+SEGR and SEGR case results are associated with applying the 2nd generation of Polaris membrane with CO_2 permeance of 2200 GPU.

Table 6-10. Capital and operating cost estimation for all considered cases

Cost parameter (M$)	NGCC W/O CCS	Baseline case	EGR+SEGR	SEGR
Feedwater & misc. Bop systems	72.3	77.5	81.6	83.7
Combustion turbine/accessories	186.1	186.1	196.6	196.6
HRSG, ducting & stack	79.2	77.0	82.5	87.4
Steam turbine generator	105.2	92.9	96.6	102.7
Cooling water system	27.5	36.4	46.2	47.2
Accessory electric plant	66.1	86.8	89.7	94.0
Instrumentation & control	23.5	27.0	27.3	27.4
Improvements to site	16.4	16.7	16.8	17.1
Buildings & structures	18.9	18.2	19.0	19.7
CO_2 compression & Drying	0	51.2	50.8	52.0
Amine-based CCS	0	394.8	247.5	203.0
Membrane-based SEGR & EGR	0	0	95.3	253.0
Solar PTC field & TES	0	0	194.8	194.8
Total TPC	595.2	1064.6	1244.6	1378.7
TOC	818.5	1291.8	1511.3	1672.7
FOM	21.7	31.6	31.6	34.7
VOM	8.9	17.9	26.9	50.6
Fuel cost	146.0	146.0	149.5	157

As can be seen from Table 6-10, the capital cost of the amine-based capture plant considerably decreases by 37% and 48% in EGR+SEGR and SEGR cases, respectively. The overall economic performance, including capital and operating expenditure (CAPEX and OPEX) of the EGR+SEGR case, is superior compared to the SEGR case, although it required higher CAPEX and OPEX compared to the baseline case without solar integration. The SEGR case required the highest capital cost mainly due to the high membrane module costs and incorporation of solar PTC field. However, it should be considered that the total electricity generated by the SEGR case is the highest among other CCS-equipped cases. Accordingly, the solar-assisted SEGR case requires a 30% higher capital cost while the rise in the generated electricity is almost 13.4%. On the other hand, the proposed EGR+SEGR case requires 17% more capital cost compared to the baseline case. In comparison, electricity generation is increased by 7.8%, and more flexible operation due to the integration of the solar PTC field has been provided.

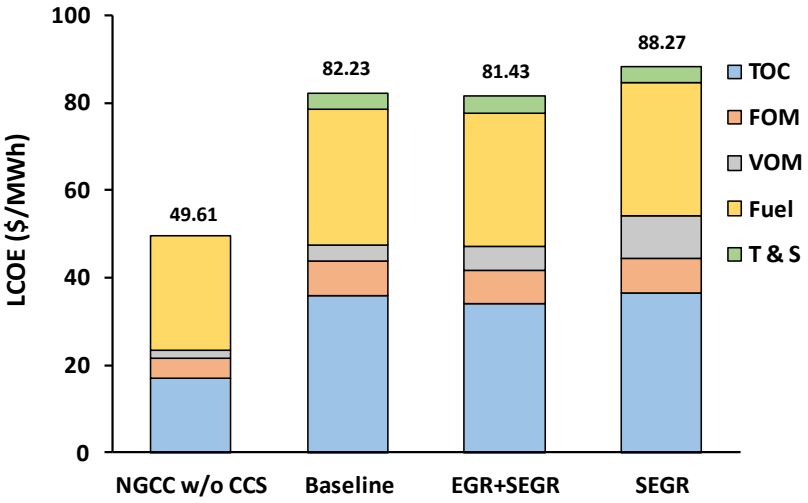

Fig. 6-17. LCOE and breakdown values for all considered cases

In order to facilitate a comprehensive comparison of the economic results across all cases, Fig. 6-17 displays the levelized cost of electricity for each considered scenario without integration of the PTC solar field. Additionally, the figure highlights the contribution of each cost parameter to determining the overall cost. The considerable increase of LCOE in the CCS integrated cases is obvious compared to the NGCC plant without CCS, which is mainly due to the high capital cost requirement of the CCS plant. Also, the cost of transport and storage (T&S) has a noticeable impact

on the LCOE, which has been assumed to be $10 per tonne of captured CO_2 for the geologic storage of CO_2. In the case of utilizing the produced CO_2 as a feedstock in other processes, this cost could be negligible and lower LCOE in the CCS-integrated cases could be achieved.

The LCOE results prove that the EGR+SEGR case represents the case with the lowest LCOE, 81.43 $/MWh, among the CCS-equipped scenarios. On the other hand, LCOE in the SEGR case is equal to 88.27 $/MWh, which is 8.4% higher than the EGR+SEGR case. Moreover, by decarbonization of the NGCC plant, the LCOE is increased by at least 64%. Furthermore, it is worth noting that the fuel cost and capital cost of the integrated system play a significant role in determining the overall cost of electricity generation.

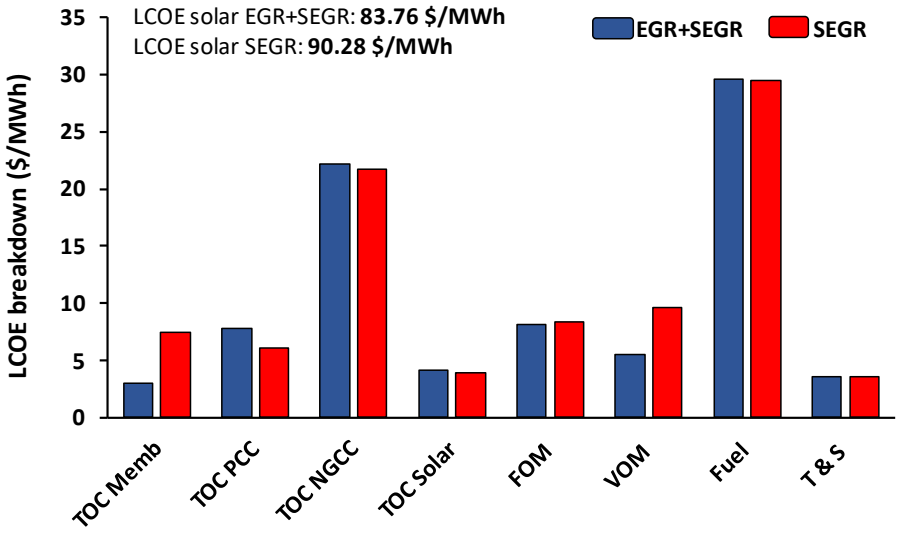

Fig. 6-18. Detail of LCOE values for the EGR+SEGR and SEGR cases by solar filed integration

The comparison of the LCOE breakdown for the case of PTC solar filed integration for the EGGR+SEGR and SEGR case is presented in Fig. 6-18. By the integration of the solar PTC field, the LCOE increases by 2.33 and 2.01 $/MWh for the EGR+SEGR and SEGR cases, respectively. Also, in the case of SEGR, the contribution of variable operating cost is more significant compared

to other cases, which is mainly due to the high required membrane area and the replacement cost associated with the membrane modules.

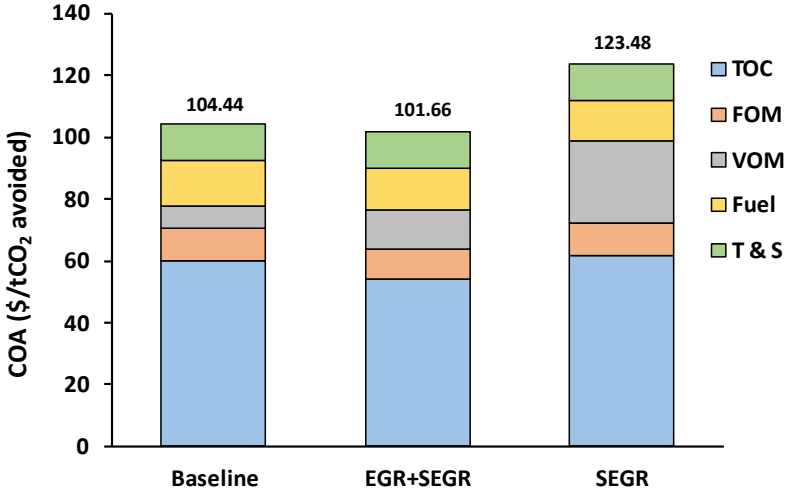

Fig. 6-19. COA and breakdown values for CCS integrated cases

Also, the cost of CO_2 avoided for the CCS-equipped cases is presented in Fig. 6-19. As can be seen, the case of EGR+SEGR has the lowest COA value, equal to 101.66 $ per tonne of avoided CO_2, while the SEGR case represents the highest COA value among the evaluated cases. The economic assessment results proved that the Cost of CO_2 captured (COC), which represents the production cost of CO_2 as it doesn't include the transport and storage cost of CO_2 in the LCOE calculation, for the EGR+SEGR case, is 76.3 $ per tonne of captured CO_2, while this value is 77.03 $ per tonne of captured CO_2. It is significant to highlight that the cost associated with CO_2 transport and storage contributes approximately 12 $/t$CO_2$. This cost is specifically related to the storage of CO_2 in a saline reservoir or its utilization in enhanced oil recovery (EOR) processes.

Sensitivity analysis of the economic indicators

As mentioned in the previous section, fuel cost is one of the major contributors to LCOE and COA values in all cases. The natural gas price is not fixed and varies based on supply/demand and other economic factors. Accordingly, the effect of fuel price on the LCOE and COA values of the proposed designs is presented in Fig. 6-20. As can be seen, by the reduction of fuel price, the LCOE and COA values of both cases could decrease significantly, although the rate of reduction

in LCOE and COA below 4 $/MMBTU decreases compared to the higher price. This is mainly due to the major contribution of fuel cost in the LCOE and COA at high fuel prices.

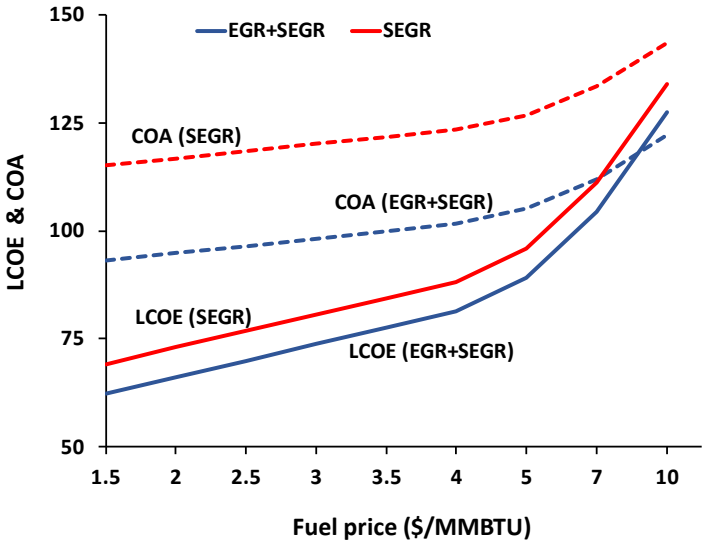

Fig. 6-20. Effect of variation in fuel price on the LCOE and COA value of the proposed designs

The development of membrane materials with better performance for CO_2 separation technologies is an active area of research, specifically at low-pressure conditions applications such as SEGR. Extensive efforts are being made in the field, including advancements in materials, design, and manufacturing processes to enhance membrane permeability and durability and reduce the manufacturing costs associated with these systems. As a result, there are inherent uncertainties in estimating the costs of membrane modules, and the current estimates of membrane cost are based on available literature and assumptions.

The influence of uncertainties in the membrane cost and membrane CO_2 permeability on the LCOE and COA are presented in Fig. 6-21. As seen, the SEGR case has more potential to become the optimal process by considerably improving CO_2 permeability and manufacturing cost. For instance, in the case of membrane cost to be 10 $/m^2 and CO_2 permeance becoming higher than 3500 GPU (similar to 3rd generation of Polaris membrane, which is under development), the LCOE of SEGR becomes lower than EGR+SEGR case with similar improvements. Moreover,

even with the 50 $/m^2 membrane module cost, with significant improvements in CO_2 permeance (above 8000 GPU), the SEGR case becomes the most optimal case in terms of LCOE and COA.

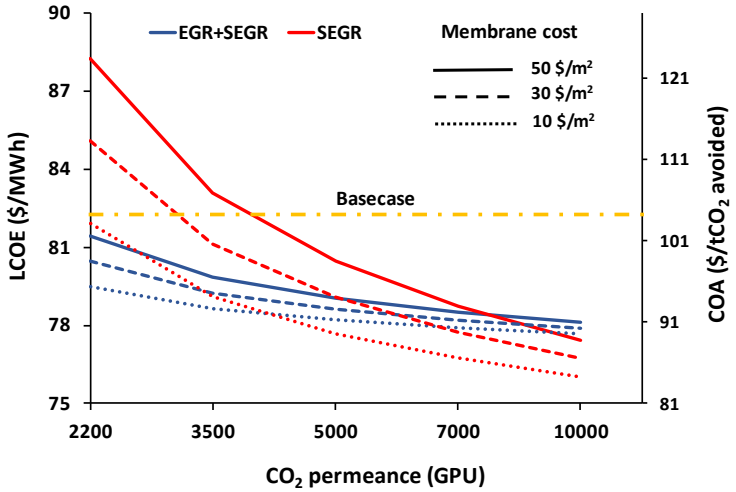

Fig. 6-21. Influence of membrane cost and CO_2 permeance on the LCOE and COA

Considering the research progress and technological advancements in membrane gas separation processes, it is expected that the costs associated with membrane modules will decrease and their CO_2 permeance will improve in the near future. Therefore, ongoing research and development efforts in membrane technology play a crucial role in realizing the full potential of solar-assisted hybrid membrane CCS and achieving cost reductions that will make these systems more economically attractive and commercially viable.

Finally, the impact of PTC field location on the generated power as well as LCOE and COA of the EGR+SEGR cases, is presented in Fig. 22 considering four cities in the US with different climate data: Oklahoma City, OK (DNI: 5.73 kWh/m^2/day); Tucson (DNI: 7.46 kWh/m^2/day), AZ; Houston (DNI: 4.89 kWh/m^2/day), TX; and Barstow (DNI: 7.86 kWh/m^2/day), CA. The PTC solar filed design is similar in all cities, and the information regarding climate data of the typical metrological year (TMY) for the considered locations is extracted from the NREL database.

According to Fig. 6-22, Tuscan and Barstow cities are more appropriate cities for PTC solar filed integration with the NGCC plant due to the high DNI and efficiency of the solar system at these locations. The results showed that the LCOE of the EGR+SEGR case in Barstow, the highest annual average DNI in the considered cities, could be as low as 82.93 $/MWh, which is

less than 1 $/MWh compared to the LCOE in Houston. This difference is more noticeable in the cost of CO_2 avoided, as the COA in Houston is higher by 3.32 $/tonne$CO_2$ compared to the COA in Barstow. Furthermore, the results showed that for the EGR+EGR case located in Barstow, the increase in generated electricity power could be as high as 9.11% compared to the baseline case (conventional amine-based CCS without solar integration), while this value in Houston is 7.48%. In summary, it can be inferred that while the specific location of the EGR+SEGR case may influence the economic performance of the system, this influence is relatively small, resulting in a 1.25% change in the LCOE. However, this small change should not overshadow the significant economic and technical benefits associated with the EGR+SEGR design.

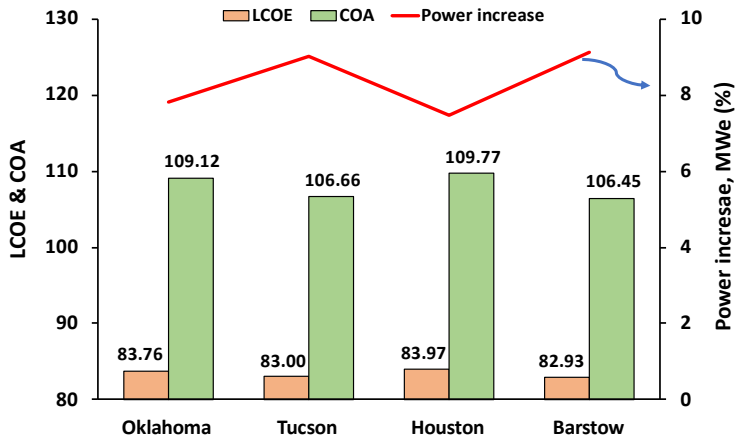

Fig. 6-22. LCOE, COA and power generation increase in four considered cities in US

Overall, by decarbonizing the NGCC power plant, both the LCOE and COA of the plant considerably increase due to the cost-intensive nature of the capture plant. The proposed design, the solar-assisted hybrid EGR+SEGR case, represents an improved techno-economic performance compared to the conventional system. Importantly, both the EGR+SEGR and SEGR cases have the potential to achieve even greater cost reduction and energy savings in the future since recent research works on the advanced membrane indicate promising results, suggesting a significant improvement in CO_2 permeance and manufacturing cost. The anticipated improvement not only enhances the economic viability of EGR+SEGR and SEGR designs but also makes them more competitive in comparison to other CO_2 capture technologies for widespread implementation.

6.7 Chapter Summary

This chapter delves into two main research questions, RQ6 and RQ7, to comprehensively assess the impacts of deploying the proposed hybrid design on various aspects of the system. The objective of the study is to thoroughly investigate the part load performance and economic feasibility of integrating the solar-assisted hybrid carbon capture system with a natural gas combined cycle power plant. The obtained new knowledge provides valuable insights into the performance and economic viability of the proposed hybrid design when applied to real-world conditions, particularly during off-design and partial load operations.

The proposed system integrates a multi-stage CO_2 selective membrane module with exhaust gas recirculation (EGR) to increase the CO_2 concentration in the flue gas. It also incorporates a solar parabolic trough collector (PTC) field with thermal energy storage to provide the necessary thermal energy for CO_2 capture. A process modeling and simulation framework, utilizing software such as Aspen Plus, Aspen Custom Modeler, Thermoflex, and SAM, was used to analyze the system's performance in off-design conditions where the gas turbine load decreases from 100% to 50%. Furthermore, an economic model is developed to calculate the levelized cost of electricity and CO_2 avoided cost. The economic performance of the system is evaluated, and a detailed comparison with other cases, as well as sensitivity analysis of parameters on the economic indicators, are provided.

The part load operation of the proposed system revealed that both EGR+SEGR and SEGR cases show acceptable performance, while the EGR+SEGR part load operation is slightly superior to the SEGR case. Furthermore, the results demonstrate that all cases show considerably better performance at full load conditions, and efficiency degradation should be expected during partial loads. The NGCC gross efficiency drops by 5.45% and 4.84% for the EGR+SEGR and baseline cases, respectively. During partial loads from 100% to 50%, the CO_2 concentration in the flue gas experiences a slight decrease from 10.87 mole% to 10.23 mole% in the EGR+SEGR case. Also, the exhaust gas flowrate at 50% of the load is approximately 64% of the flue gas flowrate at the full load operation. The part load performance of all considered PCC plants showed that the specific reboiler duty increases at partial loads, and the PCC plant deviates from its optimal operation at full load conditions. The part load performance of membrane-based SEGR proved its flexible operation as some membrane modules could be bypassed during partial loads. The fraction

of the operating membrane module is calculated to be 64% during 50% load of the gas turbine for the EGR+SEGR case. Moreover, the PTC solar filed provided efficient performance during partial loads. The surplus thermal energy during partial loads is effectively stored in the thermal energy storage system, leading to significant improvement in the system's flexibility in response to the variability of solar irradiance.

The economic analysis of the integrated system indicates a significant reduction of 37% and 48% in the capital cost of the amine-based capture plant in the EGR+SEGR and SEGR cases, respectively. The EGR+SEGR case demonstrates superior overall economic performance, considering both capital and operating expenditures, compared to the SEGR case, although the EGR+SEGR case requires higher capital and operating cost compared to the baseline case. Importantly, the LCOE results revealed that the EGR+SEGR case represents the case with the lowest LCOE and COA, 81.43 $/MWh and 101.66 $/tonne$CO_2$, among the CCS-equipped designs, which highlight the advantages of this design over baseline and SEGR case. The sensitivity analysis proved that the proposed hybrid systems have great potential for even greater cost reduction and energy savings in the future since the recent research on the advanced membrane has shown promising results, indicating a significant improvement in both CO_2 permeance and manufacturing cost. These advancements further enhance the economic feasibility and attractiveness of the proposed hybrid systems, making them increasingly favorable for widespread implementation. Also, energy and climate policies are vital drivers by incentivizing innovation and creating market opportunities for CCS technologies to establish themselves.

Chapter 7. Conclusion and Future Works

7.1 Conclusion

The advent of renewable sources has changed the traditional expectation of carbon capture technologies. In the near future, fossil fuel power plants will need to work in an integrated and fully connected grid that involves new and advanced components such as renewable sources and energy storage. In such a complex energy system, a carbon capture system needs to satisfy other requirements to be effectively integrated with other components. There are significant challenges in the field of CO_2 capture technologies to make them technically and commercially viable and appropriate for the large-scale decarbonization of fossil-fueled power plants. As the operational parameters of fossil fuel power plants change due to intermittent renewable sources, the energy requirement, operational expenses, and flexible operation of carbon capture technologies are important criteria that need to be evaluated and optimized in order to make CCS technologies a viable option for decarbonization. The main problem that the dissertation is dealing with is addressing these challenges associated with the design, operation, and integration of CCS technologies with fossil-fueled power plants. Accordingly, after a critical evaluation of the literature performed in Chapter 2, several research questions based on the identified gaps in the field of CO_2 capture technologies have been proposed that addressing them makes significant contributions and generates new knowledge. Table 7-1 presents the summary of new knowledge documented in each chapter of this dissertation. In the following paragraphs, the research questions and the primary findings derived from the approaches employed to address these questions are summarized.

Table 7-1. Summary of new knowledge documented in each chapter

Chapter 2	Overview of recent progresses, developments, and challenges in CO_2 capture technologies
Chapter 3	The technical performance and cost of membrane technologies in various designs scenarios and operation conditions imposed by upstream power plants

Chapter 4	Optimal multi-stage membrane-based CCS process and possible trade-offs for energy and cost penalty - Flexible operation and transient behavior of membrane process for integration with power plant under load following operation
Chapter 5	Efficient and robust design of a CCS process by hybridization of membrane-amine process and solar heating field for flexible and sustainable decarbonization of NGCC power plant
Chapter 6	Insight into part load performance and economic viability of the natural gas combined cycle power plant integrated with the proposed design

The first research question (RQ1) deals with the current status and progress of CO_2 capture technologies for integrating with fossil-fueled power plants and has been discussed and addressed in Chapter 2 by performing a critical literature review. The conclusion drawn from this investigation is that although there have been significant advancements in this field, there are still persistent challenges in achieving sustainable design and flexible operation, and seamless integration of carbon capture systems with fossil-fueled power plants. These challenges primarily revolve around reducing costs, minimizing energy penalties, and enhancing the flexible operation of solar-integrated systems.

Chapter 3 focuses on addressing the second research question (RQ2), which pertains to the design and operation of membrane-based carbon capture and storage (CCS) systems when integrated with fossil-fueled power plants. The approach to address this question is based on performing component and system-level simulations and techno-economic investigation of the membrane-based CCS. Various designs and operating parameters of the membrane-based CCS are investigated for improving the techno-economic performance and flexibility of the system as a potential option for integrating into the future low-carbon energy system. To this end, four designs of the double-stage membrane process and three polymeric membranes with various transport properties were considered, and the influence of the feed pressure, feed CO_2 concentration, retentate recycling, sweep gas, and membrane properties on their techno-economic performance have been investigated with the separation target of 90% of CO_2 recovery and 95 mol% CO_2 purity. The results revealed that by increasing the feed pressure, the required membrane area significantly decreases, although the specific energy increases due to the additional power required by compressors. Also, using a membrane with higher CO_2/N_2 selectivity, such as PVAm/PG

membrane, leads to lower specific energy. Also, analyzing the effect of retentate recycling showed that at full retentate recycling, although higher CO_2 purity of the permeate gas can be achieved, the system energy consumption and required membrane area increase compared with the case of zero retentate recycling. Furthermore, considering a portion of the retentate stream as a sweep gas remarkably reduces the required membrane area, although the system specific energy increases. Moreover, the increase of the CO_2 level in the flue gas improves the performance and economy of the membrane-based CCS. The other notable result is that improving the selectivity of membranes does not always offer a cost-saving process. On the other hand, a higher value of selectivity decreases the specific energy of the system, which is of great importance for the flexible operation of the membrane-based CCS. The economic comparison of different designs proved that considering the feed compression approach by counter-current membrane module and sweep gas is the most cost-effective design (22.76\$/tCO_2) since it has the lowest capital cost and CO_2 capture cost. On the other hand, the vacuum system with a counter-flow module design is the most energy-efficient option, which decreases the energy penalty of the power plant and may lead to the flexible operation of the system. The techno-economic analysis results demonstrated that among the various designs of membrane-based CCS, selecting a counter-flow membrane module equipped with a membrane with moderate selectivity and high permeability is the optimal design for reducing CO_2 capture cost and energy consumption and improving the system flexibility. Also, second-stage retentate recirculation, moderate sweep gas flowrate, the high CO_2 concentration of feed, and moderate pressure ratio are other operating considerations that can improve system flexibility.

Chapter 4 deals with the third and fourth research questions (RQ3 and RQ4), which are related to the optimal design and operation of membrane-based CCS as well as the flexible operation of the membrane modules toward various changes in the flue gas conditions. The research objective of this chapter is to develop an economically viable design of multi-stage membrane-based CCS with a flexible operation for integration with a power plant under load-following operation.

To address RQ3, the design and operation of membrane-based CCS are optimized, given that their energy consumption and economics are crucial to their large-scale deployment. To this end, a numerical model based on the solution-diffusion mechanism for a multicomponent gas separation process with a hollow fiber membrane module is developed using Aspen Custom

Modeler. The model was imported into Aspen Plus to examine the effects of feed pressure, CO_2 concentration, retentate recycling, and membrane properties on separation efficiency, power consumption, and economic performance of a double-stage membrane process. Following that, Aspen Plus and MATLAB are linked to determine the optimal operating and design conditions of the process using the MLMOPSO technique. With increasing CO_2 concentration in the feed gas, CO_2 removal improves, and CO_2 capture costs decrease significantly, although the process energy requirement increases slightly. Analyzing the best possible trade-offs between objective functions confirms that there is significant potential to improve the sustainability of the process. The CO_2 capture cost and energy penalty of the process could be as low as 13.1 $/tonne CO_2 and 10% at optimal design and operating conditions. The result of this research is beneficial for decision-makers to optimize and improve the sustainable performance of the system with the aim of facilitating the commercial implementation of membrane-based CCS.

Furthermore, in Chapter 4, to address RQ4 regarding the flexible operation of membrane-based CCS, the transient behavior of the system is discussed by applying step changes in the membrane module pressure, feed flow rate, feed CO_2 concentration, and recycling percentage. The results show that the response of the membrane module to a step-change in pressure is relatively fast; the membrane module requires 11 s to reach a steady-state, while the system response to a step-change in feed composition is slower and goes to a steady state after 20 s. The permeate and retentate concentration present a fast response to step-change in the feed pressure, and the system reaches to steady state in less than 13 s. Also, the results show that the higher selectivity and permeability of the membrane, the larger the length of overshooting and undershooting in the transient response of the membrane module. Furthermore, the fast dynamic behavior of the membrane system by step change at feed flowrate makes this system a good option for future flexible carbon capture systems, in which the membrane system needs to operate in partial load conditions typically.

In Chapter 5, the fifth research question (RQ5) regarding novel designs and integration of CCS plant with power plant is addressed by developing a novel solar-assisted hybrid membrane-amine carbon capture system for flexible and sustainable decarbonization of natural gas-fired combined cycle power plant. In the proposed hybrid design, a multi-stage CO_2 selective membrane module with the aid of exhaust gas recirculation (EGR) is used to selectively recirculate CO_2 to the turbine inlet air and increase the CO_2 concentration of flue gas. Furthermore, the solar PTC

field with 4-hour thermal energy storage is integrated with the MEA-based CCS reboiler to provide the required thermal energy for capturing 90% of generated CO_2. In this design, the CO_2 concentration of the NGCC plant flue gas increases from 3.9 mole% in the conventional design to 10.87 mole% in the EGR+SEGR case, while the SEGR case demonstrates 18.08 CO_2 mole% in the flue gas. Due to the change in the inlet air properties and integration of the solar PTC field, the output power of the system in SEGR and EGR+SEGR cases could be increased by 19.4% and 13.8% in comparison to the baseline case. Furthermore, due to the higher driving force in the PCC plant, resulting from high CO_2 concentration, along with lower flue gas flowrate entering MEA-based PCC in the proposed designs, the specific reboiler duty and required packing material volume in the absorber and stripper considerably improves. Also, the power plant carbon intensity in the proposed solar-assisted hybrid design could be reduced by 10.3% based on the solar irradiance data in Oklahoma City, US. The comparative analysis results prove that for a fixed gas turbine design (GE 7FA.05), the SEGR case is able to generate more power compared to the EGR+SEGR case (approximately 5%), and the reboiler duty and columns size of the PCC plant is slightly smaller in the SEGR case compared the EGR+SEGR case. However, the EGR+SEGR case offers an optimal solution as it requires a significantly smaller membrane area compared to the SEGR case (reduced by approximately 71%). Sensitivity analysis of the membrane-based SEGR system showed that improving membrane CO_2 permeation is an important factor affecting the required membrane area and cost of the system. In this chapter, a cutting-edge hybrid carbon capture system is developed that utilizes solar energy to optimize the decarbonization process in NGCCs. The innovative design and flexibility of this system hold promising potential for reducing greenhouse gas emissions and improving the overall sustainability of the energy sector.

The sixth and seventh research questions (RQ6 and RQ7) are addressed in Chapter 6, which involve addressing associated challenges in the commercial-scale deployment of the proposed hybrid design. The approach considered to deal with these questions is based on the investigation of part load performance and economic viability of the natural gas combined cycle power plant integrated with a solar-assisted hybrid carbon capture system. A process modeling and simulation framework, utilizing software such as Aspen Plus, Aspen Custom Modeler, Thermoflex, and SAM, was used to analyze the performance of the system in off-design conditions where the gas turbine load decreases from 100% to 50%. The part load operation of the proposed system revealed that both EGR+SEGR and SEGR cases demonstrate acceptable performance, while the EGR+SEGR

part load operation is slightly superior to the SEGR case. Furthermore, the results reveal that all cases perform considerably better at full load conditions, and efficiency degradation should be expected during partial loads. The NGCC gross efficiency drops by 5.45% and 4.84% for the EGR+SEGR and baseline cases, respectively. During partial loads from 100% to 50%, the CO_2 concentration in the flue gas experiences a slight decrease from 10.87 mole% to 10.23 mole% in the EGR+SEGR case. Also, the exhaust gas flowrate at 50% of the load is approximately 64% of the flue gas flowrate at the full load operation. The part load performance of all considered PCC plants showed that the specific reboiler duty increases at partial loads, and the PCC plant deviates from its optimal operation at full load conditions. The results obtained from the part load performance of the proposed design prove the flexible operation of the design, as some membrane modules could be bypassed during partial loads. The fraction of the operating membrane modules is calculated to be 64% during 50% load of the gas turbine for the EGR+SEGR case. Moreover, the PTC solar filed provided efficient performance during partial loads. The surplus thermal energy during partial loads is effectively stored in the thermal energy storage system, leading to significant improvement in the system's flexibility in response to the variability of solar irradiance. The economic analysis of the integrated system indicates a significant reduction of 37% and 48% in the capital cost of the amine-based capture plant in the EGR+SEGR and SEGR cases, respectively. The EGR+SEGR case demonstrates superior overall economic performance, considering both capital and operating expenditures, compared to the SEGR case, although the EGR+SEGR case requires higher capital and operating cost compared to the baseline case. Importantly, the LCOE results revealed that the EGR+SEGR case represents the case with the lowest LCOE and COA, 81.43 \$/MWh and 101.66 \$/tonneCO_2, among the CCS-equipped designs, which highlight the advantages of this design over baseline and SEGR case. The sensitivity analysis proved that the proposed hybrid systems have great potential for even greater cost reduction and energy savings in the future since the recent research on the advanced membrane has shown promising results, indicating a significant improvement in both CO_2 permeance and manufacturing cost. These advancements further enhance the economic feasibility and attractiveness of the proposed hybrid systems, making them increasingly favorable for widespread implementation. Also, energy and climate policies play a vital role as drivers by incentivizing innovation and creating market opportunities for CCS technologies to establish themselves.

Journal and conference publications

1. J. Asadi, P. Kazempoor, " Advancing Power Plant Decarbonization with a Flexible Hybrid Carbon Capture System" Under Review
2. J. Asadi, P. Kazempoor, " Dynamic Performance and Economics of Solar-Assisted Hybrid Carbon Capture for Natural Gas Combined Cycle Power Plant" Under Review
3. J. Asadi, P. Kazempoor, " Dynamic response and flexibility analyses of a membrane-based CO_2 separation module" Journal: International Journal of Greenhouse Gas Control, 2022
4. J. Asadi, P. Kazempoor, "Sustainability Enhancement of Fossil-Fueled Power Plants by Optimal Design and Operation of Membrane-Based CO_2 Capture Process", Atmosphere, 2022
5. J. Asadi, P. Kazempoor, " Techno-economic Analysis of Membrane-based Processes for Flexible CO2 Capturing from Power Plant" Journal: Energy Conversion and Management, 2021
6. L. Jolaoso, J. Asadi, P. Kazmepoor, " A novel green hydrogen production using water-energy nexus framework", Energy Conversion and Management, 2023
7. P. Kazempoor, J. Asadi, R.J. Braun, "Validation Challenges in Solid Oxide Electrolysis Cell Modeling Fueled by Low Steam/CO_2 Ratio", International Journal of Hydrogen Energy, 2022
8. J. Asadi, L. Jolaoso, P. Kazempoor, "Efficiency and Flexibility Improvement of Amine-Based Post Combustion CO2 Capturing System in Full and Partial Load Conditions", ASME ES 2022 Conference
9. J. Asadi, P. Kazempoor, "Sustainability Improvement of Membrane Separation Process for Post-Combustion CO2 Capturing Using Multi-Objective Optimization", ASME ES 2022 Conference
10. J. Asadi, E. Yazdani, Y. Hosseinzadeh, P. Kazempoor, " Technical evaluation and optimization of a flare gas recovery system for improving energy efficiency and reducing emissions", Journal: Energy Conversion and Management, 2021
11. E. Yazdani, J. Asadi, Y. Hosseinzadeh, P. Kazempoor, " Flare gas recovery by liquid ring compressors-system design and simulation " Journal: Journal of Natural Gas Science and Engineering, 2021

7.2 Limitations and Recommendations for Future works

Here, the imitations of the current works and some recommendations for future research in the field of optimal and flexible CO_2 capture systems and integration with fossil-fueled power plants are presented. By addressing these detailed recommendations, further research can enhance our understanding of the integrated solar-NGCC-CO_2 capture plant, design and flexible operation of CCS, process optimization, economic viability, and environmental impact of the integrated systems. This will contribute to the development of more sustainable and efficient energy systems

that integrate renewable energy sources, carbon capture technologies, and conventional power generation. The future works are categorized as follows based on their contribution to different areas of membrane-based and hybrid CCS technologies.

Membrane materials and module

- This research utilized the mathematical modeling approach to prove the influence of membrane properties on the energy and cost penalties of the CO_2 capture process and determined the optimal permeability and selectivity of the membrane (Chapters 3 and 4) without conducting experimental investigations. These results can be considered as an objective in the experimental research to develop new membrane materials with optimum selectivity and permeability, which can lead to a cost-effective and flexible membrane-based CCS. In order to enhance the performance of membrane-based CO_2 capture processes, the synthesis of CO_2-philic membranes with improved flux (the rate at which gases permeate through the membrane) and selectivity (the ability to capture CO_2 selectively over other gases) is a crucial step. Besides polymeric membranes that are currently commercialized, the potential membranes in the future CO_2 capture system could be facilitated transport membranes and mixed matrix membranes.
- Research plans should primarily concentrate on identifying new materials that are also both ecologically friendly and economically viable. These membranes can be specifically designed to have a high affinity for CO_2, allowing for efficient separation and capture. To evaluate the effectiveness of these candidate membranes, they should be tested in a permeation setup, which simulates real-world conditions and measures the permeation rate and selectivity of the membranes when exposed to a gas stream. In this case, it would be beneficial to use real syngas, which typically contains impurities and various gas components found in the gas stream of interest.

Membrane-based CO_2 capture process design and flexible operation

The results of Chapters 3 and 4 proved the potential and possible designs and improvements for improving the performance and flexible operation of the membrane-based CCS process. Future studies can investigate the following points in the membrane CO_2 capture system:

- The modeling of the membrane process has been performed based on the following widely-used assumptions:

- Identical and uniform membrane fiber.
- Negligible variation of concentration and pressure in the radial axis.
- The gas mixtures are assumed to be ideal gas.
- The pressure drop is calculated by the Hagen-Poiseuille equation.
- The effect of concentration polarization is neglected.

To create a more detailed model of the membrane process, it is beneficial to avoid these assumptions. Specifically, this involves taking into account the mass transfer resistance in the radial axis and also considering the effects of concentration polarization on the membrane's performance. By incorporating these factors, the model can better capture the intricacies of the membrane process and provide more accurate predictions and insights.

- This dissertation focuses on CO_2-selective membranes for power plant decarbonization. The performance of membrane-based CCS using other membrane types, such as N_2-selective membranes, could be interesting since the concentration of N_2 in the flue gas is higher than CO_2. This membrane type could also combine with a CO_2-selective membrane. However, this type of membrane is still in the early stage of development.
- The results of this dissertation proved that the membrane process is a flexible option for CO_2 capture application as it responds quickly to possible changes in feed conditions. This result is achieved by focusing on the capture side of the integrated system and performing a dynamic simulation of the CCS plant. Future research could be implemented to study the long-term dynamic operation of power plants integrated with membrane-CCS and evaluate cost and energy savings in various scenarios, including process start-up, shut-down, ramp-up, and ramp-down.
- By utilizing the modeling and optimization approach proposed in this dissertation, future works could analyze the membrane performance by including the impacts of other parameters, such as the presence of gas contaminants, water condensation, and non-ideal gas streams.
- Future work needs to study the possible uncertainties in the design, operation, and cost of the membrane-based system. Some of these uncertainties are membrane fouling, degradation, and the impact of impurities, which need to be better understood for the long-term operation of the membrane system.

- Hybridization of membrane processes with other technologies, such as cryogenic process, adsorption, and direct air capture systems, need to be investigated in terms of technical and economic performance.
- In this research, the process optimization involved multiple conflicting objective functions, and the focus was on finding the best possible trade-offs among these objectives. As the nature of the objectives and constraints was complex, including nonlinearity, nonconvexity, and varying levels of achievability, it was impossible to achieve a single-optimal solution that meets the Karush-Kuhn-Tucker (KKT) conditions. It is recommended to apply optimization approaches based on satisficing solutions for large-scale optimization problems. These methods, such as decision support problems and the adaptive linear programming algorithm, could be considered to tackle the optimization problem. By adopting these methods, satisficing solutions could be obtained, which may not be optimal but are still robust, easily attainable, and generally sufficient to meet the objectives.

Hybrid CO_2 capture processes

The results of Chapters 5 and 6 substantiate the potential of the membrane process for improving the conventional integration of NGCC plants with amine-based CCS through hybridization and solar energy incorporation. Future work should continue in the field of hybrid CCS in order to further improve the system's performance. Some recommendations in the field are as follows:

- In the current work, pinch analysis and possible thermal integrations of various streams have not been investigated thoroughly. The proposed hybrid design for the CCS plant could also be further optimized and improved in terms of overall plant thermal efficiency by performing thermal integration and pinch analysis. One potential integration could be the evaluation of preheating the rich solvent using the heat available in the flue gas from the power plant. It is worth exploring the potential of fully or partially integrating the power plant condenser as a heat source for preheating the CO_2 capture plant.
- The other limitation of the current study is that a fixed 30 wt% aqueous MEA solvent has been considered, as it is widely used in industry, to examine the impact of increased CO_2 concentration in flue gas on the CO_2 capture process. The extent of potential benefits relies heavily on the thermodynamics, kinetics, and mass transfer limitations of the solvent. To gain further insights, it is recommended to investigate the effect using different solvents with higher

CO_2 absorption capacity and/or lower enthalpy of absorption are likely to result in significantly reduced reboiler duty. Tertiary amines like methyldiethanolamine (MDEA) or hindered amines like 2-amino-2-methyl-1-propanol (AMP) could be potential alternatives for the proposed designs.

- Various modifications to the absorber and stripper units, such as intercooler and multi-column configurations for the absorber, as well as split flow, vacuum, vapor compression, and multi-pressure setups for the stripper, can be assessed in the hybrid design to achieve cost reduction and minimize energy penalties. These modifications aim to optimize the overall performance of the CO_2 capture process, ensuring efficient operation while minimizing expenses and energy consumption. Evaluating these enhancements can lead to innovative and economically viable solutions that effectively mitigate CO_2 emissions from power plants.

Integration of CO_2 capture technology with fossil-fueled power plants

- In pursuit of a sustainable energy system, this dissertation's findings in Chapters 5 and 6 proved the potential of solar-assisted hybrid CCS process for integration with fossil-fueled power plants. It is imperative to conduct further research on the optimal integration of CO_2 capture technologies that effectively reduce greenhouse gas emissions. Future works could work on the improvement of CCS integration with various power plants, including IGCC with high renewable energy penetration in dynamic operation.
- Incorporating novel energy storage solutions into renewable energy sources is vital to address flexibility limitations and optimize profitability. However, the current research is limited to the utilization of conventional thermal energy storage for this purpose. Utilizing state-of-the-art technologies such as novel batteries to store excess power from hybrid systems or selling stored energy during peak demand periods could further improve the reliability of the proposed design.
- The control system is a vital part of each process, especially in the highly integrated system. This topic was out of the scope of the current work; however, important results could be achieved by analyzing and improving the control system. Therefore, developing advanced control strategies and optimization algorithms can enhance the overall performance and efficiency of the integrated solar-NGCC-CO_2 capture plant. This involves dynamically managing the operation of the different components, optimizing energy flow, and coordinating the solar and NGCC systems to maximize power generation and CO_2 capture efficiency.

- In the current study, Therminol-VP1 is utilized as a heat transfer fluid in thermal energy storage, considering the operating temperature range. However, there is a fire hazard for this type of heat transfer fluid. Accordingly, considering other heat transfer fluids, such as molten salt, and studying their impact on the system performance will provide useful information.
- Life Cycle Assessment (LCA) and water and heat management are crucial in the CO_2 capture process as it allows for a comprehensive evaluation of its environmental impact throughout its entire life cycle. LCA provides insights into the potential environmental burdens associated with CO_2 capture technologies, including resource depletion, emissions, energy consumption, and waste generation. By considering the entire life cycle, from raw material extraction to end-of-life disposal, LCA helps identify areas where improvements can be made to minimize environmental impacts and increase sustainability. This information is essential for making informed decisions regarding the deployment of CO_2 capture technologies and ensuring their compatibility with broader sustainability goals.
- Power plant decarbonization through CO_2 capture and storage (CCS) technology is a promising approach to mitigate greenhouse gas emissions. However, there are several uncertainties and challenges associated with its implementation. Some uncertainties regarding the fuel cost, plant location, and possible advances in membrane properties have been studied. However, the other limitation of the current work is conducting a detailed uncertainty analysis of the proposed design for power plant decarbonization. Some of these uncertainties that need to be investigated are as follows:
    - **Cost and economic viability:** The overall cost of implementing CCS technology on a large scale includes high uncertainty. The expenses associated with capturing, transporting, and storing CO_2 are significant and can impact the economic viability of the technology.
    - **Energy penalty:** CCS processes require additional energy to capture, compress, and transport CO_2. This energy penalty may reduce the overall efficiency of power plants, leading to increased fuel consumption and potential impacts on power generation costs. Considering associated uncertainties for energy penalty calculation are essential.
    - **Long-term storage integrity:** The long-term stability and integrity of CO_2 storage sites are uncertain. Ensuring that CO_2 remains securely stored underground for extended periods without leakage is a critical concern. Also, identifying suitable

geological formations for CO_2 storage and assessing their capacity is a challenge. Uncertainty exists regarding the availability of suitable storage locations and the amount of CO_2 that can be safely stored.

- **Regulatory and policy environment:** The regulatory framework and government policies related to CCS may change over time, affecting the feasibility and investment decisions of power plant operators. This uncertainty is very important and needs to be investigated in detail.
- **Public acceptance and perception:** The public's perception of CCS technology and its benefits, along with its potential environmental and health impacts, may influence its widespread adoption. The uncertainties regarding social acceptance and concerns about CO_2 leakage or other environmental risks could pose challenges.
- **Technological readiness:** Some CCS technologies are still in the early stages of development and demonstration. The maturity of different CCS methods may vary, affecting their readiness for large-scale deployment.
- **Infrastructure requirements:** Building the necessary infrastructure for CO_2 capture, transportation, and storage is a complex and resource-intensive process. The availability and scalability of the required infrastructure are uncertain.
- **Integration with renewable energy:** Decarbonization efforts often involve integrating renewable energy sources with CCS. Uncertainties exist about the optimal balance between renewable energy and fossil-fuel-based CCS in the energy mix.
- **Carbon pricing and incentives:** The effectiveness of CCS implementation may depend on the presence and stability of carbon pricing mechanisms and incentives. Changes in carbon pricing policies could impact the financial viability of CCS projects.
- **Operational challenges:** Operating CCS facilities over the long term may present challenges, such as maintenance, monitoring, and managing potential operational risks.

Addressing these uncertainties is crucial to unlocking the full potential and robustness of CO_2 capture and storage technology as a viable tool for power plant decarbonization and combating climate change. Accordingly, it is recommended that future work focus on incorporating and

addressing the mentioned uncertainties within the CCS and power plant. This will allow for a better understanding of how these uncertainties impact economic performance and optimal solutions.

- The robustness of the proposed design for power plant decarbonization needs to be further investigated. Robust design can be classified into three primary types, as referenced in sources [315,316]. The proposed hybrid CCS design in this dissertation encompasses Type I and II of robust design, which include systematic procedures to identify various design alternatives and generate robust design solutions by minimizing the effect of both noise and control factors by formulating and solving a multiobjective decision problem. Future works can cover Type III of robust design, in which the focus is on creating design solutions that are resilient to variations and uncertainties present in the model used. This type of robust design aims to ensure that the proposed solutions remain effective and reliable even in the face of potential changes or uncertainties in the operating conditions, environmental factors, or input parameters.
- The availability of the experimental works and operation data for the performance of gas turbines at high temperatures and CO_2 presence is scarce. Due to the material properties of gas turbines and temperature requirements, it is recommended to perform comprehensive experiment studies on the operation of gas turbine and CO_2 capture plants at high CO_2 concentrations. These studies could shed light on the long-run operation of gas turbines with high CO_2 concentration in the entering air. Investigating the impact of exhaust gas recirculation on plant transient response and equipment health would provide valuable insights.

References

[1] Morison JIL, Lawlor DW. Interactions between increasing CO2 concentration and temperature on plant growth. Plant Cell Environ 1999;22:659–82.

[2] Kellogg WW. Climate change and society: consequences of increasing atmospheric carbon dioxide. Routledge; 2019.

[3] Singh A, Abbhishek K, Kuttippurath J, Raj S, Mallick N, Chander G, et al. Decadal variations in CO2 during agricultural seasons in India and role of management as sustainable approach. Environ Technol Innov 2022;27:102498.

[4] Li L, Wong-Ng W, Huang K, Cook LP. Materials and Processes for CO2 Capture, Conversion, and Sequestration. 2018.

[5] Inventory of U.S. Greenhouse Gas Emissions and Sinks | US EPA. US EPA 2021.

[6] Singh BR, Singh O. Study of impacts of global warming on climate change: rise in sea level and disaster frequency. Glob Warm Futur Perspect 2012.

[7] Holechek JL, Geli HME, Sawalhah MN, Valdez R. A global assessment: can renewable energy replace fossil fuels by 2050? Sustainability 2022;14:4792.

[8] CO2 Emissions in 2022 – Analysis - IEA. IEA 2022.

[9] IEA. Net Zero by 2050: A Roadmap for the Global Energy Sector. 2021.

[10] Tollefson J. IPCC says limiting global warming to 1.5 C will require drastic action. Nature 2018;562:172–3.

[11] Cormos A-M, Sandu V-C, Cormos C-C. Assessment of main energy integration elements for decarbonized gasification plants based on thermo-chemical looping cycles. J Clean Prod 2020;259:120834.

[12] Tramošljika B, Blecich P, Bonefačić I, Glažar V. Advanced Ultra-Supercritical Coal-Fired Power Plant with Post-Combustion Carbon Capture: Analysis of Electricity Penalty and CO2 Emission Reduction. Sustain 2021;13.

[13] Kuehn NJ, Mukherjee K, Phiambolis P, Pinkerton LL, Varghese E, Woods MC. Current

and future technologies for natural gas combined cycle (NGCC) power plants. National Energy Technology Laboratory (NETL), Pittsburgh, PA, Morgantown, WV …; 2013.

[14] Wilson IAG, Staffell I. Rapid fuel switching from coal to natural gas through effective carbon pricing. Nat Energy 2018;3:365–72.

[15] Quang DV, Milani D, Abu Zahra M. A review of potential routes to zero and negative emission technologies via the integration of renewable energies with CO2 capture processes. Int J Greenh Gas Control 2023;124:103862.

[16] Global CCS Institute-website. Glob CCS Inst 2023.

[17] McQueen N, Gomes KV, McCormick C, Blumanthal K, Pisciotta M, Wilcox J. A review of direct air capture (DAC): scaling up commercial technologies and innovating for the future. Prog Energy 2021;3:32001.

[18] Peridas G, Mordick Schmidt B. The role of carbon capture and storage in the race to carbon neutrality. Electr J 2021;34:106996.

[19] Global Status of CCS. GlobalccsinstituteCom 2022.

[20] Jones AC. Carbon Capture and Sequestration (CCS) in the United States. Congressional Research Service; 2021.

[21] IEA RE– A-. Renewable Electricity – Analysis - IEA. IEA 2022.

[22] Osman AI, Hefny M, Abdel Maksoud MIA, Elgarahy AM, Rooney DW. Recent advances in carbon capture storage and utilisation technologies: a review. Environ Chem Lett 2021;19:797–849.

[23] Brown LR. The great transition: Shifting from fossil fuels to solar and wind energy. WW Norton & Company; 2015.

[24] Zantye MS, Arora A, Hasan MMF. Renewable-integrated flexible carbon capture: a synergistic path forward to clean energy future. Energy Environ Sci 2021.

[25] Boot-Handford ME, Abanades JC, Anthony EJ, Blunt MJ, Brandani S, Mac Dowell N, et al. Carbon capture and storage update. Energy Environ Sci 2014;7:130–89.

[26] Abdilahi A, Mustafa M, Reviews SA-… E, 2018 undefined. Harnessing flexibility

potential of flexible carbon capture power plants for future low carbon power systems. Elsevier n.d.

[27] IEA. World Energy Outlook. 2021.

[28] Goto K, Yogo K, Higashii T. A review of efficiency penalty in a coal-fired power plant with post-combustion CO2 capture. Appl Energy 2013;111:710–20.

[29] Rahman FA, Aziz MMA, Saidur R, Bakar WAWA, Hainin MR, Putrajaya R, et al. Pollution to solution: Capture and sequestration of carbon dioxide (CO2) and its utilization as a renewable energy source for a sustainable future. Renew Sustain Energy Rev 2017;71:112–26.

[30] Adu E, Zhang YD, Liu D, Tontiwachwuthikul P. Parametric process design and economic analysis of post-combustion CO2 capture and compression for coal-and natural gas-fired power plants. Energies 2020;13:2519.

[31] Lin X, Liu Y, Song H, Guan Y, Wang R. Concept design, parameter analysis, and thermodynamic evaluation of a novel integrated gasification chemical-looping combustion combined cycle power generation system. Energy Convers Manag 2023;279:116768.

[32] Díaz-Herrera PR, Alcaraz-Calderón AM, González-Díaz MO, González-Díaz A. Capture level design for a natural gas combined cycle with post-combustion CO2 capture using novel configurations. Energy 2020;193:116769.

[33] M. Montañés R, GarÐarsdóttir SÓ, Normann F, Johnsson F, Nord LO. Demonstrating load-change transient performance of a commercial-scale natural gas combined cycle power plant with post-combustion CO2 capture. Int J Greenh Gas Control 2017;63:158–74.

[34] Mechleri E, Lawal A, Ramos A, Davison J, Dowell N Mac. Process control strategies for flexible operation of post-combustion CO2 capture plants. Int J Greenh Gas Control 2017;57:14–25.

[35] Adeosun A, Abu-Zahra MRM. Evaluation of amine-blend solvent systems for CO2 post-combustion capture applications. Energy Procedia 2013;37:211–8.

[36] Ye B, Jiang J, Zhou Y, Liu J, Wang K. Technical and economic analysis of amine-based

carbon capture and sequestration at coal-fired power plants. J Clean Prod 2019;222:476–87.

[37] Rodríguez N, Mussati S, Scenna N. Optimization of post-combustion CO2 process using DEA–MDEA mixtures. Chem Eng Res Des 2011;89:1763–73.

[38] Oh H-T, Kum J, Park J, Dat Vo N, Kang J-H, Lee C-H. Pre-combustion CO2 capture using amine-based absorption process for blue H2 production from steam methane reformer. Energy Convers Manag 2022;262:115632.

[39] Agbonghae EO, Hughes KJ, Ingham DB, Ma L, Pourkashanian M. Optimal process design of commercial-scale amine-based CO2 capture plants. Ind Eng Chem Res 2014;53:14815–29.

[40] Knudsen JN, Bade OM, Askestad I, Gorset O, Mejdell T. Pilot plant demonstration of CO2 capture from cement plant with advanced amine technology. Energy Procedia 2014;63:6464–75.

[41] Romeo LM, Minguell D, Shirmohammadi R, Andrés JM. Comparative analysis of the efficiency penalty in power plants of different amine-based solvents for CO2 capture. Ind Eng Chem Res 2020;59:10082–92.

[42] Míguez JL, Porteiro J, Pérez-Orozco R, Gómez MÁ. Technology evolution in membrane-based CCS. Energies 2018;11:3153.

[43] Wang S, Li X, Wu H, Tian Z, Xin Q, He G, et al. Advances in high permeability polymer-based membrane materials for CO2 separations. Energy Environ Sci 2016;9:1863–90.

[44] Kehlhofer R. Combined-cycle gas and steam turbine power plants 1991.

[45] Cebrucean D, Cebrucean V, Ionel I. Modeling and evaluation of a coal power plant with biomass cofiring and CO2 capture. Recent Adv Carbon Capture Storage 2017:31–55.

[46] Environment Baseline, Volume 1: Greenhouse Gas Emissions from the U.S. Power Sector. 2016.

[47] to. It’s critical to tackle coal emissions – Analysis - IEA. IEA 2021.

[48] Ibrahim TK, Rahman MM. Effect of compression ratio on performance of combined cycle

gas turbine. Int J Energy Eng 2012;2:9–14.

[49] Robert E, Kearins D, Turner M, Woods M, Kuehn N, Zoelle A. Cost and performance baseline for fossil energy plants volume 1: bituminous coal and natural gas to electricity. National Energy Technology Laboratory (NETL), Pittsburgh, PA, Morgantown, WV …; 2019.

[50] Singh B, Strømman AH, Hertwich E. Life cycle assessment of natural gas combined cycle power plant with post-combustion carbon capture, transport and storage. Int J Greenh Gas Control 2011;5:457–66.

[51] U.S. electric-generating capacity for combined-cycle natural gas turbines is growing. EiaGov 2022.

[52] Asano T. 22 - Case study: Nakoso IGCC power plant, Japan. In: Wang T, Stiegel GBT-IGCC (IGCC) T, editors., Woodhead Publishing; 2017, p. 799–815.

[53] Fact Sheet: “Clean Coal” Power Plants (IGCC) - Energy Justice Network. 2014.

[54] Kheirinik M, Ahmed S, Rahmanian N. Comparative Techno-Economic Analysis of Carbon Capture Processes: Pre-Combustion, Post-Combustion, and Oxy-Fuel Combustion Operations. Sustainability 2021;13.

[55] Raza A, Gholami R, Rezaee R, Rasouli V, Rabiei M. Significant aspects of carbon capture and storage – A review. Petroleum 2019;5:335–40.

[56] Zhang Z, Wang T, Blunt MJ, Anthony EJ, Park A-HA, Hughes RW, et al. Advances in carbon capture, utilization and storage. Appl Energy 2020;278:115627.

[57] Pardemann R, Meyer B. Pre-Combustion Carbon Capture. Handb Clean Energy Syst 2015:1–28.

[58] Siefert NS, Hopkinson DP. Physical Solvent Development for Pre-Combustion Carbon Capture. NETL; 2019.

[59] Olabi AG, Obaideen K, Elsaid K, Wilberforce T, Sayed ET, Maghrabie HM, et al. Assessment of the pre-combustion carbon capture contribution into sustainable development goals SDGs using novel indicators. Renew Sustain Energy Rev

2022;153:111710.

[60] Nataly Echevarria Huaman R, Xiu Jun T. Energy related CO2 emissions and the progress on CCS projects: A review. Renew Sustain Energy Rev 2014;31:368–85.

[61] Gür TM. Carbon Dioxide Emissions, Capture, Storage and Utilization: Review of Materials, Processes and Technologies. Prog Energy Combust Sci 2022;89:100965.

[62] Franz J, Maas P, Scherer V. Economic evaluation of pre-combustion CO2-capture in IGCC power plants by porous ceramic membranes. Appl Energy 2014;130:532–42.

[63] Jonshagen K, Sipöcz N, Genrup M. A novel approach of retrofitting a combined cycle with post combustion CO2 capture. J Eng Gas Turbines Power 2011;133.

[64] Bernhardsen IM, Knuutila HK. A review of potential amine solvents for CO2 absorption process: Absorption capacity, cyclic capacity and pKa. Int J Greenh Gas Control 2017;61:27–48.

[65] Yun S, Oh S-Y, Kim J-K. Techno-economic assessment of absorption-based CO2 capture process based on novel solvent for coal-fired power plant. Appl Energy 2020;268:114933.

[66] Sultan H, Quach T-Q, Muhammad HA, Bhatti UH, Lee YD, Hong MG, et al. Advanced post combustion CO2 capture process–A systematic approach to minimize thermal energy requirement. Appl Therm Eng 2021;184:116285.

[67] Bao J, Zhang L, Song C, Zhang N, Guo M, Zhang X. Reduction of efficiency penalty for a natural gas combined cycle power plant with post-combustion CO2 capture: Integration of liquid natural gas cold energy. Energy Convers Manag 2019;198:111852.

[68] Di Lorenzo G, Barbera P, Ruggieri G, Witton J, Pilidis P, Probert D. Pre-combustion carbon-capture technologies for power generation: an engineering-economic assessment. Int J Energy Res 2013;37:389–402.

[69] Sifat NS, Haseli Y. A critical review of CO2 capture technologies and prospects for clean power generation. Energies 2019;12:4143.

[70] Bao J, Zhang L, Song C, Zhang N, Guo M, Zhang X. Reduction of efficiency penalty for a natural gas combined cycle power plant with post-combustion CO2 capture: Integration of

liquid natural gas cold energy. Energy Convers Manag 2019;198:111852.

[71] Hu Y, Yan J. Characterization of flue gas in oxy-coal combustion processes for CO2 capture. Appl Energy 2012;90:113–21.

[72] Madejski P, Chmiel K, Subramanian N, Kuś T. Methods and techniques for CO2 capture: Review of potential solutions and applications in modern energy technologies. Energies 2022;15:887.

[73] Borgert KJ, Rubin ES. Oxy-combustion carbon capture for pulverized coal in the integrated environmental control model. Energy Procedia 2017;114:522–9.

[74] Yadav S, Mondal SS. A review on the progress and prospects of oxy-fuel carbon capture and sequestration (CCS) technology. Fuel 2022;308:122057.

[75] Wang M, Lawal A, Stephenson P, Sidders J, Ramshaw C. Post-combustion CO2 capture with chemical absorption: A state-of-the-art review. Chem Eng Res Des 2011;89:1609–24.

[76] Khallaghi N, Abbas SZ, Manzolini G, De Coninck E, Spallina V. Techno-economic assessment of blast furnace gas pre-combustion decarbonisation integrated with the power generation. Energy Convers Manag 2022;255:115252.

[77] Kunze C, Spliethoff H. Assessment of oxy-fuel, pre- and post-combustion-based carbon capture for future IGCC plants. Appl Energy 2012;94:109–16.

[78] Son S, Heo JY, Kim N Il, Jamal A, Lee JI. Reduction of CO2 emission for solar power backup by direct integration of oxy-combustion supercritical CO2 power cycle with concentrated solar power. Energy Convers Manag 2019;201:112161.

[79] Mancini ND, Mitsos A. Conceptual design and analysis of ITM oxy-combustion power cycles. Phys Chem Chem Phys 2011;13:21351–61.

[80] Luis P, Van der Bruggen B. The role of membranes in post-combustion CO2 capture. Greenh Gases Sci Technol 2013;3:318–37.

[81] Wang M, Joel AS, Ramshaw C, Eimer D, Musa NM. Process intensification for post-combustion CO2 capture with chemical absorption: A critical review. Appl Energy

2015;158:275–91.

[82] Zhang X, He X, Gundersen T. Post-combustion carbon capture with a gas separation membrane: parametric study, capture cost, and exergy analysis. Energy & Fuels 2013;27:4137–49.

[83] Xi H, Liao P, Wu X. Simultaneous parametric optimization for design and operation of solvent-based post-combustion carbon capture using particle swarm optimization. Appl Therm Eng 2021;184:116287.

[84] Han C, Zahid U, An J, Kim K, Kim C. CO2 transport: design considerations and project outlook. Curr Opin Chem Eng 2015;10:42–8.

[85] Niemi A, Bear J, Bensabat J. Geological storage of CO2 in deep saline formations. vol. 29. Springer; 2017.

[86] Roefs P, Moretti M, Welkenhuysen K, Piessens K, Compernolle T. CO2-enhanced oil recovery and CO2 capture and storage: an environmental economic trade-off analysis. J Environ Manage 2019;239:167–77.

[87] Luo J, Xie Y, Hou MZ, Xiong Y, Wu X, Lüddeke CT, et al. Advances in subsea carbon dioxide utilization and storage. Energy Rev 2023:100016.

[88] Cao C, Liu H, Hou Z, Mehmood F, Liao J, Feng W. A review of CO2 storage in view of safety and cost-effectiveness. Energies 2020;13:600.

[89] Tan Y, Nookuea W, Li H, Thorin E, Yan J. Property impacts on Carbon Capture and Storage (CCS) processes: A review. Energy Convers Manag 2016;118:204–22.

[90] Kárászová M, Zach B, Petrusová Z, Červenka V, Bobák M, Šyc M, et al. Post-combustion carbon capture by membrane separation, Review. Sep Purif Technol 2020;238:116448.

[91] Li Y, Huang W, Zheng D, Mi Y, Dong L. Solubilities of CO2 capture absorbents 2-ethoxyethyl ether, 2-butoxyethyl acetate and 2-(2-ethoxyethoxy) ethyl acetate. Fluid Phase Equilib 2014;370:1–7.

[92] Park SH, Lee SJ, Lee JW, Chun SN, Lee J Bin. The quantitative evaluation of two-stage pre-combustion CO2 capture processes using the physical solvents with various design

parameters. Energy 2015;81:47–55.

[93] Lee AS, Eslick JC, Miller DC, Kitchin JR. Comparisons of amine solvents for post-combustion CO2 capture: A multi-objective analysis approach. Int J Greenh Gas Control 2013;18:68–74.

[94] Sanchez Fernandez E, Goetheer EL V, Manzolini G, Macchi E, Rezvani S, Vlugt TJH. Thermodynamic assessment of amine based CO2 capture technologies in power plants based on European Benchmarking Task Force methodology. Fuel 2014;129:318–29.

[95] Ahn H, Luberti M, Liu Z, Brandani S. Process configuration studies of the amine capture process for coal-fired power plants. Int J Greenh Gas Control 2013;16:29–40.

[96] Chao C, Deng Y, Dewil R, Baeyens J, Fan X. Post-combustion carbon capture. Renew Sustain Energy Rev 2021;138:110490.

[97] Oyenekan BA, Rochelle GT. Alternative stripper configurations for CO2 capture by aqueous amines. AIChE J 2007;53:3144–54.

[98] Zhang Y, Que H, Chen C-C. Thermodynamic modeling for CO2 absorption in aqueous MEA solution with electrolyte NRTL model. Fluid Phase Equilib 2011;311:67–75.

[99] Manzolini G, Sanchez Fernandez E, Rezvani S, Macchi E, Goetheer EL V, Vlugt TJH. Economic assessment of novel amine based CO2 capture technologies integrated in power plants based on European Benchmarking Task Force methodology. Appl Energy 2015;138:546–58.

[100] Osagie E, Biliyok C, Di Lorenzo G, Hanak DP, Manovic V. Techno-economic evaluation of the 2-amino-2-methyl-1-propanol (AMP) process for CO2 capture from natural gas combined cycle power plant. Int J Greenh Gas Control 2018;70:45–56.

[101] Vega F, Cano M, Camino S, Fernández LMG, Portillo E, Navarrete B. Solvents for carbon dioxide capture. Carbon Dioxide Chem Capture Oil Recover 2018:142–63.

[102] Aghel B, Janati S, Wongwises S, Shadloo MS. Review on CO2 capture by blended amine solutions. Int J Greenh Gas Control 2022;119:103715.

[103] Vega F, Baena-Moreno FM, Fernández LMG, Portillo E, Navarrete B, Zhang Z. Current

status of CO2 chemical absorption research applied to CCS: Towards full deployment at industrial scale. Appl Energy 2020;260:114313.

[104] Barzagli F, Mani F, Peruzzini M. Novel water-free biphasic absorbents for efficient CO2 capture. Int J Greenh Gas Control 2017;60:100–9.

[105] Ahn H, Luberti M, Liu Z, Brandani S, Le Moullec Y, Neveux T, et al. A comparative review between amines and ammonia as sorptive media for post-combustion CO2 capture. Appl Energy 2015;148:109–16.

[106] Rochelle GT. Thermal degradation of amines for CO 2 capture. Curr Opin Chem Eng 2012;1:183–90.

[107] Bravo J, Drapanauskaite D, Sarunac N, Romero C, Jesikiewicz T, Baltrusaitis J. Optimization of energy requirements for CO2 post-combustion capture process through advanced thermal integration. Fuel 2021;283:118940.

[108] Fu W, Wang L, Yang Y. Optimal design for double reheat coal-fired power plants with post-combustion CO2 capture: A novel thermal system integration with a carbon capture turbine. Energy 2021;221:119838.

[109] Shirmohammadi R, Aslani A, Ghasempour R, Romeo LM, Petrakopoulou F. Exergoenvironmental analysis and thermoeconomic optimization of an industrial post-combustion CO2 capture and utilization installation. J CO2 Util 2022;59:101927.

[110] Damartzis T, Papadopoulos AI, Seferlis P. Process flowsheet design optimization for various amine-based solvents in post-combustion CO2 capture plants. J Clean Prod 2016;111:204–16.

[111] Favre E. 2.6 Polymeric Membranes for Gas Separation. In: Drioli E, Giorno L, Fontananova EBT-CMS and E (Second E, editors., Oxford: Elsevier; 2017, p. 124–75.

[112] Graham T. LXIX. On the absorption and dialytic separation of gases by colloid septa. London, Edinburgh, Dublin Philos Mag J Sci 1866;32:503–31.

[113] Henis JMS, Tripodi MK. The developing technology of gas separating membranes. Science (80-) 1983;220:11–7.

[114] Bernardo P, Drioli E, Golemme G. Membrane gas separation: a review/state of the art. Ind Eng Chem Res 2009;48:4638–63.

[115] Khalilpour R, Mumford K, Zhai H, Abbas A, Stevens G, Rubin ES. Membrane-based carbon capture from flue gas: a review. J Clean Prod 2015;103:286–300.

[116] Luis P, Van Gerven T, Van der Bruggen B. Recent developments in membrane-based technologies for CO2 capture. Prog Energy Combust Sci 2012;38:419–48.

[117] Liang CZ, Chung T-S, Lai J-Y. A review of polymeric composite membranes for gas separation and energy production. Prog Polym Sci 2019;97:101141.

[118] Li H, Haas-Santo K, Schygulla U, Dittmeyer R. Inorganic microporous membranes for H2 and CO2 separation—Review of experimental and modeling progress. Chem Eng Sci 2015;127:401–17.

[119] Rui Z, James JB, Lin YS. Highly CO2 perm-selective metal-organic framework membranes through CO2 annealing post-treatment. J Memb Sci 2018;555:97–104.

[120] Vilardi G, Bassano C, Deiana P, Verdone N. Exergy and energy analysis of three biogas upgrading processes. Energy Convers Manag 2020;224:113323.

[121] Pazani F, Maleh MS, Shariatifar M, Jalaly M, Sadrzadeh M, Rezakazemi M. Engineered graphene-based mixed matrix membranes to boost CO2 separation performance: Latest developments and future prospects. Renew Sustain Energy Rev 2022;160:112294.

[122] Sunder N, Fong YY, Bustam MA, Suhaimi NH. Development of Amine-Functionalized Metal-Organic Frameworks Hollow Fiber Mixed Matrix Membranes for CO2 and CH4 Separation: A Review. Polymers (Basel) 2022;14:1408.

[123] Janakiram S, Santinelli F, Costi R, Lindbråthen A, Nardelli GM, Milkowski K, et al. Field trial of hollow fiber modules of hybrid facilitated transport membranes for flue gas CO2 capture in cement industry. Chem Eng J 2021;413:127405.

[124] Karim SS, Shaikh H, Farrukh S, Memon SA, Qureshi T, Memon S. Facilitated Transport Membranes (FTMs) for CO2 Separation from Flue Gas (CO2/N2). Facil. Transp. Membr. CO2 Capture Overv. Futur. Trends, Springer; 2023, p. 173–208.

[125] Teramoto M, Takeuchi N, Maki T, Matsuyama H. Facilitated transport of CO2 through liquid membrane accompanied by permeation of carrier solution. Sep Purif Technol 2002;27:25–31.

[126] White LS, Amo KD, Wu T, Merkel TC. Extended field trials of Polaris sweep modules for carbon capture. J Memb Sci 2017;542:217–25.

[127] Merkel TC, Lin H, Wei X, Baker R. Power plant post-combustion carbon dioxide capture: An opportunity for membranes. J Memb Sci 2010;359:126–39.

[128] Tong Z, Ho WSW. Facilitated transport membranes for CO2 separation and capture. Sep Sci Technol 2017;52:156–67.

[129] Vakharia V, Salim W, Wu D, Han Y, Chen Y, Zhao L, et al. Scale-up of amine-containing thin-film composite membranes for CO2 capture from flue gas. J Memb Sci 2018;555:379–87.

[130] Zhao S, Feron PHM, Deng L, Favre E, Chabanon E, Yan S, et al. Status and progress of membrane contactors in post-combustion carbon capture: A state-of-the-art review of new developments. J Memb Sci 2016;511:180–206.

[131] Wijmans JG, Baker RW. The solution-diffusion model: a review. J Memb Sci 1995;107:1–21.

[132] Nath K. Membrane separation processes. PHI Learning Pvt. Ltd.; 2017.

[133] Favre E. Membrane processes and postcombustion carbon dioxide capture: Challenges and prospects. Chem Eng J 2011;171:782–93.

[134] Baker RW. Membrane technology and applications. John Wiley & Sons; 2012.

[135] Scholes CA. Pilot plants of membrane technology in industry: Challenges and key learnings. Front Chem Sci Eng 2020;14:305–16.

[136] Ramezani R, Di Felice L, Gallucci F. A Review on Hollow Fiber Membrane Contactors for Carbon Capture: Recent Advances and Future Challenges. Processes 2022;10.

[137] Mat NC, Lou Y, Lipscomb GG. Hollow fiber membrane modules. Curr Opin Chem Eng 2014;4:18–24.

[138] Shah C, Raut S, Kacha H, Patel H, Shah M. Carbon capture using membrane-based materials and its utilization pathways. Chem Pap 2021:1–17.

[139] Cai L, Wu X, Zhu X, Ghoniem AF, Yang W. High-performance oxygen transport membrane reactors integrated with IGCC for carbon capture. AIChE J 2020;66:e16427.

[140] Wang X, Huang Y, Li D, Zeng L, He Y, Boubeche M, et al. High oxygen permeation flux of cobalt-free Cu-based ceramic dual-phase membranes. J Memb Sci 2021;633:119403.

[141] Li D, Wang X, Tan W, Huang Y, Zeng L, He Y, et al. Influences of Al substitution on the oxygen permeability through 60 wt%Ce0.9La0.1O2-δ-40 wt%La0.6Sr0.4Co1-xAlxO3-δ composite membranes. Sep Purif Technol 2021;274:119042.

[142] Batoon V, Borsaly A, Casillas C, Hofmann T, Huang I, Kniep J, et al. Scale-Up Testing of Advanced Polaris^{TM} Membrane CO2 Capture Technology. Available SSRN 4281208 2022.

[143] Dhoke C, Cloete S, Krishnamurthy S, Seo H, Luz I, Soukri M, et al. Sorbents screening for post-combustion CO2 capture via combined temperature and pressure swing adsorption. Chem Eng J 2020;380:122201.

[144] Webley PA. Adsorption technology for CO2 separation and capture: a perspective. Adsorption 2014;20:225–31.

[145] Jiang N, Shen Y, Liu B, Zhang D, Tang Z, Li G, et al. CO2 capture from dry flue gas by means of VPSA, TSA and TVSA. J CO2 Util 2020;35:153–68.

[146] Song C, Liu Q, Deng S, Li H, Kitamura Y. Cryogenic-based CO2 capture technologies: State-of-the-art developments and current challenges. Renew Sustain Energy Rev 2019;101:265–78.

[147] Lee AS, Eslick JC, Miller DC, Kitchin JR. Comparisons of amine solvents for post-combustion CO2 capture: A multi-objective analysis approach. Int J Greenh Gas Control 2013;18:68–74.

[148] Siqueira RM, Freitas GR, Peixoto HR, Do Nascimento JF, Musse APS, Torres AEB, et al. Carbon dioxide capture by pressure swing adsorption. Energy Procedia 2017;114:2182–92.

[149] Xu J, Lin W. A CO2 cryogenic capture system for flue gas of an LNG-fired power plant. Int J Hydrogen Energy 2017;42:18674–80.

[150] Rezazadeh F, Gale WF, Hughes KJ, Pourkashanian M. Performance viability of a natural gas fired combined cycle power plant integrated with post-combustion CO2 capture at part-load and temporary non-capture operations. Int J Greenh Gas Control 2015;39:397–406.

[151] Jørsboe JK, Vinjarapu SHB, Neerup R, Møller AC, Jensen S, Abildskov J, et al. Mobile pilot plant for CO2 capture in biogas upgrading using 30 wt% MEA. Fuel 2023;350:128702.

[152] Muhammad HA, Sultan H, Lee B, Imran M, Baek IH, Baik Y-J, et al. Energy minimization of carbon capture and storage by means of a novel process configuration. Energy Convers Manag 2020;215:112871.

[153] Law LC, Azudin NY, Shukor SRA. Optimization and economic analysis of amine-based acid gas capture unit using monoethanolamine/methyl diethanolamine. Clean Technol Environ Policy 2018;20:451–61.

[154] Bravo J, Charles J, Neti S, Caram H, Oztekin A, Romero C. Integration of solar thermal energy to improve NGCC with CO2 capture plant performance. Int J Greenh Gas Control 2020;100:103111.

[155] Wang F, Deng S, Zhao J, Zhao J, Yang G, Yan J. Integrating geothermal into coal-fired power plant with carbon capture: A comparative study with solar energy. Energy Convers Manag 2017;148:569–82.

[156] Abu-Zahra MRM, Schneiders LHJ, Niederer JPM, Feron PHM, Versteeg GF. CO2 capture from power plants: Part I. A parametric study of the technical performance based on monoethanolamine. Int J Greenh Gas Control 2007;1:37–46.

[157] Aboudheir A, Elmoudir W. Optimization of an existing 130 tonne per day CO2 capture plant from a flue gas slipstream of a coal power plant. Energy Procedia 2013;37:1509–16.

[158] Damartzis T, Papadopoulos AI, Seferlis P. Optimum synthesis of solvent-based post-combustion CO 2 capture flowsheets through a generalized modeling framework. Clean

Technol Environ Policy 2014;16:1363–80.

[159] Le Moullec Y, Neveux T, Al Azki A, Chikukwa A, Hoff KA. Process modifications for solvent-based post-combustion CO2 capture. Int J Greenh Gas Control 2014;31:96–112.

[160] Sultan H, Bhatti UH, Muhammad HA, Nam SC, Baek IH. Modification of postcombustion CO2 capture process: A techno-economic analysis. Greenh Gases Sci Technol 2021;11:165–82.

[161] Gbadago DQ, Oh H-T, Oh D-H, Lee C-H, Oh M. CFD simulation of a packed bed industrial absorber with interbed liquid distributors. Int J Greenh Gas Control 2020;95:102983.

[162] Zhang Y, Chen H, Chen C-C, Plaza JM, Dugas R, Rochelle GT. Rate-Based Process Modeling Study of CO2 Capture with Aqueous Monoethanolamine Solution. Ind Eng Chem Res 2009;48:9233–46.

[163] Razi N, Svendsen HF, Bolland O. Validation of mass transfer correlations for CO2 absorption with MEA using pilot data. Int J Greenh Gas Control 2013;19:478–91.

[164] Khalilpour R, Abbas A. Optimal synthesis and design of solvent-based PCC process using a rate-based model. Sep Purif Technol 2014;132:149–67.

[165] Herraiz L, Fernández ES, Palfi E, Lucquiaud M. Selective exhaust gas recirculation in combined cycle gas turbine power plants with post-combustion CO2 capture. Int J Greenh Gas Control 2018;71:303–21.

[166] Jung J, Jeong YS, Lee U, Lim Y, Han C. New Configuration of the CO2 Capture Process Using Aqueous Monoethanolamine for Coal-Fired Power Plants. Ind Eng Chem Res 2015;54:3865–78.

[167] Cho H, Binns M, Min K-J, Kim J-K. Automated process design of acid gas removal units in natural gas processing. Comput Chem Eng 2015;83:97–109.

[168] Gao H, Zhou L, Liang Z, Idem RO, Fu K, Sema T, et al. Comparative studies of heat duty and total equivalent work of a new heat pump distillation with split flow process, conventional split flow process, and conventional baseline process for CO2 capture using monoethanolamine. Int J Greenh Gas Control 2014;24:87–97.

[169] Le Moullec Y, Kanniche M. Screening of flowsheet modifications for an efficient monoethanolamine (MEA) based post-combustion CO2 capture. Int J Greenh Gas Control 2011;5:727–40.

[170] Mores PL, Manassaldi JI, Scenna NJ, Caballero JA, Mussati MC, Mussati SF. Optimization of the design, operating conditions, and coupling configuration of combined cycle power plants and CO2 capture processes by minimizing the mitigation cost. Chem Eng J 2018;331:870–94.

[171] Choi J, Cho H, Yun S, Jang M-G, Oh S-Y, Binns M, et al. Process design and optimization of MEA-based CO2 capture processes for non-power industries. Energy 2019;185:971–80.

[172] Yulia F, Sofianita R, Prayogo K, Nasruddin N. Optimization of post combustion CO2 absorption system monoethanolamine (MEA) based for 320 MW coal-fired power plant application – Exergy and exergoenvironmental analysis. Case Stud Therm Eng 2021;26:101093.

[173] Wu Y, Dai Y, Xie W, Chen H, Zhu Y. System integration for combined heat and power (CHP) plants with post-combustion CO2 capture. Energy Convers Manag 2022;258:115508.

[174] Zoelle A, Keairns D, Pinkerton LL, Turner MJ, Woods M, Kuehn N, et al. Cost and performance baseline for fossil energy plants volume 1a: Bituminous coal (PC) and natural gas to electricity revision 3. National Energy Technology Laboratory (NETL), Pittsburgh, PA, Morgantown, WV …; 2015.

[175] Li K, Leigh W, Feron P, Yu H, Tade M. Systematic study of aqueous monoethanolamine (MEA)-based CO2 capture process: Techno-economic assessment of the MEA process and its improvements. Appl Energy 2016;165:648–59.

[176] Asadi J, Kazempoor P. Dynamic response and flexibility analyses of a membrane-based CO2 separation module. Int J Greenh Gas Control 2022;116:103634.

[177] Belaissaoui B, Willson D, Favre E. Membrane gas separations and post-combustion carbon dioxide capture: Parametric sensitivity and process integration strategies. Chem

Eng J 2012;211:122–32.

[178] Xu J, Wang Z, Qiao Z, Wu H, Dong S, Zhao S, et al. Post-combustion CO2 capture with membrane process: Practical membrane performance and appropriate pressure. J Memb Sci 2019;581:195–213.

[179] Gabrielli P, Gazzani M, Mazzotti M. On the optimal design of membrane-based gas separation processes. J Memb Sci 2017;526:118–30.

[180] Atlaskin AA, Petukhov AN, Stepakova AN, Tsivkovsky NS, Kryuchkov SS, Smorodin KA, et al. Membrane Cascade Type of «Continuous Membrane Column» for Power Plant Post-Combustion Carbon Dioxide Capture Part 1: Simulation of the Binary Gas Mixture Separation. Membranes (Basel) 2023;13.

[181] Maghami S, Mehrabani-Zeinabad A, Sadeghi M, Sánchez-Laínez J, Zornoza B, Téllez C, et al. Mathematical modeling of temperature and pressure effects on permeability, diffusivity and solubility in polymeric and mixed matrix membranes. Chem Eng Sci 2019;205:58–73.

[182] Chu Y, Lindbråthen A, Lei L, He X, Hillestad M. Mathematical modeling and process parametric study of CO2 removal from natural gas by hollow fiber membranes. Chem Eng Res Des 2019;148:45–55.

[183] Trubyanov MM, Kirillov SY, Vorotyntsev A V, Sazanova TS, Atlaskin AA, Petukhov AN, et al. Dynamic behavior of unsteady-state membrane gas separation: Modelling of a closed-mode operation for a membrane module. J Memb Sci 2019;587:117173.

[184] He X, Chen D, Liang Z, Yang F. Insight and Comparison of Energy-efficient Membrane Processes for CO2 Capture from Flue Gases in Power Plant and Energy-intensive Industry. Carbon Capture Sci Technol 2022;2:100020.

[185] Zhao L, Riensche E, Blum L, Stolten D. Multi-stage gas separation membrane processes used in post-combustion capture: Energetic and economic analyses. J Memb Sci 2010;359:160–72.

[186] Bhattacharyya D. Design and optimization of hybrid membrane–solvent-processes for post-combustion CO2 capture. Curr Opin Chem Eng 2022;36:100768.

[187] Brunetti A, Drioli E, Lee YM, Barbieri G. Engineering evaluation of CO2 separation by membrane gas separation systems. J Memb Sci 2014;454:305–15.

[188] Giordano L, Roizard D, Bounaceur R, Favre E. Evaluating the effects of CO2 capture benchmarks on efficiency and costs of membrane systems for post-combustion capture: A parametric simulation study. Int J Greenh Gas Control 2017;63:449–61.

[189] Asadi J, Kazempoor P. Techno-economic analysis of membrane-based processes for flexible CO2 capturing from power plants. Energy Convers Manag 2021;246:114633.

[190] Mores PL, Arias AM, Scenna NJ, Mussati MC, Mussati SF. Cost-based comparison of multi-stage membrane configurations for carbon capture from flue gas of power plants. Int J Greenh Gas Control 2019;86:177–90.

[191] Arias AM, Mussati MC, Mores PL, Scenna NJ, Caballero JA, Mussati SF. Optimization of multi-stage membrane systems for CO2 capture from flue gas. Int J Greenh Gas Control 2016;53:371–90.

[192] Song C, Liu Q, Ji N, Deng S, Zhao J, Li Y, et al. Reducing the energy consumption of membrane-cryogenic hybrid CO2 capture by process optimization. Energy 2017;124:29–39.

[193] Mat NC, Lipscomb GG. Membrane process optimization for carbon capture. Int J Greenh Gas Control 2017;62:1–12.

[194] Ramírez-Santos ÁA, Bozorg M, Addis B, Piccialli V, Castel C, Favre E. Optimization of multistage membrane gas separation processes. Example of application to CO2 capture from blast furnace gas. J Memb Sci 2018;566:346–66.

[195] Lee S, Yun S, Kim J-K. Development of novel sub-ambient membrane systems for energy-efficient post-combustion CO2 capture. Appl Energy 2019;238:1060–73.

[196] Yuan M, Teichgraeber H, Wilcox J, Brandt AR. Design and operations optimization of membrane-based flexible carbon capture. Int J Greenh Gas Control 2019;84:154–63.

[197] Fujikawa S, Selyanchyn R, Kunitake T. A new strategy for membrane-based direct air capture. Polym J 2021;53:111–9.

[198] Pohlmann J, Bram M, Wilkner K, Brinkmann T. Pilot scale separation of CO2 from power plant flue gases by membrane technology. Int J Greenh Gas Control 2016;53:56–64.

[199] Ko D. Development of a dynamic simulation model of a hollow fiber membrane module to sequester CO2 from coalbed methane. J Memb Sci 2018;546:258–69.

[200] Mikulčić H, Skov IR, Dominković DF, Alwi SRW, Manan ZA, Tan R, et al. Flexible Carbon Capture and Utilization technologies in future energy systems and the utilization pathways of captured CO2. Renew Sustain Energy Rev 2019;114:109338.

[201] Abdilahi AM, Mustafa MW, Abujarad SY, Mustapha M. Harnessing flexibility potential of flexible carbon capture power plants for future low carbon power systems. Renew Sustain Energy Rev 2018;81:3101–10.

[202] Szima S, Arnaiz del Pozo C, Cloete S, Chiesa P, Jiménez Alvaro Á, Cormos A-M, et al. Finding synergy between renewables and coal: Flexible power and hydrogen production from advanced IGCC plants with integrated CO2 capture. Energy Convers Manag 2021;231:113866.

[203] Ho MT, Wiley DE. Flexible strategies to facilitate carbon capture deployment at pulverised coal power plants. Int J Greenh Gas Control 2016;48:290–9.

[204] Rúa J, Bui M, Nord LO, Mac Dowell N. Does CCS reduce power generation flexibility? A dynamic study of combined cycles with post-combustion CO2 capture. Int J Greenh Gas Control 2020;95:102984.

[205] Hentschel J, Spliethoff H. A parametric approach for the valuation of power plant flexibility options. Energy Reports 2016;2:40–7.

[206] Rua J, Bui M, Nord LO, Mac Dowell N. Does CCS reduce power generation flexibility? A dynamic study of combined cycles with post-combustion CO2 capture. Int J Greenh Gas Control 2020;95:102984.

[207] Li J, Mi Z, Wei Y-M, Fan J, Yang Y, Hou Y. Flexible options to provide energy for capturing carbon dioxide in coal-fired power plants under the Clean Development Mechanism. Mitig Adapt Strateg Glob Chang 2019;24:1483–505.

[208] Jang M-G, Yun S, Kim J-K. Process design and economic analysis of membrane-

integrated absorption processes for CO2 capture. J Clean Prod 2022;368:133180.

[209] Bui M, Gunawan I, Verheyen V, Feron P, Meuleman E. Flexible operation of CSIRO's post-combustion CO2 capture pilot plant at the AGL Loy Yang power station. Int J Greenh Gas Control 2016;48:188–203.

[210] Tait P, Buschle B, Milkowski K, Akram M, Pourkashanian M, Lucquiaud M. Flexible operation of post-combustion CO2 capture at pilot scale with demonstration of capture-efficiency control using online solvent measurements. Int J Greenh Gas Control 2018;71:253–77.

[211] Bui M, Tait P, Lucquiaud M, Mac Dowell N. Dynamic operation and modelling of amine-based CO2 capture at pilot scale. Int J Greenh Gas Control 2018;79:134–53.

[212] Bui M, Flø NE, de Cazenove T, Mac Dowell N. Demonstrating flexible operation of the Technology Centre Mongstad (TCM) CO2 capture plant. Int J Greenh Gas Control 2020;93:102879.

[213] Flø NE, Kvamsdal HM, Hillestad M. Dynamic simulation of post-combustion CO2 capture for flexible operation of the Brindisi pilot plant. Int J Greenh Gas Control 2016;48:204–15.

[214] Cohen SM. A techno-economic plant-and grid-level assessment of flexible CO2 capture 2012.

[215] Lawal A, Wang M, Stephenson P, Koumpouras G, Yeung H. Dynamic modelling and analysis of post-combustion CO2 chemical absorption process for coal-fired power plants. Fuel 2010;89:2791–801.

[216] Wu X, Wang M, Liao P, Shen J, Li Y. Solvent-based post-combustion CO2 capture for power plants: A critical review and perspective on dynamic modelling, system identification, process control and flexible operation. Appl Energy 2020;257:113941.

[217] White LS, Wei X, Pande S, Wu T, Merkel TC. Extended flue gas trials with a membrane-based pilot plant at a one-ton-per-day carbon capture rate. J Memb Sci 2015;496:48–57.

[218] Van Der Spek M, Bonalumi D, Manzolini G, Ramirez A, Faaij A. Techno-economic comparison of combined cycle gas turbines with advanced membrane configuration and

monoethanolamine solvent at part load conditions. Energy & Fuels 2018;32:625–45.

[219] Bouton GR, Luyben WL. Optimum economic design and control of a gas permeation membrane coupled with the hydrodealkylation (HDA) process. Ind Eng Chem Res 2008;47:1221–37.

[220] Katoh T, Tokumura M, Yoshikawa H, Kawase Y. Dynamic simulation of multicomponent gas separation by hollow-fiber membrane module: Nonideal mixing flows in permeate and residue sides using the tanks-in-series model. Sep Purif Technol 2011;76:362–72.

[221] Scholz M, Alders M, Lölsberg J, Wessling M. Dynamic process simulation and process control of biogas permeation processes. J Memb Sci 2015;484:107–18.

[222] Rao AD. Combined cycle systems for near-zero emission power generation 2012.

[223] Energy G. Global Energy and CO2 Status Report. Int Energy Agency Paris, Fr 2019.

[224] Lindqvist K, Jordal K, Haugen G, Hoff KA, Anantharaman R. Integration aspects of reactive absorption for post-combustion CO2 capture from NGCC (natural gas combined cycle) power plants. Energy 2014;78:758–67.

[225] Jordán PS, Javier Eduardo AM, Zdzislaw MC, Alan Martín ZG, Liborio HP, Jesús Antonio FZ, et al. Techno-economic analysis of solar-assisted post-combustion carbon capture to a pilot cogeneration system in Mexico. Energy 2019;167:1107–19.

[226] Powell KM, Edgar TF. Modeling and control of a solar thermal power plant with thermal energy storage. Chem Eng Sci 2012;71:138–45.

[227] Wang J, Zhao J, Deng S, Sun T, Du Y, Li K, et al. Integrated assessment for solar-assisted carbon capture and storage power plant by adopting resilience thinking on energy system. J Clean Prod 2019;208:1009–21.

[228] Alcaraz Calderón AM, Jaramillo Salgado OA, Velazquez Limón N, Robles Perez M, Aguilar JO, González Díaz MO, et al. Optimisation of an Integrated System: Combined Heat and Power Plant with CO2 Capture and Solar Thermal Energy. Processes 2023;11.

[229] Elmohlawy AE, Ochkov VF, Kazandzhan BI. Thermal performance analysis of a concentrated solar power system (CSP) integrated with natural gas combined cycle

(NGCC) power plant. Case Stud Therm Eng 2019;14:100458.

[230] Zhao R, Deng S, Zhao L, Liu Y, Tan Y. Energy-saving pathway exploration of CCS integrated with solar energy: Literature research and comparative analysis. Energy Convers Manag 2015;102:66–80.

[231] Mokhtar M, Ali MT, Khalilpour R, Abbas A, Shah N, Hajaj A Al, et al. Solar-assisted Post-combustion Carbon Capture feasibility study. Appl Energy 2012;92:668–76.

[232] Wu Y, Dai Y, Xie W, Chen H, Zhu Y. Performance analysis for post-combustion CO2 capture in coal-fired power plants by integration with solar energy. Energy 2022;261:125239.

[233] Baker RW, Freeman B, Kniep J, Wei X, Merkel T. CO2 capture from natural gas power plants using selective exhaust gas recycle membrane designs. Int J Greenh Gas Control 2017;66:35–47.

[234] Zhang Z, Oh D-H, Dat Nguyen V, Lee C-H, Lee J-C. Techno-Economic Assessment of Natural Gas Combined Cycle Power Plants with Carbon Capture and Utilization. Energy & Fuels 2023.

[235] Merkel TC, Wei X, He Z, White LS, Wijmans JG, Baker RW. Selective Exhaust Gas Recycle with Membranes for CO2 Capture from Natural Gas Combined Cycle Power Plants. Ind Eng Chem Res 2013;52:1150–9.

[236] Ali U, Agbonghae EO, Hughes KJ, Ingham DB, Ma L, Pourkashanian M. Techno-economic process design of a commercial-scale amine-based CO2 capture system for natural gas combined cycle power plant with exhaust gas recirculation. Appl Therm Eng 2016;103:747–58.

[237] Akram M, Ali U, Best T, Blakey S, Finney KN, Pourkashanian M. Performance evaluation of PACT Pilot-plant for CO2 capture from gas turbines with Exhaust Gas Recycle. Int J Greenh Gas Control 2016;47:137–50.

[238] Biliyok C, Yeung H. Evaluation of natural gas combined cycle power plant for post-combustion CO2 capture integration. Int J Greenh Gas Control 2013;19:396–405.

[239] Elena Diego M, Bellas J-M, Pourkashanian M. Process analysis of selective exhaust gas

recirculation for CO2 capture in natural gas combined cycle power plants using amines. J Eng Gas Turbines Power 2017;139.

[240] Pan M, Aziz F, Li B, Perry S, Zhang N, Bulatov I, et al. Application of optimal design methodologies in retrofitting natural gas combined cycle power plants with CO2 capture. Appl Energy 2016;161:695–706.

[241] Díaz-Herrera PR, Romero-Martínez A, Ascanio G. Cost projection of combined cycle power plants equipped with post-combustion carbon capture. Front Energy Res 2022;10:1855.

[242] Li H, Haugen G, Ditaranto M, Berstad D, Jordal K. Impacts of exhaust gas recirculation (EGR) on the natural gas combined cycle integrated with chemical absorption CO2 capture technology. Energy Procedia 2011;4:1411–8.

[243] Li H, Ditaranto M, Berstad D. Technologies for increasing CO2 concentration in exhaust gas from natural gas-fired power production with post-combustion, amine-based CO2 capture. Energy 2011;36:1124–33.

[244] Giorgetti S, Bricteux L, Parente A, Blondeau J, Contino F, De Paepe W. Carbon capture on micro gas turbine cycles: Assessment of the performance on dry and wet operations. Appl Energy 2017;207:243–53.

[245] Freeman B, Hao P, Baker R, Kniep J, Chen E, Ding J, et al. Hybrid membrane-absorption CO2 capture process. Energy Procedia 2014;63:605–13.

[246] Torres FB, Gutierrez JP, Ruiz LA, Bertuzzi MA, Erdmann E. Comparative analysis of absorption, membrane, and hybrid technologies for CO2 recovery. J Nat Gas Sci Eng 2021;94:104082.

[247] Diego ME, Bellas J-M, Pourkashanian M. Techno-economic analysis of a hybrid CO2 capture system for natural gas combined cycles with selective exhaust gas recirculation. Appl Energy 2018;215:778–91.

[248] Qureshi Y, Ali U, Sher F. Part load operation of natural gas fired power plant with CO2 capture system for selective exhaust gas recirculation. Appl Therm Eng 2021;190:116808.

[249] Alcaráz-Calderon AM, González-Díaz MO, Mendez Á, González-Santaló JM, González-

Díaz A. Natural gas combined cycle with exhaust gas recirculation and CO2 capture at part-load operation. J Energy Inst 2019;92:370–81.

[250] Shindo Y, Hakuta T, Yoshitome H, Inoue H. Calculation methods for multicomponent gas separation by permeation. Sep Sci Technol 1985;20:445–59.

[251] Han Y, Wu D, Ho WSW. Nanotube-reinforced facilitated transport membrane for CO2/N2 separation with vacuum operation. J Memb Sci 2018;567:261–71.

[252] Picaud-Vannereux S, Lutin F, Favre E, Roizard D. Energy efficiency of membrane vs hybrid membrane/cryogenic processes for propane recovery from nitrogen purging vents: A simulation study. Sep Purif Technol 2020;240:116613.

[253] Khalilpour R, Abbas A, Lai Z, Pinnau I. Modeling and parametric analysis of hollow fiber membrane system for carbon capture from multicomponent flue gas. AIChE J 2012;58:1550–61.

[254] Yang D, Ren H, Li Y, Wang Z. Suitability of cross-flow model for practical membrane gas separation processes. Chem Eng Res Des 2017;117:376–81.

[255] Haydary J. Chemical process design and simulation: Aspen Plus and Aspen Hysys applications. John Wiley & Sons; 2019.

[256] Bounaceur R, Lape N, Roizard D, Vallieres C, Favre E. Membrane processes for post-combustion carbon dioxide capture: a parametric study. Energy 2006;31:2556–70.

[257] Shao P, Dal-Cin MM, Guiver MD, Kumar A. Simulation of membrane-based CO2 capture in a coal-fired power plant. J Memb Sci 2013;427:451–9.

[258] Cerveira GS, Borges CP, Kronemberger F de A. Gas permeation applied to biogas upgrading using cellulose acetate and polydimethylsiloxane membranes. J Clean Prod 2018;187:830–8.

[259] Wu D, Sun C, Dutta PK, Winston Ho WS. SO2 interference on separation performance of amine-containing facilitated transport membranes for CO2 capture from flue gas. J Memb Sci 2017;534:33–45.

[260] Hussain A, Hägg M-B. A feasibility study of CO2 capture from flue gas by a facilitated

transport membrane. J Memb Sci 2010;359:140–8.

[261] He X, Fu C, Hägg M-B. Membrane system design and process feasibility analysis for CO2 capture from flue gas with a fixed-site-carrier membrane. Chem Eng J 2015;268:1–9.

[262] Finkenrath M. Cost and performance of carbon dioxide capture from power generation 2011.

[263] Bui M, Gunawan I, Verheyen V, Feron P, Meuleman E, Adeloju S. Dynamic modelling and optimisation of flexible operation in post-combustion CO2 capture plants—A review. Comput Chem Eng 2014;61:245–65.

[264] Belaissaoui B, Cabot G, Cabot M-S, Willson D, Favre E. An energetic analysis of CO2 capture on a gas turbine combining flue gas recirculation and membrane separation. Energy 2012;38:167–75.

[265] Franz J, Schiebahn S, Zhao L, Riensche E, Scherer V, Stolten D. Investigating the influence of sweep gas on CO2/N2 membranes for post-combustion capture. Int J Greenh Gas Control 2013;13:180–90.

[266] Thundyil MJ, Koros WJ. Mathematical modeling of gas separation permeators—for radial crossflow, countercurrent, and cocurrent hollow fiber membrane modules. J Memb Sci 1997;125:275–91.

[267] Cerveira GS, Borges CP, Kronemberger F de A. Gas permeation applied to biogas upgrading using cellulose acetate and polydimethylsiloxane membranes. J Clean Prod 2018;187:830–8.

[268] Asadi J, Yazdani E, Hosseinzadeh Dehaghani Y, Kazempoor P. Technical evaluation and optimization of a flare gas recovery system for improving energy efficiency and reducing emissions. Energy Convers Manag 2021;236:114076.

[269] Shokrian M, High KA. Application of a multi objective multi-leader particle swarm optimization algorithm on NLP and MINLP problems. Comput Chem Eng 2014;60:57–75.

[270] Fouladvand MT, Asadi J, Lotfollahi MN. Simulation and optimization of aromatic extraction from lube oil cuts by liquid-liquid extraction. Chem Eng Res Des

2021;165:118–28.

[271] Shokrian M, High KA. An efficient multi criteria process optimization framework: Sustainable improvement of the Dimethyl Ether Process. Comput Chem Eng 2014;60:213–30.

[272] Asadi J, Amani P, Amani M, Kasaeian A, Bahiraei M. Thermo-economic analysis and multi-objective optimization of absorption cooling system driven by various solar collectors. Energy Convers Manag 2018;173:715–27.

[273] Sipöcz N, Tobiesen FA. Natural gas combined cycle power plants with CO2 capture – Opportunities to reduce cost. Int J Greenh Gas Control 2012;7:98–106.

[274] Lee W-S, Kang J-H, Lee J-C, Lee C-H. Enhancement of energy efficiency by exhaust gas recirculation with oxygen-rich combustion in a natural gas combined cycle with a carbon capture process. Energy 2020;200:117586.

[275] Zhai R, Qi J, Zhu Y, Zhao M, Yang Y. Novel system integrations of 1000 MW coal-fired power plant retrofitted with solar energy and CO2 capture system. Appl Therm Eng 2017;125:1133–45.

[276] THERMOFLEX® Version 30, Thermoflow Inc., USA, https://www.thermoflow.com 2023.

[277] Jonshagen K. Modern Thermal Power Plants-Aspects on Modelling and Evaluation 2011.

[278] Madeddu C, Errico M, Baratti R. CO2 Capture by Reactive Absorption-Stripping: Modeling, Analysis and Design. Springer; 2018.

[279] Rezazadeh F, Gale WF, Akram M, Hughes KJ, Pourkashanian M. Performance evaluation and optimisation of post combustion CO2 capture processes for natural gas applications at pilot scale via a verified rate-based model. Int J Greenh Gas Control 2016;53:243–53.

[280] Omehia KC, Clements AG, Michailos S, Hughes KJ, Ingham DB, Pourkashanian M. Techno-economic assessment on the fuel flexibility of a commercial scale combined cycle gas turbine integrated with a CO2 capture plant. Int J Energy Res 2020;44:9127–40.

[281] Canepa R, Wang M. Techno-economic analysis of a CO2 capture plant integrated with a

commercial scale combined cycle gas turbine (CCGT) power plant. Appl Therm Eng 2015;74:10–9.

[282] System Advisor Model Version 2022.11.21 (SAM 2022.11.21). National Renewable Energy Laboratory. Golden, CO. Accessed April 10, 2023. sam.nrel.gov . n.d.

[283] Jain A, Vu T, Mehta R, Mittal SK. Optimizing the cost and performance of parabolic trough solar plants with thermal energy storage in India. Environ Prog Sustain Energy 2013;32:824–9.

[284] Liu G, Liu J, E J, Li Y, Zhang Z, Chen J, et al. Effects of different sizes and dispatch strategies of thermal energy storage on solar energy usage ability of solar thermal power plant. Appl Therm Eng 2019;156:14–22.

[285] Notz R, Mangalapally HP, Hasse H. Post combustion CO2 capture by reactive absorption: Pilot plant description and results of systematic studies with MEA. Int J Greenh Gas Control 2012;6:84–112.

[286] González-Díaz A, Alcaráz-Calderón AM, González-Díaz MO, Méndez-Aranda Á, Lucquiaud M, González-Santaló JM. Effect of the ambient conditions on gas turbine combined cycle power plants with post-combustion CO2 capture. Energy 2017;134:221–33.

[287] Razi N, Svendsen HF, Bolland O. Cost and energy sensitivity analysis of absorber design in CO2 capture with MEA. Int J Greenh Gas Control 2013;19:331–9.

[288] Liang CZ, Yong WF, Chung T-S. High-performance composite hollow fiber membrane for flue gas and air separations. J Memb Sci 2017;541:367–77.

[289] Han H, Scofield JMP, Gurr PA, Webley PA, Qiao GG. Ultrathin membrane with robust and superior CO2 permeance by precision control of multilayer structures. Chem Eng J 2023;462:142087.

[290] Cousins A, Wardhaugh LT, Feron PHM. Preliminary analysis of process flow sheet modifications for energy efficient CO2 capture from flue gases using chemical absorption. Chem Eng Res Des 2011;89:1237–51.

[291] Liu Z, Karimi IA. Simulation and optimization of a combined cycle gas turbine power

plant for part-load operation. Chem Eng Res Des 2018;131:29–40.

[292] Zhang G, Zheng J, Xie A, Yang Y, Liu W. Thermodynamic analysis of combined cycle under design/off-design conditions for its efficient design and operation. Energy Convers Manag 2016;126:76–88.

[293] Mitterrutzner B, Sanz W, Nord LO. A part-load analysis and control strategies for the Graz Cycle. Int J Greenh Gas Control 2022;113:103521.

[294] Zhang Y, Liu P, Li Z. Gas turbine off-design behavior modelling and operation windows analysis under different ambient conditions. Energy 2023;262:125348.

[295] Kim TS. Comparative analysis on the part load performance of combined cycle plants considering design performance and power control strategy. Energy 2004;29:71–85.

[296] Li Y, Zhang G, Wang L, Yang Y. Part-load performance analysis of a combined cycle with intermediate recuperated gas turbine. Energy Convers Manag 2020;205:112346.

[297] Li Y, Zhang G, Bai Z, Song X, Wang L, Yang Y. Backpressure adjustable gas turbine combined cycle: A method to improve part-load efficiency. Energy Convers Manag 2018;174:739–54.

[298] Apan-Ortiz JI, Sanchez-Fernández E, González-Díaz A. Use of steam jet booster as an integration strategy to operate a natural gas combined cycle with post-combustion CO2 capture at part-load. Energy 2018;165:126–39.

[299] Rovira A, Valdés M, Durán MD. A model to predict the behaviour at part load operation of once-through heat recovery steam generators working with water at supercritical pressure. Appl Therm Eng 2010;30:1652–8.

[300] Zhang G, Zheng J, Yang Y, Liu W. Thermodynamic performance simulation and concise formulas for triple-pressure reheat HRSG of gas–steam combined cycle under off-design condition. Energy Convers Manag 2016;122:372–85.

[301] Theis J. Quality Guidelines for Energy Systems Studies: Cost Estimation Methodology for NETL Assessments of Power Plant Performance - Feb 2021. United States: 2021.

[302] Zoelle A, Kuehn N. Quality Guidelines for Energy System Studies: Capital Cost Scaling

Methodology: Revision 4 Report. United States: 2019.

[303] Datta A, Krishnamoorti R. Analysis of direct air capture integrated with wind energy and enhanced oil recovery. Environ Sci Technol 2023;57:2084–92.

[304] Turton R, Bailie RC, Whiting WB, Shaeiwitz JA. Analysis, synthesis and design of chemical processes. Pearson Education; 2008.

[305] Mazzotti M, Baciocchi R, Desmond MJ, Socolow RH. Direct air capture of CO2 with chemicals: optimization of a two-loop hydroxide carbonate system using a countercurrent air-liquid contactor. Clim Change 2013;118:119–35.

[306] Chen L. Heat-integrated Crude Oil Distillation System Design (Ph. D. Thesis) UMIST. Manchester, UK 2008.

[307] Du Y, Gao T, Rochelle GT, Bhown AS. Zero-and negative-emissions fossil-fired power plants using CO2 capture by conventional aqueous amines. Int J Greenh Gas Control 2021;111:103473.

[308] Hu S, Yang Z, Li J, Duan Y. Optimal solar thermal retrofit for geothermal power systems considering the lifetime brine degradation. Renew Energy 2022;186:628–45.

[309] Yılmaz İH, Mwesigye A, Kılıç F. Prioritization of heat transfer fluids in parabolic trough solar systems using CFD-assisted AHP-VIKOR approach. Renew Energy 2023;210:751–68.

[310] Liu T, Yang J, Yang Z, Duan Y. Techno-economic feasibility of solar power plants considering PV/CSP with electrical/thermal energy storage system. Energy Convers Manag 2022;255:115308.

[311] Shagdar E, Shuai Y, Lougou BG, Mustafa A, Choidorj D, Tan H. New integration mechanism of solar energy into 300 MW coal-fired power plant: performance and techno-economic analysis. Energy 2022;238:122005.

[312] Zhai H, Rubin ES. Techno-economic assessment of polymer membrane systems for postcombustion carbon capture at coal-fired power plants. Environ Sci Technol 2013;47:3006–14.

[313] Lee S, Kim J-K. Process-integrated design of a sub-ambient membrane process for CO2 removal from natural gas power plants. Appl Energy 2020;260:114255.

[314] Mehanovic D, Al-Haiek A, Leclerc P, Rancourt D, Fréchette L, Picard M. Energetic, GHG, and economic analyses of electrified steam methane reforming using conventional reformer tubes. Energy Convers Manag 2023;276:116549.

[315] McDowell DL, Panchal J, Choi H-J, Seepersad C, Allen J, Mistree F. Integrated design of multiscale, multifunctional materials and products. Butterworth-Heinemann; 2009.

[316] Nellippallil AB, Allen JK, Gautham BP, Singh AK, Mistree F. Architecting robust co-design of materials, products, and manufacturing processes. Springer; 2020.